2002

Flow unit prediction with limited permeability data using artificial neural network analysis

Benjamin Hale Thomas
West Virginia University

FLOW UNIT PREDICTION WITH LIMITED PERMEABILITY DATA USING ARTIFICIAL NEURAL NETWORK ANALYSIS

Benjamin Hale Thomas

Dissertation submitted to the
College of Engineering and Mineral Resources
at West Virginia University
in partial fulfillment of the requirements
for the degree of

Doctor of Philosophy
in
Petroleum and Natural Gas Engineering

Khashayar Aminian, Ph.D., Chair
Samuel Ameri, M.S.
Michael Hohn, Ph.D.
Robert Chase, Ph.D.
H. Ilkin Bilgesu, Ph.D.
Shahab Mohaghegh, Ph.D.

Morgantown, West Virginia
2002

Keywords: Reservoir Simulation, Artificial Neural Networks, Reservoir Characterization, Flow Units, Permeability Prediction, Waterflooding, Gordon Sandstone, Jacksonburg-Stringtown Field

ABSTRACT

FLOW UNIT PREDICTION WITH LIMITED PERMEABILITY DATA USING ARTIFICIAL NEURAL NETWORK ANALYSIS

Benjamin Hale Thomas

The Appalachian Basin has numerous abandoned or marginally producing oilfields having significant recoverable oil remaining in place. Typically production records and reservoir data is not available. Presented is a new methodology, applicable to any field having limited records, designed for reservoir characterization via flow unit identification.

This methodology utilizes limited core permeability data from a few wells as a key to predicting flow units within a field when only log-based data is available. Primary software tools used include NeuroShell 2, an artificial neural network (ANN) program, and the Boast98 numerical simulator.

Various techniques for flow unit identification including graphic approaches using the permeability-porosity relationship within a given flow unit and ANN (Kohonen) analysis are utilized as a part of the methodology developed. The core data and flow units are utilized in neural network models designed to predict flow units and permeability field-wide using only electric well logs. Field wide prediction of flow units and permeability are products of the study.

The study field selected was the Jacksonburg-Stringtown field. The producing horizon is the Upper Devonian Gordon sandstone. Discovered in 1895, waterflood operations were commenced in 1981. The characterization study utilizes core data and electric logs (gamma ray- density) from six core wells for flow unit identification.

Two dual five spots were selected in the field for verification of this new methodology. Reservoir simulation analysis utilizing the predicted flow units and permeability was completed for comparison to actual production records. A close match was achieved. As another comparison step a single layer simulation model for the two patterns was generated. The single layer model included the same inputs as the flow unit model except for thickness and average permeability. The simulation model utilizing flow units was a far more accurate prediction method.

ACKNOWLEDGEMENTS

As I complete the final stages of my research project and doctoral studies, I have much to be thankful for. I thank God for our safe travel during the many long trips to the university, good health and blessing me with supporting family, friends, professors, and fellow graduate research students - all of whom played a significant part in this accomplishment.

I extend my appreciation to Dr. Khashayar Aminian, my graduate advisor and committee Chairman. His experience, knowledge and willingness to support my efforts are a big part of my success.

In 1994, I began my graduate studies. Chairman Ameri has always offered positive support, in every aspect, as the Department Chairman and a committee member.

Having been through the doctoral process I have gained a deep appreciation for my committee members. They have willingly given their time and energy. I extend my sincere appreciation to Dr. Ilkin Bilgesu, Dr. Robert Chase, Dr. Michael Hohn and Dr. Shahab Mohaghegh, my other committee members.

I also would like to thank Dr. Ronald McDowell and David Matchen of the West Virginia Geologic Surveys. Their geologic expertise and assistance was greatly appreciated.

My son, Jeremy, has watched my efforts for these many years. By example, I hope my perseverance, sacrifice and passion influence his life goals and aspirations.

Lastly and most importantly, I write of my wife, Connie. Her tireless support and believing that we could accomplish my goal has been steadfast. She has endured long days and nights of travel, managed the household with little help from me, and willingly gave up our time together for several years in order that I could accomplish my goal. She has earned my endless respect and appreciation for her unselfish support. I look forward to spending time with her, the one I love.

TABLE OF CONTENTS

LIST OF TABLES

LIST OF FIGURES

NOMENCLATURE

ANN:	**Artificial Neural Network**
Bo:	**Oil Formation Volume Factor, RB/STB**
BOPD:	**Barrels of Oil per Day**
Bg:	**Gas Formation Volume Factor, RCF/SCF**
DX:	**x-direction Grid Block Dimension, ft.**
FZI:	**Flow Zone Indicator**
GR:	**Gamma Ray**
GRNN:	**General Regression Neural Network**
h:	**Thickness, ft.**
k:	**Permeability, md**
k_r**:**	**Relative Permeability**
Pc_{corr}**:**	**Capillary Pressure Corrected for an Oil-Water System, psia**
Pc_{exp}**:**	**Capillary Pressure Obtained for a Water-Air System, psia**
PID:	**Flow Index per Layer, STB/D**
r:	**Linear Correlation Coefficient**
r^2**:**	**Coefficient of Determination**
R^2**:**	**Coefficient**
RQI:	**Reservoir Quality Indicator**
Rs:	**Gas-Oil Ratio, SCF/STB**
r_w**:**	**Wellbore Radius, ft.**
Sv_{gr}**:**	**Specific Surface Area per Grain Unit Volume**
K_z**:**	**Kozeny Constant**
σ**w-o:**	**Interfacial Tension for Water-Oil, dyne/cm**
σ**w-a:**	**Interfacial Tension for Air-Water, dyne/cm**
ϕ_e**:**	**Effective Porosity**
ϕ_n**:**	**Normalized Porosity Index (also seen as** $\varnothing_{z)}$
ϕ**:**	**Porosity, %**

CHAPTER 1

INTRODUCTION

1.1 Introductory Discussion

Reservoir characterization is the ongoing process of defining reservoir properties and geological conditions for evaluating reservoir performance and forecasting future behavior (Neog, 2000). The ability to predict reservoir performance via simulation work is enhanced as reservoir properties are better defined. Flow unit identification can be utilized during the reservoir characterization process. The flow unit is a volume of total reservoir rock within which geological and petrophysical properties that affect fluid flow are internally consistent and different from properties of other rock volumes (Ebanks, 1987). A given flow unit exhibits a certain permeability-porosity relationship and has similar properties for fluid flow. Within each flow unit, utilizing fluid flow properties enhances reservoir simulation. The flow unit division allows fluid flow within the reservoir to be better understood and categorized in a useful manner for simulation analysis.

1.2 Research Objectives

The Appalachian Basin has numerous abandoned or marginally productive oilfields in the region. Typically production

records are nonexistent which hampers further development interest. The objective of this research is to develop a methodology for reservoir characterization specifically modeled for the Appalachian Basin when reservoir records are limited.

The permeability-porosity relationship within each flow unit allows us to identify the flow units using various techniques. However, without permeability distribution, flow unit prediction is not possible. This research seeks to predict flow units using only well log data when a limited number of cores are available for analysis. By following this methodology the researcher is able to:

- **Identify flow units based on well log data (gamma ray-density)**
- **Predict the flow unit properties in wells having only well log data**
- **Determine the distribution of flow units within the reservoir.**

1.3 Primary Research Tools

In order to test this methodology an Appalachian Basin oilfield was selected which has far more complete production records than typically available in the Appalachian Basin. The 9,000-acre Jacksonburg-Stringtown field is currently being waterflooded. Field record retention by the operator is far better than what is normally encountered in the Appalachian Basin. This offered the unique opportunity to verify the methodology developed by comparing

simulator results (predicted) against actual secondary recovery production results. It is important to clarify that this research and the methods identified for flow unit identification has application to all reservoirs. The Jacksonburg-Stringtown field offered a unique opportunity to test and verify the methodology developed.

For Appalachian reservoirs this methodology requires that a limited number of cores be secured from wells at the time of drilling. The cores are utilized to secure permeability and porosity measurements. It is also recommended that a few core samples from each flow unit be tested on order to develop relative permeability data for simulation analysis. At a minimum a gamma ray-density log is required for each cored well. With this limited data, utilizing this methodology flow unit identification and permeability estimation within each flow unit can be done. The extent to which the prediction tool can be applied, to other wells in the field, is limited by the number of available logs from other existing wells.

Artificial Neural Networks (ANNs) were found to be very useful for predicting permeability and flow units. The use of ANNs to predict permeability had previously been demonstrated when geophysical log data was used. This research extends this application by developing a methodology to identify flow units within the reservoir when permeability is not known and available reservoir information is limited to electric log data. The benefit of flow unit

identification, with very limited reservoir data, improves permeability prediction within each flow unit and more enhances reservoir simulation analysis. Being able to better predict reservoir performance by identifying flow units can be significant when evaluating future potential of Appalachian based reservoirs.

1.4 Research Value

The success of this research may well lead to heightened interest in many of the previously prolific oil reservoirs situated throughout the Appalachian Basin. This procedure has application in natural gas and oil reservoirs. Most abandoned or marginally productive fields in the Appalachian Basin are primarily oil fields. As a result oil reservoirs having secondary recovery potential are the primary interest.

CHAPTER 2

VERIFICATION FIELD HISTORY

2.1 Field History

The Jacksonburg-Stringtown field was discovered in 1895. The field is located in portions of Wetzel, Tyler and Doddridge counties, West Virginia and encompasses nearly 9,000 acres (Figure 2.1). Between 1895 and 1901 over 500 wells were drilled through the Gordon sandstone. Drilled on average well spacing of 13 acres; the wells initially produced up to 300 BOPD. Standard completion called for open-hole completion through the pay with nitroglycerine being used for stimulation. The field was a solution gas drive and gravity drainage reservoir.

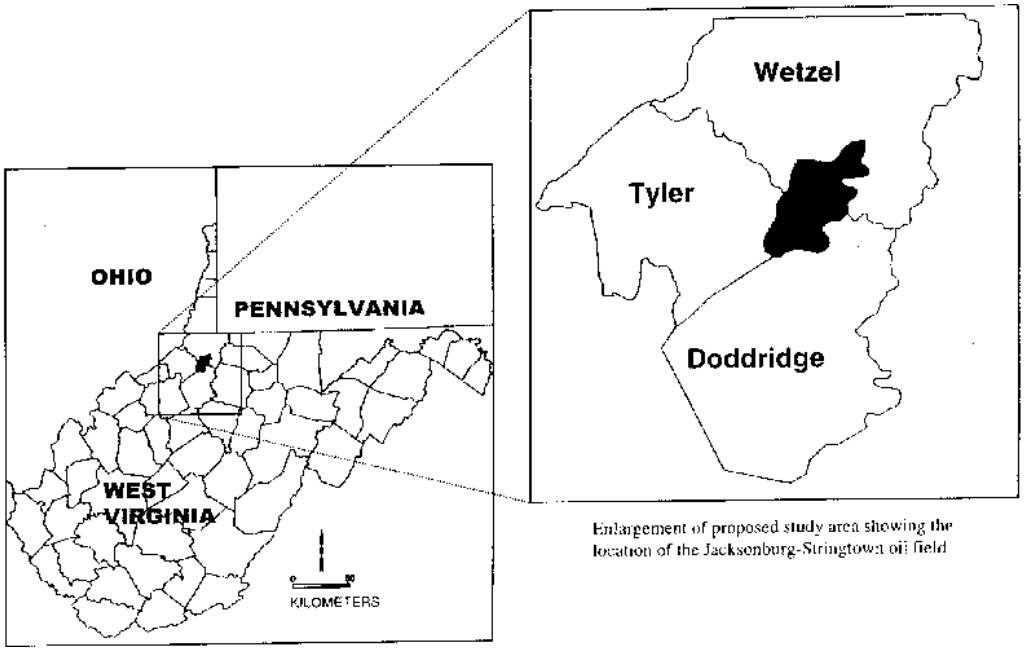

Figure 2.1 The Jacksonburg-Stringtown Field

By 1910 most of the wells were plugged and abandoned. Production records indicate 12 million barrels of oil (MMBO) were recovered. Figures 2.2 and 2.3 present the daily and cumulative oil production for the field from 1896 to 1991. Internal company records estimated initial oil in place to be 88.5 MMBO.

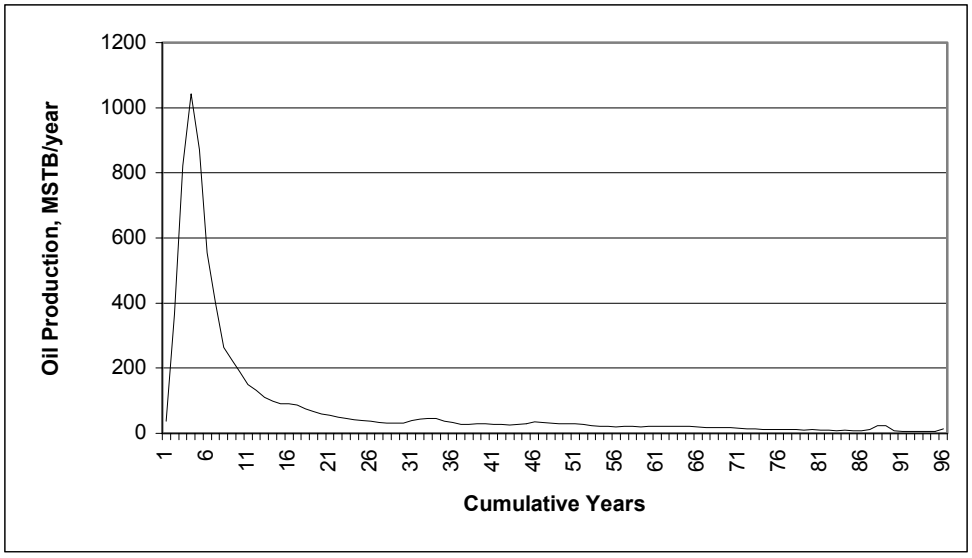

Figure 2.2 Daily Oil Production in the Jacksonburg-Stringtown Field 1896-1991

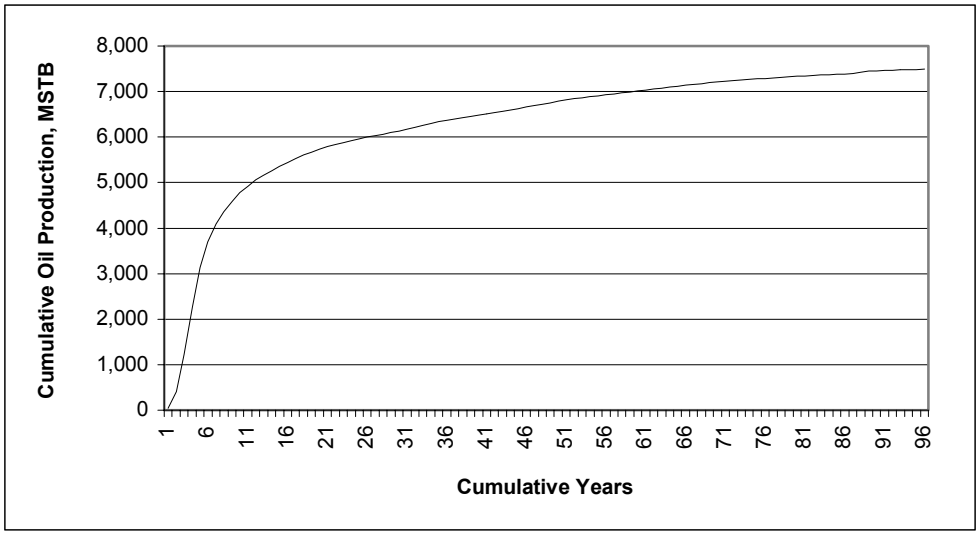

Figure 2.3 Cumulative Oil Production in the Jacksonburg-Stringtown Field 1896-1991

In the mid 1930's a gas re-injection program commenced and continued through the 1950's. Five injection wells were utilized in the field. Additional recoveries, due to gas re-injection, were limited to only portions of the field. Table 2.1 is a summary of recovery estimates from various internal company reports.

The Gordon sandstone formation depth ranges from approximately 2,800 feet to 3,100 feet. The surface elevation above sea level varies from approximately 925 feet to 1,150 feet, which accounts for nearly all of the depth variation. Company records indicated an oil viscosity of 3.5 cp at 85° F and a gravity of 45.3° API at 60° F. Table 2.2, 2.3, and 2.4 summarize the oil, gas and production water properties as reflected in company records.

Table 2.1 Field Recovery Summary

Description	Barrels Per Acre
Primary Recovery Estimate (King, 1980)	1,454
Primary Recovery Estimate (Morrison, 1991)	1,590
Gas Re-Injection Recovery (Boone, 1986)	154
34 Acre Pilot Waterflood Recovery (Boone, 1986)	1,300

(Recovery estimates captured from internal Pennzoil correspondence)

Table 2.2 Crude Oil Analysis

Property	
Crude Gravity, º API	45.3
IBF, º F	96
Viscosity @ 85 ºF	3.5 cp
Density @ 85 ºF	0.7903 g/ml
% Tar	1

Table 2.3 Gas Analysis

Property	
Specific Gravity	0.628
BTU/CF @ 14.73 psia Dry Basis Wet Basis	 989.8 972.6
Molecular Weight	18.2
Compressibility Factor	0.998

Table 2.4 Produced Water Analysis

Property	M-1	H-12
Specific Gravity @ 75 °F	1.089	1.002
PH	4.3	7.46
Total Dissolved Solids, mg/l	129116	7006

In 1981, a dual five spot pilot waterflood was commenced in the field. The pilot area covered 34 acres of the reservoir. An average of 1,300 barrels of oil per acre (BOPA) was recovered in four years (Boone, 1986).

Based on the pilot recoveries; development proceeded to a full-scale waterflood of the field. Over 140 new wells were drilled as injectors or producers. The terrain dictated that some wells be drilled directionally to their bottom hole target location. Some in-field sites remain to be drilled. Secondary recovery of the field is currently in progress.

2.2 Geologic Overview

The producing horizon in the field is the Upper Devonian Gordon sandstone. The formation is known to be extremely heterogeneous as a result of stratigraphy, structure and post diagenetic impact (Figure 2.4). Gross thickness can be up to 50 feet. The pay thickness varies from 4 feet up to 20 feet. Permeability can range from < 5md to values in excess of 250 md. This varying thickness is due to a non-uniform pre-depositional surface and erosional impact during post deposition. The sand is a shallow marine, shoreline deposit trending in a northeast-southwest direction. In portions of the field the pay zone is situated below a conglomerate. Permeability within the conglomerate varies widely.

As a result the conglomerate can act either as a highly permeable thief zone for injected fluids or be impermeable for fluid flow. Figure 2.5 presents a core description and associated electric log for the Ball # 18 well. This well is one of the core wells in the field and is also in the portion of the field used for verification.

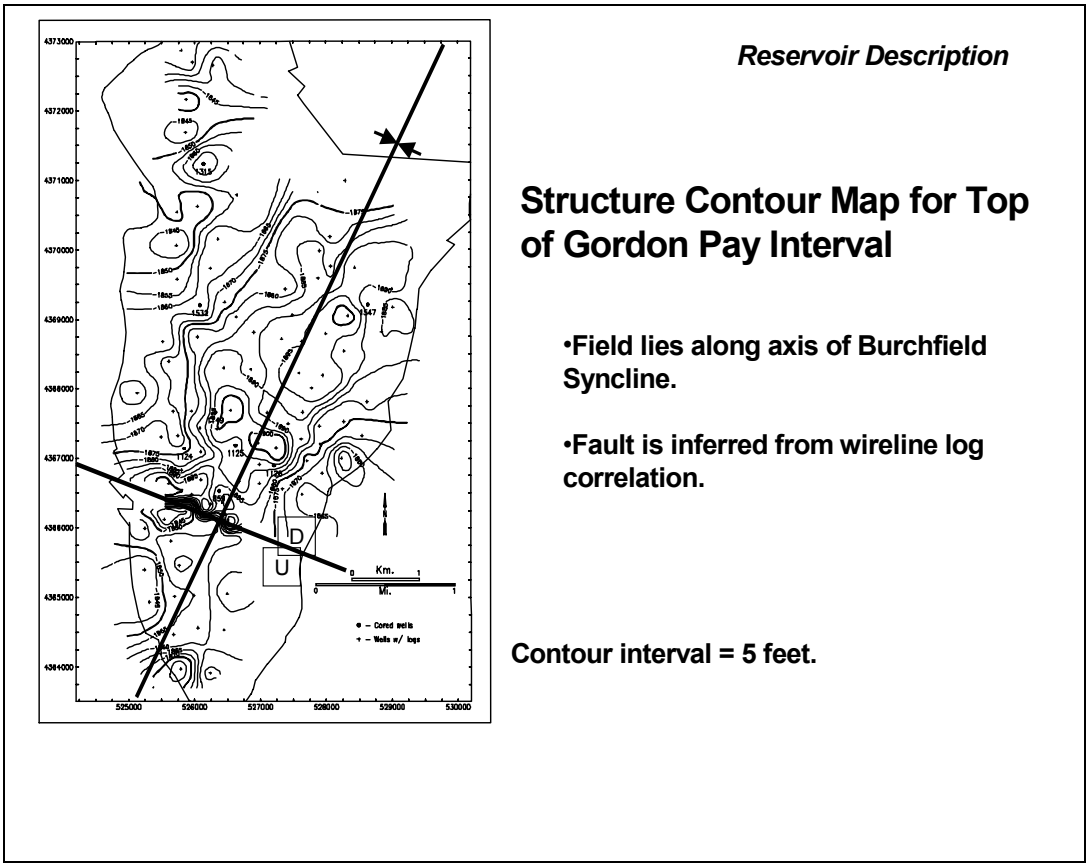

Figure 2.4 Structure Contour Map - Top of Gordon Sand

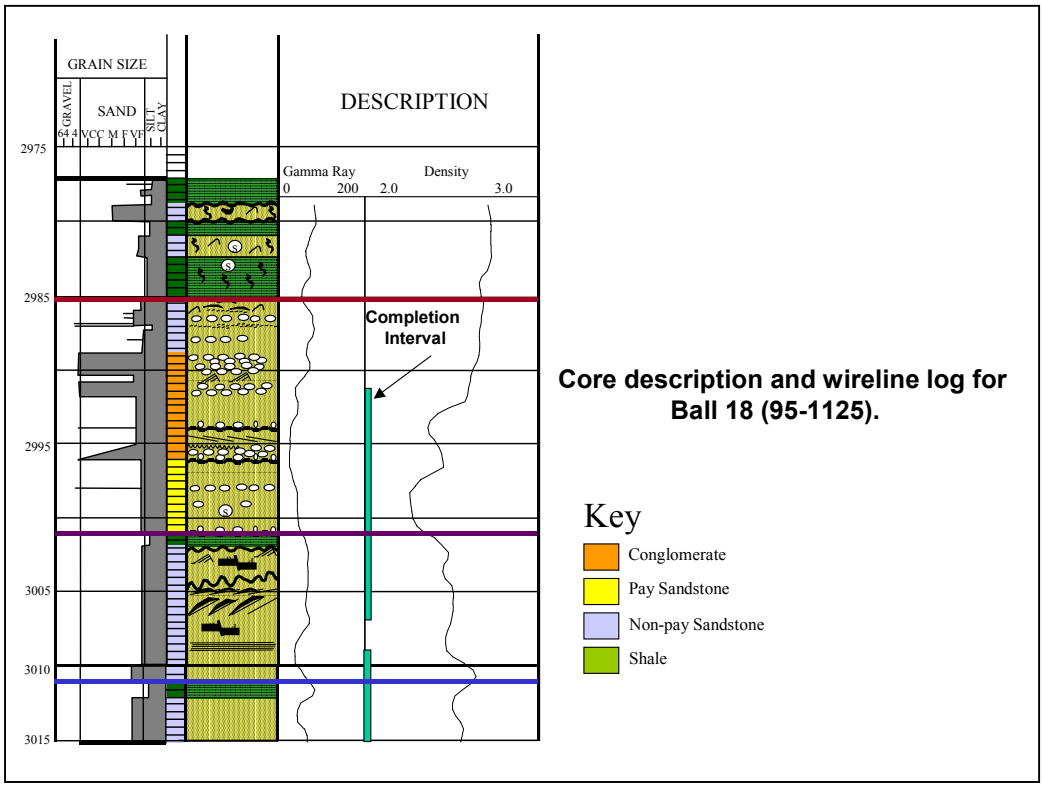

Figure 2.5 Core Description and Electric Log for Ball # 18

CHAPTER 3

RESERVOIR CHARACTERIZATION AND THE FLOW UNIT

3.1 Introductory Discussion

In 1977 Forrest F. Craig authored a paper titled "Optimized Recovery Through Continuing Interdisciplinary Cooperation" (Craig, 1977). Craig noted that prior to numerical simulation reservoir models - detailed geological and performance data was not useful for the common hand calculations frequently done for reservoir prediction. The reservoir engineer had more data than could be used in the model(s). As a result, there was little need for close communication between the geologist and engineer.

However, as more advanced technology became available to the reservoir engineer, the need for information flow within the organization began to increase. The author recognized that we had entered a period where the capability of the tools to use reservoir data exceeded the availability of the data. As a result of the additional capability, the reservoir engineer finds himself seeking more data, both in quantity and detail from the geologist, production engineer, and other technical staff members. The geologist, as well, is able to use this open flow of information to enhance his understanding of the geologic process. Accordingly engineering and geologic skills, strengthened by ongoing information exchange,

interpretation and judgment, guide our understanding of the reservoir.

Reservoir characterization is an ongoing process of defining reservoir properties and geological conditions for evaluating reservoir performance and forecasting future behavior (Neog, 2000). As a result geology, geophysics, and engineering are utilized in order to fully characterize a given reservoir.

3.2 Reservoir Description

Ideally the economic benefit of reservoir characterization is being realized in new and existing fields. In the United States most field discovery and development has occurred. Reservoir characterization is a process whereby ultimate recoverable reserves can be increased. "Only when a clear picture of the reservoir is developed can it be determined whether new technology should be applied, which reservoirs to apply it to, and what the timing of the application should be" (Holtz, 1996). The process of developing of a reservoir description should be initiated during the early stage of reservoir development. However, some companies elect to postpone the investment of staff and expenses required for characterization work.

The development of a reservoir description or the characterization process can be broken down into four major study areas (Willhite, 1986).

- **Rock Studies**
- **Framework Studies**
- **Reservoir Quality Studies**
- **Integration Studies**

Rock Studies

Identifying the depositional environment is an essential step in order to estimate reservoir properties. The geologist will study the cores, analyze thin sections, and develop a vertical sequence of sedimentation. One objective is a three-dimensional analysis of the reservoir rock distribution as a result of depositional conditions. The rock study is to correlate the rock properties of permeability, porosity, and capillary pressure with the identified rock types. As a part of this study, other considerations may include vertical versus horizontal permeability, water saturation versus permeability and porosity versus permeability. The geologist will also identify various "facies" within the reservoir. This term is used to describe a sedimentary body having distinct physical, chemical and biological attributes (Monroe, 1992).

Framework Studies

The purpose of the framework study is to determine the number and distribution of reservoir zones. Efforts to determine reservoir continuity identify flow barriers and non-reservoir zones are essential. Correlation work between wells using logs, cores, core descriptions and seismic data are needed to complete the framework step. In sandstone formations understanding the shale barriers and the separation of sand units in the reservoir occurs as a part of the framework analysis.

Reservoir Quality Studies

The objective of the reservoir quality study is to identify and describe variations in rock properties and fluid saturations in the reservoir. In the event more than one zone or intervals with different properties exist the properties are defined for each zone. This includes net sand thickness and fluid saturations. Net sand is an essential part of the study. Minimum values of hydrocarbon saturation, porosity or permeability values are frequently used. Relationships between porosity and permeability are often analyzed graphically. In addition, directional permeability can also be evaluated. The geologist's understanding of the depositional environment coupled with core results greatly enhances the level of reservoir knowledge. An understanding of directional permeability

can also have significant impact on reservoir development and recovery design.

Within a given facies the reservoir properties can vary significantly. This variation has lead to a further subdivision known as Flow Units (FU). Flow units are regions in the sedimentary sequence that are judged to control the movement of injected or produced fluids within the reservoir (Hearn, 1984). Further discussion will be dedicated to this concept in section 3.7.1.

Integration Studies

The final step during the process of developing a reservoir description is to transfer the study results into a three-dimensional model of the reservoir. Generally the three-dimensional model of the reservoir is designed as a mathematical model. The objective is to build a model that will predict production similar to actual results and handle field modifications in order to simulate future reservoir performance.

As new production history is gained, wells are drilled and/or updated reservoir data is gained the reservoir description can be adjusted. During field development until the field approaches abandonment this process should be considered ongoing. After a valid model is built various future development alternatives can be tested via the model. As a result, the ultimate recoverable reserves,

estimated development costs and risk adjusted economic analysis can be developed in order to identify the optimal development plan for a given reservoir.

3.3 Permeability-Porosity Relationship

The classic scatter plot of permeability versus porosity on semi-log scale has historically been utilized to aid in identifying the relationship between core permeability and core porosity. Amaefule and others (1993) noted that there is apparently no theoretical basis to support this traditional cross plot and that permeability plotted as a function only appears to be log normally distributed. Often times the scatter of the data negates the value of this technique. Using the core data the empirical permeability is estimated from the log derived porosity equation:

$$\text{Log } k = a\phi + b$$

It has been documented that porosity is generally not dependent upon grain size. As a general rule permeability is very much grain size dependent. Amaefule and others (1993) illustrated this by considering a reservoir having high and low permeability zones. In their example the porosity was equal for two cores having high and low permeability. As a result the researchers noted the limitation of the classic approach. However, it was observed that

different porosity-permeability relationships are supporting detail regarding the presence of multiple flow units.

3.4 Pore Geometry

Davies (1999) further discussed the permeability-porosity relationship. In the case study the plot of all data exhibited significant scatter. Davies sought to characterize the reservoir in terms of pore geometry. Changes in pore geometry in the reservoir can occur due to changes in lithology, the depositional environment and chemical changes that have occurred post deposition. Such events impact grain size, grain shape, sorting and packing. Using pore geometry as a basis the researchers identified individual rock types in the reservoir. As a result of the subdivision plots of permeability versus porosity supported the rock type breakdown.

The researchers presented a methodology for reservoir characterization directed at permeability prediction and the resulting improvement in predicting production or injection behavior. Davies and others (1999) investigated and analyzed the “rock type” in two reservoirs. They characterized rock types based on unique pore geometry. The method utilized image analysis via a scanning electron microscope specially equipped for automated image analysis procedures in order to identify various pore geometries. When integrated with other petrophysical measurements (porosity,

permeability, etc.), rock types of non-cored sections were identified from the logs. As a result the reservoir can be defined in terms of flow units.

Pore geometry analysis coupled with log data allow for significant reservoir characterization. The parameters of pore geometry measurement consider several different aspects of the pore and pore system in order to identify and/or differentiate the rock types. Core samples and at times, under favorable circumstances, samples from drill cuttings are utilized for pore geometry analysis. Ideally core samples are removed from the core for testing at predetermined intervals (.5-1.0 feet) through the entire pay section. These samples are used to determine typical petrophysical properties (porosity, permeability, relative permeability, capillary pressures etc.). Thin section and scanning electron analysis related to pore geometry modeling must be taken from the same core plug sample area. This is essential in order to correlate the pore geometry analysis with the petrophysical properties.

At the microscopic level a core description was developed which categorized the texture and lithology for each core sample. The thin section and electron microscope analysis results in direct measurement of shale and clay volumes, grain size detail, sorting analysis, and mineral composition. This analysis is done at each core point for correlation with the petrophysical and log properties.

Davies and others (1999) classified pore types in terms of several parameters. The scanning electron microscope is essential for this type of analysis:

- **Pore Size and Shape - Determined via scanning electron work.**
- **Pore Throat Size - Determined via scanning electron work and capillary tests.**
- **Aspect Ratio - Ratio of pore body to throat size.**
- **Coordination Number - The number of pore throats intersecting each pore.**
- **Pore Arrangement - Pore distribution is analyzed via the scanning electron work.**

The researchers utilized the pore typing method and other analysis to characterize the rock at the pore structure level. Davies and others noted that the pore geometry directly controls hydrocarbon displacement efficiency. In many reservoirs the original depositional environment or lithology are not adequate to properly characterize the reservoir. Digenetic processes are known to alter the permeability-porosity relationships.

Pore geometry analysis does not consider depositional environment of lithology. Within each rock type porosity and permeability is related strictly to pore structure. The traditional semi-log plot of permeability versus porosity resulted in a high degree of scatter in the Davies and others (1999) research. In this case study porosity and permeability were closely related for each

rock type or pore structure. Regression analysis equations were developed for each rock type. The equations were then used for a field wide permeability prediction.

The North Robinson Clearfork Unit selected by Davies and others (1999) as a case study field has a thick productive pay section. Historically the producing and injection wells had been perforated based on porosity detail gained from electric logs (perforate and stimulate the highest porosity sections). The log suite included the gamma ray, photoelectric factor, bulk density, neutron porosity and dual laterolog. Higher permeability rock types had lower porosity. The highest porosity sections occurred in rock types having low permeability. The method of perforation selection and zone completion needed modification.

Flow units were identified by evaluating the rock type and the petrophysical properties within each rock type. Flow units having different hydraulic properties will have different pore throat properties as well. Accurate flow unit identification can occur by detailing changes in the pore throat system. This analysis leads to a layering profile, which was useful in identifying distinct flow units. As a result the outcome of reservoir modeling more closely matched actual production results. In addition future in-fill wells could be better identified.

3.5 Outcrop Derived Models of Permeability

The ability to predict reservoir permeability within the reservoir remains difficult variable to determine. Often times the data gained by core analysis from the reservoir is not adequate to predict permeability distribution in the reservoir. As the reservoir becomes more heterogeneous the ability to predict becomes further reduced. One approach to better understand the scales and magnitude of reservoir heterogeneity of a given reservoir is to evaluate exposed outcrops having similar or analogous sediments.

Successful outcrop studies can lead to permeability modeling within a given reservoir by gaining valuable permeability data from the outcrop. Outcrops selected typically exhibit similar lithologic and sedimentologic features and are approximately the same geologic age. The outcrop is exposed and as a result the measured permeability can be impacted.

Lewis (1988) noted that the main cause of reservoir heterogeneity is depositional architecture. The researcher suggested that a series of scales could be used to classify the variables resulting from reservoir heterogeneity. Such a classification system could be from outcrops. The results can then be applied to a specific reservoir - adjusted to the reservoir based on actual core data. A major assumption of this approach is that the "porosity and permeability measured at the outcrop is analogous to

those in similar sediment types in the subsurface" (Lewis, 1988). Lewis limited his study to carbonates and did not discuss digenetic impact. This application is limited in the Appalachian Basin due to the lack of outcrops from producing or analogous formations that can be utilized.

3.6 Pre-Flow Unit Review

D.G. Harris (1975) discussed the role of geology in reservoir simulation studies. The primary thrust of Harris's work was to describe the geologic activities needed for building realistic mathematic reservoir models. Harris identified and discussed four stages of the geologic activity. In 1986 Willhite drew heavily from this work and incorporated more of the teaming aspect (engineering and geology) in the four steps.

- **Step One: Rock studies to establish lithology, to determine depositional environment and to distinguish reservoir rock from non-reservoir rock;**
- **Step Two: Framework studies to establish the structural style and determine the three dimensional continuity character and gross thickness trends of the reservoir rock;**
- **Step Three: Reservoir quality studies to determine the framework variability of the reservoir rock in terms of porosity, permeability and capillary properties and**
- **Step Four: Integration studies to develop the hydrocarbon pore volume and fluid transmissibility pattern in three dimensions.**

Of particular interest in this very detailed process is the identification of the "key" rock units. This description was for identifying the lithological unit and included shale, siltstone and sandstone. By 1975 researchers recognized the value of characterizing the lithology of the reservoir.

Craig and others (1975) discussed the need for reservoir development and management to occur through teams developed from various technical disciplines. The researcher noted that the progress of reservoir simulation software to handle reservoir data had necessitated the need for increased communication and information sharing between the geologist, production engineer and reservoir engineer. Craig recognized the need to call upon the geologist, with his knowledge of depositional processes, to provide more reservoir descriptions for use in engineering calculations. Further, he recognized the reservoir engineer's need, with his understanding of fluid flow mechanisms, to relate all available pressure and production data to the geologic descriptions so that the most likely possibilities may be considered.

In 1981 researchers Hunt and Hearn (Hearn, 1981) presented an initial case study titled "Reservoir Management of the Hartzog Draw Field". This case study is important to this research for two reasons:

1. **The research and analysis of this field ultimately leads to the recognition, identification and definition of the flow unit.**

2. **This case study demonstrates the value of bringing technical expertise together in order to fully interpret a reservoir for maximum understanding.**

The Hartzog Draw Field is located in the Powder River Basin. The field was discovered in 1975 and is twenty-two miles long and varies in width from one to four miles. Within the field, the working interest ownership was held by 85 different operators. In 1977 the Hartzog Draw Operators Committee was formed. The operators were interested in unitizing the field so that secondary or enhanced recovery could be considered as field development progressed. The committee organization formed several producer sub-committees as follows:

- **Technical Committee**
- **Geologic Committee**
- **Formation Evaluation Committee**
- **Fluids and Pressure Committee**
- **Special Studies Committee**

In order to accomplish the unitization objective the process required a complete reservoir analysis. As a result of bringing the various producers together onto the various committees field data and knowledge transfer was maximized. Open communication between the committees was an integral part of the process. The primary objective of the case study was to present the unitization process which included the gathering and processing of all technical field data and required cooperation between the various working interest owners of tracts in the field.

The process presented the opportunity to review actual results with predicted pilot flood results for a field, which received significant technical attention and analysis. The planned pilot called for a 160-acre pilot waterflood. A layered reservoir approach was used as a means of accounting for the varying permeability.

3.7 The Flow Unit

3.7.1 The Hartzog Draw Field

In 1984 researchers Hearn, Ebanks, Tye and Ranganthan published research results for the Hartzog Draw Field titled "Geological factors Influencing Reservoir Performance of the Hartzog Draw Field, Wyoming". Intense data gathering and interpretation had previously occurred. In addition the researchers had the performance results of a pilot waterflood. Nine new wells

drilled as a part of the pilot program were fully cored. The earlier work of breaking the reservoir down into lithology units did not work well. There was significant variability in the reservoir properties of each facies.

The "Flow Unit" concept was introduced. The reservoir was subdivided into different intervals. Flow units were used to determine the distribution of rock types that most strongly controlled behavior as fluids were produced or injected. Hearn, Ebanks and others (1984) defined the flow unit as a reservoir zone that is continuous laterally and vertically, and has similar permeability, porosity, and bedding characteristics.

"The stratigraphic sequence of the facies is based on their occurrence in vertical sections, such as outcrops or cores. This sequence is the framework in which the flow units are defined on the basis of not only their geologic characteristics and position in the vertical sequence but also on their petrophysical properties, especially porosity and permeability. Certain ranges of porosity and permeability that occur in a particular part of the sedimentary sequence are used to subdivide the reservoir along lines that represent gradations in reservoir quality - i.e., the ability of the rocks to transmit fluids, both laterally and vertically" (Hearn, Ebanks and others, 1984).

The flow unit concept provided for a more:

- **quantitative definition and mapping of the parts of the reservoir in terms of reservoir behavior and**

- **realistic building block for reservoir zonation which was beneficial to numerical simulation of the reservoir performance.**

In the case study the researchers analyzed potential variables that resulted in different flow units being identified. These included:

1. **Pore Size Distribution: Pore size distribution was determined on various core samples from mercury injection data. Average pore size distribution curves were generated for each flow unit. The data plots of the saturated pore volume (%) versus radius of pores supported five flow units having different pore networks.**

2. **Bedding: The reservoir in the case study contained different sedimentary structures in different facies of the Shannon sandstone. In three flow units it was determined that the shale laminae did not have significant lateral extent. This lead to the conclusion that the laminae in these units would not impact reservoir continuity between the producer and injector wells. The analysis of the other unit and the lowest section of one of the above units confirmed "more continuous" shale laminae between the thin sandbeds and would therefore impact flood performance.**

3. **Vertical Permeability: Although not useful for flow unit identification in the case study, the authors briefly discussed the value of vertical/horizontal core permeability ratios as a potential tool to identify different flow units.**

4. **Mineral and Pore Geometry: "Pore geometry is a resultant of several different diagenetic, that is, post depositional, physical and chemical processes" (Hearn, 1984). Different facies will contain different proportions of minerals. Diagenetic processes operate differently as the proportions of minerals vary. The authors evaluated the cores in terms of percent of clay, the compaction of ductile grains and the resulting loss of primary porosity due to glauconite, chert, and rock fragments.**

In addition, porosity enhancement resulted from dissolution of portions of the carbonate - primarily the calcite. This resulted in significant changes to the geometry of the pore system. For portions of the reservoir having high percentages of clay (20% versus 3%), the pores were clay lined. This clay, which serves as a cementing agent has reduced the porosity. This portion of the reservoir had very low permeability.

5. Water Saturation: Connate water saturation was found to vary based on rock type and porosity. Reservoir performance is impacted by rock composition and texture.

In the study two wells were drilled on an oil-based mud in order to gain connate saturation data. The various facies were grouped into three general categories. Table 3.1 summarizes the research results.

Table 3.1 Values of Porosity and Water Saturation from Analysis of Wells Cored with Oil-Based Muds (Hearn, 1984)

Rock Type	Flow Units	Porosity %	Water Saturation %
Least Clay Matrix - No Shale Laminae	3,4,5	14-20	5-24
Moderate Clay - Few Laminae	2,3	8-14	15-40
Abundant Clay - Many Laminae Burrows	1	5-11	36-60

Hearn, Ebanks and others (1984), was able to recognize and map five flow units in the pilot area. The basis for the flow units included stratigraphic and petrographic analysis of cores, correlation of logs, and major rock types were determined. The flow

units identified had similar porosity, permeability, bedding characteristics and by their position in the vertical sequence. Each flow unit included stratigraphic units with similar properties for fluid flow.

Although the study lacked specific details it was noted that the identified flow units as a part of the reservoir characterization process resulted in good correlation with injection and production histories in the pilot area.

3.7.2 The Flow Unit Concept and Discussion

In 1987 at the annual convention of the American Association of Petroleum Geologist Ebanks presented an abstract titled "Flow Unit Concept - Integrated Approach to Reservoir Description for Engineering Projects (Ebanks, 1987). The presentation was at a round table session and no complete paper was included as a part of the proceedings. The abstract captures the flow unit concept in a concise manner and is included herein in its entirety:

"The successful application of secondary and tertiary technology requires an accurate understanding of the internal architecture of the reservoir. Engineers have difficulty incorporating geological heterogeneity in their numerical models for simulating reservoir behavior. The concept of flow units has been developed to integrate geological and engineering data into a system for reservoir description.

A flow unit is a volume of the total reservoir rock within which geological and petrophysical properties that affect fluid flow are internally consistent and predictably different from properties of other rock volumes (i.e. flow units). Flow units are defined by

geological properties, such as texture, mineralogy, sedimentary structures, bedding contacts, and the nature of permeability barriers, combined with quantitative petrophysical properties, such as porosity, permeability, capillary, and fluid saturations. Studies in the subsurface and in surface outcrops have shown that flow units do not always coincide with geological lithofacies.

The flow unit approach provides a means of uniquely subdividing reservoirs into volumes that approximate the architecture of a reservoir at a scale consistent with reservoir simulations. Thus reservoir engineers can incorporate critical geological information into a reservoir simulation without greatly increasing the complexity of their models. This approach has advantages over more traditional methods of reservoir zonation whereby model layers are determined on the basis of vertical distributions of permeability and porosity from core analysis and wireline logs."

3.7.3 Comparison of Depositional, Layered and Flow Unit Models – A Case Study

Slatt (1988) developed three types of reservoir description models for the Balmoral field, North Sea. These included the depositional model, layer model and the flow unit model. Slatt determined that the flow unit model provided the most complete reservoir description based on well data due to the flow unit model including a variety of geological and petrophysical properties. The researcher also noted that the model can provide inputs for reservoir simulation work and has value for reservoir development and improved management. Tables 3.2 and 3.3 summarize the properties of the layered versus the flow unit model.

The depositional model was developed via a core analysis of sixteen wells. The detailed core analysis was used to correlate to the

log responses. Other tools used to interpret the environment were isopached stratigraphic intervals and correlations with other similar field examples.

Table 3.2 Properties of the Layered Model (Slatt, 1988)

LAYER	FACIES	AVERAGE POROSITY %	AVERAGE PERMEABILITY (md)
I	Channel Sand	26.4	956
II	Slope Claystone	Low	Low
III	Channel Sand	27.1	1378
IV	Fan Lobe Sand	28.2	593
V	Fan Lobe Channel Sand	28.4	489

Table 3.3 Properties of the Flow Unit Model (Slatt, 1988)

FLOW UNIT	PERM md	Poro-sity %	Md GRAIN SIZE (mm)	Md PORE THRT SIZE (mm)	SATURATION BRINE @ 200 psi (%)	CHARACTER-ISTICS
E	> 1000	23-34	.182-.304	.01-.013	6-12	Large Sand Channel Facies
G	100-1000	20-34	.083-.242	.007	11-24	Massive Sand Channel/ Lobe Facies
Pc	.01-> 1000	4-28	.113-.245	.002	30-37	Massive Sand with Calcite Cement Zones Channel Lobe Facies
Pi	.1-> 1000	7-32	.1-.23	.002	31	Interbedded Sand Mud Channel Lobe Facies
Pm	No k	No k	-	-	-	Clay Mudstone

The researchers followed with a second case study report on the Balmoral field in 1990. Slatt (1990) noted that the flow unit model allowed for the interpretation of many of the geological and

petrophysical properties into the reservoir description. As a result the level of reservoir understanding is increased and the best inputs for simulation models are developed which leads to improved recovery and reservoir management (Slatt, 1990).

The depositional model was useful for identifying regional trends of given facies and providing valuable information regarding sediment transport paths and the depositional environment. However, the model could not be utilized in terms of useful engineering applications.

The layered model was designed to meet three criteria in addition to being utilized to calculate volumetrics of the reservoir. The model was to:

1. **Have a simple design and offer simple layers.**
2. **Layers selected should have a geologic basis.**
3. **The reservoir properties should vary between layers.**
4. **The core plug porosity and permeability data must be used in the model developed.**

The core data utilized included 818 core plugs. It was determined that the various reservoir facies would be used to satisfy condition three. Accordingly a five-layer model was designed that was useful for more accurate reservoir volumetrics. Electric logs include gamma ray-density log, sonic log and resistivity logs. Other logs were not referenced in the case study.

3.7.4 Identifying Flow Units Using Flow Capacity and Storage Capacity as Indicators

Guangming, etal (1993) examined the Endicott Field situated on the North Slope of Alaska. The researchers sought to use core data and well log data as a means to predict permeability and the resulting flow units previously identified in the core wells. Regression analysis between core data and well log data was utilized. The researchers had full interval core data available for every 1/2 foot of the interval for the cored wells. Data included vertical and horizontal permeability and porosity. Digitized log data was compiled in a like manner. Some of the logs utilized in the study included gamma ray density porosity, sonic porosity, and resistivity logs. The figures presented indicate that productive intervals are up to 1,000 feet thick. Core data at 1/2 foot intervals from eleven wells situated across the field were utilized.

The researchers broke the formation down into facies (depositional environment) representing major zones. The major zones were further broken down into sub-zones. The mechanism to determine the flow units considered k- h, ϕ- h, and the ratio of net to gross sand within the sub zones. The researchers utilized three screening methods to differentiate the sub zones:

1. $\frac{\text{(Point Permeability) – (Average Permeability of the Zone)}}{\text{(Average Permeability of the Zone)}}$

2. $\frac{\text{(Shale Content of .5 ft Section) – (Average Shale of the Zone)}}{\text{(Average Shale of the Zone)}}$

3. $\frac{\text{(Porosity of .5 ft Section) – (Average Porosity of the Zone)}}{\text{(Average Porosity of the Zone)}}$

The researchers defined the flow unit as a volume of rock body having similar properties that influence the flow of fluids through it (Guangming, 1993). As a result they proposed to group the sub zones based on their transmissibility, storativity, and net to gross ratio.

Cluster analysis was used to break out the sub zones into four specific flow units. The researchers used a statistical analysis procedure to predict permeability. Observations regarding this research include:

1. **The core database was extensive. Approximately 20,000 data points were available.**

2. **The permeability prediction via the statistical analysis procedure was for all data. It was not specific to unique porosity-permeability relationships within each flow unit.**

3.7.5 The Flow Zone Indicator

Amaefule, Tiab and others (1993) proposed a new method to identify and characterize flow units. The technique developed by Amaefule, Tiab and others is focused at extracting characterization detail at the pore throat level or scale. Further discussion regarding pore throat analysis is included in the reservoir characterization section (Davies). The pore geometry determines the hydraulic quality of the rock. Amaefule, Tiab and others (1993) demonstrated a methodology by which reservoir pore throats are analyzed which results in the ability to identify flow units with similar hydraulic properties.

The researchers developed this new methodology by modifying the Kozeny-Carmen equation. This equation expressed permeability in terms of porosity and specific surface area. Three new terms were defined as a part of the research:

Flow Zone Indicator (FZI) : $1 / ((Sv_{gr})(k_z)^{.5})$

Reservoir Quality Index ($_{um}$) : $.0314 \ (k / \phi_e)^{.5}$

Normalized Porosity Index ($\phi_{z)}$: $\phi_e / (1- \phi_e)$
= effective pore volume to grain volume ratio

Where Sv_{gr} is defined as the specific surface area per unit grain volume, k_z is the Kozeny constant, which reflects grain shape, pore

shape and tortuosity for the flow unit. The FZI value is considered to be constant within a flow unit.

FZI is also defined as:

$$FZI = RQI * \phi_z$$

The derivation from the Kozeny-Carmen equation yields the following logarithmic relationship:

$$\log RQI = \log \phi_z + \log FZI$$

A log-log plot of data from a given flow unit or similar FZI value will be situated on a straight line with a slope of 1.0. The researchers further demonstrated that other flow units will fall on adjacent parallel lines. Each flow unit will have a separate FZI value. The FZI value or indicator will be for a given flow unit having similar pore throat characteristics (Tiab, Donaldson, 1996). Further the value of FZI can be determined from the intercept at $\phi_z = 1.0$. The researchers also presented a permeability prediction equation utilizing the FZI value:

$$k = 1{,}014\ (FZI)^2\ \ (\phi^3_e / \phi^2_e)$$

The flow zone indicator incorporates the geological considerations including flow unit specific pore geometry. As a result, flow unit analysis can occur when complete petrophysical data from the core is available. Lacking geological input and guidance results in statistical techniques being used to identify flow

units. These may include frequency diagrams, error analysis, cluster analysis and normality tests.

Amaefule, Tiab and others (1993) presented summaries of six reservoir cases. The validation of the FZI concept was confirmation work using the scanning electron analysis and pore throat characterization via mercury saturation analysis.

The researchers did not include in the study results specific core plug detail regarding the number of samples or distance between core plug testing points. However, for boundary definition of the flow units core plugs for testing would need to occur at regular intervals through the entire reservoir. In addition for certain reservoirs it seems reasonable to expect transition zones between flow units. This also was not discussed in the research.

Gunter and others (1997) endeavored to develop graphical tools that would determine the number of flow units within the reservoir. This method requires continuous core porosity, permeability and saturation detail for the entire horizon. The researchers considered the flow unit to be a stratigraphically continuous layer of similar reservoir process speed that maintains the geologic framework and characteristics of rock types. The rock type is considered to be reservoir units having distinct porosity-permeability relationships and unique water saturations for the position in the reservoir above the free water level. A given rock

type would be deposited under similar processes and experienced similar diagenetic processes resulting a unique permeability-porosity relationship. The graphical tools determined to be key and utilized by the authors were:

1. Winland Porosity-Permeability Cross Plot

This graphical tool is a semi-log plot of permeability versus porosity. The plot has isopore throat lines, which have been calculated from the Winland equation during a capillary test run at 35% mercury saturation. The Winland equation uses permeability input in md and porosity as a percentage:

$$\text{Log R35} = .732 + .588(k) - .864(\log \phi)$$

2. Stratigraphic Flow Profile

This graphical tool is a plot used to present the flow unit interpretation and includes a correlation log such as a gamma ray, a geologic core description, columns showing porosity, permeability, the R35 value, the permeability/porosity ratio, storage capacity and percent flow capacity. The profile is presented in various columns and is correlated with the selected log.

3. Stratigraphic Modified Lorenz Plot (SMLP)

(SMLP) is a plot of Percentage of Flow Capacity versus Percentage of Storage Capacity. The process is to display the

cumulative percentages in stratigraphic order including each core sample. Points of inflection indicate potentially different flow units. It is important to note that water saturation must be taken into account when calculating the storage capacity. The shape and slope of the plot can provide insight into the reservoir flow characteristics. This information is then tied back to the Stratigraphic Flow Profile for correlation and analysis.

4. Modified Lorenz Plot

The Modified Lorenz Plot is a plot similar to the SMLP plot except the plot is based on the flow units developed prior to this step. The stratigraphic position is maintained.

Gunter and others tested the methodology on a series of reservoirs. After the flow units were identified a reservoir simulator was used for verification. The researchers did not provide any details about the simulator results for the case study reservoirs. The researchers made reference to permeability corrections which were done to take into account the affect of stress and relative permeability data at the given water saturation levels in each reservoir. No details regarding the corrections were included in the case study.

Soto and others (October, 2001) presented a case study predicting permeability using hydraulic flow units and soft

computing systems. This study called for using the soft computing systems for predicting the flow zone indicator (FZI) which is a constant within a given flow unit or hydraulic flow unit.

The authors demonstrated that core permeability could be predicted with a high degree of confidence if the FZI value is known. The focus of the study was then directed at predicting the FZI value. The authors used a correlation model to analyze the various log variables in order to determine which were dominant. The statistical analysis determined that the gamma ray, deep resistivity and effective porosity measurements were required to generate a trustworthy model, which could predict the log of FZI.

The next step called for the application of an adaptive network based fuzzy inference system (ANFIS). The fuzzy logic toolbox from MATLAB was used. The model output was then compared to actual FZI values from core well data. The resulting R^2 value for the log-log plot of FZI core versus FZI ANFIS model was .88.

After the FZI is calculated the permeability is predicted using the equation for permeability prediction drawn from the previously presented work of Amaefule, Tiab, and others. Using the predicted permeability and FZI, the flow zones can be determined.

The authors utilized 412 core plug data points in the sample case. The log suites ran on the wells included resistivity, gamma ray as well as some additional specialized gamma ray logs such as

gamma ray spectrometry measurement. Specific log information is not provided in the study. However, based on the results presented significant log information was available for this study.

CHAPTER 4

ARTIFICIAL NEURAL NETWORKS

4.1 Overview

Artificial Neural Networks (ANN) are designed to mimic the biological brain in terms of pattern recognition and the learning process. Researchers have hypothesized that millions of neurons in the brain work together in parallel, each trying to solve the given problem at hand. Artificial Neural Networks are information process systems that are a rough approximation and a simplified simulation of the biological process and have performance characteristics similar to those of biological neural networks (Mohaghegh, 2000).

ANNs work very well at solving problems when it is difficult to propose exact mathematical models. Mohaghegh and others (1994) noted pattern recognition as one of the neural network's strengths. Artificial neural networks learn the nature of the dependency between input and output variables. Learning is based on pattern recognition. The network classifies new patterns and predicts an output based on the learned patterns. Neural networks often have application when relationships of parameters are too complicated or require too much time to solve via conventional methods.

There are two types of neural networks - supervised and unsupervised. Supervised networks classify patterns and make decisions based on the patterns of inputs and outputs they have

learned. In other words during learning the output is provided as a means of training the network. Providing correct answers is an integral part of the learning/training process. Backpropagation is a common supervised network type.

The unsupervised network classifies a set of training data into a specified number of categories. The network will classify the data into the number of categories specified by the modeler. The Kohonen network is one of the most common unsupervised networks. The Kohonen network has a simple architecture of one layer of input and output. As with all unsupervised networks, the Kohonen network is provided the input data and learns without being shown the correct output for the input data. The Kohonen network is useful for separating data into a specified number of categories.

4.2 The Neuron

The neuron is the primary element of the ANN. The purpose of the neuron is to receive an input(s) and generate output(s) or simply stated to execute a given task. The neuron processes the information received by applying a mathematical activation function to the input thus producing an output signal. As illustrated by Figure 4.0 a typical ANN has three layers of neurons (input, middle or hidden, and output layer). Each “layer of neurons” is connected to the next neuron layer. As a result, the output of the first layer

becomes the input for the next layer. The neuron output is "weighted" by the model in order to produce results that are close to the correct outputs in the training set. The mathematical function described above occurs in the middle layer. The ANN learns by repeatedly adjusting the weighting of the neuron outputs until the results produced are similar to the correct outputs in the training set. A useful ANN must be able to predict an output with good results for data not previously seen by the network.

4.3 The Backpropagation Model

Soto and others, (2001) noted that most artificial neural networks use multi-layer backpropagation architecture to apply knowledge gained from training experiences, which allows the network to make new decisions, classifications, and predictions. Often referred to as supervised training or a supervised network, the back propagation models are trained using the nodes, which reflect the input and target variables. The connections between inputs and outputs are hidden layers (the neurons).

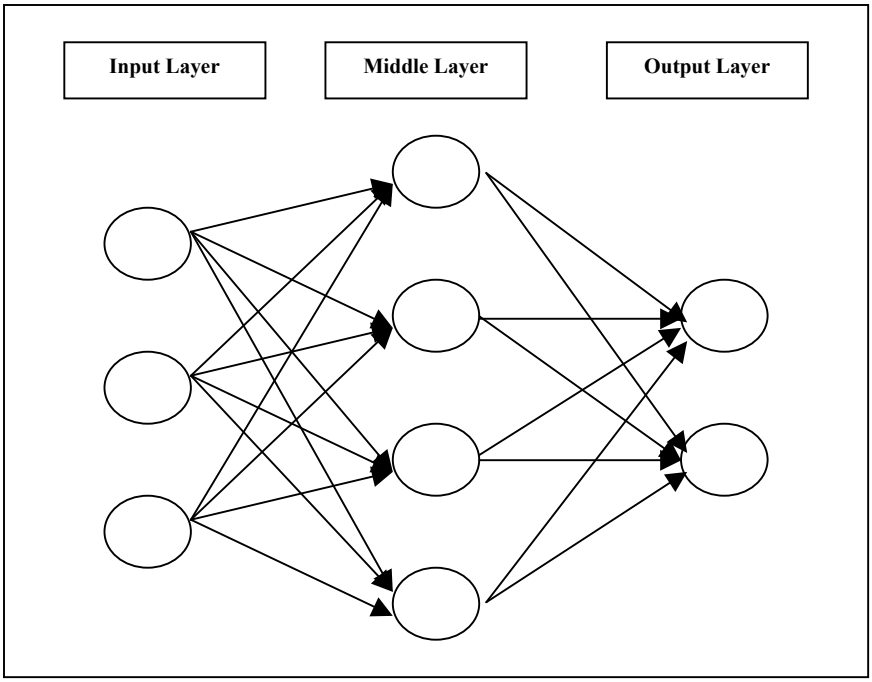

Figure 4.0 A Simplified Neural Network

At each neuron the input is composed of the weighted outputs of the previous layer. As a result of the non-linear weighting the neural network can handle very complex problems. The weighting of the inputs by the model is determined during the testing and training phase. The model-building phase continues until the error during the testing phase is minimized - or the model is optimized.

The backpropagation network compares the known output to the model prediction. The models are trained using the user selected inputs and the known outputs. The difference between the known and predicted output is propagated back through the network. The network adjusts the weighting of each neuron

connection and learning continues until an acceptable level of error is reached. More complex neural networks can also be built that have multiple outputs as opposed to single outputs.

The database to be introduced to the neural network is broken down into three groups (training, test, verification). The training set is used to train and create the network. The actual output of the training set data is used to develop weighting of the neurons in the network. During training, as a part of the learning process, at established intervals (epoch), the test set is used as a means of testing the network. The test patterns are used to determine how well the network is working. Training continues as long as the computed output error between the actual and predicted outputs of the test set is decreasing. The weighting of the neurons is adjusted and utilizing the training set data, learning continues. In other words, training continues until the best test set output results is obtained. In summary, the final ANN is identified as the network producing of the lowest amount of error between the predicted and actual output and is based on the best test set performance.

Typically approximately 80% of the data is used for testing and training. The other 20% of the data is categorized as verification data or the production set. This real data is not used during testing and training. The verification data has not been seen by the network. This data set is used as a test to determine if the newly built network

can accurately predict output results. The predicted output results are compared to the actual output results.

4.4 The NeuroShell Program

During this research a commercially available ANN program was utilized. The NeuroShell 2 program, a product of the Ward Systems Group, was used for this research. The program automatically defaults to backpropagation architecture. It includes multiple hidden slabs with different activation functions. The program offers the user the option to select other architectures. However, earlier researchers working with similar data found that the back propagation architecture selected by the program created the best prediction model.

The NeuroShell program offers a set of statistical tools to assist in model building and analysis. They include linear and multiple correlation tools. The linear correlation (r) measures the strength of the linear relationship between paired values of x and y in a given sample. Karl Pearson developed the linear correlation coefficient. Also referred to as the Pearson product moment correlation coefficient, this tool is also an important statistical tool in most popular spreadsheet programs such as Microsoft Excel. The linear correlation coefficient (r) is defined by the following formula:

$$r = \frac{n\sum xy - \left(\sum x\right)\left(\sum y\right)}{\sqrt{\left[n\sum x^2 - \left(\sum x\right)^2\right]\left[n\sum y^2 - \left(\sum y\right)^2\right]}}$$

The value for r is between –1.0 and 1.0. When r approaches zero there is no significant linear correlation between x and y or as r approaches –1.0 or 1.0 this indicates significant correlation between x and y. A negative value for r indicates that the x – y relationship has a negative correlation. The computed value for r measures the strength of the linear relationship. If the relationship is not linear this coefficient should not be applied.

The linear relationship can be defined by a straight line equation which best describes the regression line. The commonly used equation describes the relationship between the two variables (x and y) and is referred to as the regression line, line of best fit or least squares line. The general formula for the regression equation is:

$$y = b + mx$$

Although the regression equation is not a part of the NeuroShell program, the linear correlation (r) describes the strength of the linear relationship defined by the regression equation. The regression line, which best fits the data, is determined via the least squares method. When using the regression equation to predict y it

is always recommended to limit the application inside the data set area. The regression line and associated equation are readily available in commercial spreadsheet programs.

The NeuroShell statistical package also includes the coefficient of determination. This value describes the amount of variance in y that is explained by the regression line. It is computed utilizing the linear correlation coefficient (r):

$$r^2 = (\text{explained variance}) \ / \ (\text{total variance})$$

The coefficient of determination (r^2) is useful to consider the portion of variance which is explained by the regression line. As an example, if r^2 = .75 then 75% of the total variance is explained by the regression line. Accordingly 25% of the total variation in y remains unexplained.

The coefficient of determination is used regularly during neural network analysis work. It is often used to compare various model results. During model building and the analysis process it is also important to view the actual versus model predicted output graphically. A visual sense of the results in conjunction with statistical analysis is a more useful approach as opposed to solely relying upon the statistical output.

Multiple regression is a means to express a linear relationship between an independent variable y and two or more independent variables (x_1,x_2,….x_n) (Triola, 1998). The coefficient of multiple determination (R^2) is a measure of how well the multiple regression equation fits the sample data. It is defined as follows:

$$R^2 = \frac{\sum (y - \hat{y})^2}{\sum (y - \bar{y})^2}$$

When the value of R^2 value is near 1.0 this indicates a good fit. A very poor fit would be near 0.0 and a perfect fit would be 1.0. Triola (1998) noted that the coefficient of multiple determination increases as more variables are added included. As a result the highest R^2 is achieved by including all possible or available variables. The NeuroShell program includes this statistical program as an option. However, most of the model analysis used during this research has been related to comparing predicted model output to actual output, a linear relationship.

Another feature of the NeuroShell program is the contribution factor detail. The input variables have a different weighting or importance in the model developed. The program allows the modeler to view the contribution factor; a measure of the importance of each variable or input in predicting the output of the network. This option is only used for backpropagation networks. The

contribution factors are developed from an analysis of the weighting of the trained neural networks.

The NeuroShell program also offers the option to run the Kohonen network. The Kohonen is a self-organizing map network. Unlike the supervised network, which includes the backpropagation model, unsupervised networks do not compare actual and predicted output. The Kohonen network learns from the input data provided and categorizes the data into the number of sets defined by the modeler. This application has use when the data has different characteristics or properties. The network can also interpret observations having properties similar to more than one group. As a result such observations would be identified as a category between the two other categories.

4.5 Neural Network Core and Log Data Inputs

For the Jacksonburg-Stringtown field core data was available from eight wells. One core well was situated on the edge of the field and was excluded from the study. A second excluded well was cored however; core recovery was not successful. The six remaining wells had varying amounts of core data. For the thicker sections of sand a core plug was secured every foot. In some instances sections were skipped due to shale breaks or low permeability sections and core plugs were taken as determined by the geologist. No standardized approach appeared to have been used.

In order to identify the artificial neural network best able to predict a given output, it is necessary to try various inputs. The inputs tested during modeling primarily included digitized based log data. The wells in the field commonly had a gamma ray-density porosity log ran on them at the time of completion. Inputs considered included:

- **Gamma ray log value**
- **Bulk density measurement**
- **Base line value from the gamma ray log**
- **Base line value from the density log**
- **First derivative of the gamma ray log**
- **Second derivative of the gamma ray log**
- **First derivative of the bulk density log**
- **Second derivative of the bulk density log**
- **x value of the well location coordinates**
- **y value of the well location coordinates**
- **Core depths**
- **Volume of shale based on the gamma ray**
- **Gross thickness of various lithologic units**
- **Net thickness of various lithologic units**
- **Flow units**

Outputs considered included:

- **Predicted Permeability**
- **Predicted Flow Units**

Chapters 2.0 and 5.0 can be referenced for additional field background information.

CHAPTER 5

METHODOLOGY

5.1 Introductory Discussion

The main objective of this research was to develop a reservoir characterization methodology for flow unit identification using only electric log data. As a part of the methodology, preliminary flow unit identification is required using limited core and electric log data. By identifying the flow units within the reservoir, an improved method of permeability prediction is developed. The primary tool used for this research was Artificial Neural Network analysis (ANN).

To predict the reservoir flow units, the ANN backpropagation modeling required a two-step approach. Tedious preliminary work was directed at identifying the flow units in the reservoir. This required searching out and identifying the unique permeability-porosity relationships within each flow unit present. Identifying the flow units can require an interpretation of the geology, depositional environment and lithology. This type of geologic support can often guide the flow unit identification process. This process utilized actual core results of permeability-porosity for selected wells in the field and the associated gamma ray-density logs. The initial ANN model developed had permeability as the output.

After the ANN permeability model developed, the objective was to enhance the permeability prediction by identifying flow units and incorporating them into the model as an input. By identifying unique permeability-porosity relationships within each flow unit, the ANN model for predicting permeability improved. The key and essential research step was to develop an ANN for flow unit prediction within the field. This required training the ANN by using the previously identified core well flow units from the initial flow unit identification study. ANN training for flow unit prediction using only log data was possible by utilizing the flow units identified in the wells with core data.

In order to confirm the methodology is valid, a verification step was necessary. Verification of the procedure was done via utilizing a study field with far more complete records than what is typically available in the Appalachian Basin. The verification step required the utilization of the flow units identified and the permeability predictions as inputs for simulation work. The goal was to match predicted production results against actual.

This chapter presents the major steps utilized. This includes discussion of the techniques used to identify the flow units, the application of artificial neural network analysis for flow unit prediction, ANN models for permeability prediction within each

identified flow unit and the verification phase as a method to confirm the methodology.

5.2 Determining the Flow Units

5.2.1 Overview

Several methods were evaluated and tested as potential tools to assist in identifying flow units, when limited data about the reservoir is available. These methods have application for flow unit application in any reservoir. The Jacksonburg-Stringtown field was selected for this research due to excellent records retention. Previously discussed in the literature review chapters, the methods found to have application are summarized in the following sections. This methodology is designed for reservoir evaluation when good records retention is lacking or reservoir characterization data is absent. Due to the lack of typical data, flow unit identification utilizing these methods should be done in a comprehensive manner utilizing all of the methods discussed. Individually no single method identified herein should be relied upon for flow unit identification.

An essential part of this methodology is the flow identification phase. During this phase preliminary flow units are identified for the core well data. The techniques utilized are discussed in sections 5.2.2 through 5.2.7. Final flow unit designations are developed during the ANN modeling phase for permeability prediction

discussed in section 5.3. Figure 5.1 presents an overview of the initial flow identification methodology.

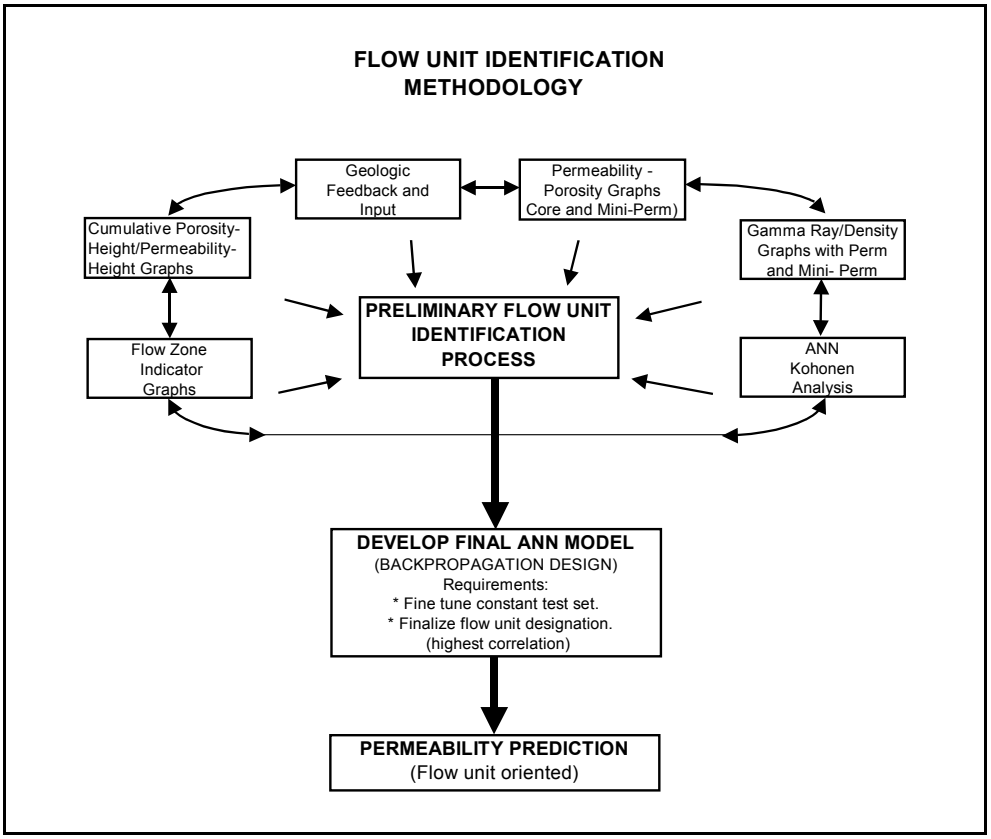

Figure 5.1 Flow Unit Identification Methodology

5.2.2 Manual Review of the Digitized Log Data

During the interpretive steps - as the flow unit identification process proceeds, it is important to routinely review and become most familiar with the log data. Graphing the digitized gamma ray-density log values along with permeability against depth for each well proved to be a valuable analytical tool. The researcher may be able to begin to develop a sense of potential flow unit breaks that can guide the research. The lack of other data related to the cored

interval, such as thin section and grain size analysis, places greater reliance upon the correlation between the methods outlined. Becoming intimately familiar with each well log characteristic proved to be very useful to the research progress. Appendix A. presents the log information for each well log with permeability measurements in graphic and table form. The operator tested a few core data points outside the sand intervals. These are not included in Appendix A. The permeability values include core permeability and minipermeameter values. The Horner # 11 does not have miniperm values due to the core no longer being available.

5.2.3 Cumulative Porosity-Height vs Cumulative Permeability-Height

An initial well screening tool utilized a graph of cumulative storage capacity (ϕ - h) versus cumulative flow capacity (k – h). Changes in the slope of the data, referred to as deflection points, are potential indicators of flow unit boundaries. In addition, this method can be helpful in identifying flow units having high or low flow capacity and/or storage capacity. This can be helpful during the simulation phase of reservoir modeling. The data for each core well was tabulated, plotted on an individual well basis and potential boundaries identified (Appendix B). The distance between core points varies. For some core wells, the operator did core analysis

for each foot of a selected section of sand. In other wells, there could be up to four feet between certain core points. Therefore, potential flow unit boundaries can be narrowed down to the interval between the two core points. The exact location or depth is more difficult to pinpoint using this method when data gaps exist.

In a similar manner, a second series of cumulative storage capacity versus cumulative flow capacity graphs were developed based on the minipermeameter measurements. For this analysis only five cores were available. The minipermeameter measurements were secured from the cores several years after the actual coring operation. The porosity values were taken from the log data. The data for each minipermeameter measurement of the well cores were tabulated and each well graphed and potential boundaries identified (Appendix C). These results were compared to those of the actual cores in Appendix B.

5.2.4 Semi-Log Graph of Permeability versus Porosity

The semi-log scatter graph of core permeability versus core porosity has been commonly used in industry. The correlation of permeability-porosity data within a given flow unit is generally much greater than the total core data correlation when multiple flow units are included. The procedure used in this analysis was a trial and error approach searching out flow unit breaks for each well that

offered the highest correlation of data within each flow unit for all six wells. In other words, one or two flow units were identified for each well. The highest correlation within each flow unit for all six wells was the ultimate objective of this graphing technique. The initial analysis was completed based on the individual scatter plot for a given well along with the earlier discussed cumulative plots of storage versus flow capacity, log graphs and geologic input. In some instances the lack of several core data points within a given flow unit limited the ability to develop a high correlation within a flow unit or identify the flow unit boundaries. Appendix D. can be referenced for the scatter plots for each well and the composite plots of the flow units for all six wells.

5.2.5 FZI Analysis

The flow zone indicator (FZI) was used in conjunction with the semi-log graph of permeability versus porosity. The typical procedure required both plots to be done at each break point selected. The correlations of the entire data and the intervals broken down were compared. This was done on an individual well basis for each core well. Both of these graphing techniques were done based on the permeability and porosity values obtained from the Core Lab's report. The log porosity values and permeability were also analyzed. However, the overall correlations were enhanced when the

core porosity was utilized. The FZI values tabulated for each core well and FZI scatter plots are presented in Appendix E.

5.2.6 ANN Kohonen Self Organizing Map

Artificial neural network analysis included Kohonen networks or "unsupervised" training. The objective was to utilize the Kohonen method to categorize the log and core data as a tool for flow unit identification.

The ANN was provided with selected log inputs and core permeability for each core well. The inputs for the ANN were gamma ray, density, gamma ray slope, density slope, gamma ray baseline, density baseline and core permeability. Three ANN models were run separating the data into two, three and four categories or groups. The option selected within the program called for a "normalized" approach meaning the winning neuron output was designated to have the highest value. The second option utilized designated the winning cluster as one and all others as zero. As opposed to generating the actual neuron value within each category, the normalized approach coupled with the whole number assigned to the category was designed to more clearly identify potential flow units. Simply put, given log input and permeability data from the core results; could the data set be dissected into categories that represented flow units?

Certain wells exhibited a transition zone between the two flow units. In these zones the data appears to represent a mixture of the characteristics unique to each flow unit. This mixture would be reflective of a heterogeneous reservoir. For these transition points the data point is categorized based on the prevailing category identified. Categorizing data using the ANN was another identification and verification tool for determining the number of flow units present. Appendix F. presents the data inputs and the ANN outputs of the various ANN outputs. Two phases of ANN Kohonen analysis occurred during the research. Initial analysis was done using all core data. No screening of the data had yet occurred. Certain core points would later be disqualified - typically due to not being a part of the flow units identified. More refined confirmation ANN Kohonen analysis was done on the final ANN.

5.2.7 Geologic Input

Flow units can be independent of changes in lithology or depositional environment. As an example, diagenetic structure can impact flow unit designation. However, in many cases the flow units will correspond to variation in the lithology or depositional environment. An integral part of flow unit identification is to incorporate geologic understanding of the depositional environment into the analysis. For this research the participating geologists of

the Appalachian Oil and Natural Gas Research Consortium proved invaluable. Geologic input assisted the flow unit identification process as well as the simulation phase.

5.3 Developing the Final ANN Permeability Model

5.3.1 Utilizing the Preliminary Flow Unit

As can be seen in Figure 5.1 it is necessary to finalize the ANN model for permeability prediction after developing preliminary flow unit designations using the various techniques. The ANN for permeability prediction is developed using the core data from six core wells and the associated log based data (from gamma ray-density logs).

5.3.2 Initial Flow Unit Designation

Drawing from the preliminary flow unit identification process, flow units for each core well was selected. These initial flow unit selections were designated as the initial flow unit input in the backpropagation model for permeability prediction.

5.3.3 Developing the ANN Model for Permeability Prediction

The permeability model inputs were selected based on developing the highest correlation between predicted and actual

core permeability. The ANN for permeability prediction was developed using the core data from six wells. Several log-based inputs were tested. Possible inputs were discussed in chapter three. Ultimately six log-based inputs were found to develop the highest R squared values between predicted versus actual permeability. The log-based inputs are listed in section 5.2.6. It was found that the addition of the flow unit significantly strengthened the ANN model for permeability prediction.

5.3.4 Permeability Prediction Utilizing the Neural Network

Two artificial neural network models were ultimately developed for permeability prediction. In both models a backpropagation network was trained to predict permeability. Several inputs were utilized during testing in order to determine the best inputs for modeling. Model improvement was determined by comparing predicted output to actual permeability. Both final permeability output models required seven inputs. The digitized gamma ray and density electric log values were used to generate ANN inputs (digitized log values, their first derivative values, base lines). This accounted for six inputs.

The permeability prediction was improved when the flow unit designation was added to the ANN as the seventh input. In order to develop the strongest permeability prediction model various flow

unit designations were tested. Flow unit designations between flow unit boundaries and the beginning or ending points of flow units were varied on a per well basis in order to develop the strongest model. A single core data point that moves from one flow unit to the other impacts the resulting ANN model. Core data between the flow units were moved back and forth in order to improve the model and finalize the flow units in each well.

Two ANN permeability prediction models were developed. The significant model difference was in the cut-off points of the core data. The cut-off points determine the beginning of flow unit one or the end of flow unit two. The "Model 1-K" permeability model provides for a tighter definition of the flow units. Core data at the upper and lower most portions of the reservoir were removed when the porosity and permeability values were more typical of shale. The excluded core data points fell outside of either flow unit. As a result model 1-K is built using fewer core data points. The points excluded were largely determined by ANN results during the permeability model building stage.

"Model 2-K" permeability model includes nearly all of core data points. The research identifies two productive flow units and a third potential non-productive flow unit. Model 2-K was primarily developed to incorporate a lower permeability-porosity sand below the recognized flow unit two sand. The prediction accuracy for flow

unit one improves when additional core data below flow unit two was included in the model. The ANN results of model 2-K suggest the lower sand has properties similar to the above flow unit one and the model is strengthened. For the purposes of model building, model 2-K expands the boundaries of the flow unit. For this research the model 2-K was ultimately used. Model selection is further discussed in chapter six as results are presented. The final permeability model can be utilized to predict permeability for wells in the field when log based data and flow unit designations are known. The flow unit designation is an essential input in the model for permeability prediction. The flow unit designation is required in order to utilize either ANN permeability model.

5.3.5 Utilizing the Predetermined Test Set

During ANN modeling the six core wells were regularly used. The total number of core data points used was 95. The initial standard procedure was to designate one of the six wells as the verification or production well. The verification well is excluded from testing and training of the network. As a result the verification well contains data points not previously seen by the model. The other five wells were used for testing and training. Typically analysis of the model was based on how well the new model predicted permeability as compared to actual results.

The model developed has a given set of selected inputs. Using the same inputs, an ANN model is built - each time setting aside a different core well as the verification well. This means each ANN model developed does vary - as a result of being built with different sets of data. The testing, training and verification sets are different. When six core wells are used there are six different ANN models generated as each well is set aside for the verification step. The predictive strength of the ANN model is based on the data set used for test and training. If the verification well is unique or has characteristics not previously encountered during modeling, the predicted output when compared to actual results, may not be satisfactory.

The problem becomes more acute as the data set varies and unique inputs of the verification well are not included in the ANN model. The properties of each core well vary in terms of log response and core data. This is likely reflects the heterogeneity of the reservoir. It can become very difficult to determine which set of inputs build the strongest model due to having six R squared values as each verification well is set aside.

A unique approach utilized in this research has been to identify the "best test" set. The test set is held constant for the data set regardless of which well is selected as the verification well. A given set of test data is designated and applied to all of the wells.

Regardless each which well is used for verification, the same set of test data is used. Identifying the "best" constant test set requires judgment and patience by the modeler.

The objective is to pre-determine the test set which "best" reflects the characteristics of the total data set (Oyerokun, 2002). The same predetermined test set was utilized for the verification well. This approach proved to be productive in terms of analysis and identifying the best model for prediction.

5.4 Flow Unit Identification - Without Core Data

5.4.1 Discussion

The flow unit identification methodology presented in Figure 5.1 is developed utilizing the core well data. Core permeability and porosity values were available for 95 core points in six wells. The permeability and porosity data allowed the flow unit identification process to advance.

The ANN model for permeability prediction can be applied to approximately 125 wells in the field having digitized log data. A required input of the ANN model is flow unit designation. A very key issue is how to predict flow units from digitized log data when permeability values are not available. The next phase of this methodology is developed in order to address this critical issue.

Figure 5.2 presents a flow chart of the overall methodology which details the flow unit ANN building phase.

5.4.2 Flow Unit Prediction Utilizing the Neural Network

Generating a prediction of the flow unit is a prerequisite in order to utilize model 2-K for permeability prediction. An ANN for flow unit prediction can be developed by utilizing the core data and the flow units which were identified as a part of the initial permeability ANN work. Two flow unit models were developed which drew from the earlier work. In both instances the models used the flow units previously identified and discussed in section 5.3.

The "Model 2-FU" flow unit model used the same data as the previous model 2-K permeability model. Model 2-FU does not include permeability - only the six log based parameters. The output for model 2-FU is the flow unit (one or two) designation. Model 2-FU uses the log data at points where core data was available (points where permeability was measured). The predetermined test set remained the same for both model 2-K and model 2-FU (permeability and flow unit output).

The approach to develop a second ANN model for flow unit prediction was different. The preliminary flow unit screening methods and ANN model 2-K identified the flow units in the six core wells. The digitized log data was available for each core well. The

digitized log data was available on a .25 ft interval for each well. "Model 3-FU", a second model for flow unit prediction was built using the digitized log data for each core well. This ANN has significantly more data points for testing and training (306 versus 95).

5.4.3 Transition Zone near Flow Unit Boundaries

In a few core wells Kohonen analysis and back propagation modeling identified portions of the core data as having properties of both flow units. This was observed at the core data points near the boundaries of the flow units and is considered a transition section area of the reservoir. The ANN could not predict the flow unit within the transition area. As a result without a properly predicted flow unit the final permeability prediction within a transition zone could be in error. The limited core data in this transition zone does not offer the opportunity to train the network to predict permeability within this area of the reservoir. In order to be able to predict flow unit one or two on the digitized log files a methodology on how to predict flow units in the transition zone was required.

5.4.4 Predicting Permeability in the Transition Zone

The transition zone has varying porosity and permeability. Some higher permeability sections exist within the zone. However,

based on the known core permeability-porosity measurements in the transition zone, permeability is expected to be similar to flow unit one. In addition, the core results indicate low permeability shale streaks as a part of this zone. This limits any impact portions of higher permeability sand would have in this zone.

The transition zone requires the application of an intermediate ANN flow prediction model. Model 3-FU (digitized log data), the flow unit prediction model, was modified in order to recognize the transition zone. "Model 4-FU", an intermediate flow unit model is developed. The intent is to train the model to recognize the transition zone and assign the zone a separate flow unit value. By identifying the zone the modeler can then categorize the transition zone as flow unit one prior to using the predicted flow units in the permeability model. Changes are as follows to model 3-FU:

- Flow unit designation as one remains one.
- Transition zone to be designated as flow unit two.
- Flow unit two to be designated as flow unit three.
- Lower flow unit one remains flow unit one.

Model 4-FU was run on the core well digitized log data having the same six log based inputs as model 3-FU. The output was flow unit. During model testing and training, the same constant test set was used. It is necessary to designate flow units as described above

for the six digitized core wells. Flow units are an input in this model. The transition zone was identified using Kohonen analysis, the ANN permeability model and model 3-FU, for flow unit prediction, using the six log based inputs. The intermediate model 4-K successfully predicted the flow units in the transition zone.

5.4.5 Reclassifying the Predicted Flow Units for the ANN Permeability Model

The flow unit output from model 4-K was manually reclassified in order to utilize the predicted flow units in model 3-K, the permeability model. Flow unit reclassifications occurred as follows:

- Flow unit one remains flow unit one.
- Flow unit two (trans area) is classified as flow unit one.
- Flow unit three (initial two) is classified as flow unit two.
- Lower flow unit one remains flow unit one.

With the flow units reclassified, the ANN permeability prediction model could be applied to the digitized well logs in the field (approximately 125 wells). Within the transition zone the ANN permeability prediction model will predict permeability based on the (flow unit one and the transition zone) being categorized as flow unit one.

5.4.6 Model Description Summary

Model 1-K:	**ANN for permeability prediction. Has tight definition for each flow unit. Core data at upper and lower most portion of the reservoir excluded (low porosity/ permeability). Two flow units and six log based inputs used.**
Model 2-K:	**ANN for permeability prediction. Includes all applicable core data (95 core data points). Two flow units and six log based inputs used. Model selected as ANN for permeability prediction.**
Model 2-FU:	**ANN for flow unit prediction. Used the same core data points as model 2-K. Has six log based inputs. ANN developed from 95 core data points. Model 2-K was used for flow unit designation.**
Model 3-FU:	**ANN for flow unit prediction. Used 306 data points from the core well digitized well log data. Assigned flow units based on flow units designated in model 2-K.**
Model 4-FU:	**ANN for flow unit prediction. Used 306 data points from the core well digitized well log data. Intermediate ANN for identifying the transition zone.**

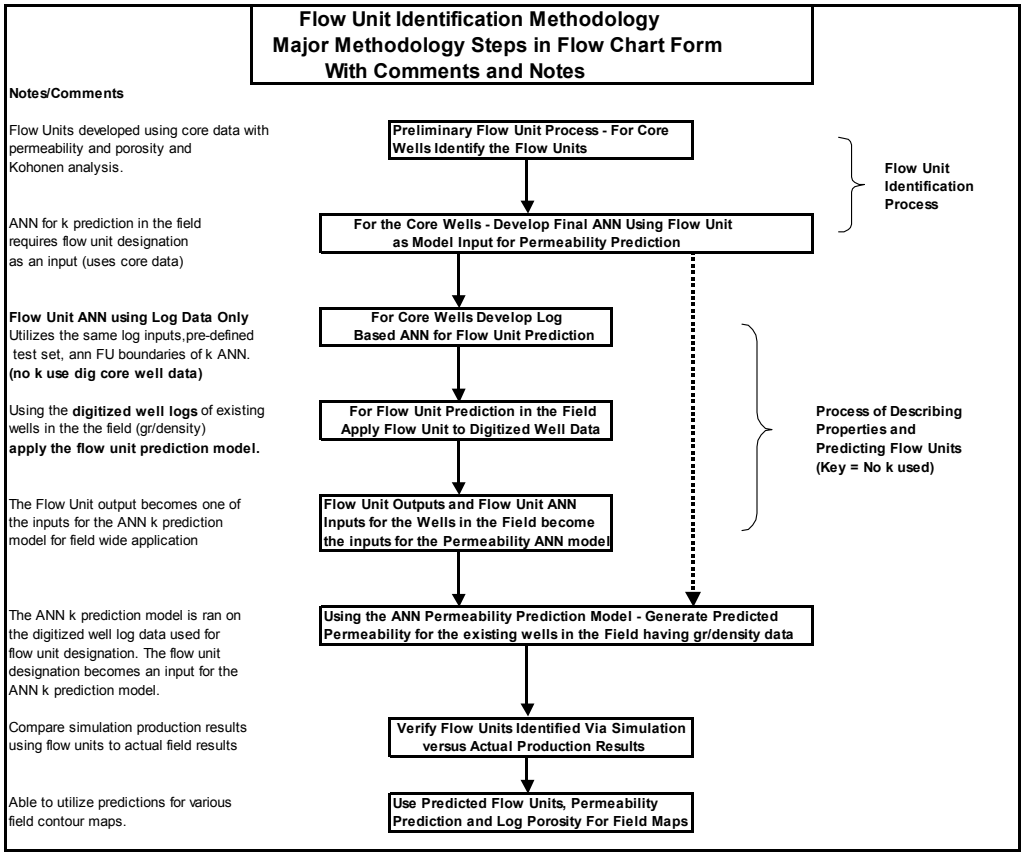

Figure 5.2 Flow Unit Identification Methodology Major Methodology Steps in Flow Chart Form with Comments and Notes

5.5 Earlier Verification Work

Gil (2000) previously researched the dual five spot pilot waterflood situated south of the current area of interest in the same field. The author demonstrated that simulated production prediction was enhanced when the producing sand was broken down into two flow units. Gil selected the flow units based strictly on porosity and permeability variation and enhanced simulation results. None of the techniques investigated herein for flow unit identification were utilized. This previous research did not include the flow unit

designation as an input for ANN modeling. However, the flow units identified and used by Gil in his simulation analysis support these research results. Accordingly, Gil's earlier work in the same field serves as a second verification of the flow units identified.

5.6 Verification Field

5.6.1 Study Area

Figure 5.3 presents the Jacksonburg-Stringtown field and highlights the core well locations within the field. Two of the original core wells were a part of the two five spot patterns included in the original pilot program. The area of interest for this research is situated north of the pilot flood patterns.

5.6.2 Core Wells Utilized in the Research

During field development a total of nine wells were cored. Three core wells were not utilized in the research. Core data could not be located for the D-14. The L-17 did not have any electric log data available. The R-13 was excluded due to the cored section taken being above the sandstone and the well being located outside of the main field area. These three wells were therefore not useful in the research.

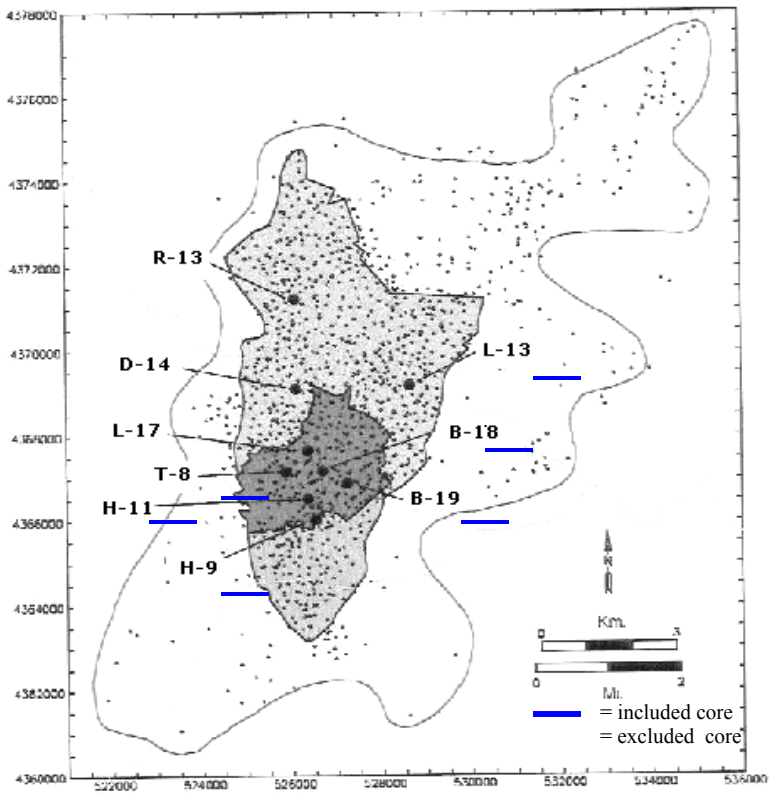

Figure 5.3 Cored Well Locations within the Jacksonburg-Stringtown Field

Six core wells within the verification field were utilized in the research. At the time of drilling, selected portions of the cored sections (core plugs) were directed to Core Laboratories, Inc. for porosity and permeability measurement analysis. In addition, relative permeability analysis was also completed on a few selected core plugs. Five of the cored sections were maintained in storage until recent research commenced. The H-11 cored section was not located for further analysis. However, the Core Laboratory report of porosity and permeability for H-11 (Horner # 11) was available.

Table 5.1 summarizes the core wells and the associated core analysis results.

Table 5.1 Summary of Jacksonburg-Stringtown Research Cores (Gil, 2000)

Well	Cored Interval, ft	Avg. porosity, %	Permeability averages, md	
			Arithmetic	Geometric
B-18	2988.5 – 3014	14.7	52	2.7
B-19	3086 – 3115	14.9	41	6.2
H-9	2980 – 2908	18.2	106	57
H-11	3083.4 – 3093.4	18.8	72	19
T-8	2781 – 2797	12.4	6.5	0.75
L-13	3032.4 – 3061.5	8.4	2.5	0.2

The gamma ray-density electric logs from each core well were digitized on a 1/4 foot basis. In a few isolated instances other types of logs were available for a given well. During the waterflood field development phase, the logging suite was typically limited to the gamma ray-density log. As a result this log is considered universal in the field.

As a part of the Department of Energy Grant (DE-AC26-98BC15104) geologists participating in the West Virginia University Research Corporation performed minipermeameter measurements at 1/4 foot intervals on the five cored sections. The TEMCO MP-401

was the model used in the study. Results as compared to the core plug measurements varied significantly. Typically when the permeability was greater than 10md the minipermeameter measurements were less than the core plug values. Appendix A. details the Core Laboratory results, minipermeameter and well log measurements for the core wells used in the study.

5.6.3 Two Five Spots Selected for Verification

The verification field includes approximately 9,000 acres of reservoir under waterflood operations. Two verfication five spot patterns were selected (Ball # 18, Ball # 21). The selection was based on:

- Prolific primary production in the section of the field selected.
- Electric logs were available on all pattern wells.
- Two cored wells exist in the patterns selected.
- The pay section appears to vary laterally across the patterns selected. Figure 5.4 is an east-west cross section of well logs and shows the stratigraphic units in the formation.
- Complete production records were available for each well.

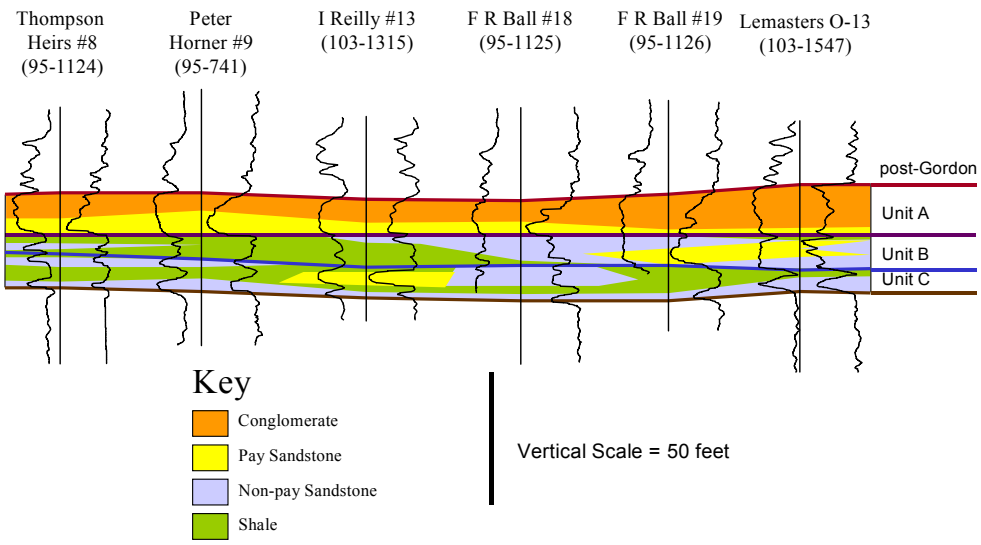

Correlation of wireline logs for cored wells. Logs are ordered roughly from east to west. Gamma Ray is on the left, Density is on the right. There is no horizontal scale for this diagram. Datum is base of Unit A. Supplemental markers are the base of the post-Gordon and the base of Unit C.

Figure 5.4 East-West Cross Section Shows Logs and Stratigraphic Units

Figures 5.5 and 5.6 present the general area of interest within the field as well as a more detailed map showing the specific patterns selected.

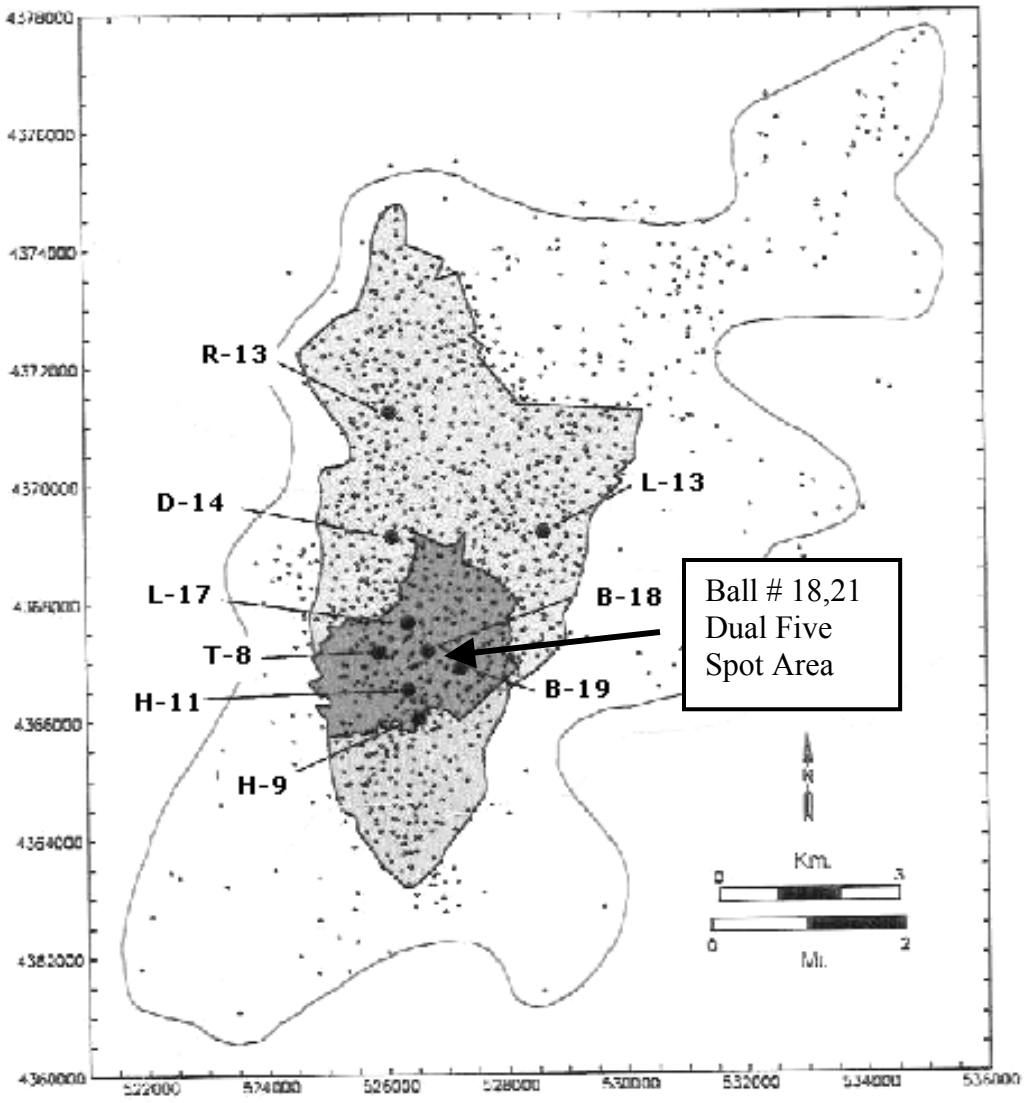

Figure 5.5 Jacksonburg -Stringtown Field Showing Verification Area

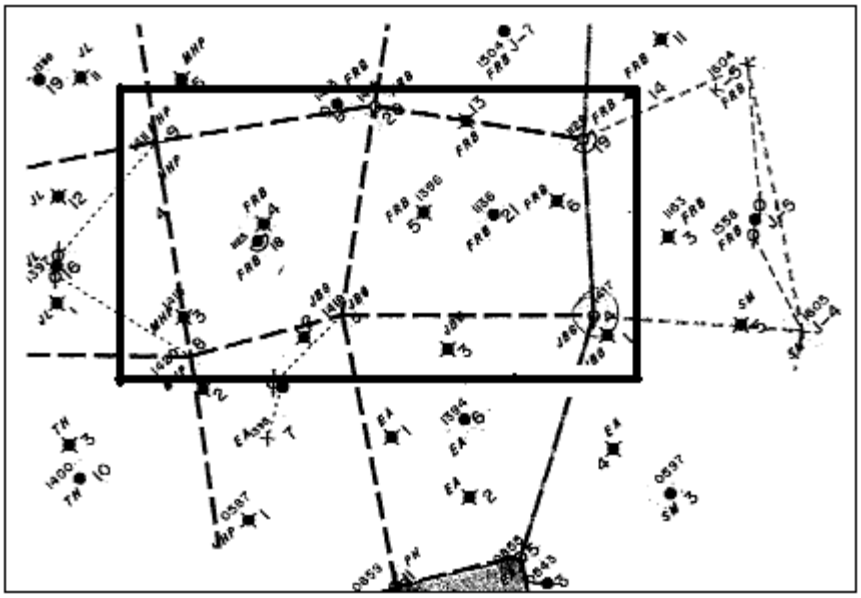

Figure 5.6 Verification Patterns Selected

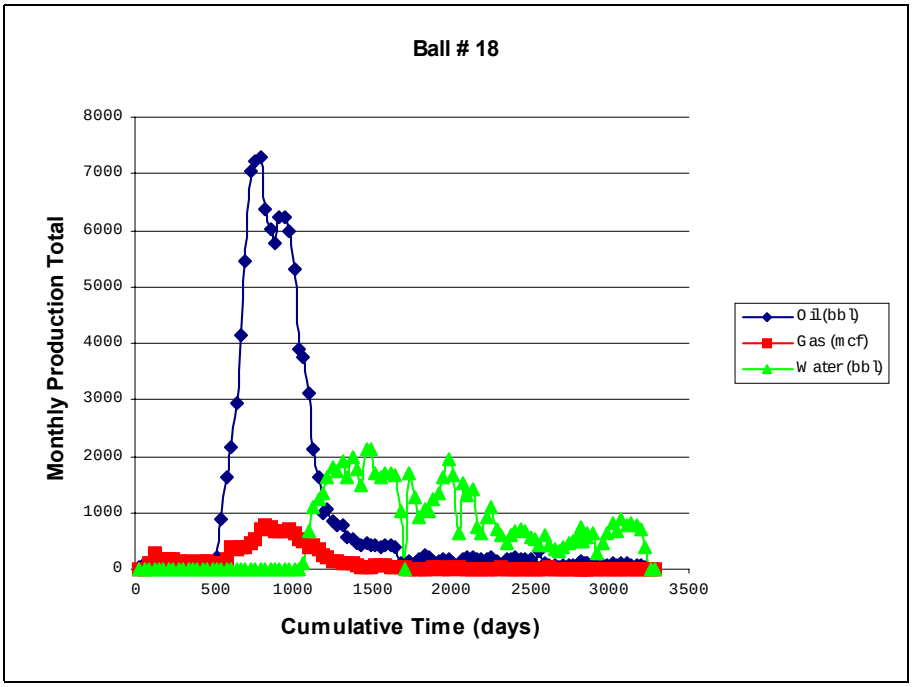

Figure 5.7 Ball # 18 Secondary Production History

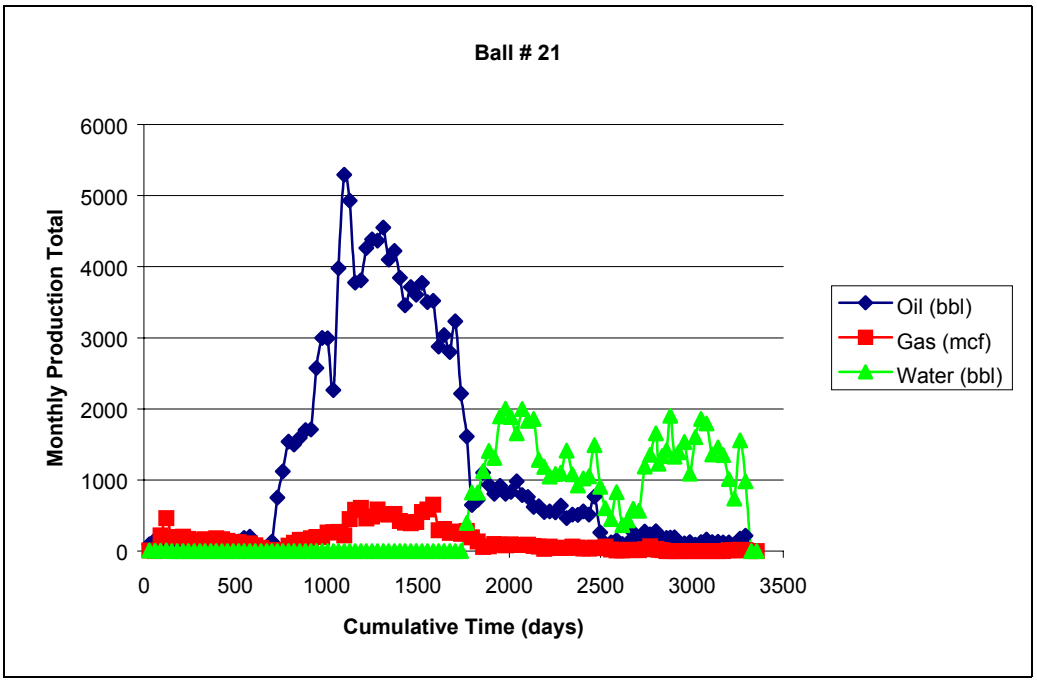

Figure 5.8 Ball # 21 Secondary Production History

Secondary recovery operations (injection) for this portion of the field and the two verification five spot patterns commenced in January, 1991. The Ball # 18, 21 production history commencing in April, 1999 is shown graphically in Figures 5.7 and 5.8. The two adjacent five spots had two common injectors in both patterns. The injected volumes and wellhead pressures for each well are presented in Figures 5.9, 5.10 and 5.11.

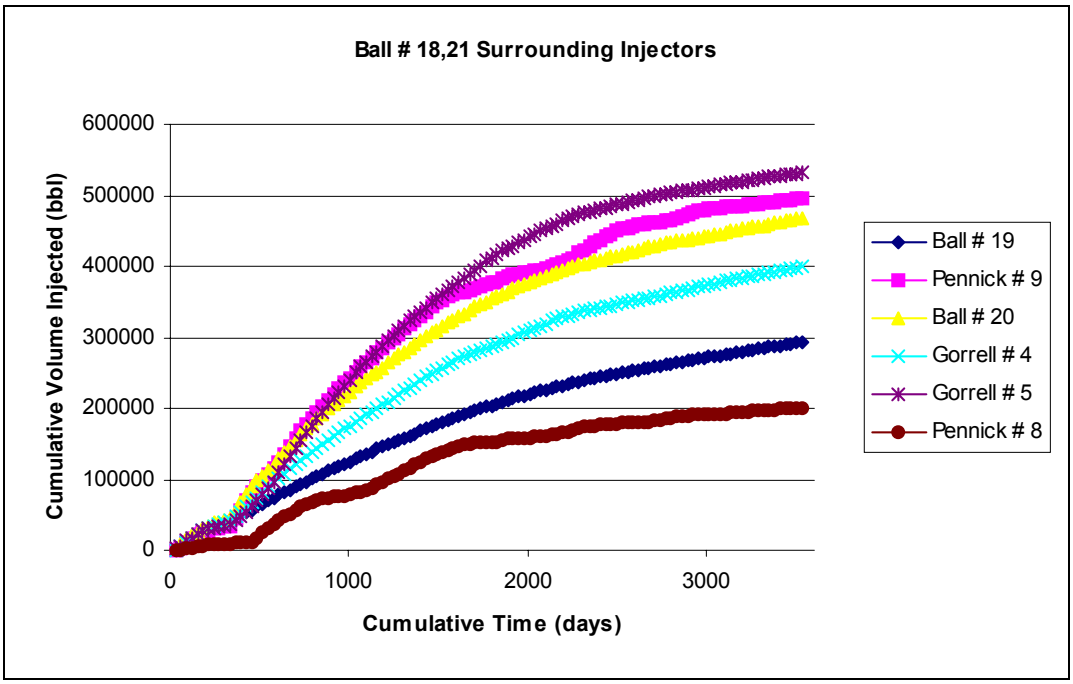

Figure 5.9 Cumulative Injected Volumes Per Well

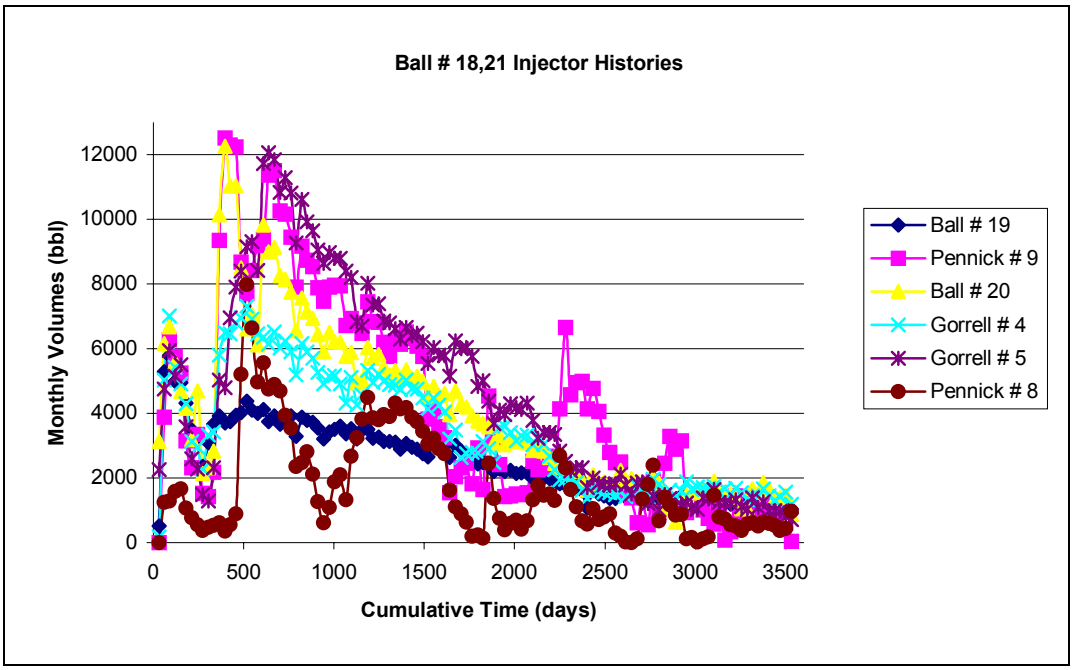

Figure 5.10 Monthly Injected Volumes Per Well

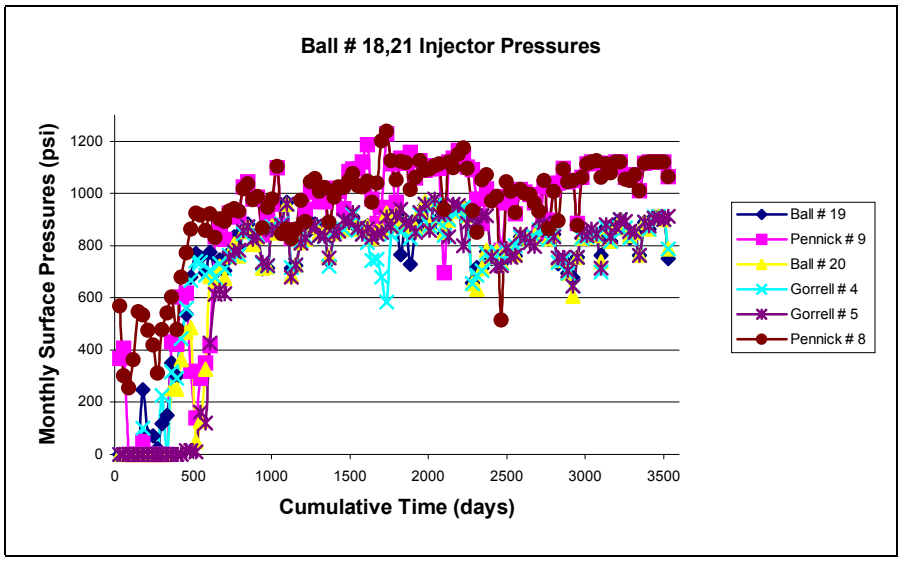

Figure 5.11 Monthly Surface Pressure for Injection Wells

5.7 Simulation Analysis - Verification Step

5.7.1 Simulator Introduction

The Boast98 simulator was used during the reservoir simulation phase. The simulator required reservoir property and fluid property inputs. In addition, for prediction matching, production and injection history was required for the area of study in the field. The flow unit ANN model 4-FU was used to predict flow units for each well in the dual five spot area - known as Ball # 18, 21 patterns. The second ANN model 2-K was used to predict permeability in each flow unit. The predicted flow unit was the model

output from model 4-FU. This flow unit output was then used as an input in the second ANN model for permeability prediction.

5.7.2 Necessary Input Data for the Simulator

The grid utilized was a 14 x 7 x 2 grid design. Each grid had an equal length and width of 194 feet. Within the two flow units the average predicted permeability from the ANN and average corresponding porosity from well log data was generated for each well in the two patterns. Permeability and porosity values between the six injectors and two producers within the study area were estimated for each grid using trends within the patterns and interpolation between the known well locations encountered during simulation. Tables 5.2, 5.3 and 5.4 present the PVT properties. Additional information regarding the fluid properties was previously presented in Tables 2.2, 2.3, and 2.4. Other parameters in the simulation model included:

- **Initial reservoir pressure @ 120 psia.**
- **Fluid saturation of oil, water, gas @ 66.8%, 17.5%, 15.7%, respectively.**
- **Irreducible water saturation @ 16%.**
- **Permeability in the x and y directions was equal.**
- **Vertical permeability was 1 md and 5 md in layers 1, 2.**

Table 5.2 Produced Oil PVT Properties

Pressure, psia	Viscosity, cp	Bo, RB/STB	Rs, SCF, STB
14.7	3.600	1.0000	0.0
80.0	3.229	1.0254	14.5
100.0	3.132	1.0275	18.9
120.0	3.038	1.0296	23.5
2500.0	0.6100	1.4234	862.5
Slope (P>Pb)	0.125E-02 cp/psia	-0.800E-06 RB/STB/psia	0.0

Table 5.3 Produced Natural Gas PVT Properties

Pressure, Psia	Visco-sity, cp	Bg, RCF/SCF	Pseudo PRS, $psia^2/cp$	Rock Comp. 1/psia
14.7	0.0112	0.1048E+01	0.00E+00	0.380E-05
120.	0.0114	0.7446E-01	0.3592E+07	0.380E-05
2500.	0.0196	0.4800E-02	0.4800E+09	0.380E-05

Table 5.4 Produced Water PVT Properties

Pressure	Viscosity, cp	Bo, RB/STB
14.7	1.4527	0.9911
120.0	1.4585	0.9909
2500.0	1.465	0.9880

Relative permeability data was available from the Horner # 9 core well. The relative permeability values used in the simulation analysis followed these results closely. In addition, the relative permeability values used in simulation mirrored that used by Gil in his earlier work. This allowed the opportunity to more closely compare Gil's reservoir simulation results to those of this study. Table 5.5 presents the relative permeability test results from the Horner # 9 well. Figure 5.12 presents a comparison of the relative permeability values associated with the Horner # 9 and those used in the simulator work.

Table 5.5 Relative Permeability - Horner #9

Sw	Krw	Kro	Kro/Krw
32.7	0.0077	0.51	66.234
37.7	0.012	0.436	36.333
41.6	0.016	0.37	23.125
46.2	0.024	0.283	11.792
48.5	0.029	0.235	8.103
50.8	0.037	0.19	5.135
52.7	0.045	0.148	3.289
54.1	0.052	0.114	2.192
55	0.06	0.098	1.633
55.6	0.066	0.089	1.348
56.2	0.074	0.076	1.027
57.3	0.08	0.05	0.625
58.2	0.096	0.033	0.344
59.5	0.107	0.0086	0.080
60.1	0.119	0.0039	0.033
60.8	0.135	0	0.000

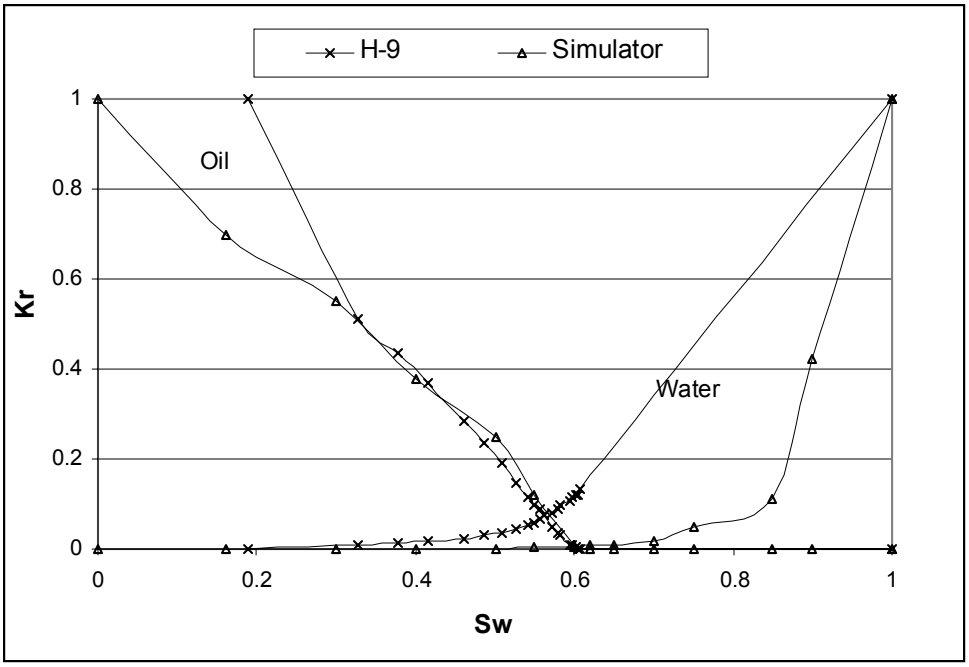

Figure 5.12 Comparisons of Relative Permeability (Gil, 2000)

5.7.3 Recurrent Data

During the simulator run the recurrent data section is used to input specifics related to initial and later changes that occur for any producing or injection well in the simulation area. The initial well location, layer completion information, and rates of injection are required inputs. As time proceeds during the simulator run it is necessary to adjust the injection rates to more accurate reflect estimates of water entering the patterns. This occurs in the recurrent data section. In addition, wells can be adjusted for skin damage problems or stimulation treatments. This also occurs in the recurrent section of the simulation program.

5.7.4 Comparing Flow Unit Simulation to Single Layer Model

The simulation results of the two flow unit model are compared to actual production results. A single layer model is also simulated. The single layer is compared to actual production as well.

5.8 Applying the Reservoir Characterization Results to the Field

The ANN results were used to construct a series of maps. The field maps include thickness isopachs of each flow unit, average permeability isopachs of each flow unit, combined kh isopachs of each flow unit. The field maps were generated by utilizing the 125 digitized well logs in the field. Figure 5.13 presents the Major Methodology Steps in Flow Chart Form.

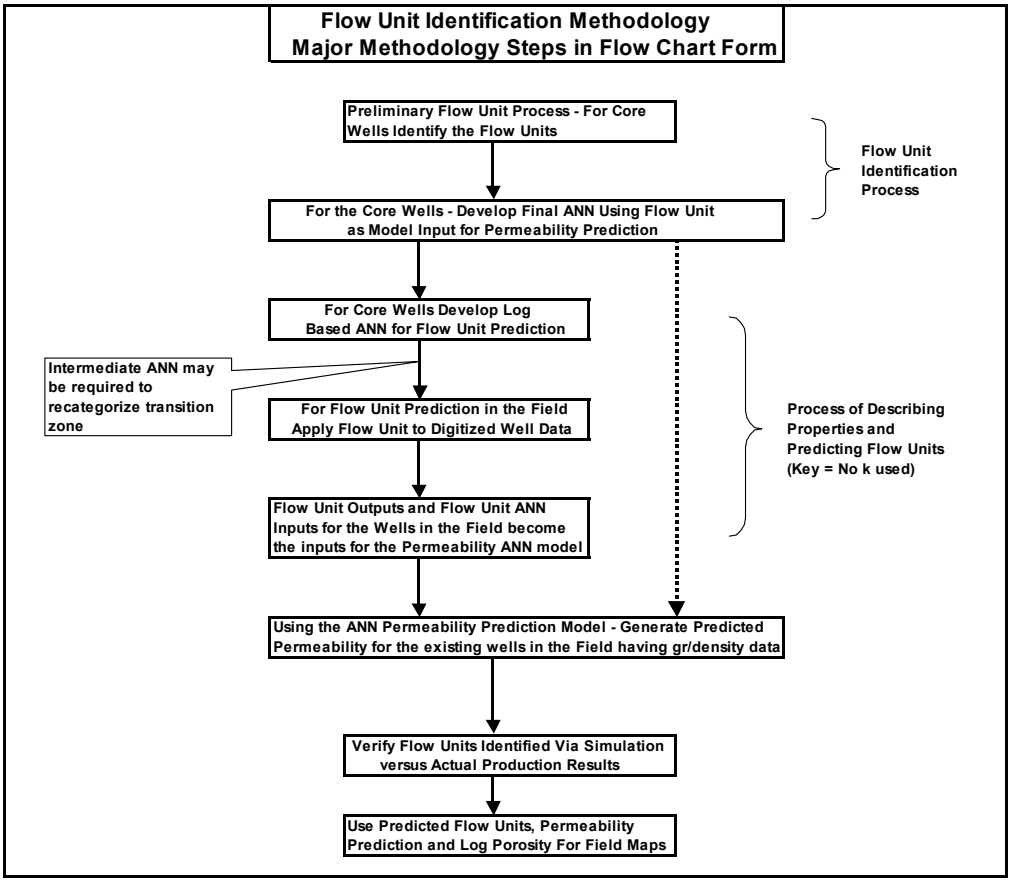

Figure 5.13 Flow Unit Identification Methodology Major Methodology Steps in Flow Chart Form

CHAPTER 6

RESULTS AND DISCUSSION

6.1 Introduction

The methodology used to identify flow units and ultimately predict permeability within each flow unit combines a series of screening tools and neural network analysis in a unique manner. The preliminary flow unit identification process proved to be very effective and provided fruitful results when used in combination with neural network analysis. Preliminary flow unit results presented herein are after multiple iterations of the preliminary flow unit tools. Previous results would be reviewed after each screening tool was utilized and further work would continue in terms of preliminary flow unit identification. Although these results appear brief and concise it is important to note that learning and enhanced interpretation occurs as the data is revisited. The preliminary flow units identified then become a part of the artificial neural network phase for flow unit prediction within the field using only log-based data.

6.2 Preliminary Flow Unit Identification Process Results

6.2.1 General Observations

Early efforts were directed at becoming more familiar with each core well by developing graphs of each well which detailed log

and core data broken out by depth. The graphs become a source of reference during the research. Table 6.1 presents general observations about cored sections in each well. Key observations are that two wells had comparatively low permeability throughout the pay zone (less than 50 md). Other wells had a zone of higher permeability in the lower section of the zone (100–250 md). Typically the sand immediately above the high permeability section had good porosity and in some instances good permeability (50–125 md) however, the upper section had noticeably less permeability and porosity than the lower portion of sand. In a few cored wells a lower permeability-porosity sand was present at the base of the high permeability section. After spending significant time with the graphs and as two flow units became more defined, trends and patterns of the gamma ray and density log measurements became more apparent.

Table 6.1 General Observations Gamma Ray-Density Log and Core Measurement versus Depth

General Observations Gamma Ray, Density Log and Core Measurements vs Depth (see Appendix A. for detail data)			
WELL NAME	**Flow Unit Interval (ft)**	**Flow Unit Interval (ft)**	**Observations**
T. Heirs # 8	2790.5 - 2794.5 Low k (7 - 10 md)	2794.5 - 2797.5 higher k (20 - 25 md)	2782 - 2790.5 no k porosity incr steadily to base of sand from 7% to 19
Horner # 9	2889 - 2892 no k 2892 - 2896 up to 100md	2896 - 2903 k jumps to 150 2903 - 2906 k jumps to 200 md	GR initially 30 increases to 60 @ deepest core point.
Ball # 19	3085 - 3098 no k 3098 - 3106 k varies	3106 - 3112 much higher k (100 - 200 md)	core porosity tracks with permeability
LeMasters # 13	3048 - 3050.5 one pt of 40 md, 20% por	3051.5 - 3053 one pt of 20 md, 15%	cored section has very low k couple of porosity streaks overall porosity 10 - 15 % up to 18 % in streaks
Ball # 18	2890 - 2894 40 - 50 md GR @ 30 md	2894 - 3000 125 - 250 md GR @ 50 md	GR is increasing as we go deeper cored from 2890 - 3000
Horner # 11	3088 - 3091 up to 70 md porosity above 20%	3091 - 3093 k jumps to 200 - 250 core porosity up to 25 % log porosity not as much	GR moved from 60 to 40 in higher pay section.

6.2.2 Cumulative k-h versus Cumulative ϕ-h for Core Data

The cumulative plots of storage capacity (ϕ-h) versus flow capacity (k-h) for each core well was a significant tool in the flow unit identification process. Figures 6.1 and 6.2 present the Ball # 19 and Ball # 18 cored wells. The two wells plot in a manner consistent with two flow units. In both cases the deflection points tie back well to the

final flow unit boundaries identified for each well. Two flow units appear to be present in the main section of the sand. Appendix B. can be referenced for all of the cumulative capacity plots for the core wells. Appendix Table B.7 further summarizes the flow unit intervals and deflection points (breaks) for each well. This approach was useful in validating flow units in five of the six wells. The T. Heirs # 8 well appeared to have two possible flow units. Further analysis supported only one flow unit. The LeMasters # 13 had no deflection points and appeared to have a single flow unit.

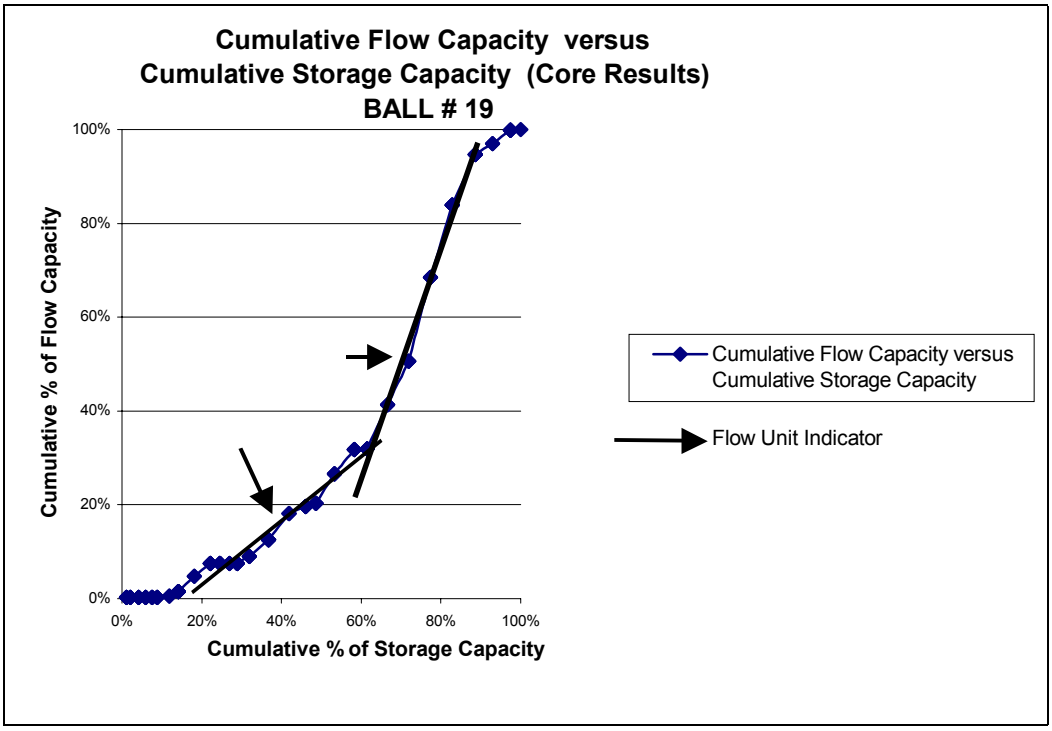

Figure 6.1 Cumulative Flow Capacity versus Cumulative Storage Capacity (Core Results) Ball # 19

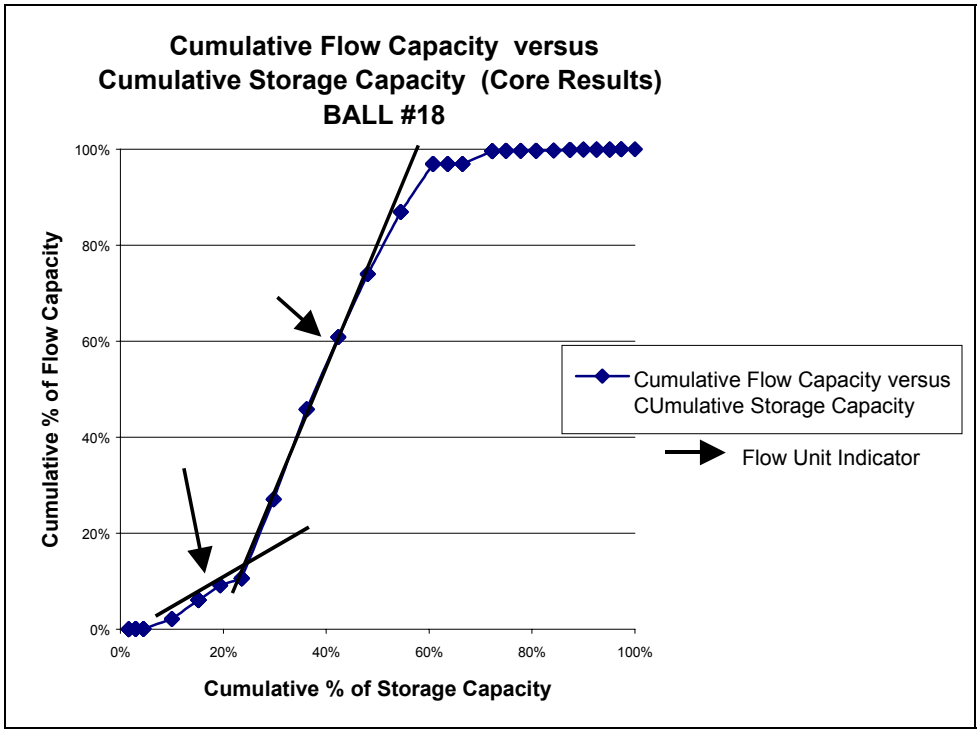

Figure 6.2 Cumulative Flow Capacity versus Cumulative Storage Capacity (Core Results) Ball # 18

6.2.3 Cumulative k-h versus Cumulative ϕ-h for Miniperm Data

Five cores were physically available for miniperm measurements. In order to utilize the miniperm measurements the log porosity was used. Results were very positive in terms of identifying the potential flow units and ratifying the earlier cumulative storage capacity plots made from the core data. Figures 6.3 and 6.4 present the Ball # 19 and Ball # 18. The overall slopes and deflection points tracked well with the cumulative storage capacity plots made from the core data. Appendix C. includes the minipermeameter plots for five of the core wells. Appendix Table C.6

summarizes the potential flow unit boundary point analysis for each well based on the minpermeameter measurements and log porosity.

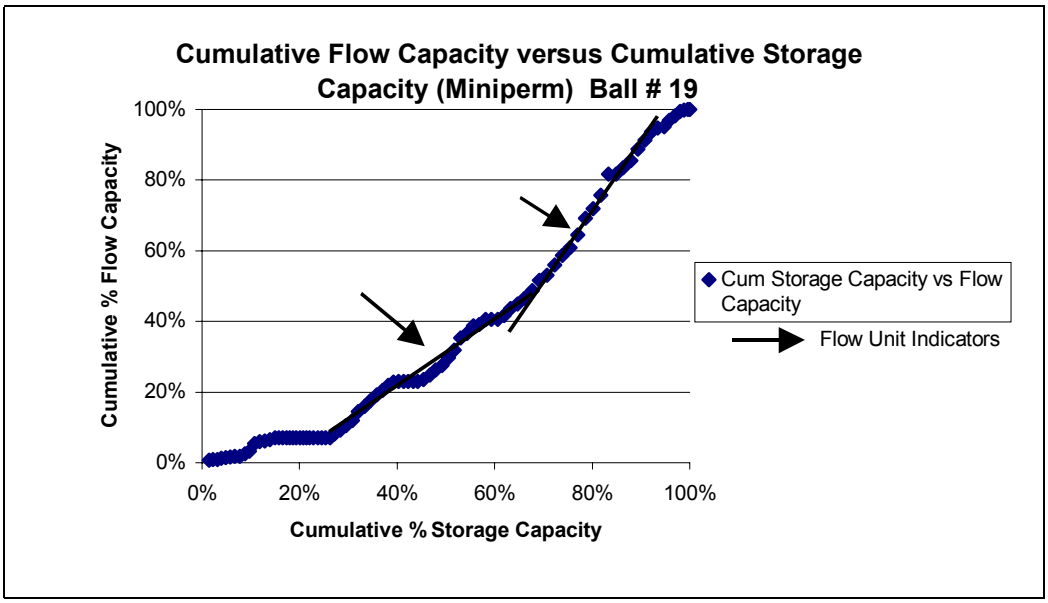

Figure 6.3 Cumulative Flow Capacity versus Cumulative Storage Capacity (Miniperm) Ball # 19

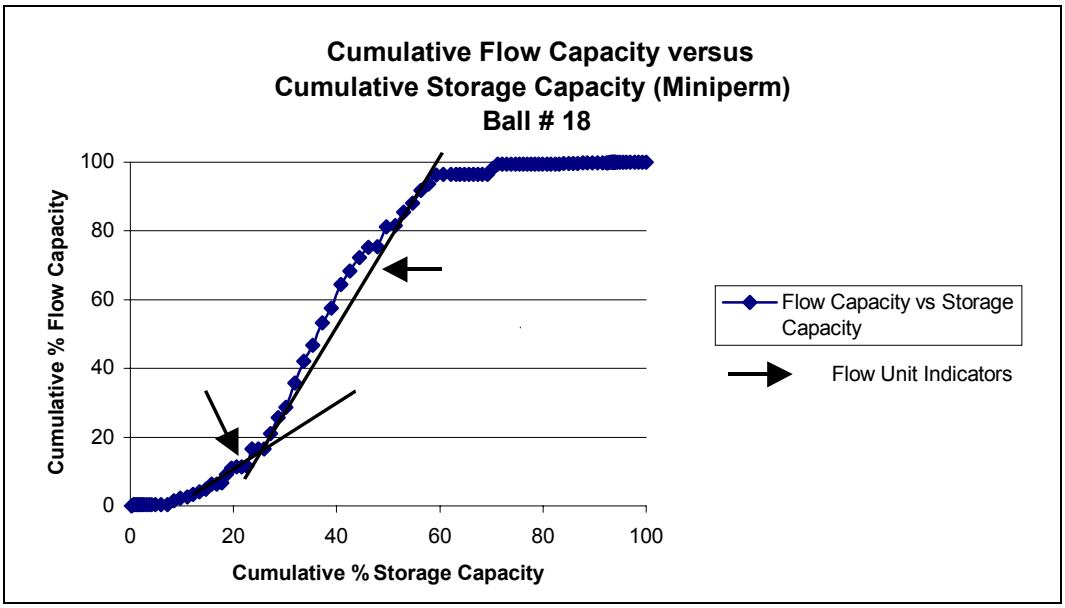

Figure 6.4 Cumulative Flow Capacity versus Cumulative Storage Capacity (Miniperm) Ball # 18

6.2.4 Cumulative k-h versus Cumulative ϕ-h - Core Data versus Miniperm Data

At the time coring and core analysis was being performed, the operator did not test the core on a per foot basis in every well. In some cases, it appears certain sections were tested (better pay) and other sections were passed over. As a result there are data gaps of a few feet between core data in a given well. The minipermeameter and the associated cumulative capacity plots offer valuable information about the gaps or lack of core analysis between core data points. Figure 6.5 (LeMasters # 13) and 6.6 (Ball # 18) present a comparison of the two cumulative plots. The miniperm cumulative plots proved to be a valuable screening tool. Appendix G. contains the comparative cumulative plots between the Core Lab report and the miniperm data with log data for the cumulative flow and storage capacity plots for the wells.

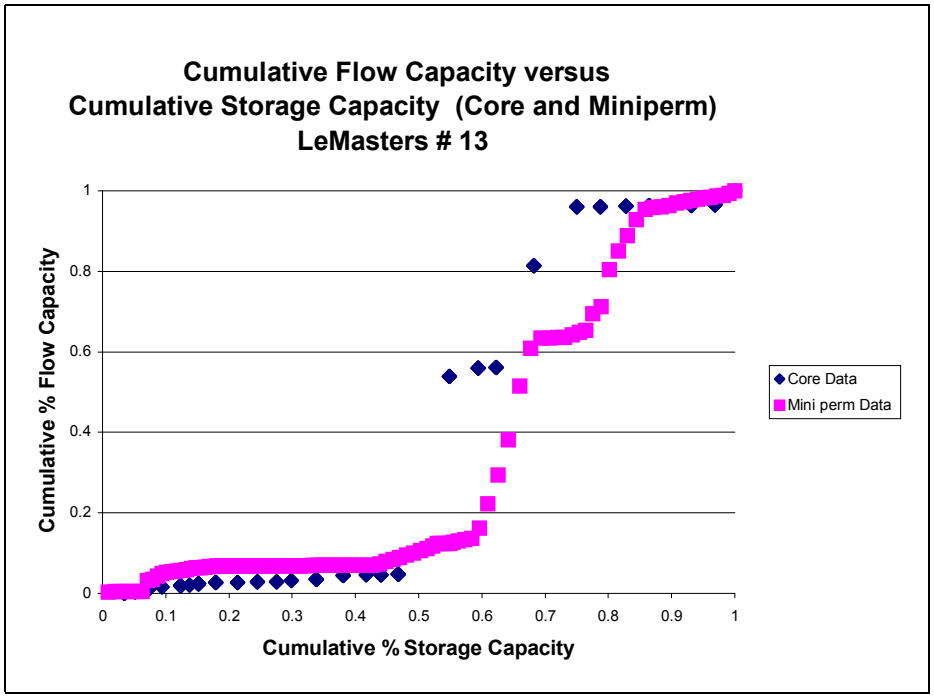

Figure 6.5 Cumulative Flow Capacity versus Cumulative Storage Capacity (Core and Miniperm) LeMasters # 13

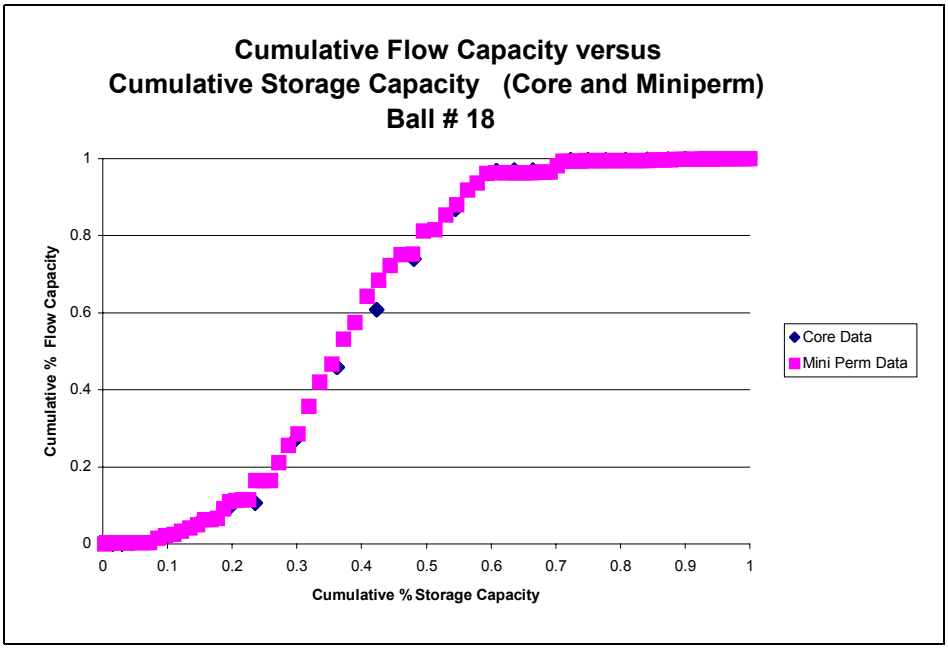

Figure 6.6 Cumulative Flow Capacity versus Cumulative Storage Capacity (Core and Miniperm) Ball # 18

6.2.5 Questionable Flow Unit Below Flow Unit Two

During the preliminary flow unit identification process the cumulative flow capacity versus storage capacity plots were revisited several times. Two flow units were clearly identified by this analysis. Flow unit one is the upper flow unit encountered. Flow unit two is situated immediately below flow unit one. Flow unit two has much higher permeability and porosity. A third potential flow unit appeared to exist in the Ball #19 well. The Ball # 18 and Horner # 11 also had limited hints of the third unit. The potential flow unit has very low permeability and porosity and was considered to be non-productive and not a part of the flow units. The low porosity-permeability sand at the top and bottom of the core data was not a part of the flow unit analysis due to the lower section being excluded (previously discussed). Figures 6.7 and 6.8 present the Ball # 19 cumulative plots showing this third potential flow unit for core data and miniperm.

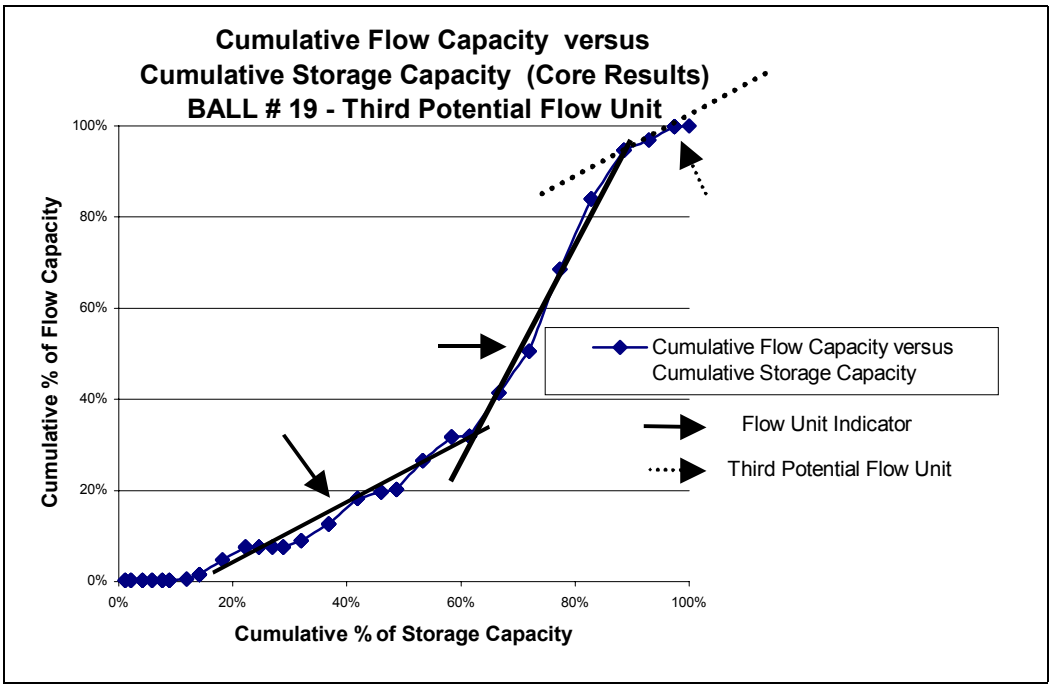

Figure 6.7 Cumulative Flow Capacity versus Cumulative Storage Capacity (Core Results) Ball #19 - Third Potential Flow Unit

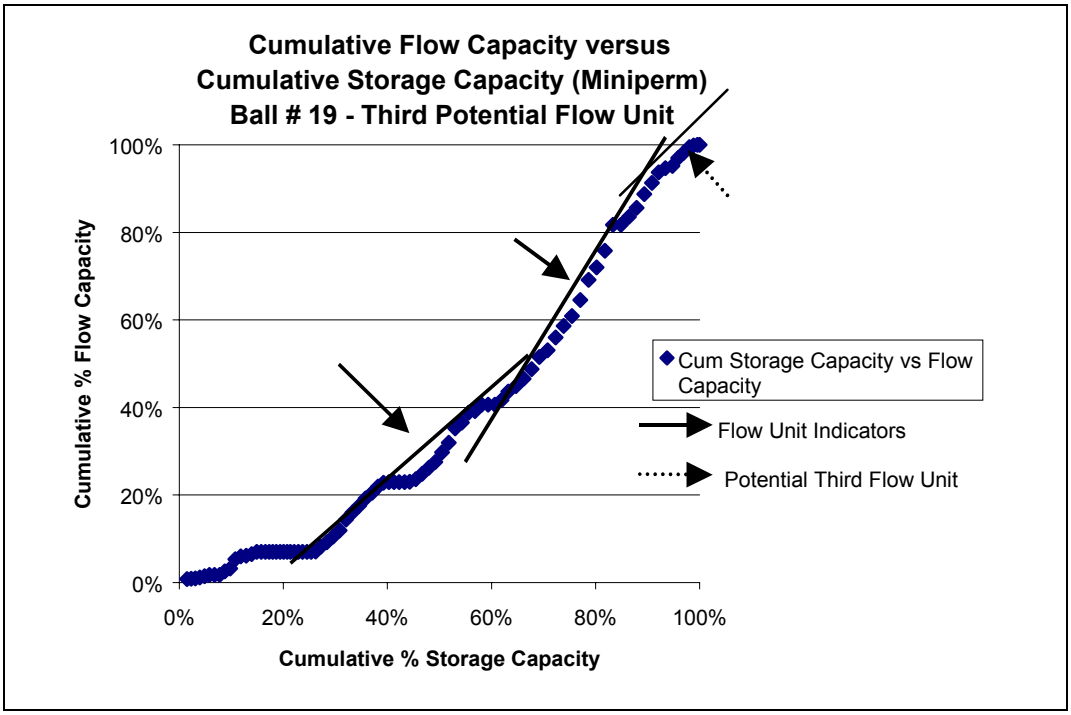

Figure 6.8 Cumulative Flow Capacity versus Cumulative Storage Capacity (Miniperm) Ball # 19 - Third Potential Flow Unit

6.2.6 Permeability-Porosity Scatter Plots

The relationship between permeability and porosity has a higher correlation within the flow unit. The permeability-porosity scatter plots of each well were developed with the objective of determining the highest correlation within the potential flow units. For wells appearing to have two flow units, boundary or edge points were shifted back and forth between the flow units until the highest correlation was obtained. The upper sand section, which became known as "Flow Unit One" typically reflected greater heterogeneity and therefore had lower correlation. The second sand section, became known as "Flow Unit Two" and is immediately below flow unit one. Flow unit two had much higher permeability and typically reflected a higher correlation.

Figures 6.9 and 6.10 present the permeability-porosity scatter plots for the T. Heirs # 8, which has a single flow unit, and the Horner # 9 which two flow units. Each core well and the supporting data for the plots are presented in Appendix D.

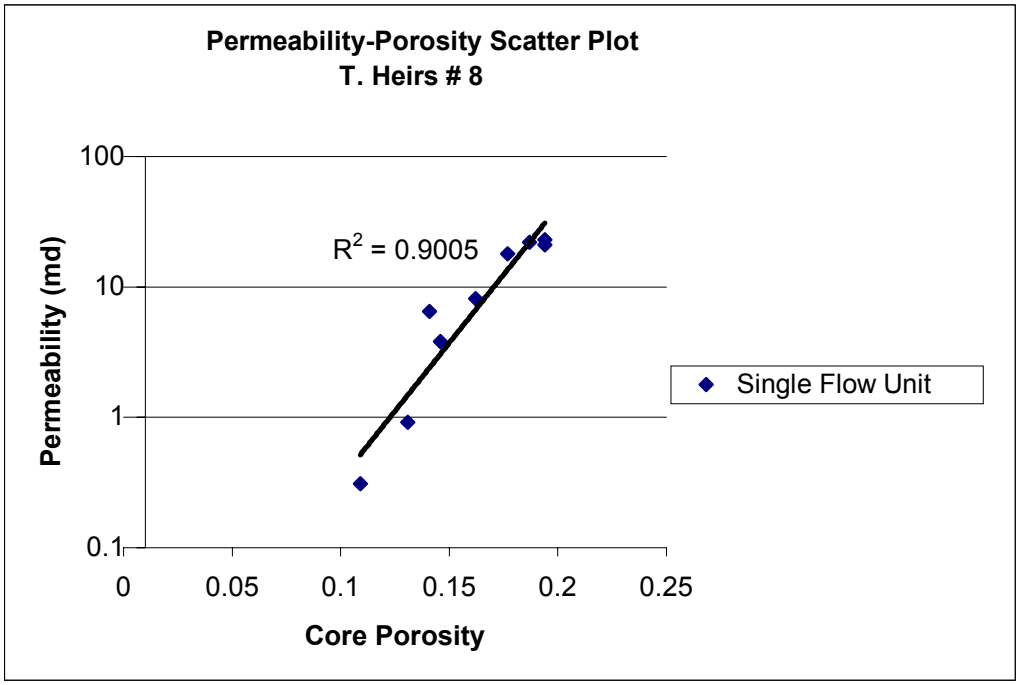

Figure 6.9 Permeability-Porosity Scatter Plot T. Heirs # 8

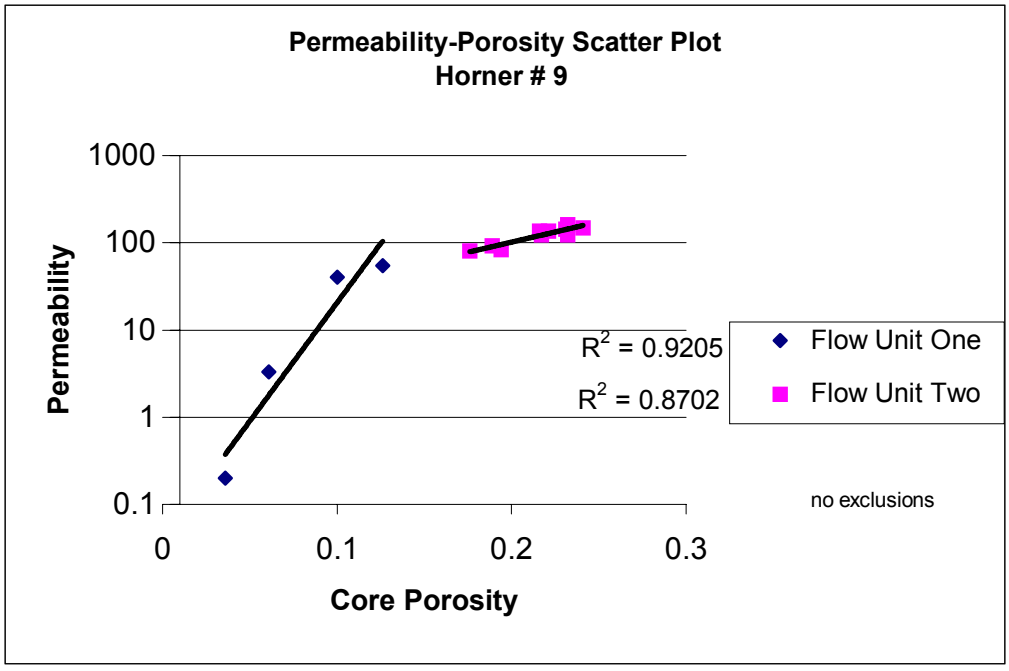

Figure 6.10 Permeability-Porosity Scatter Plot Horner # 9

Table 6.2 summarizes the correlation values for each of the core wells. As further comparison Figure 6.11 and Figure 6.12 present composite scatter plots for all six wells combined as a single flow unit (Figure 6.11) as compared to the designated two flow units (Figure 6.12) for the six wells. The R squared value for the six core wells, as a single unit, was .8173. When the data was broken down into two flow units the R squared values are .7093 and .9281 for flow unit one and two, respectively.

Table 6.2 Summary of R Squared Values for Two Flow Units for Permeability-Porosity Scatter Plots

Well Name	Flow Unit One	Flow Unit Two
T. Heirs # 8	.9005	one unit
Horner # 9	.9205	.8702
Ball # 19	.8231	.9523
LeMasters # 13	.9277	one unit
Ball # 18	.862	.9612
Horner # 11	.9089	.9999

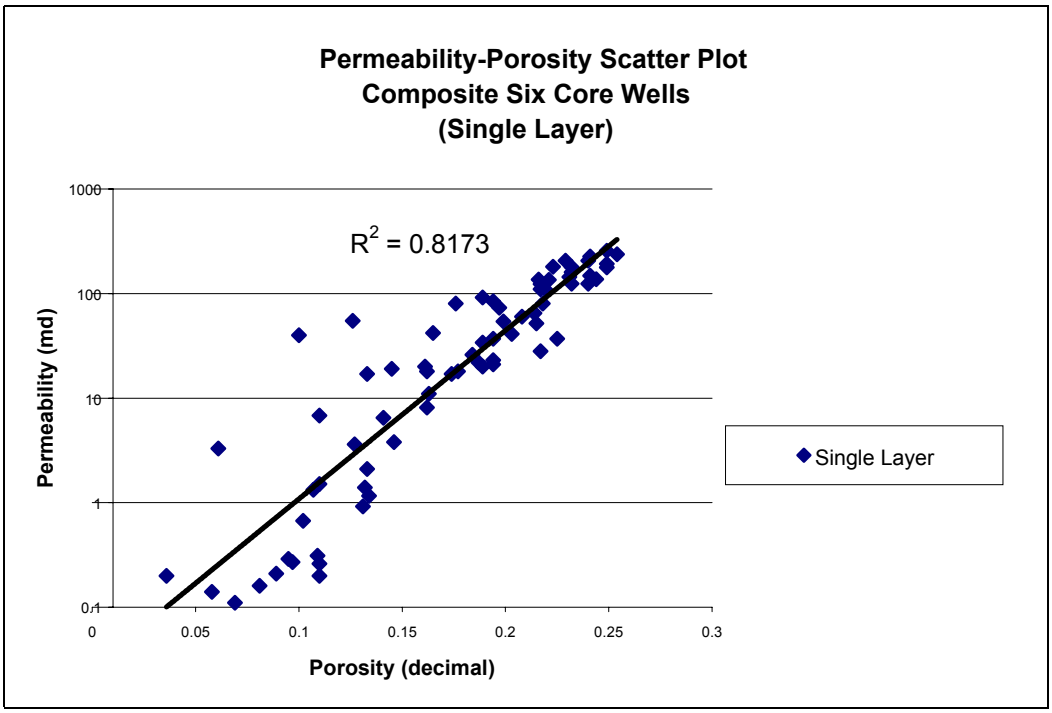

Figure 6.11 Permeability-Porosity Scatter Plot Composite Six Core Wells (Single Layer)

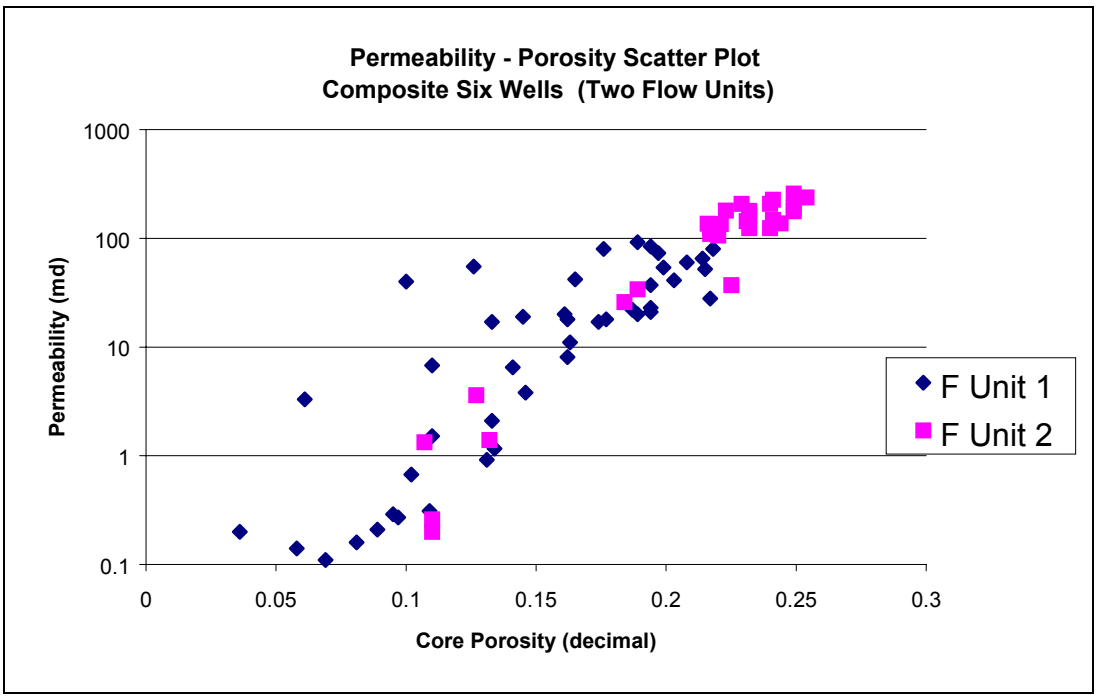

Figure 6.12 Permeability-Porosity Scatter Plot Composite Six Core Wells (Two Flow Units)

6.2.7 Flow Zone Indicator (FZI)

As compared to the permeability-porosity scatter plots, the FZI plots supported the flow unit breaks as well. However, lower R squared calculations were observed for some of the units. This was likely due to having a very limited number of data points to work with. Table 6.3 summarizes the results. FZI plots are included for the T. Heirs # 8 and Horner # 9 - Figures 6.13 and 6.14. Both wells were presented in section 6.2.6 (Permeability-Porosity Scatter Plots) for comparison.

When comparing the R squared values for the six core wells combined, the values are lower than the k-ϕ scatter plots. The R squared values are .697 for the single flow unit and for the two flow unit model the values are .555 and .9256 for flow units one and two respectively. Figures 6.13 and 6.14 are the six well composite FZI graphs for the single and two flow unit cases. Table 6.3 is a well summary of the preliminary flow units identified using the permeability-porosity scatter plots in conjunction with the FZI method.

Table 6.3 Summary of R Squared Values for Two Flow Units for Flow Zone Indicator (FZI) Plots

Well Name	Flow Unit One	Flow Unit Two
T. Heirs # 8	.9036	one unit
Horner # 9	.013	.8468
Ball # 19	.7842	.9652
LeMasters # 13	.9243	one unit
Ball # 18	.8952	.9565
Horner # 11	.8977	.9995

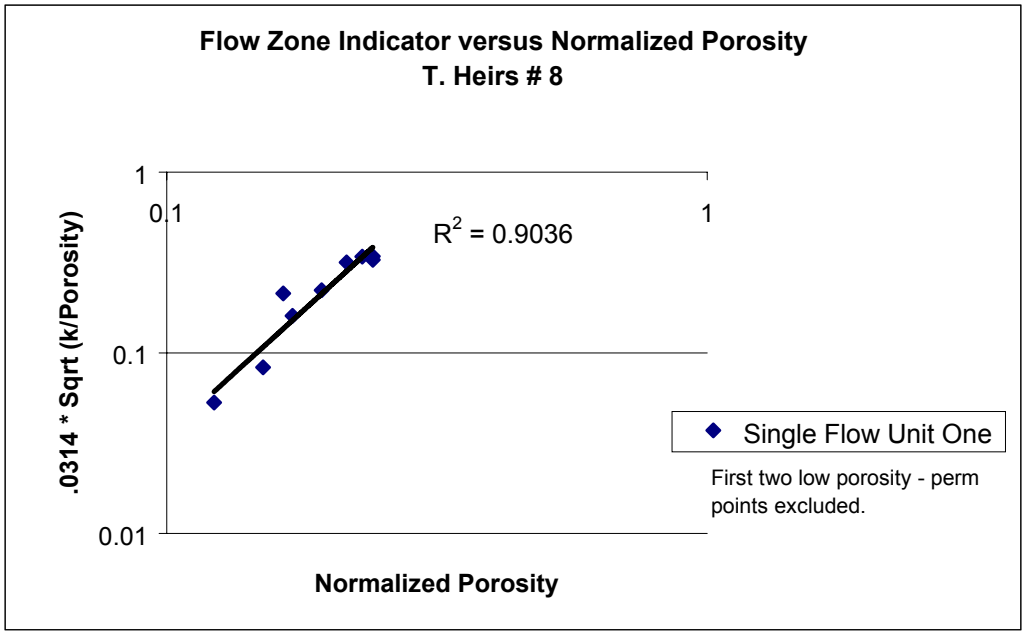

Figure 6.13 Flow Zone Indicator versus Normalized Porosity T. Heirs # 8

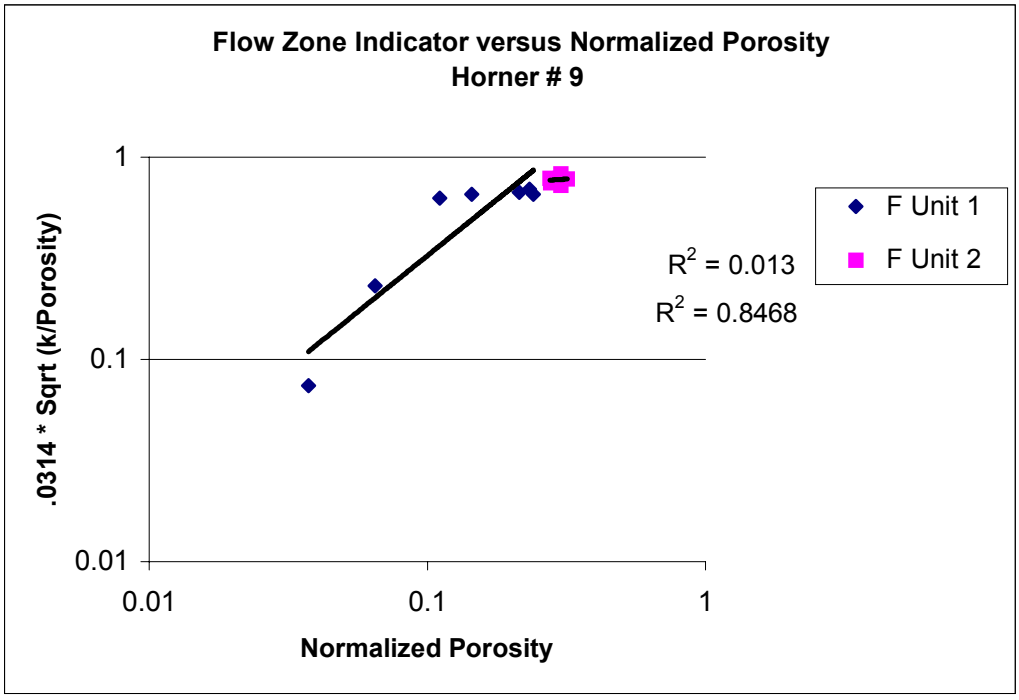

Figure 6.14 Flow Zone Indicator versus Normalized Porosity Horner # 9

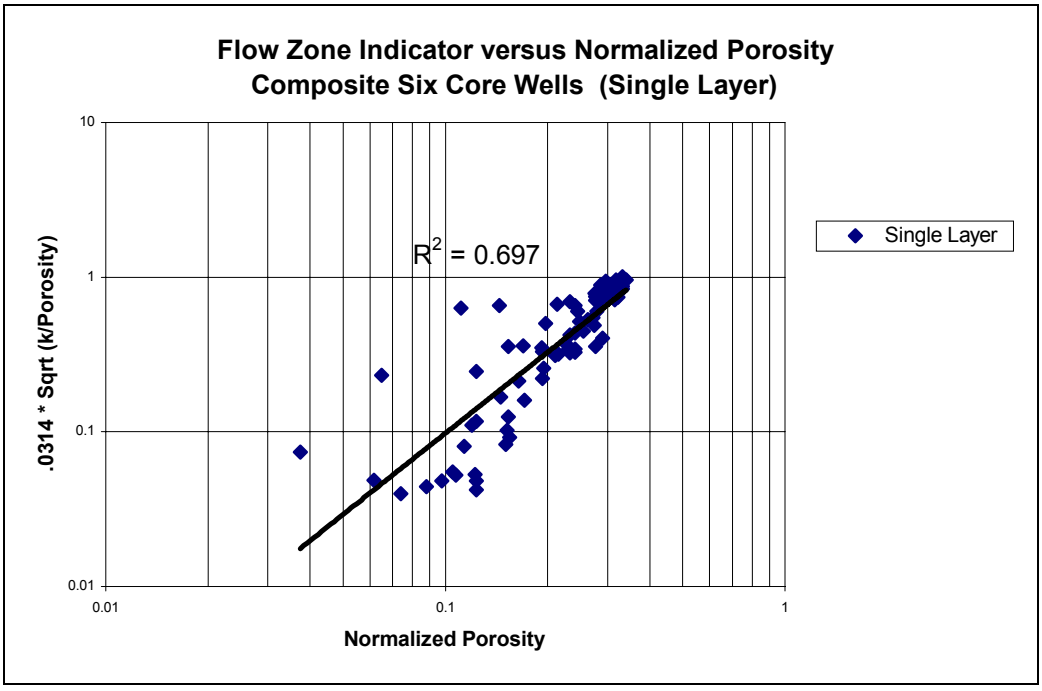

Figure 6.15 Flow Zone Indicator versus Normalized Porosity Composite Six Wells (Single Layer)

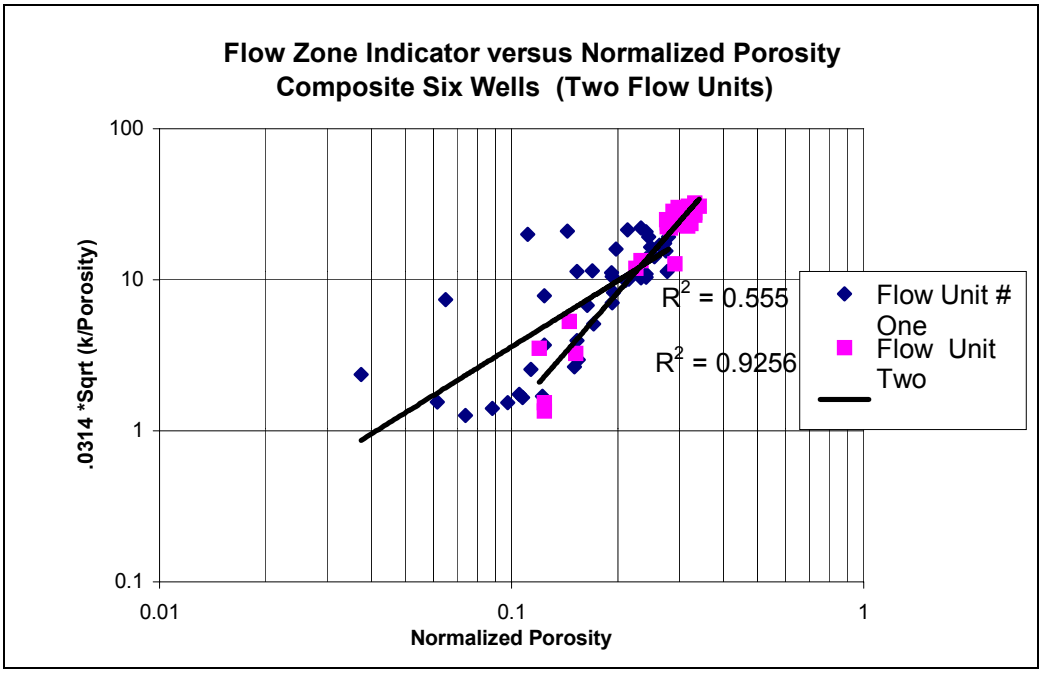

Figure 6.16 Flow Zone Indicator versus Normalized Porosity Composite Six Core Wells (Two Flow Units)

Table 6.4 Summary of the Interval Identified as Flow Units by the k - ϕ Scatter Plot and FZI Plots (Log Depth in Feet)

Well Name	Flow Unit One	Flow Unit Two
T. Heirs # 8	2788.75 – 2797.5	single unit
Horner # 9	2890 – 2896.5	2898.25 – 2903.50
Ball # 19	3097.25 – 3106	3107.25 – 3112.5
LeMasters # 13	3043.25 – 3052.75	single unit
Ball # 18	2989.50 – 2994	2995.5 – 3007.25
Horner # 11	3084.5 – 3090.5	3092 – 3093.25

6.2.8 Artificial Neural Network Kohonen Analysis

The final preliminary flow unit identification tool utilized the ANN Kohonen method to separate the data into groups. The other preliminary flow unit identification tools utilized focused strictly on identifying the permeability-porosity relationship within the flow unit. The Kohonen analysis included several log-based inputs. The log inputs included gamma ray, density, gamma ray slope, density slope, gamma ray base line, and density base line. The other input was measured permeability from the core analysis.

Kohonen analysis of all available core data was completed for two, three and four groups. The two and three category models offered very positive results (Tables F.1 and F.2). A four-category model failed as compared to the other two models. The final groups in the four-category model lacked the recognizable patterns of the two and three category models. The groups in the four-category model did not represent flow units.

Certain data points appeared to have characteristics or properties of both flow units. These core points are situated between the two flow units. The three-category Kohonen model had the ability to recognize and categorize these particular points and place them in the center group or category. There were only a few points the ANN handled in this manner. However, these transition

points became more of an area of focus as the backpropagation ANN model for permeability prediction was finalized.

For certain wells another outcome became more apparent from the two and three category models. Certain core data below flow unit two was being categorized as flow unit one. The producing flow unit one is situated above flow unit two. In a few of the wells a continuation of low quality sand below flow unit two is observed. This lower portion typically exhibits very low porosity and permeability and is considered to be non-productive. Section 6.2.5 previously discussed this additional potential flow unit as a result of the cumulative permeability-porosity analysis. Although non-productive; the Kohonen analysis suggests a porosity-permeability relationship similar to flow unit one. This discovery was further tested as the final backpropagation model was developed.

The preliminary flow unit identification processes focusing strictly on the permeability-porosity indicated a single flow unit in the Lemasters # 13. During the preliminary identification process the T. Heirs # 8 appeared to have a single flow unit and at other times appeared to have two flow units. The balance of the wells reflected two flow units during screening.

Kohonen analysis results categorized the T. Heirs # 8 data as a single flow unit. This well had appeared to have both flow units present during some of the preliminary tests (cumulative porosity-

permeability). A distinct advantage of the analysis is for the network to learn from all available core and log data of the six wells. The T. Heirs # 8 exhibits some permeability-porosity variation. However, based on the characteristics of both flow units in all six wells, the model categorized the T. Heirs well as flow unit one. This was helpful during the backpropagation modeling phase.

Additional Kohonen analysis was performed on model 1-K, the ANN backpropagation model. The difference between the initial work described above and the additional Kohonen analysis related to the core data used. Low permeability-porosity core results at the top or bottom of the sand were excluded for each well. The intent was to include only those core samples actually a part of either flow unit. Low permeability or porosity data indicated non-production sections outside the primary sand and was excluded during this analysis.

In terms of identifying the flow unit breaks between flow unit one and two, the results for this Kohonen analysis were similar to the initial analysis, which included all of the data. Tables F.3, and F.4 can be referenced for each well. Table 6.6 summarizes the per well results for flow units as determined by the Kohonen Self Organizing Map Network. The transition points between the two flow units are better assigned to a given flow unit during the backpropagation ANN modeling. The Kohonen analysis also characterized a section of

sand below flow unit two as being similar to flow unit one. Tables F.3, F.4 can be referenced for further detail.

6.2.9 Summary of the Preliminary Flow Unit Identification Process

The preliminary methods identified two flow units within the sandstone:

- Flow unit one is encountered first in the reservoir. A conglomerate is often observed in the upper part of the sand. Flow unit one is situated in the lower part of a conglomerate sand and the upper part of the sandstone section directly below the conglomerate. As compared to flow unit two, the flow unit has lower porosity and much lower permeability.

- Flow unit two is situated below flow unit one. The two flow units exhibit different values for the gamma ray and density logs (Table 6.5). Flow unit two has higher porosity and significantly more permeability.

- Another low permeability flow unit below flow unit two seems to be present in a few of the wells. This flow unit appears to have properties similar to flow unit one.

Table 6.5 Description of the Flow Units

WELL LOG PARAMETER	FLOW UNIT ONE	FLOW UNIT TWO
Bulk Density (gm/cc)	2.35 - 2.45	2.31 - 2.41
Porosity (%)	13 - 16	15 - 20
Gamma Ray (API)	31 - 41	40 - 60

Table 6.6 Kohonen Network Summary
Core Permeability and Log Measurements

Well Name	Groups Max	Groups Used	Flow Unit One	Flow Unit Two	Flow Unit Three	Observations
T.Heirs # 8	2	1	2785.3 - 2979.5	none	na	ANN sees single groups both times.
	3	1	2785.3 - 2979.5	none	none	
Horner # 9	2	2	2890 - 2893.5	2895 - 2903.5	na	Break point @ 2893.5 both same break point
	3	2	2890 - 2893.5	none	2895 - 2903.5	exact same two groups.
Ball # 19	2	2	3086.25 - 3100	3107.25 - 3110.7	na	Between two groups, 6 points back and
	3	2	3086.25 - 3100	none	3107.25 - 3110.75	forth same break points for the groups.
LeMas # 13	2	1	3031.8 - 3052.8	none	na	ANN sees single unit both times.
	3	1	3031.8 - 3052.8	none	none	
Ball # 18	2	2	2987.5 - 2990.75	2995.5 - 2999.75	na	Three common points between the two units
	3	2	2987.5 - 2990.75	none	2995.5 - 2999.75	back and forth.
Horner # 11	2	2	3084.5 - 3089.5	3090.5 - 3092.5	na	Same groups, both models see two
	3	2	3084.5 - 3089.5	none	3090.5-3092.5	groups.

6.3 The Neural Network for Permeability Prediction

6.3.1 Model 1-K for Permeability Prediction

Two neural networks were ultimately developed for permeability prediction. One ANN designated as model 1-K was defined using a tighter definition of the flow units. This was

confirmed by the neural network analysis. Other efforts to strengthen the model included revisiting the correlation between log and core depth. Although limited, a few core data points were ultimately shifted 1/4 foot in depth. The slightly changing values of the digitized logs can enhance the final ANN. Any such shift was in keeping with the characteristics of the log data. The 81 core data and log inputs used for developing the ANN model are presented in Appendix H.1. As discussed in chapter 4, the table details the ANN results for the testing, training and production verification well. For each well, the correlation value between predicted permeability and actual permeability was very good (Table 6.7). R squared values between .8924 and .9870 were observed.

Table 6.7 Permeability Prediction Model (Model 1-K) R Squared Values

WELL NAME	TST	TRN	PRO
Horner # 11	0.8017	0.8916	0.987
T Heirs # 8	0.8185	0.885	0.9021
Horner # 9	0.8085	0.8944	0.9064
Ball # 19	0.8702	0.9878	0.8924
LeMasters # 13	0.8494	0.9753	0.8942
Ball # 18	0.8396	0.9014	0.9681

6.3.2 Model 2-K for Permeability Prediction

Model 2-K is based on a total of 95 core and log data inputs. This model incorporates the core data for the lower permeability-porosity section below flow unit two. Appendix H. Table 2.0 details the data used for model developing model 2-K. As can be seen in Table 6.8, model 2-K significantly improves the LeMasters # 13 permeability prediction (.8942 increases to .9338 for the production set). Change in permeability prediction of the other core wells was not significant.

Table 6.8 Permeability Prediction Model (Model 2-K) R Squared Values

WELL NAME	TST	TRN	PRO
Horner # 11	0.7842	0.9334	0.9815
T Heirs # 8	0.9019	0.9864	0.9011
Horner # 9	0.8734	0.988	0.894
Ball # 19	0.8346	0.9866	0.888
LeMasters # 13	0.8987	0.9843	0.9338
Ball # 18	0.7468	0.9218	0.9768

6.3.3 Model 2-K Selected as the Final Model for Permeability Prediction

Model 2-K, the ANN model for permeability prediction, was chosen as the better ANN model for this particular field. Two key factors were considered. The location of the core wells within the field was significant. The LeMasters # 13 well is situated in the north part of the field. This well exhibits only flow unit one. Model 2-K will better predict the north section of the field, as well as other portions of the field where flow unit one exists either as a single flow unit or when both flow units are present. By including more data similar to flow unit one, the models ability to predict flow unit one (situated above flow unit two) is enhanced. Any impact to the model prediction ability in flow unit two was not significant.

In addition model 2-K more fully utilizes the core data during training. Model 2-K is tested and trained using 95 data points as opposed to 81 core data points included in model 1-K. As a result it is considered a stronger model. Table H. 4.0 presents a flow unit summary breakdown per well. Figures 6.17 and 6.18 graphically present actual versus predicted permeability results for Horner # 11 and Ball # 19. Figures H. 1- 6 can be referenced for graphs of all six core wells.

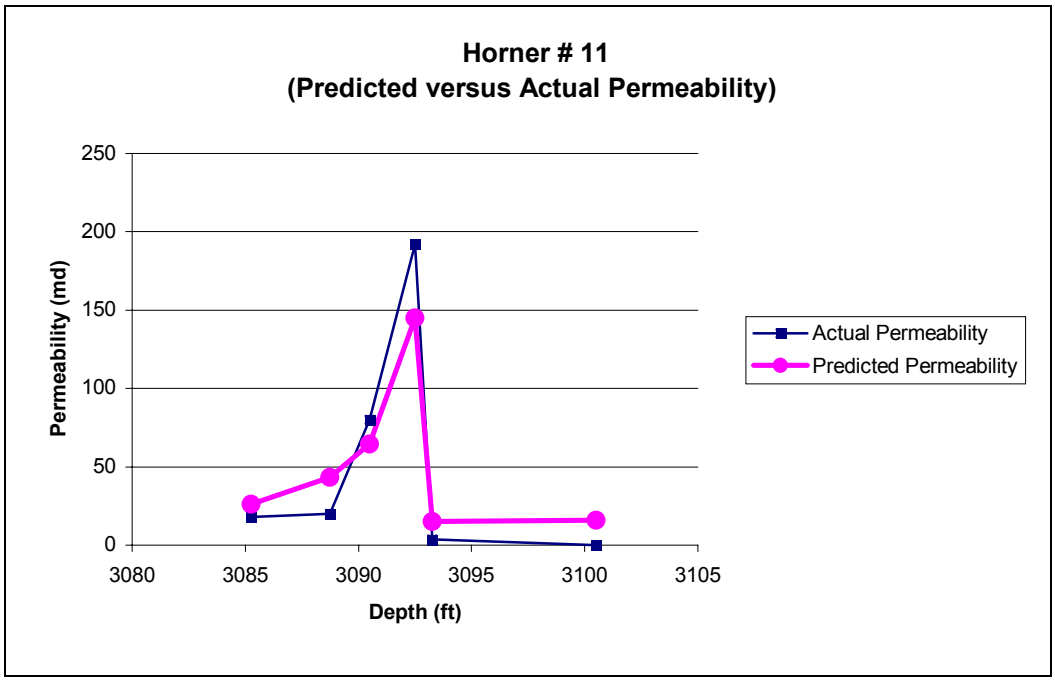

Figure 6.17 Horner # 11 Predicted versus Actual Permeability

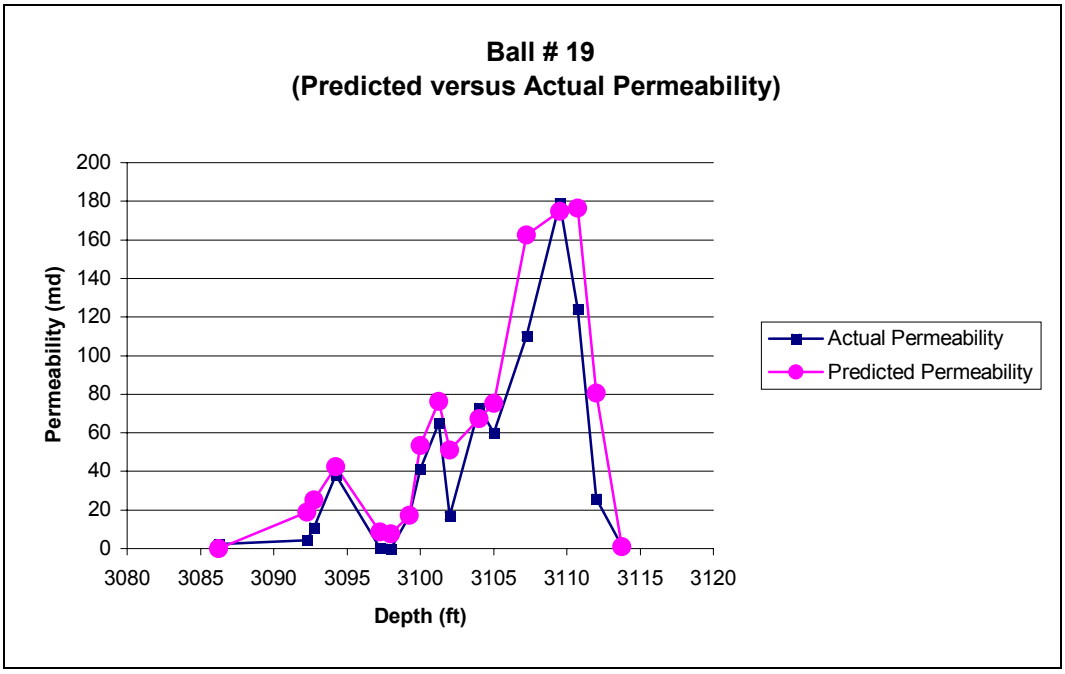

Figure 6.18 Ball # 19 Predicted versus Actual Permeability

6.4 Predicting the Flow Unit

Two flow unit models were evaluated. Model 2-FU utilized the core data and flow unit designation at each core data point (95 points). Model 3-FU utilized the digitized log data and flow units were assigned utilizing the previous flow unit identification work (306 points). Table 6.9 compares the correlation results for both models. As can be observed certain core wells exhibit excellent correlation while others appear not to correlate well.

Table 6.9 Flow Unit Prediction Model
Summary of R Squared Values

WELL NAME	2-FU Core	3-FU Dig. Log
Horner # 11	.25	.9021
T Heirs # 8	X	X
Horner # 9	.6857	.9018
Ball # 19	.8595	.5148
LeMasters # 13	1.0	1.0
Ball # 18	1.0	1.0

The ANN could not predict the flow unit within the transition area of certain core wells. Outside of the transition zone of the core wells the prediction of flow unit one or two is very accurate. Table

6.10 illustrates the problem. In the upper portion of sand predictions for flow unit one are excellent. The lower flow unit two is predicted equally well. These results suggest a combination of flow unit properties over a thin transition section. This problem occurs at or near the flow unit boundaries. Table 6.11 is a portion of Table F.2 for the Ball #19 well. This table presents the results of the Kohonen analysis during the flow unit identification process. The transition zone can readily be seen.

Table 6.10 Portion of the ANN Flow Unit Model 3-FU Ball # 19

Portion of the ANN Flow Unit Model 3-FU Well Name: Ball # 19 R Sq ==> 0.829251			
Depth (feet)	Actual Flow Unit	ANN Predicted	F Unit Assigned for R sq Purposes
3100	1	1.0388694	1
3101.25	1	1.0544004	1
3102	1	1.1242173	1
3103	1	1.3730816	1
3104	1	1.3495631	1
3105	1	1.1447512	1
3106	1	1.403694	1
3107.25	1	1.5270721	1.527 transition area
3108	1	1.476661	1.4766 transition area
3108.75	2	1.9162269	2
3109.5	2	1.9839251	2
3110.75	2	1.9939854	2

6.4.1 Predicting Permeability in the Transition Zone

The transition zone has varying porosity and permeability. Based on the core permeability-porosity measurements in the transition zone, permeability is expected to exhibit permeability similar to flow unit one. In addition, the core results indicate low permeability shale streaks as a part of this zone. This will further limit any impact pockets of higher permeability would have in the transition zone.

Table 6.11 Kohonen Network (Three Categories)
(Portion of Table F.2 for the Ball # 19)

ANN Kohonen Analysis of Core Data Set
Winning Neuron is 1.0
Analysis for Three Categories

ANN Inputs =====>		input	input	input	input	input	input	input			
										Network	
Well Name	Depth	gr	rhob	gr'	rhob'	gr bl	rhob bl	K (md)	1	2	3
Ball # 19	3096	41	2.469	-6.648	0.128	123	2.71	0.08	1	0	0
Ball # 19	3097	35.46	2.509	2.216	0.008	123	2.71	0.27	1	0	0
Ball # 19	3098	41	2.519	7.756	-0.04	123	2.71	0.16	1	0	0
Ball # 19	3099	45.43	2.477	-7.756	-0.01	123	2.71	17	1	0	0
Beginning of Transition Zone											
Ball # 19	3100	37.12	2.396	-8.864	-0.11	123	2.71	41	0	1	0
Ball # 19	3101	36.57	2.373	3.324	-0.01	123	2.71	65	0	1	0
Ball # 19	3102	41.55	2.399	7.756	0.096	123	2.71	17	1	0	0
Ball # 19	3103	43.77	2.432	0	0.008	123	2.71	6.79	1	0	0
Ball # 19	3104	44.32	2.377	2.216	-0.04	123	2.71	73	0	0	1
Ball # 19	3105	43.21	2.365	4.432	-0	123	2.71	60	0	1	0
Ball # 19	3106	43.77	2.367	-4.432	0.004	123	2.71	1.16	1	0	0
Beginning of FU 2 and End of Transition											
Ball # 19	3107	39.89	2.362	-2.216	-0.01	123	2.71	110	0	0	1
Ball # 19	3108	40.44	2.307	5.54	-0.01	123	2.71	106	0	0	1
Ball # 19	3109	43.21	2.293	-1.108	0	123	2.71	207	0	0	1

6.4.2 Two Step Process to Model Flow Unit Designation for ANN Permeability Model

In order to utilize model 2-K to predict permeability using the digitized well logs from 125 wells, the transition area had be properly categorized. A two step process was developed to:

- **recognize the transition zone and to**
- **classify the transition zone as flow unit one prior to running the ANN permeability prediction model on the 125 digitized well logs.**

This was accomplished by developing an intermediate ANN flow unit prediction model - model 4-FU. Except for changes to flow unit designations, this model is identical to model 3-FU which utilized the digitized log data. Flow unit designation changes are as follows to the model:

- **Flow unit designation as one remains flow unit one.**
- **Transition zone to be designated as flow unit two.**
- **Flow unit two to be designated as flow unit three.**
- **Lower flow unit one to remain as flow unit one.**

Model 4-K was ran on the digitized log data having the same six log based inputs as the model 3-K. The same constant test set is used. The output was flow unit one, two, or three. The only difference between model 3-FU and model 4-FU is the reclassification of flow units.

It was necessary to designate the flow units for the six digitized core wells. The transition zone was identified using the Kohonen analysis results in Appendix F. along with model 2-K and model 2-FU. The correlation results of model 4-FU are summarized in Table 6.12. This intermediate model successfully predicted the flow units and the transition zone. Table H.3 can be referenced for data utilized in the 1,3,2,1 ANN model.

Table 6.12 Summary of R Squared Values
Flow Unit Prediction for Model 4-FU

WELL	TST	TRN	PRO
Horner # 11	0.9183	0.9719	0.7858
T. Heirs # 8	0.9662	0.9735	1
Horner # 9	0.9472	0.9551	0.9031
Ball # 19	0.9576	0.9858	0.9137
LeMasters # 13	0.9596	0.9797	1
Ball # 18	0.9924	0.9761	0.8759

6.4.3 Preparing the Predicted Flow Units for the ANN Permeability Model

Model 4-FU was applied to the 125 digitized well logs. The flow unit outputs from model 4-FU were manually changed in order to run model 2-K (permeability prediction) on the 125 digitized well logs. In order to predict permeability via model 2-K the unit

designations were re-categorized. The reclassified flow unit designations were the output product of model 4-FU. Figure 6.19 presents the flow unit designations of the intermediate model needed to address the transition zone.

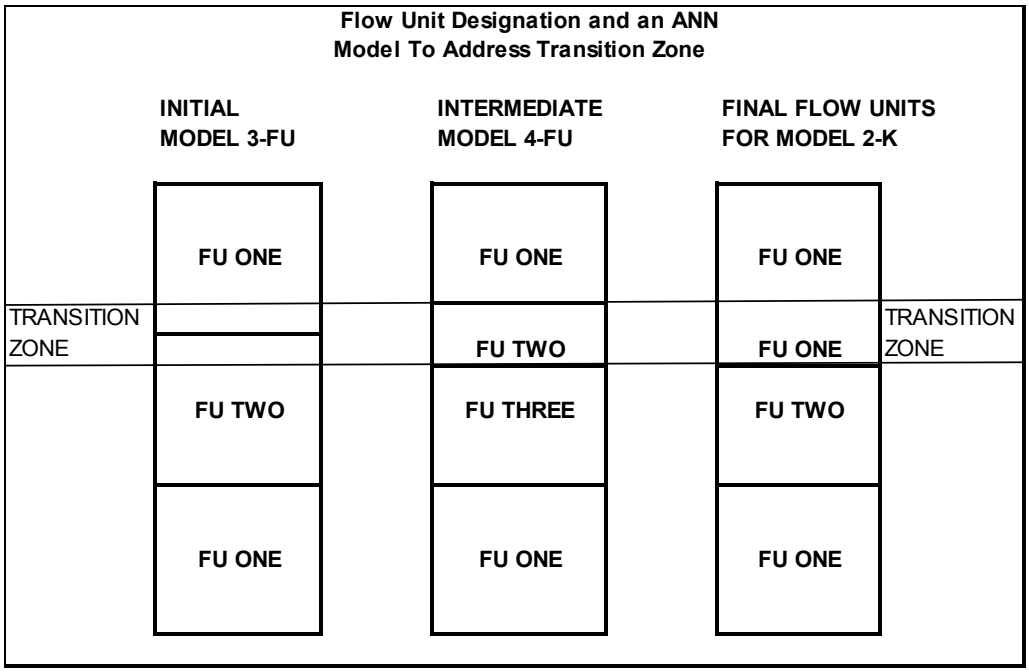

Figure 6.19 Flow Unit Designation and an ANN Model to Address Transition Zone

Flow unit reclassifications occurred as follows:

- **Flow unit one remains flow unit one.**
- **Flow unit two (transition area) is reclassified as flow unit one.**
- **Flow unit three (initial two) is reclassified as flow unit two.**
- **Lower flow unit one remains flow unit one.**

Model 2-K, the selected permeability prediction model was trained using the core data of the six core wells and utilized two flow unit designations for permeability prediction. Due to the success of the intermediate step the model treated the transition zone as flow unit one. Model 2-K for permeability prediction was applied to the digitized well logs in the field (approximately 125 wells). Permeability was predicted within each flow unit every 1/4 foot.

6.5 Two Flow Unit Model Verified via Simulation Results

The Boast98 simulator was utilized on the two flow unit model. The operator had previously used a 12% porosity cut-off for determining the productive interval of the sand. This was the initial screening criteria used for building the simulator model. Simulation runs resulted in the net thickness being reduced further as simulation progressed. Table 6.13 offers additional reservoir properties used in the simulation runs. For each well the table includes net thickness, average permeability and average porosity within each flow unit.

Figures 6.20 and 6.21 graphically detail the cumulative actual production versus predicted (oil and water) for the Ball # 18 well. Figures 6.22 and 6.23 offer a similar presentation for the Ball # 21.

Figures 6.24 and 6.25 are cumulative graphs for both producers combined.

Table 6.13 Average Properties Used in the Simulation

	Flow Unit One			Flow Unit Two		
Well Name	Thickness	Porosity	k (md)	Thickness	Porosity	k (md)
Pennick # 9	2	11	29	6.5	25	186
Pennick # 8	2	12	20	6	25	140
Ball # 18	3	14	31	5	24	190
Ball # 20	1	11	5	7	25	175
Gorrell # 5	3.5	16	16	5	26	137
Ball # 21	5	15	38	7	23	211
Ball # 19	4	15	18	7	22	140
Gorrell # 4	4	16	44	6	24	185

Declining rates of injection in the field appeared to be a common problem in certain wells. The operator recognized an early problem with water quality. This problem was addressed by the operator. However, certain wells have continued to require periodic treatment as a means of maintaining acceptable injection rates. Records and pressure build-up information to estimate an after treatment skin value was very limited. A specific records search was made of the well files to refine the PID input. Only a few treatment

records were found. For the simulation analysis a PID value for each well was calculated which included an assumed skin value of –1. The skin value of –1 had been used by company engineers in other internal work product.

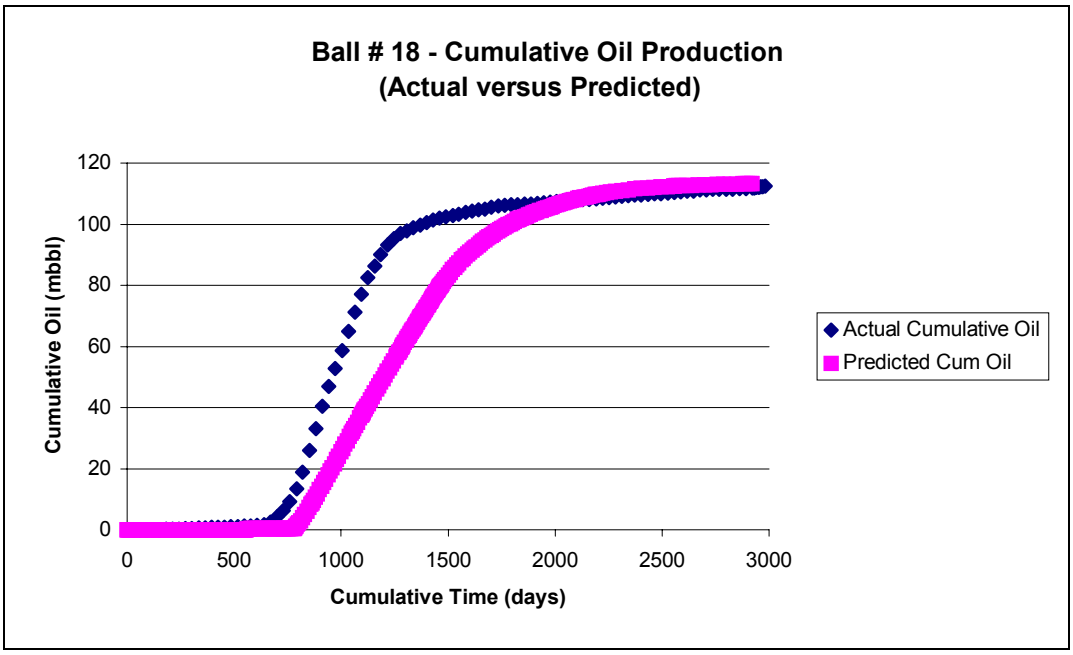

Figure 6.20 Ball # 18 Cumulative Oil Production (Actual versus Predicted)

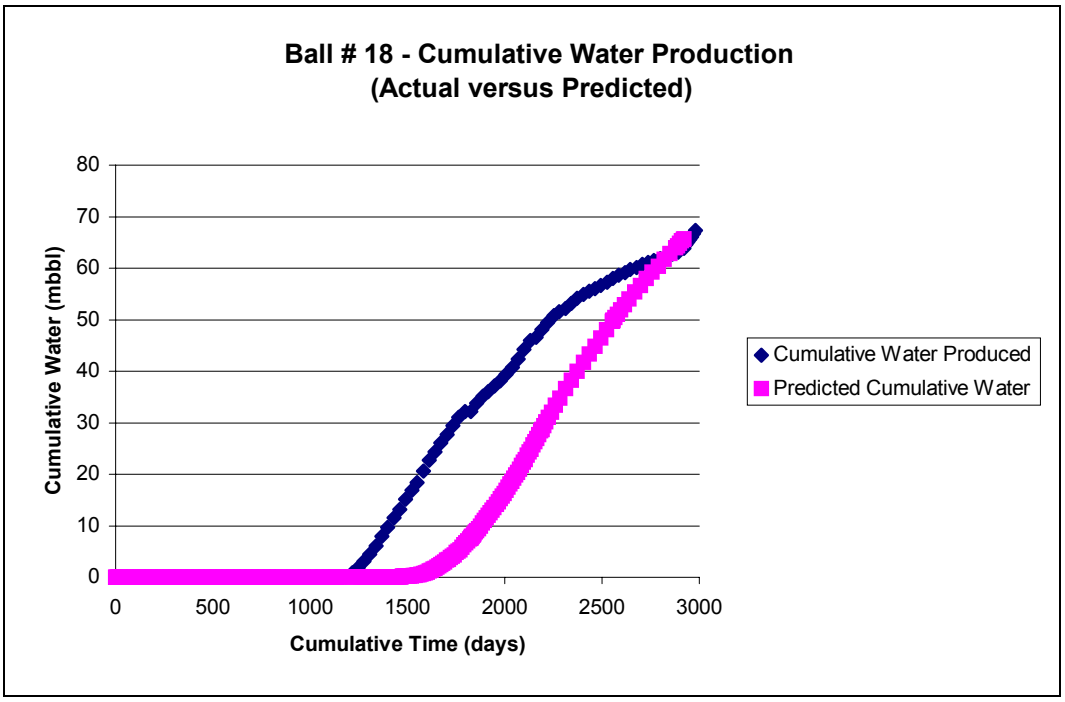

Figure 6.21 Ball # 18 Cumulative Water Production (Actual versus Predicted)

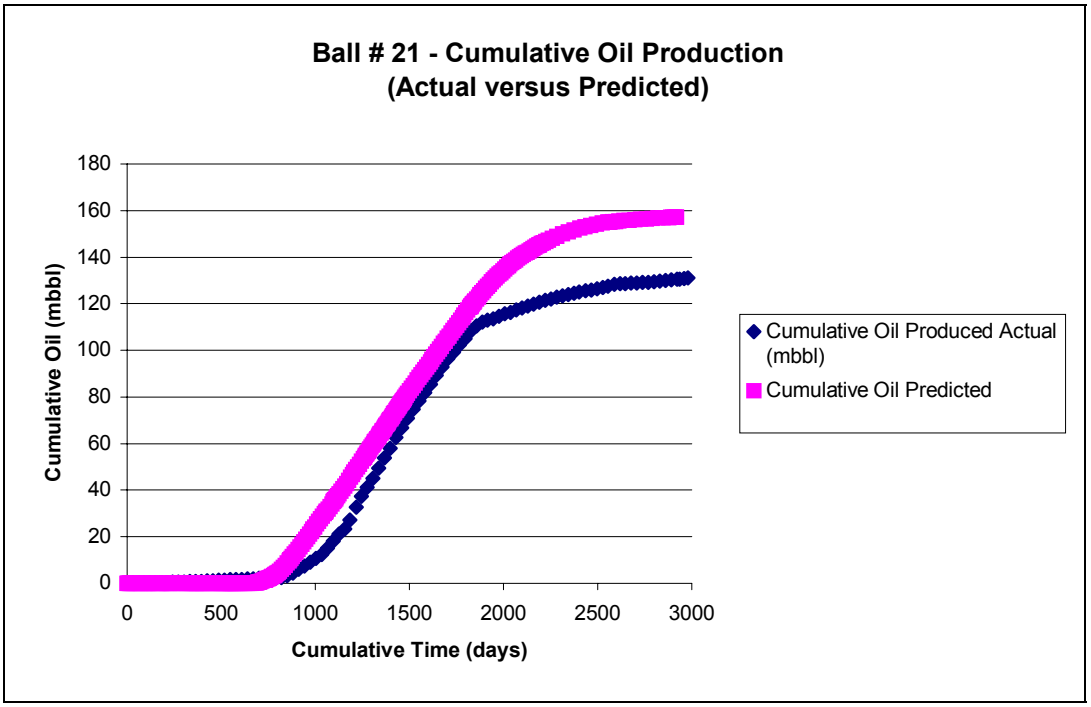

Figure 6.22 Ball # 21 Cumulative Oil Production (Actual versus Predicted)

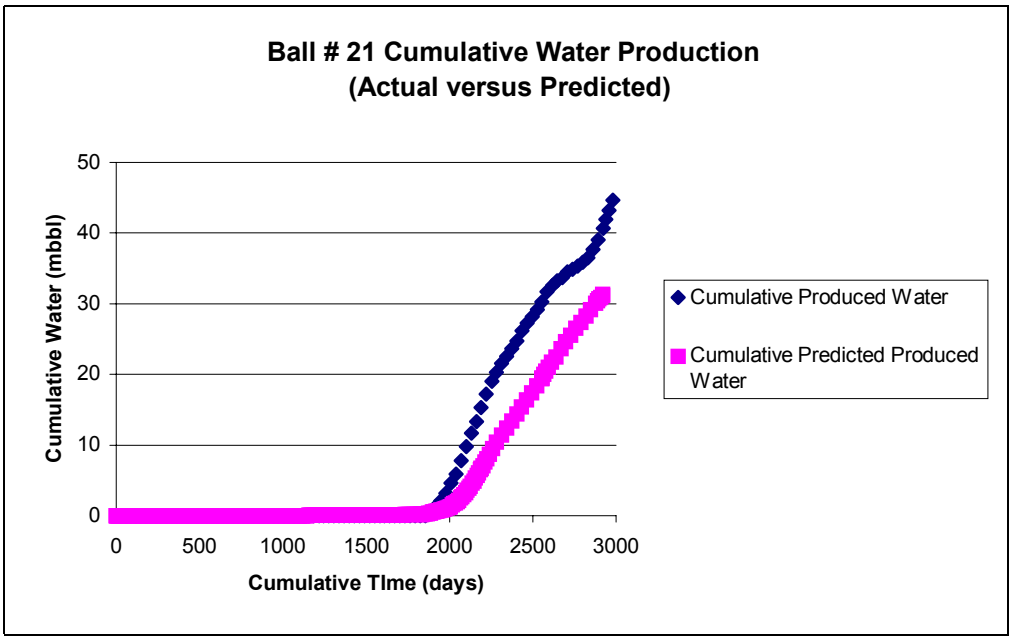

Figure 6.23 Ball # 21 Cumulative Water Production (Actual versus Predicted)

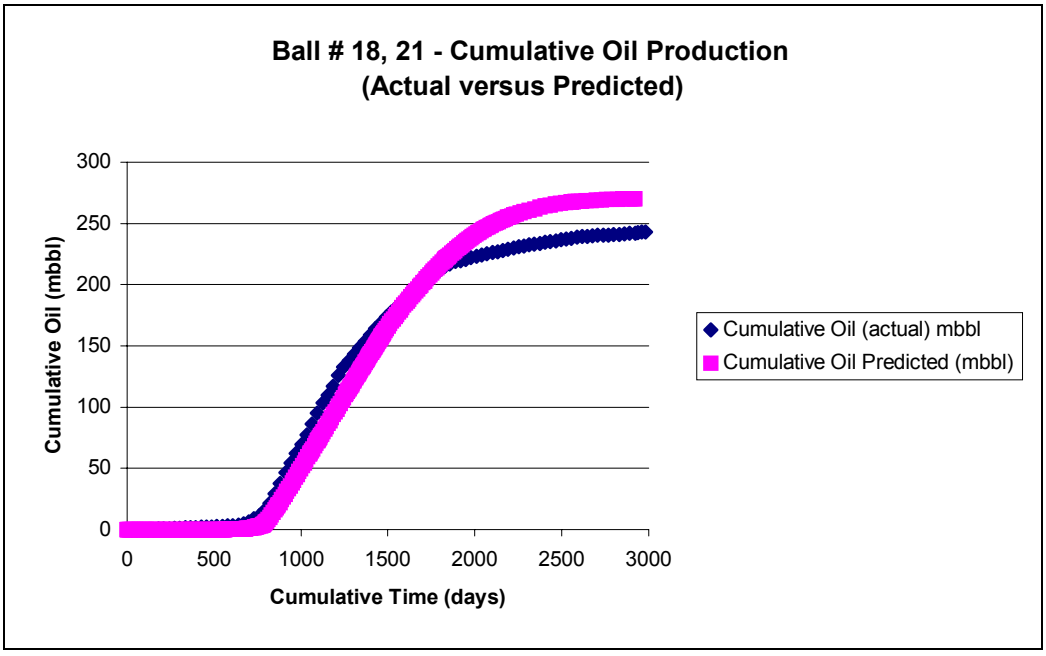

Figure 6.24 Ball #18, 21 Cumulative Oil Production (Actual versus Predicted)

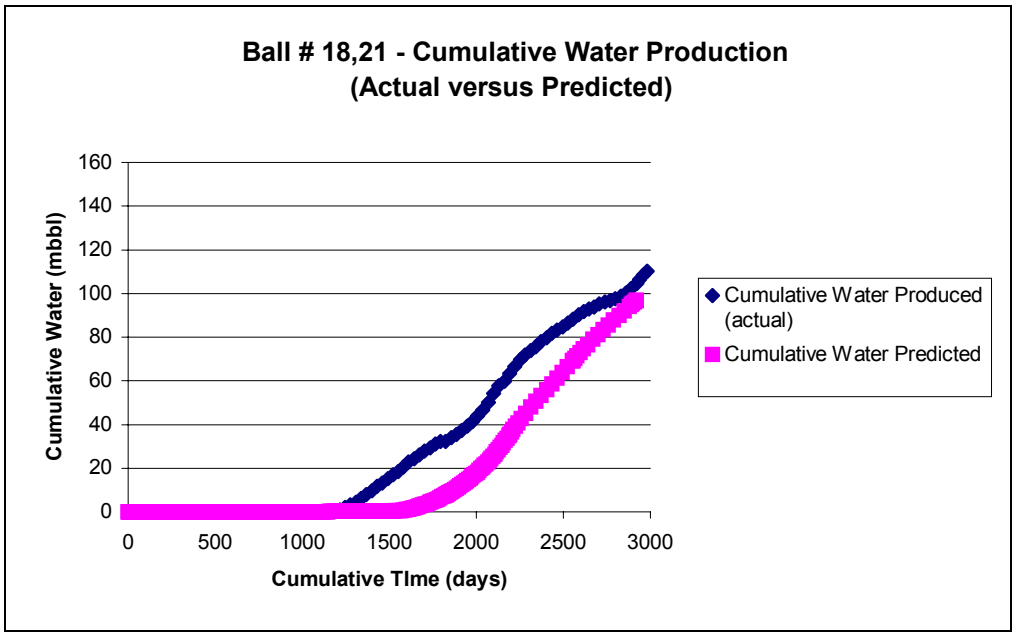

Figure 6.25 Ball #18, 21 Cumulative Water Production (Actual versus Predicted)

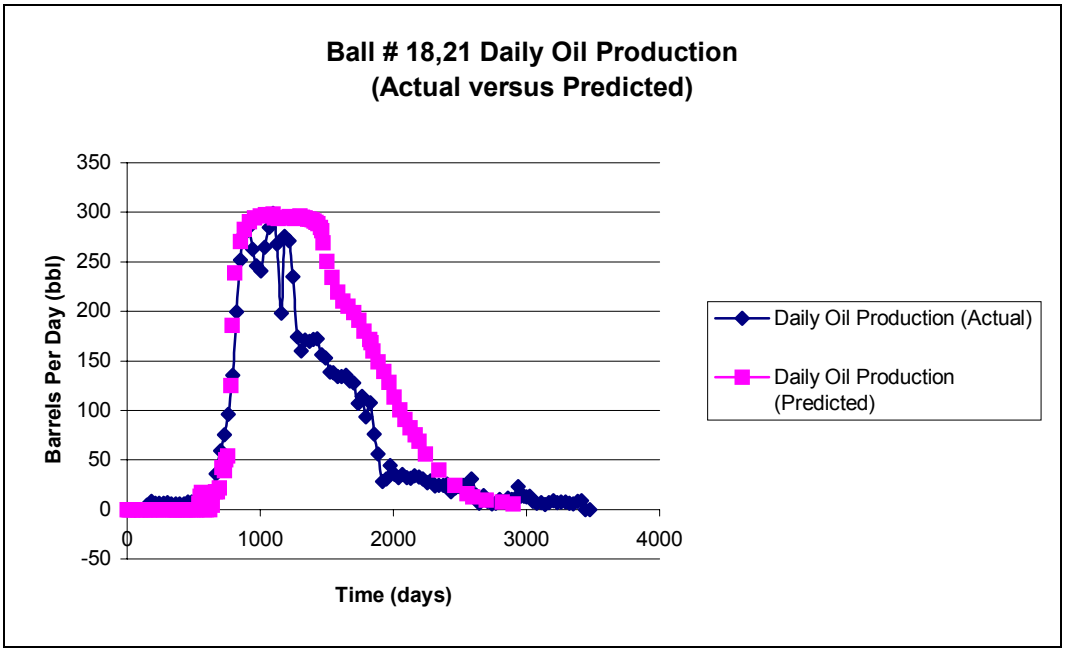

Figure 6.26 Ball # 18, 21 Daily Oil Production (Actual versus Predicted)

6.6 Single Layer Simulation Comparison

As further study of the Ball # 18, 21 patterns a single layer simulation was completed. The simulation was done using the core permeability data for the Ball # 18, 19 wells. Both core wells are situated in the two verification patterns. In order to predict permeability from the digitized logs in the pattern a plot of core permeability versus log porosity was completed for the two core wells (Figure 6.27). An exponential equation was developed as a method of predicting permeability from the best fit trendline. The R squared is .6864.

The digitized logs for each well in the pattern were used to predict permeability for the given wells in the pattern. The porosity cut-off was 12%, a historical value used by the operator. Values for average porosity and permeability between the wells in the pattern were extrapolated.

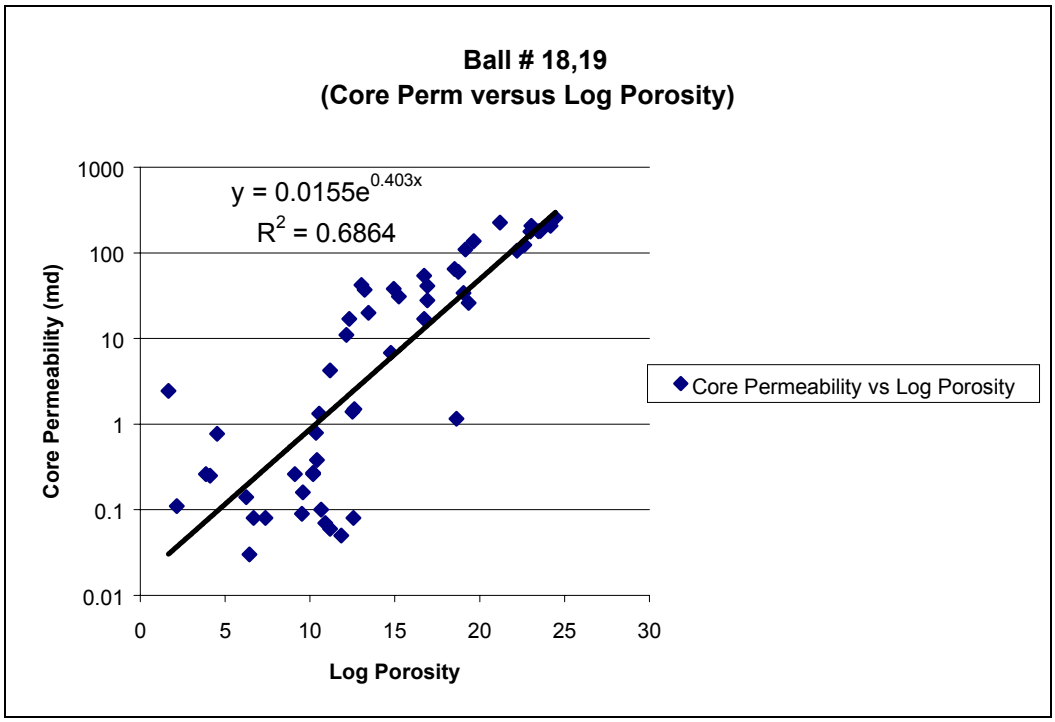

Figure 6.27 Ball # 18,19 (Core Perm versus Log Porosity)

All other simulation inputs were the same as those used in the two layer simulation model. This included water volumes scheduled into the patterns, relative permeability data and flowing pressures at each producing well. The intent was to develop a valid comparison of the single layer system to the two flow unit model. Figures 6.28 and 6.29 present cumulative oil and water production comparisons of actual versus predicted production for both wells combined. Figures 6.30 and 6.31 present both wells individually.

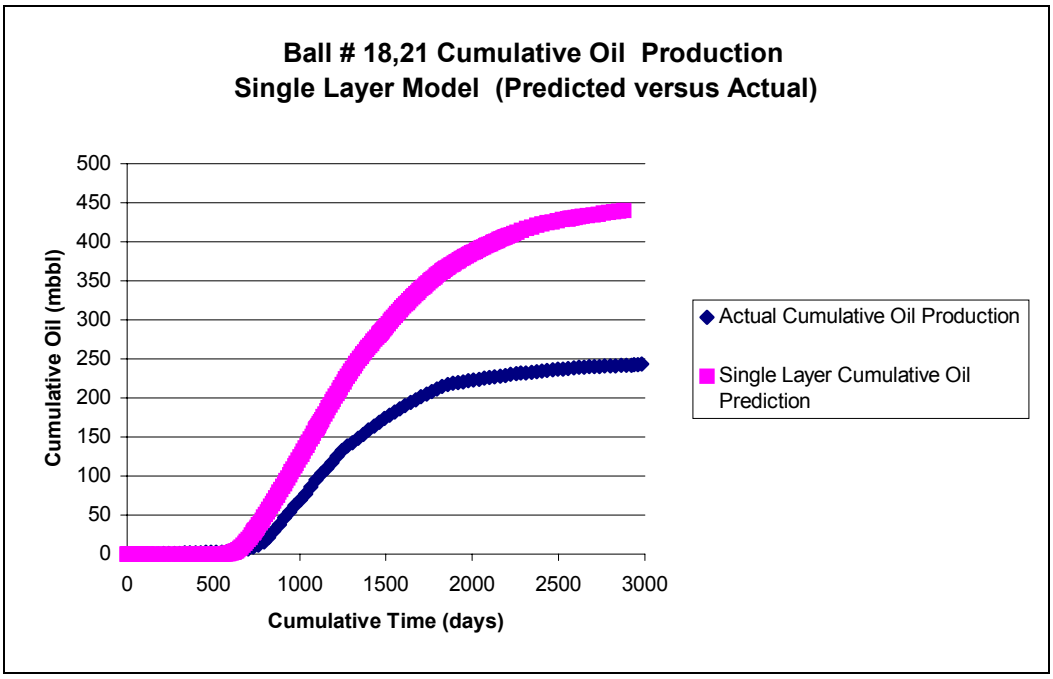

Figure 6.28 Ball # 18, 21 Cumulative Oil Production Single Layer Model (Predicted versus Actual)

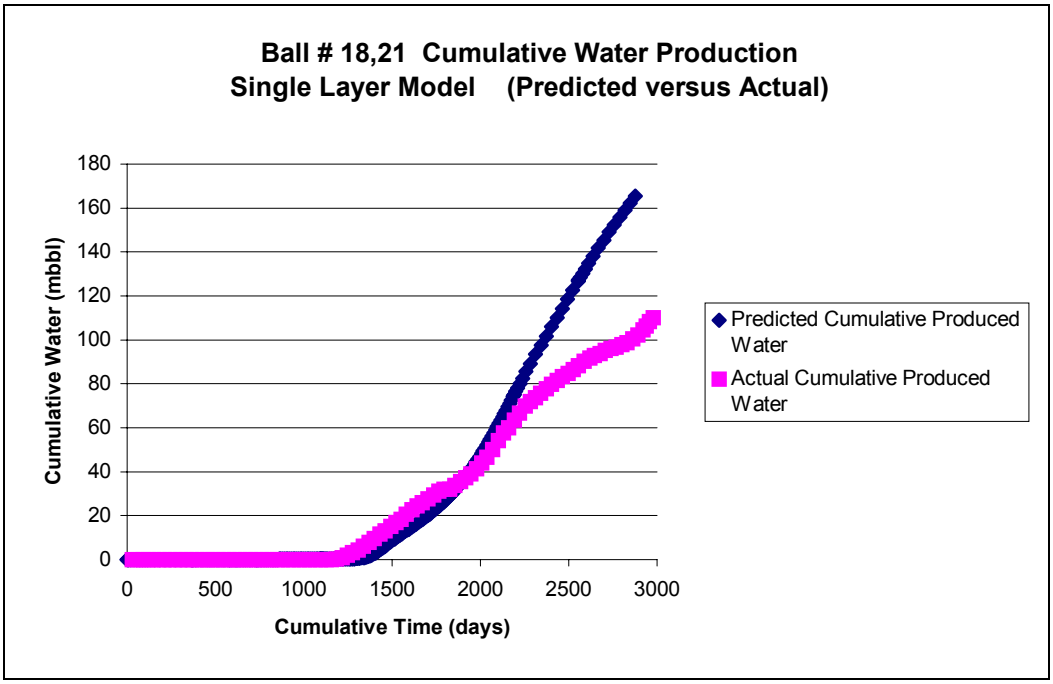

Figure 6.29 Ball # 18, 21 Cumulative Water Production Single Layer Model (Predicted versus Actual)

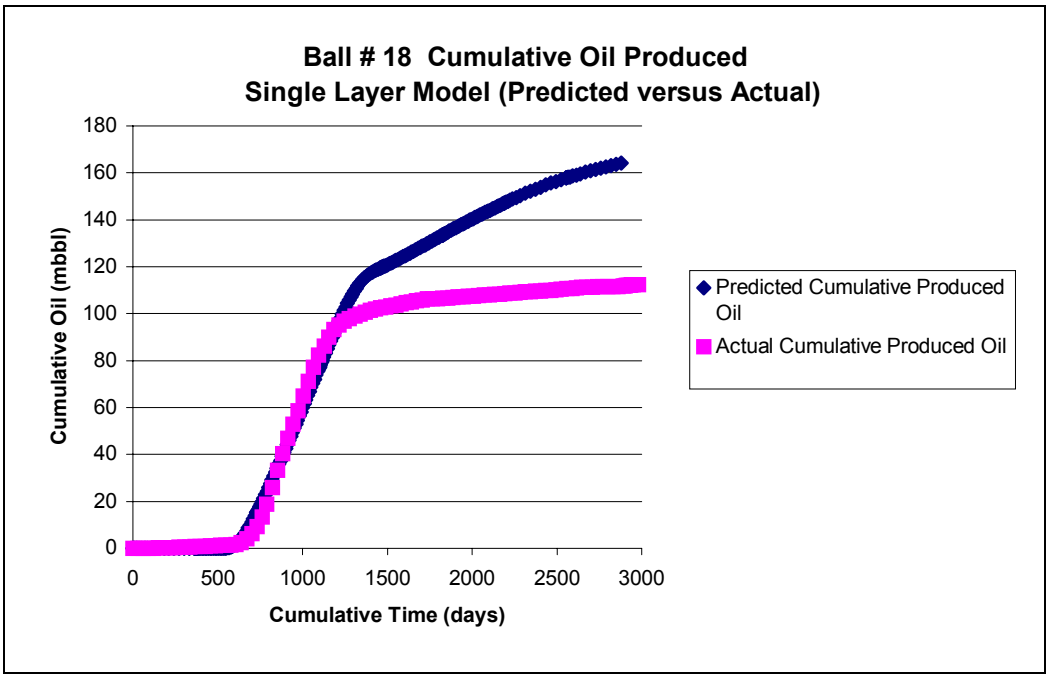

Figure 6.30 Ball # 18 Cumulative Oil Produced Single Layer Model (Predicted versus Actual)

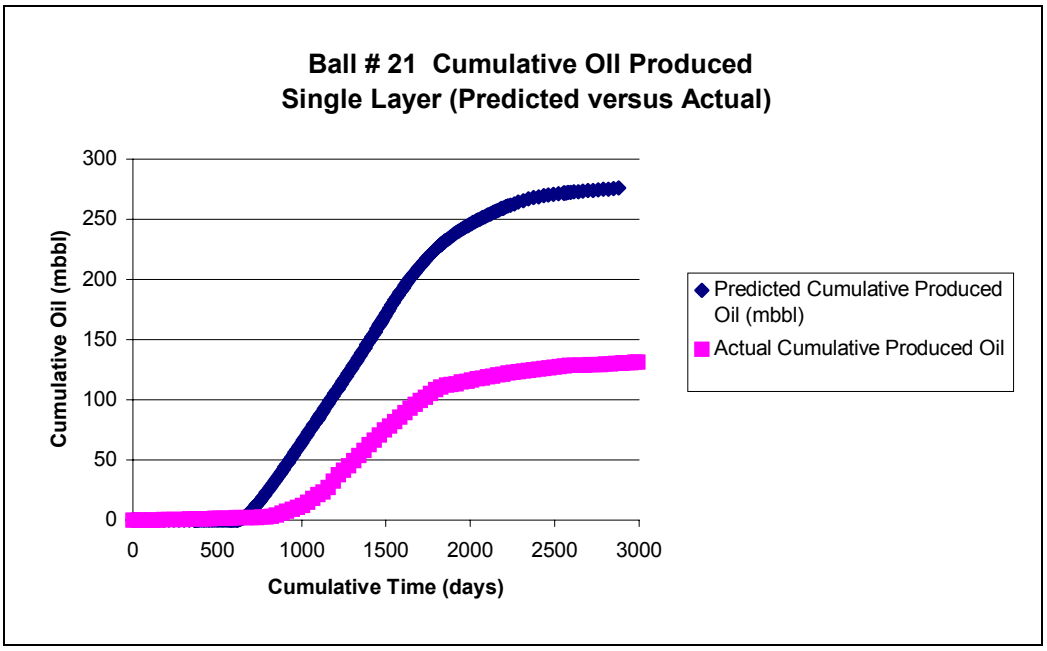

Figure 6.31 Ball # 21 Cumulative Oil Produced Single Layer Model (Predicted versus Actual)

6.7 Field Maps Generated

The two final neural network models were applied to the digitized well data for 125 wells in the field. Model 4-FU (flow unit prediction) was initially utilized to predict flow units. The flow unit results were then prepared for use as an input in model 3-K (permeability prediction). The results of the neural network permeability prediction were combined with the flow unit thickness data. For each flow unit average permeability and thickness was determined. Appendix Tables I.1 and I.2 detail the 125 well summary data. This well data was utilized to generate a series of field maps showing the distribution of average permeability, thickness, and flow capacity (kh) for each flow unit in the field. Figures 6.32 - 6.37 present the field maps for each individual flow unit. It is important to note that only flow units one and two are included on the referenced maps. Other productive intervals of sand do exist in parts of the field at lower intervals.

Figure 6.38 is a field map based on cumulative production records secured from the operator. The production history was maintained on a farm/lease basis. In order to develop a cumulative per well production map, the total farm production was divided by the number of wells on each farm. Figures 6.35 - 6.37 present flow unit two. The primary production map for the field correlates well with the predicted flow unit two. Flow two has higher porosity and

largely accounts for the flow capacity. This further confirms the methodology used to predict flow units and permeability.

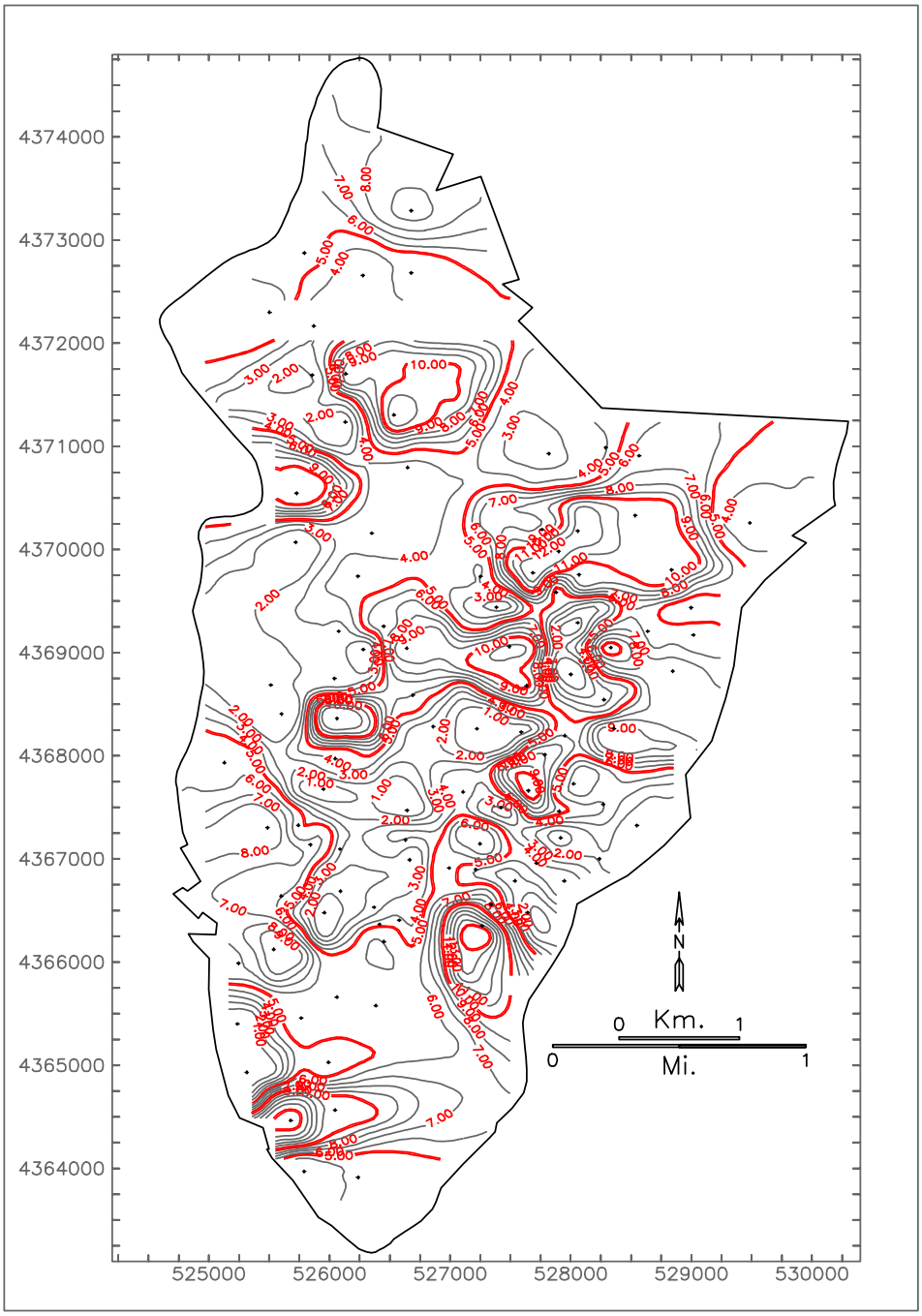

Figure 6.32 Flow Unit One (Thickness)

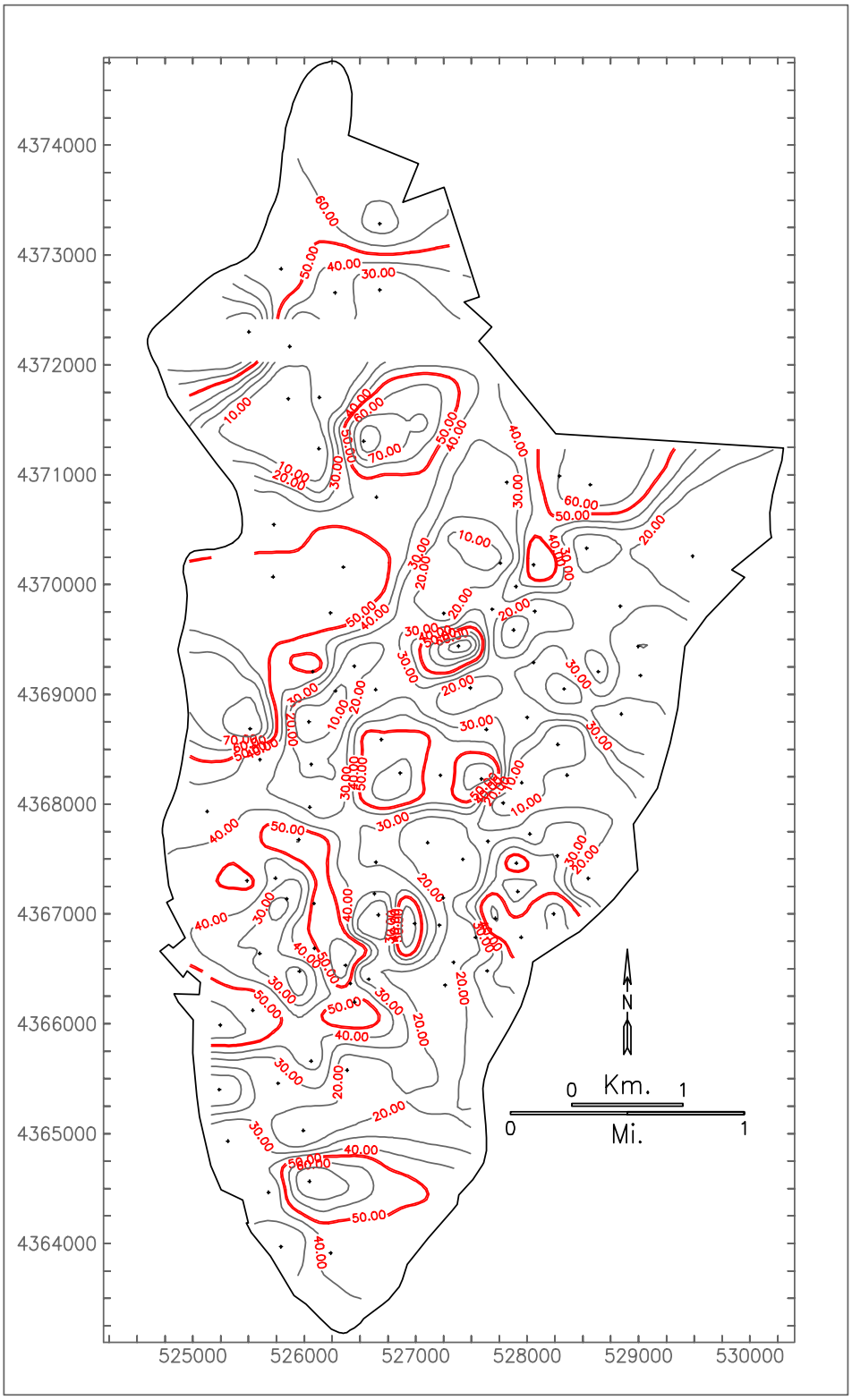

Figure 6.33 Flow Unit One (Average Permeability)

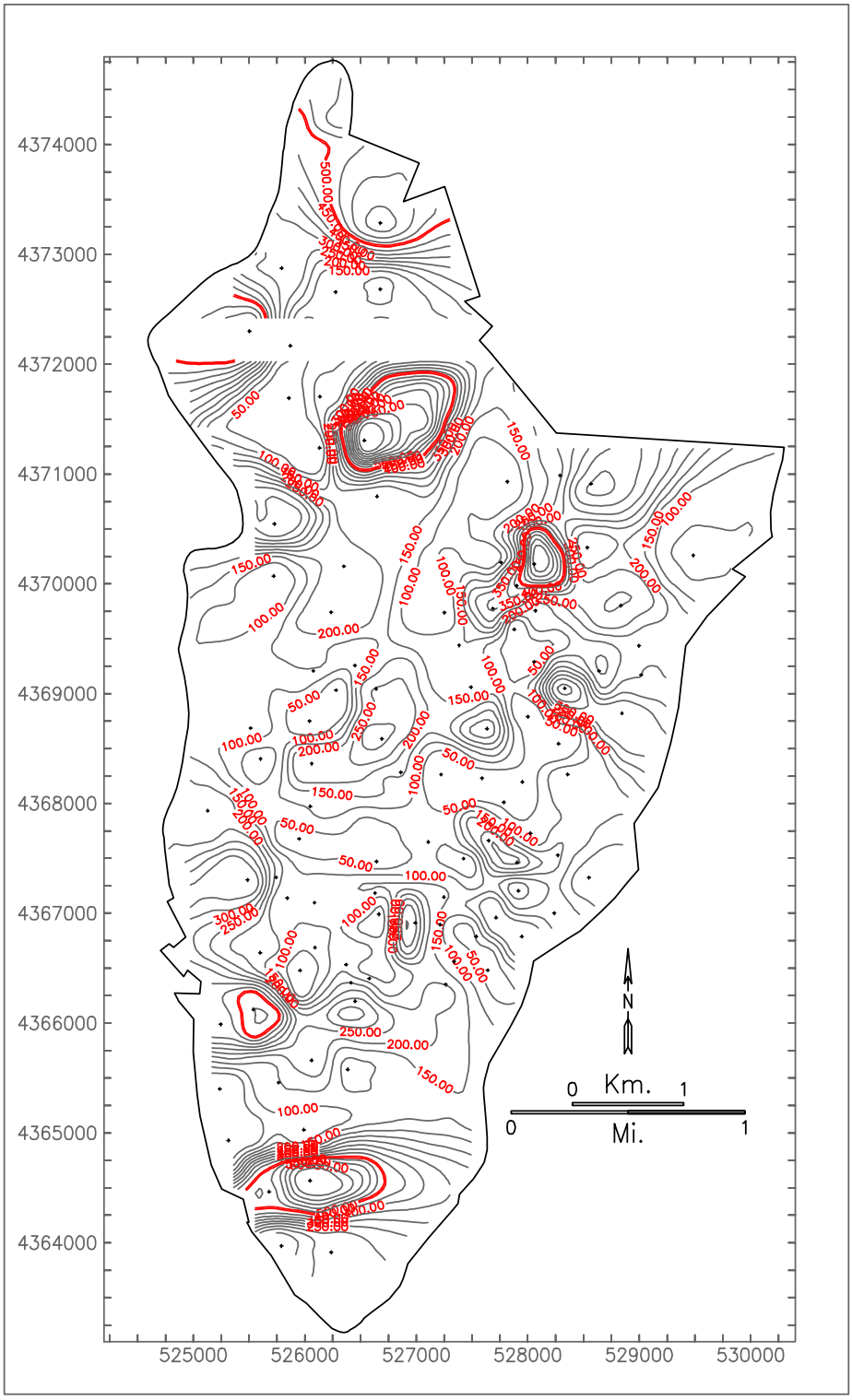

Figure 6.34 Flow Unit One (kh)

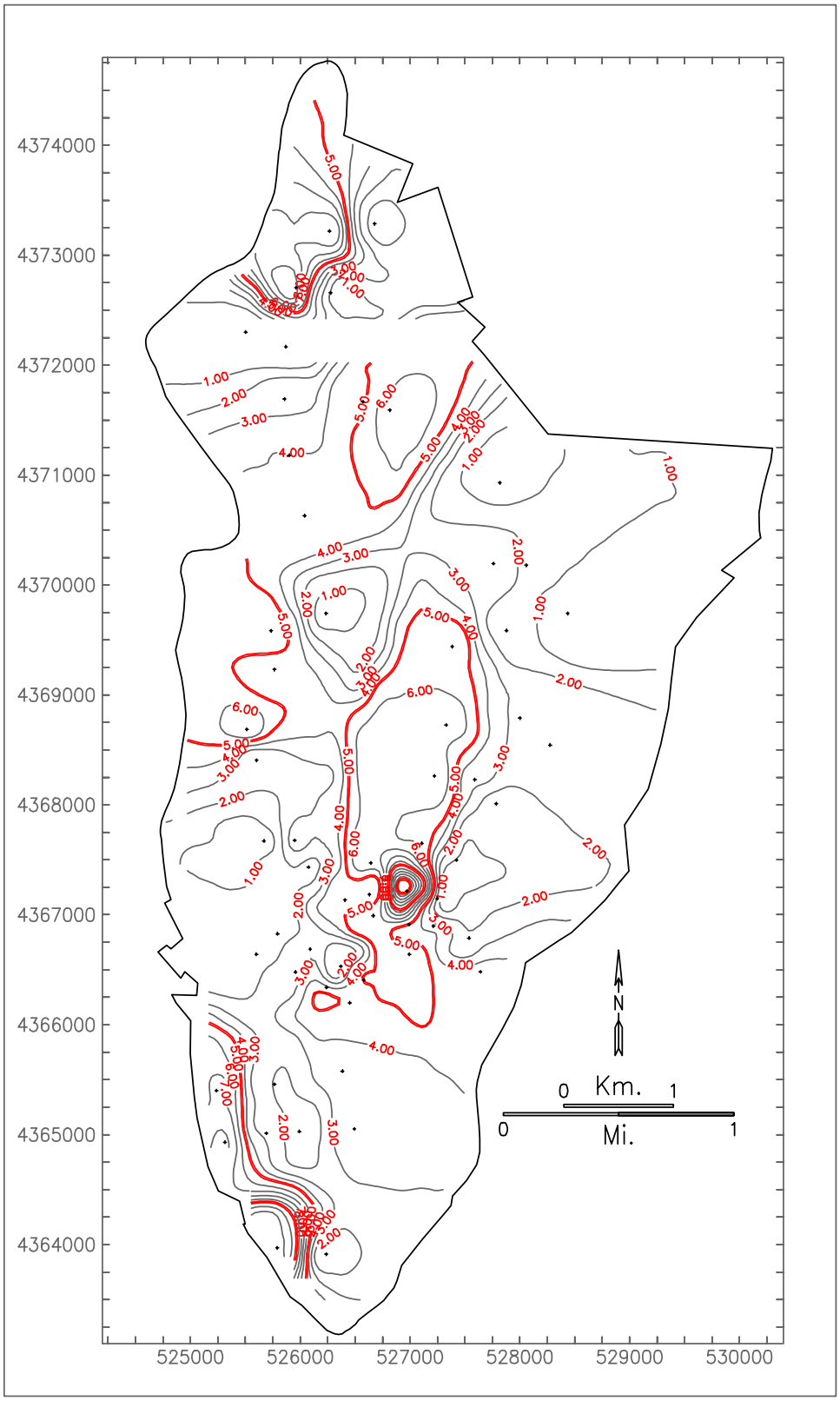

Figure 6.35 Flow Unit Two (Thickness)

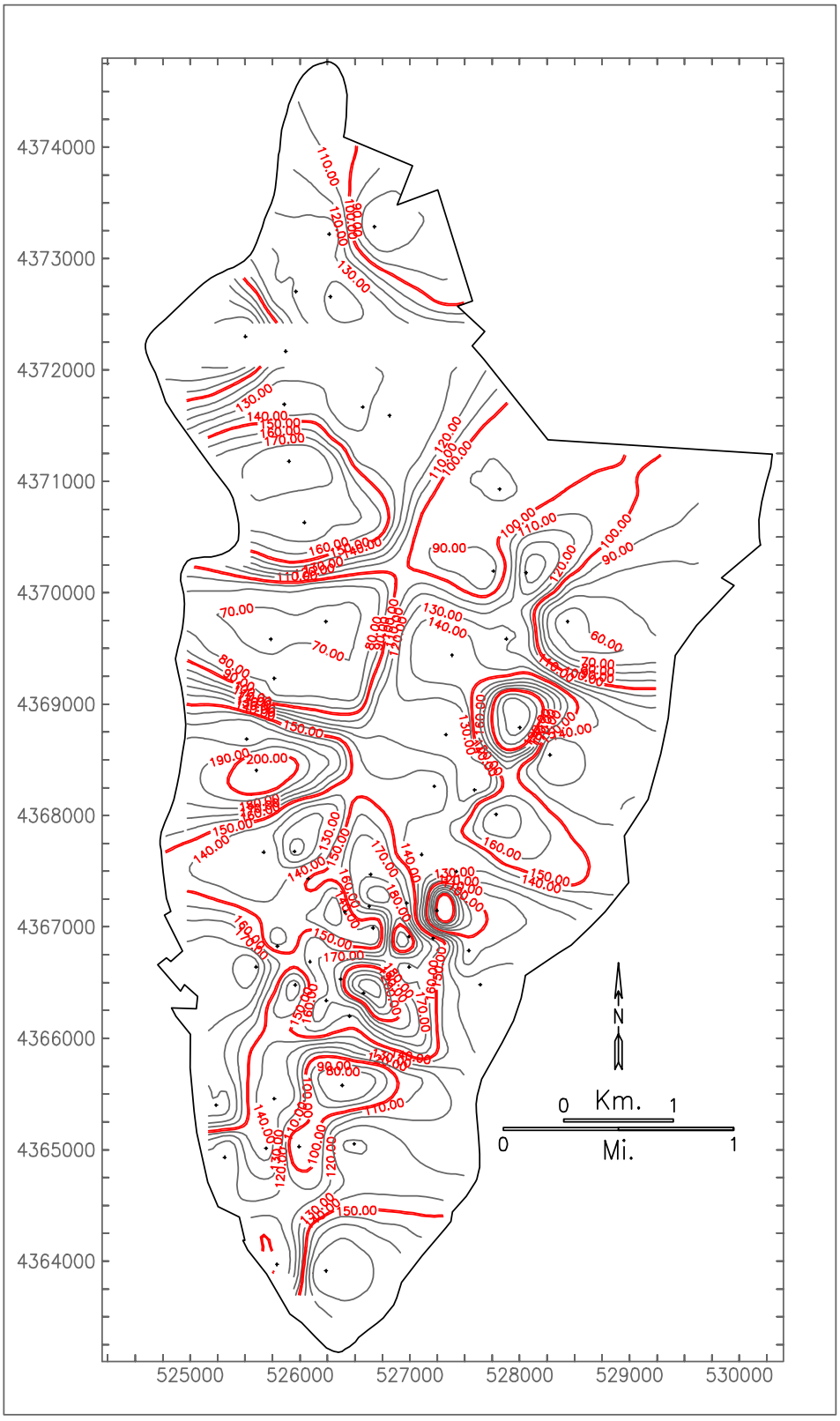

Figure 6.36 Flow Unit Two (Average Permeability)

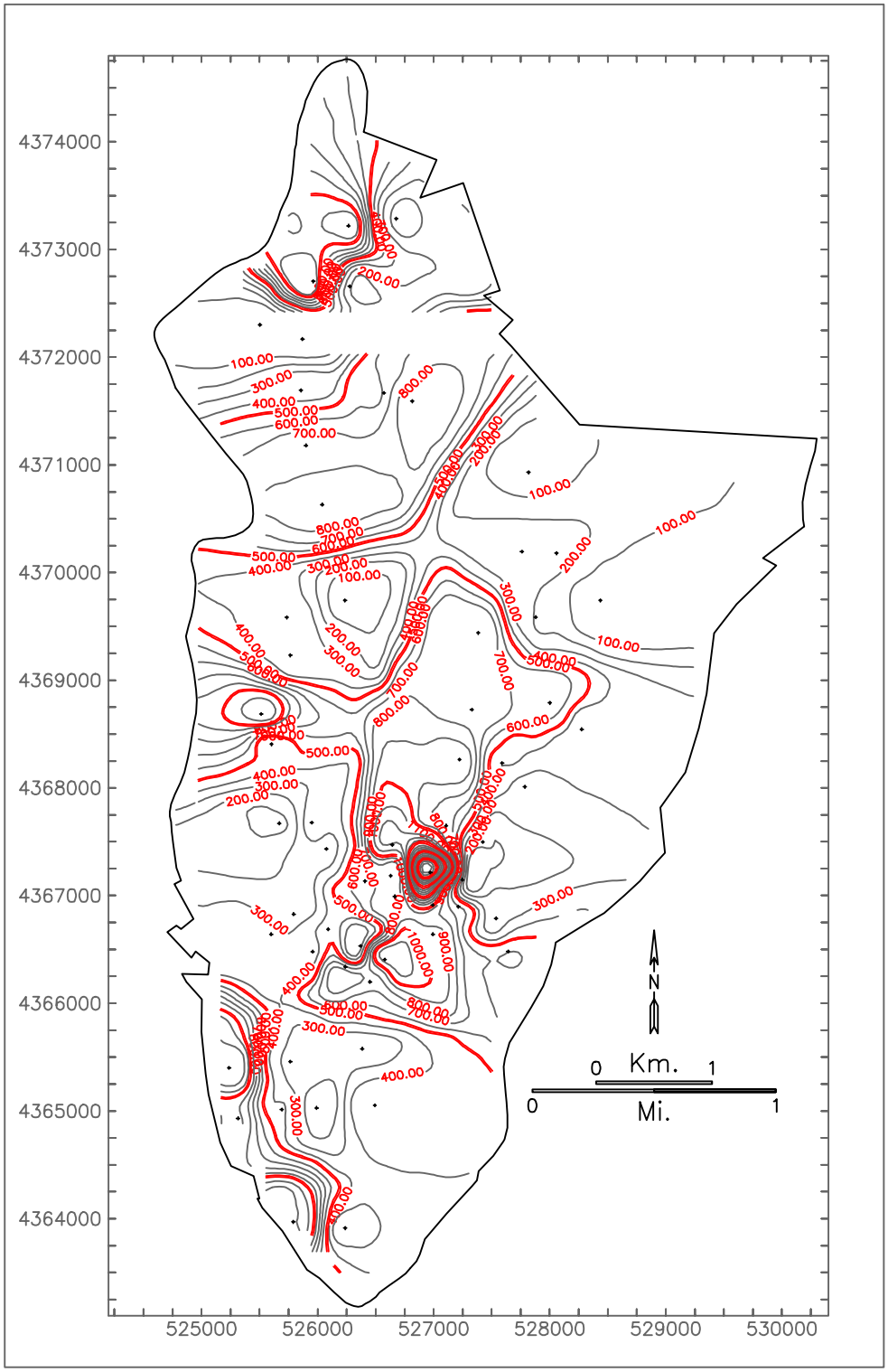

Figure 6.37 Flow Unit Two (kh)

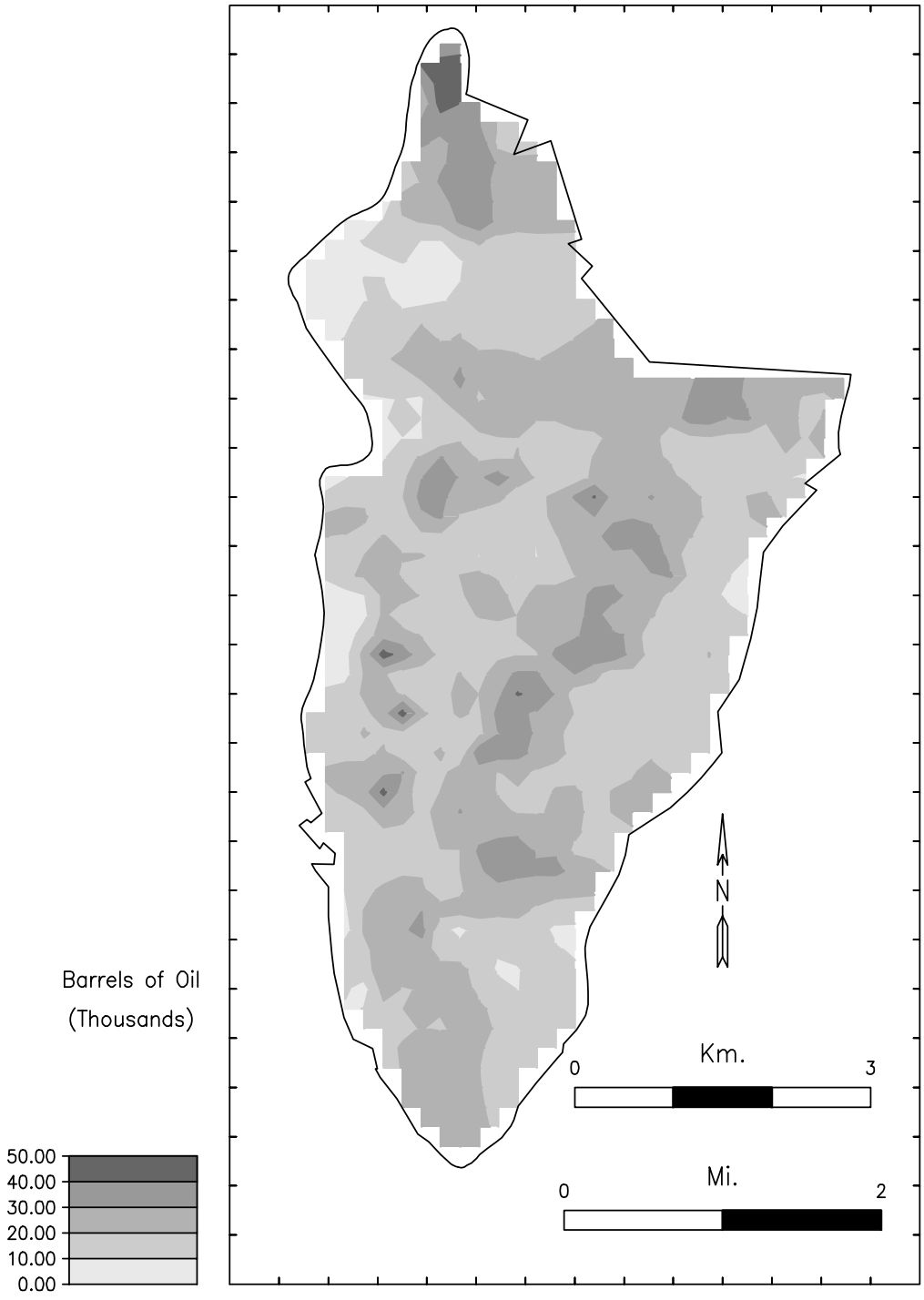

(records available per farm only – per well production averaged by farm)

Figure 6.38 Cumulative Primary Production Map - Per Well Basis

6.8 Methodology Summary - Overview

6.8.1 Flow Unit Value

Identifying flow units for a given well can be done using complete core data, thin sections and ex-ray diffraction. The ability to predict permeability is improved when flow units are known. However, many fields have limited core data from only a few wells in a given field. Further no special testing of the cores exists as a means of defining flow units. This flow unit prediction methodology for wells having only electric log data is new and can be utilized with limited permeability data.

6.8.2 Methodology Summary

This methodology requires a few wells in a given field have some core plug data. From these core plugs, permeability and porosity measurements can be obtained. The core wells should also have electric log data. The methodology calls for utilizing the core data and electric logs to identify the flow units and to build an ANN model to predict flow units. A separate ANN model to predict permeability is also constructed that includes flow unit as an input. The work to this point of the methodology has been strictly using the core wells and their associated logs. The core wells and the ANN models developed are then utilized to predict flow units in the field

for wells having only log data. Within each predicted flow unit in the field permeability can be predicted using the predicted flow unit as an input in the ANN permeability model.

6.8.3 Steps Leading to Flow Unit Identification Using Only Well Log Data

Initial flow unit identification occurs by using the limited core permeability and porosity data from a few wells (in this case six wells - 95 data points). As a part of the methodology, the preliminary flow unit identification is utilized in order to identify flow units in the core wells. Techniques utilized include graphic analysis of the core data to identify the permeability-porosity relationships within each flow unit. In addition neural network analysis of the core wells is performed on the log-based data along with the core permeability.

A backpropagation ANN model was developed to predict permeability. Within each flow unit the log response to permeability is related. The inclusion of the identified flow units as an input significantly enhanced permeability prediction. The use of the ANN model to predict permeability is also a method to confirm that the flow units have been identified correctly. The strongest ANN permeability model occurs when flow units have been correctly identified.

Permeability prediction field wide is a useful product of reservoir characterization. However, the permeability prediction

model requires flow unit designation. The flow unit was identified in the six core wells due to core data being available. In order to predict permeability the flow unit must be identified in non-cored well. In this study there were 125 digitized electric logs (gamma ray-density) from existing wells in the field.

Having identified the flow units in the core wells a new approach is utilized as a means of flow unit identification. Flow unit identification is accomplished by developing a new backpropagation model for flow unit prediction. The flow units identified in the six core wells and the digitized logs are used for developing an ANN for flow unit prediction. The ANN for flow unit prediction is built using six log-based inputs. The resulting model can predict flow unit using only log-based data. No core permeability data is required. No additional special core testing is required.

By being able to predict the flow unit in the field - we can then predict permeability utilizing the previously developed permeability prediction model. The prediction of flow units can be accomplished for wells having only log data in the field. The permeability field wide can then follow as a result of the key step of flow unit identification using only well logs.

CHAPTER 7

CONCLUSIONS

1. **The artificial neural network was successfully developed to predict flow units utilizing only well log data.**

2. **By including flow unit as an input in the artificial neural network significantly improved permeability prediction.**

3. **Minipermeameter measurement is a valuable source of information for flow unit identification. The measurements correlated well with actual core permeability-porosity measurements when comparing cumulative storage capacity versus cumulative flow capacity. As a result they provided significant flow unit boundary clues between core data points.**

4. **The permeability-porosity methods for flow unit identification coupled with neural network analysis successfully identified the flow units in the reservoir.**

5. **Neural network analysis (Kohonen) of log based well data with permeability data is a useful tool for flow unit identification. The Kohonen analysis identified a lower flow unit as being the same as flow unit one and identified a transition zone between flow units one and two.**

6. **Utilizing the predetermined test set resulted in a stronger ANN model being developed for permeability prediction.**

7. **The flow units identified by the methodology were verified via simulation and the earlier Gil (2000) research.**

8. **This reservoir characterization methodology has application in any reservoir having multiple flow units.**

CHAPTER 8

RECOMMENDATIONS

1. **Although not directly a part of this research thin section analysis evaluated the grain size of samples taken from selected core sections. It would have been helpful if the thin section work had been from samples adjacent to the core plugs used as a part of this research. The opportunity to include grain size as another flow unit identification method could have been further strengthened the flow unit boundaries identified herein.**

2. **During simulation the percentage of total water entering the patterns from each injector was low. Corner and center injectors were 19% and 32%, respectively. Ideal percentages would have been 25% and 50%. The low percentage of water scheduled into the pattern may be inherent of the simulator or may have actually occurred. In the event another part of the field is simulated another simulator may be useful to interpret the injection results.**

3. **The minipermeameter measurements were done on old, partially preserved cores. Measurements on fresh cores offer obvious advantages. If coring is planned a plan to measure miniperm measurements for the entire cored section is recommended.**

4. **Further investigation of the transition zone in another part of the reservoir should be considered.**

REFERENCES

Amaefule, J., Altunbay, M., Taib, D., Kersey, D., "Enhanced Reservoir Description: Using Core and Log Data to Identify Hydraulic (flow units) and Predict Permeability in Uncored Intervals/Wells," Society of Petroleum Engineers paper 26436. Presented at the sixty eighth Annual SPE Conference. October 1993.

Aminian, K., Ameri, S., Avary, K.L., Bilgesu, H.I., Hohn, M.E., McDowell, R.R., and Matchen, D.L., "Reservoir Characterization of the Upper Devonian Gordon Sandstone, Jacksonburg, Stringtown Oil Field, Northwestern West Virginia," Semi-Annual Report, October 1, 1999 - March 31, 2000. October 1999.

Aminian, K., Ameri, S., Avary, K.L., Bilgesu, H.I., Hohn, M.E., McDowell, R.R., and Matchen, D.L., "Reservoir Characterization of the Upper Devonian Gordon Sandstone, Jacksonburg, Stringtown Oil Field, Northwestern West Virginia," Semi-Annual Report, April 1, 1999 - September 30, 1999. October 1999.

Boone, D.A., King, P.E., Jr., Ferrebee, Mack, "Stringtown Field Report and 1986 Proposed Waterflood Development, Tyler and Wetzel Counties, West Virginia" internal Pennzoil memo. April 14, 1986, p. 25.

Craig, F., Wilcox, P., Ballard, J., Nation, W., "Optimized Recovery Through Continuous Interdisciplinary Cooperation," Society of Petroleum Engineers paper 6108. Journal of Petroleum Technology. July 1977. 755-60.

Davies, D., Vessell, R., Auman, J., "Improved Prediction of Reservoir Behavior Through Integration of Quantitative Geological and Petrophysical Data," Society of Petroleum Engineers Reservoir Evaluation & Engineering, April 1999. 149-160.

Ebanks, W. J., "Flow Unit Concept - Integrated Approach for Engineering Projects," Abstract presented June 8, 1987 during the roundtable sessions at the 1987 American Association of Petroleum Geologists Annual Convention.

Gil, E., "Improving The Simulation of a Waterflood Recovery Process Using Artificial Neural Networks," West Virginia University. Thesis Publication 2000.

Gunter, G., Finneran, J., Hartmann, D., Miller, J., "Early Determination of Reservoir Flow Units Using An Integrated Petrophysical Method," Society of Petroleum Engineers paper 38679. Presented at the 1997 SPE Annual Technical Conference. October 1997.

Harris, D.G., "The Role of Geology in Reservoir Simulation Studies," Society of Petroleum Engineers paper 5022.

Hearn, C. L., "Geological Factors Influencing Reservoir Performance of the Hartzog Draw Field," Journal of Petroleum Technology. August 1984. 1335-1346.

Holtz, M.H., Hamilton, D.S., "Reservoir Characterization Methodology to Identify Reserve Growth Potential," Society of Petroleum Engineers paper 35434. Presented at the 1996 SPE/DOE Tenth Symposium on Improved Oil Recovery.

Lewis, J.J.M., "Outcrop-Derived Quantitative Models of Permeability Heterogeneity for Genetically Different Sand Bodies," Society of Petroleum Engineers paper 18153. Presented at the sixty third Annual Technical Conference and Exhibit of the Society of Petroleum Engineers. 1988.

Monroe, J. S., Wicander R., "Physical Geology - Exploring The Earth," West Publishing Company, St. Paul, MN. 1992.

NeuroShell tutorial program, © Ward Systems Group, Inc.

Mohaghegh, S., Arefi, R., Ameri, S., Rose, D., "Design and Development of an Artificial Neural Network for Estimation of Formation Permeability," Society of Petroleum Engineers paper 28237. Presented at the SPE Petroleum Computer Conference. 1994.

Mohaghegh, S., Arefi, R., Ameri, S., Hefner, M., "A Methodology Approach For Reservoir Heterogeneity Characterization Using Artificial Neural Networks," Society of Petroleum Engineers paper 28394. Presented at the SPE Annual Technical Conference and Exhibit. September 1988.

Mohaghegh, S., "Virtual-Intelligence Applications in Petroleum Engineering: Part 1-Artificial Neural Networks," Journal of Petroleum Technology. September 2000.

Neog, P.K., Borah, N.M., "Reservoir Characterization Through Well Test Analysis Assists in Reservoir Simulation - A Case Study," Society of Petroleum Engineers paper 64447.

Oyerokun, A.A., "A New Approach For Training and Testing Artificial Neural Networks For Permeability Prediction," West Virginia University. Thesis Publication 2002.

Petroleum Technology Transfer Council (PTTC)., "New Methods of Acquiring Permeability Data from Appalachian Basin Reservoir Rocks," NRCCE/WVU, Morgantown, WV. October 11, 2000.

Slatt, R.M., Hopkins, G.L., "Scales of Geological Reservoir Description for Engineering Applications: North Sea Oilfield Example," Society of Petroleum Engineers paper 18136. Presented at the sixty third Annual Technical Conference and Exhibition of the SPE. October 1988.

Soto, R.B., Torres, F., Arango, S., Cobaleda, G., "Improved Permeability Models from Flow Units and Soft Computing Techniques: A Case Study, Suria and Reforma-Libertad Fields, Columbia," Society of Petroleum Engineers paper 69625. Presented at the SPE Lation American and Caribbean Petroleum Engineering Conference. March 2001.

Soto, R.B., Garcia, J.C., Torres, F., Perez, G.S., "Permeability Using Hydraulic Flow Units and Hybrid Soft Computing Systems," Society of Petroleum Engineers paper 71455. Presented at the 2001 annual SPE Conference. October 2001.

Tiab, D., Donaldson, E., "Petrophysics - Theory and Practice of Measuring Reservoir Rock and Fluid Transport Properties," Gulf Publishing Company, Houston, Texas. 1996.

Triola, M.F., "Elementary Statistics," Seventh Edition, Addison Wesley Longman, Inc., Reading, Massachusetts. 1998.

Willhite, G. P., Waterflooding, Monogram Series, Society of Petroleum Engineers, Richardson, Texas (1986). Chapter 7 referred to extensively.

APPENDIX A.

Appendix A. presents graphs of core porosity, log density, core permeability, minipermeability and gamma ray versus depth for each core well. The associated tables used to develop graphs are also included.

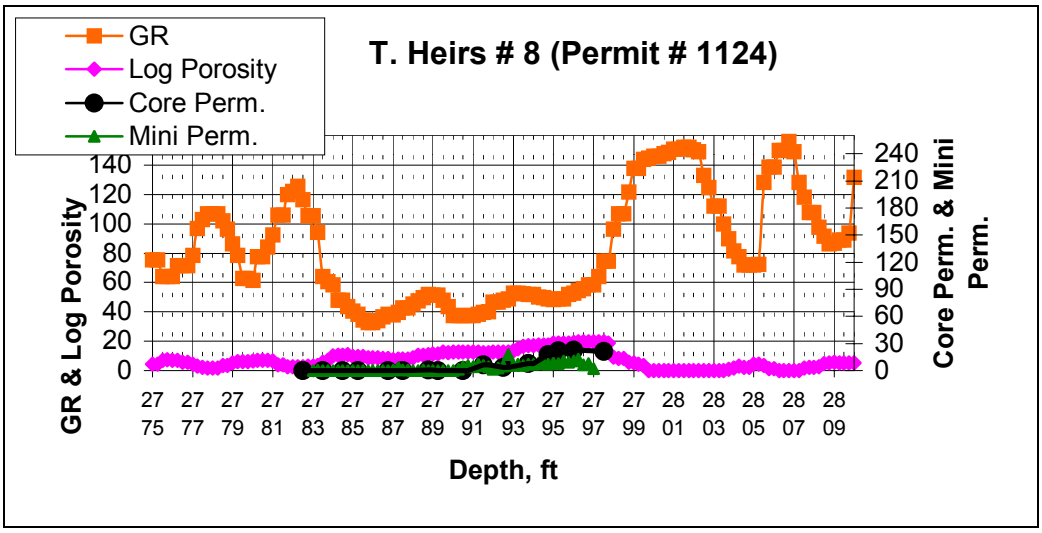

Figure A.1 T. Heirs # 8 Gamma Ray-Log Porosity and Core Measurements

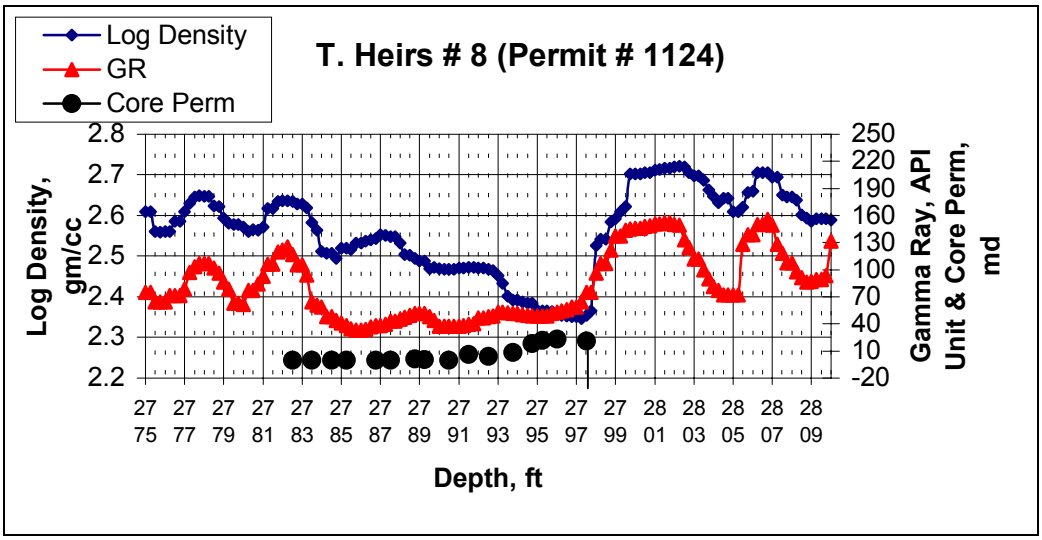

Figure A.2 T. Heirs # 8 Gamma Ray-Log Density and Core Permeability

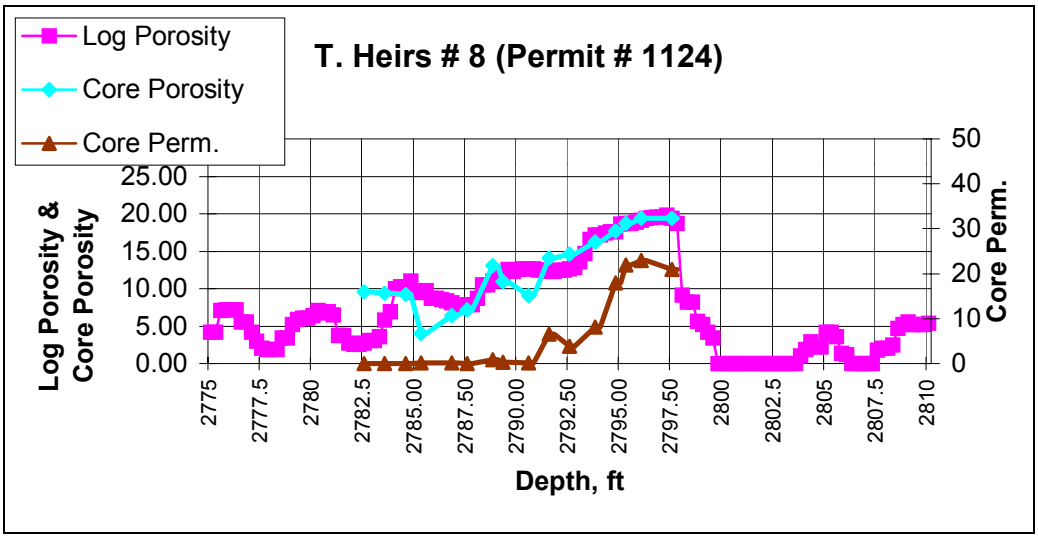

Figure A.3 T. Heirs # 8 Log Porosity versus Core Porosity with Core Permeability

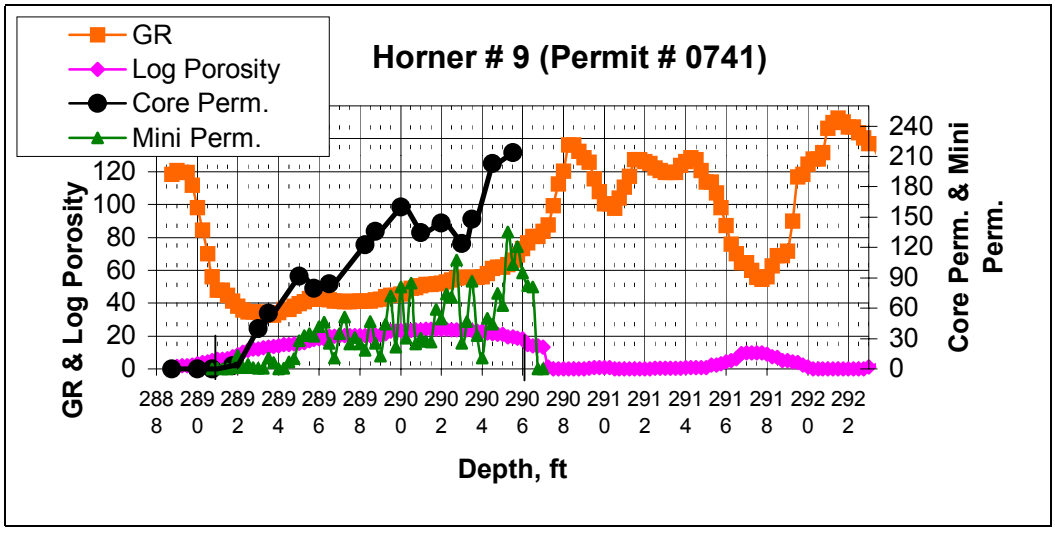

Figure A.4 Horner # 9 Gamma Ray-Log Porosity and Core Measurements

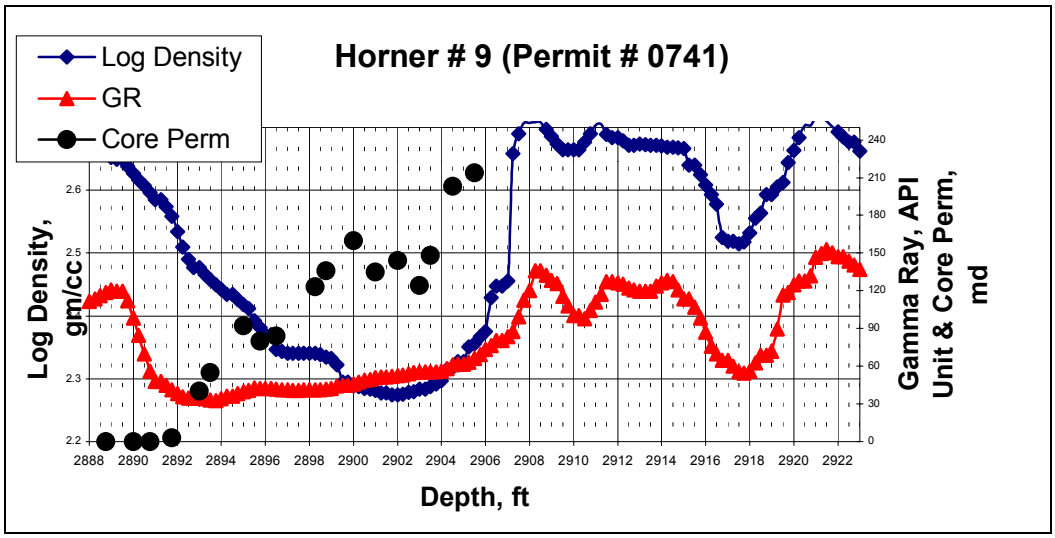

Figure A.5 Horner # 9 Gamma Ray-Log Density and Core Permeability

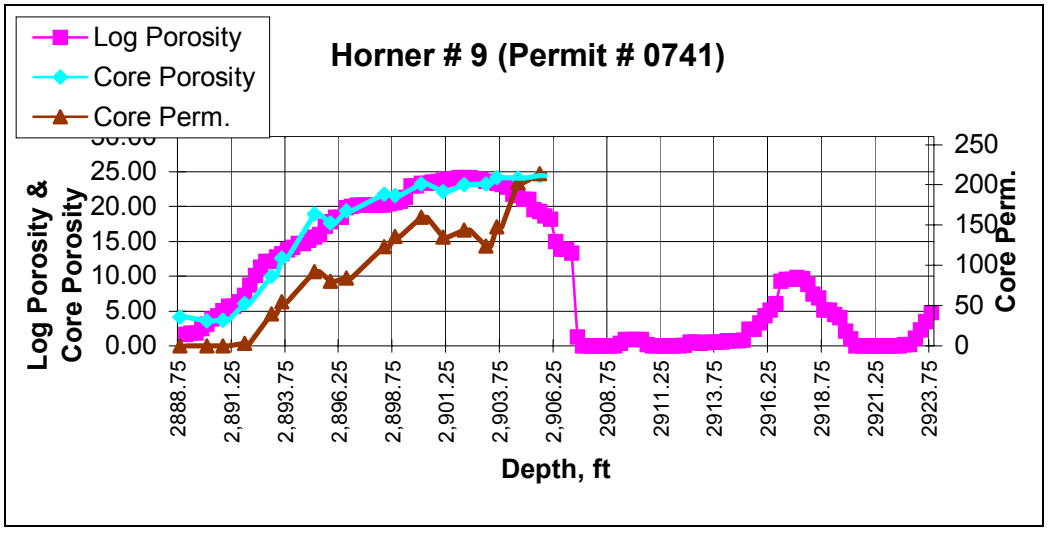

Figure A.6 Horner # 9 Log Porosity versus Core Porosity with Core Permeability

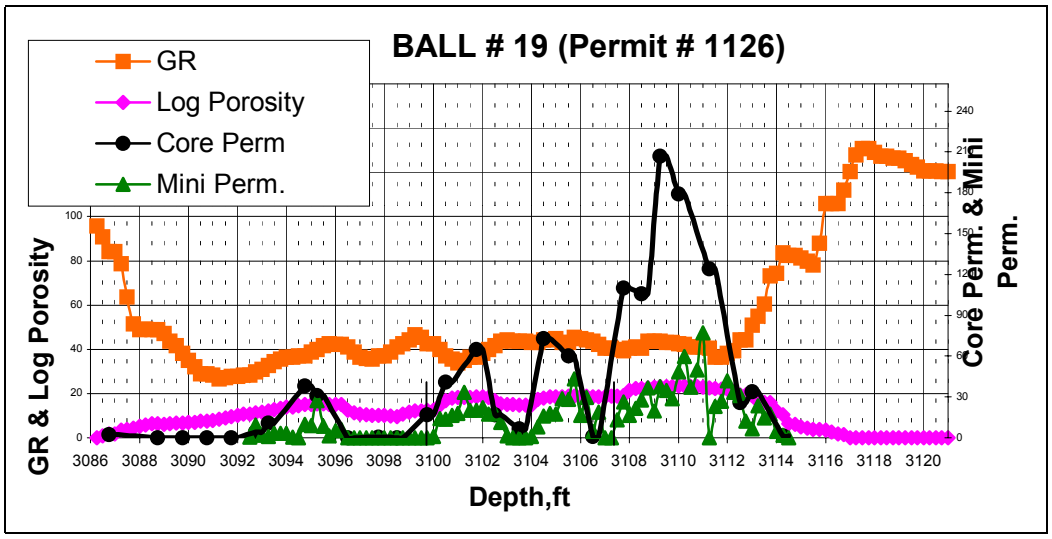

Figure A.7 Ball # 19 Gamma Ray-Log Porosity and Core Measurements

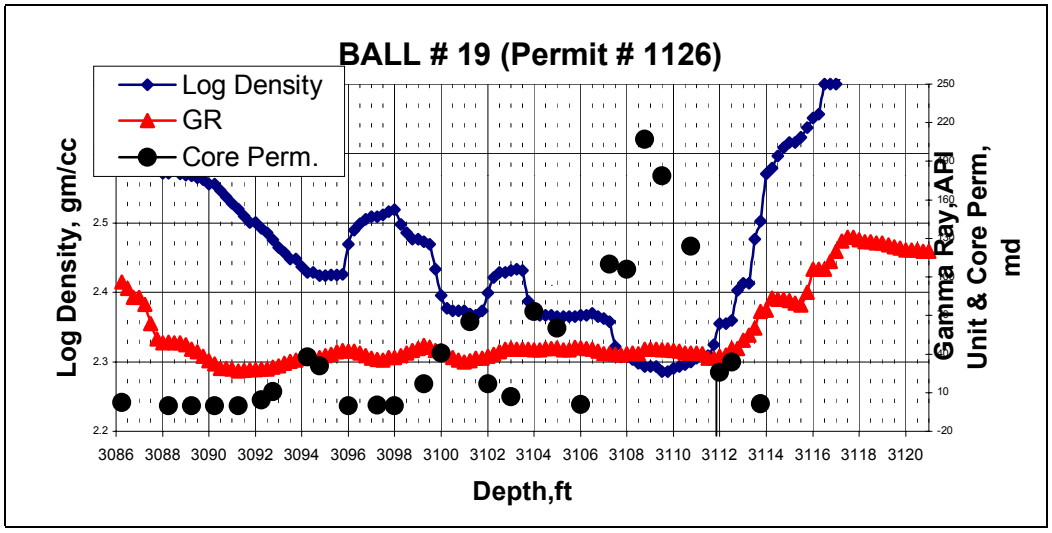

Figure A.8 Ball # 19 Gamma Ray-Log Density and Core Permeability

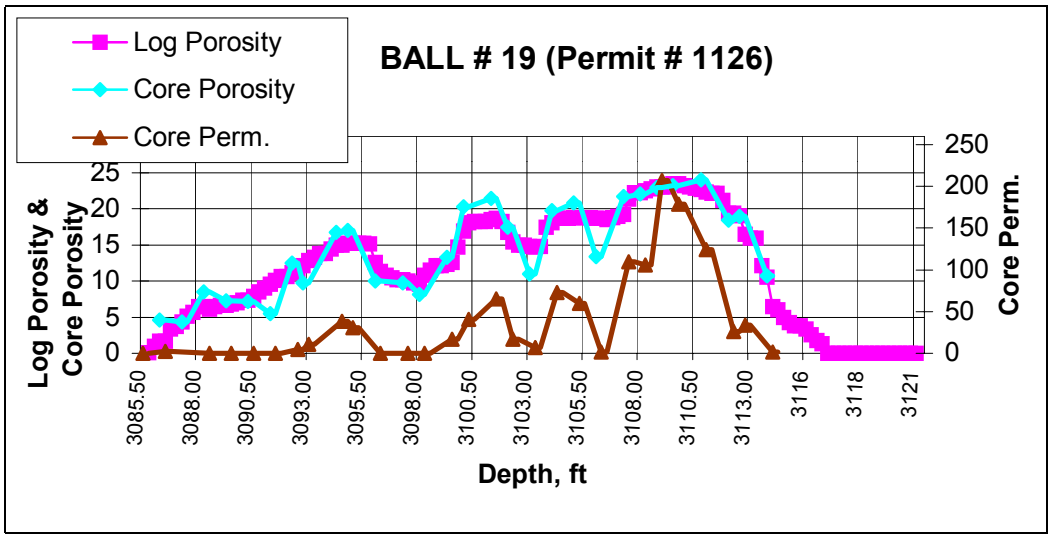

Figure A.9 Ball # 19 Log Porosity versus Core Porosity with Core Permeability

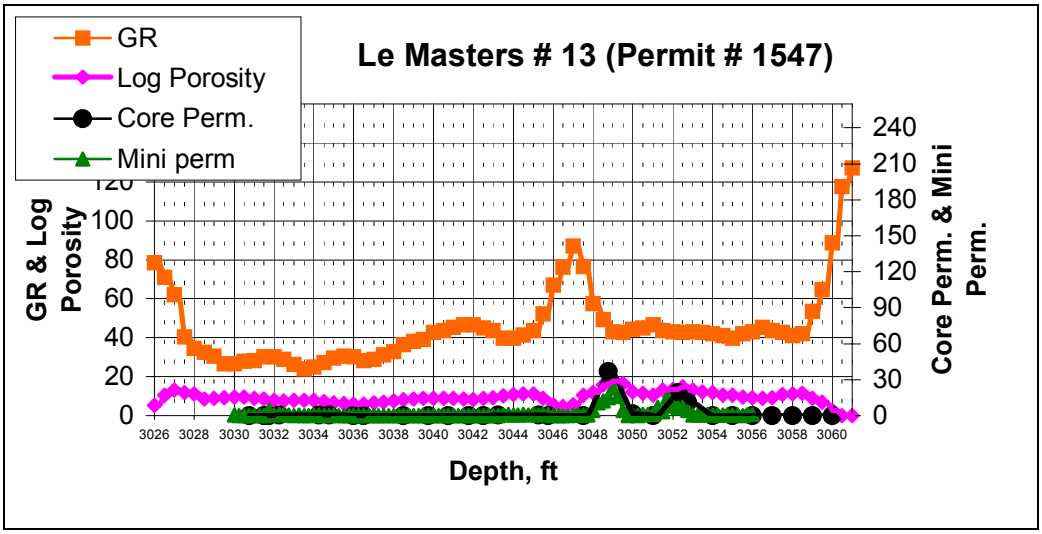

Figure A.10 LeMasters # 13 Gamma Ray-Log Porosity and Core Measurements

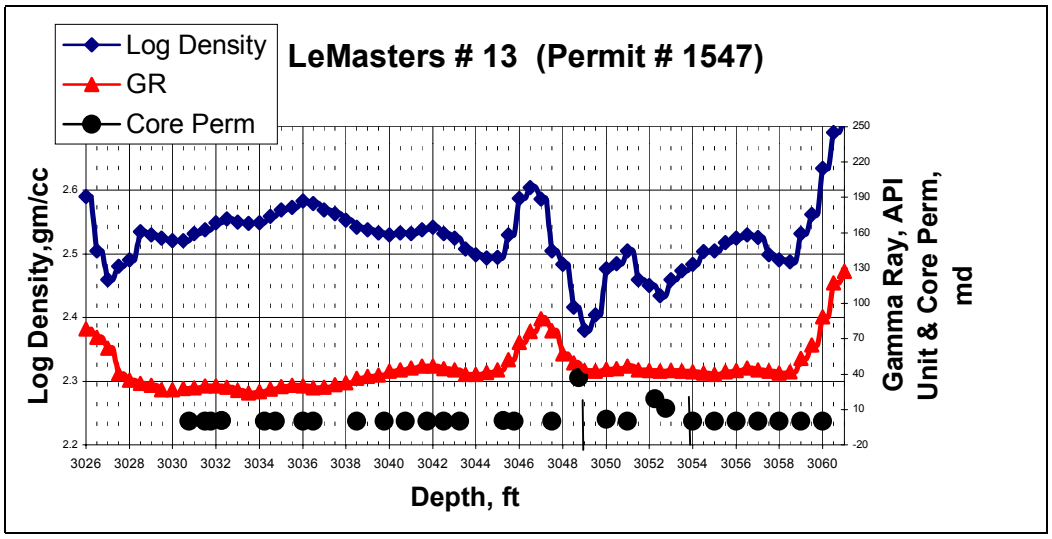

Figure A.11 LeMasters # 13 Gamma Ray-Log Density and Core Permeability

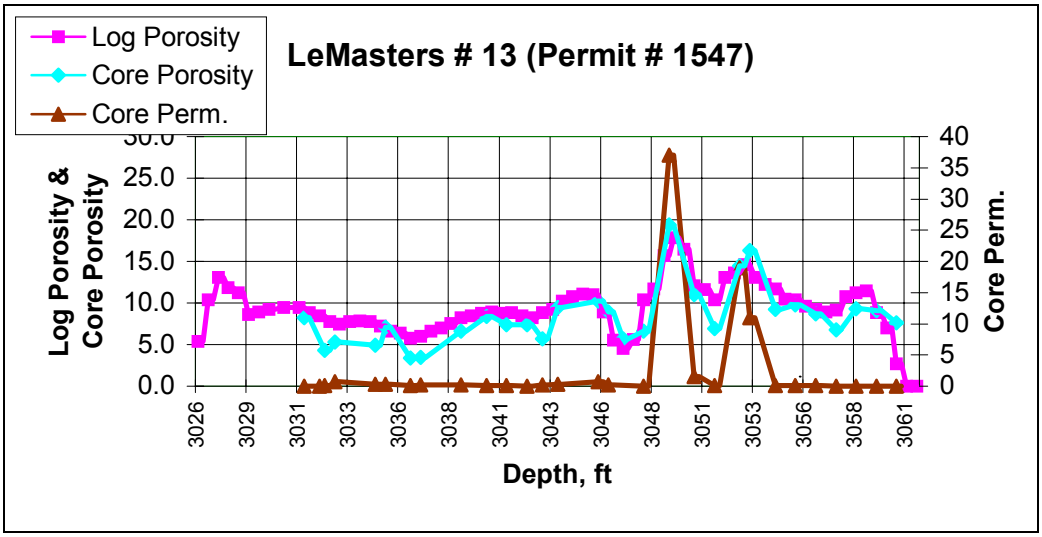

Figure A.12 LeMasters # 13 Log Porosity versus Core Porosity with Core Permeability

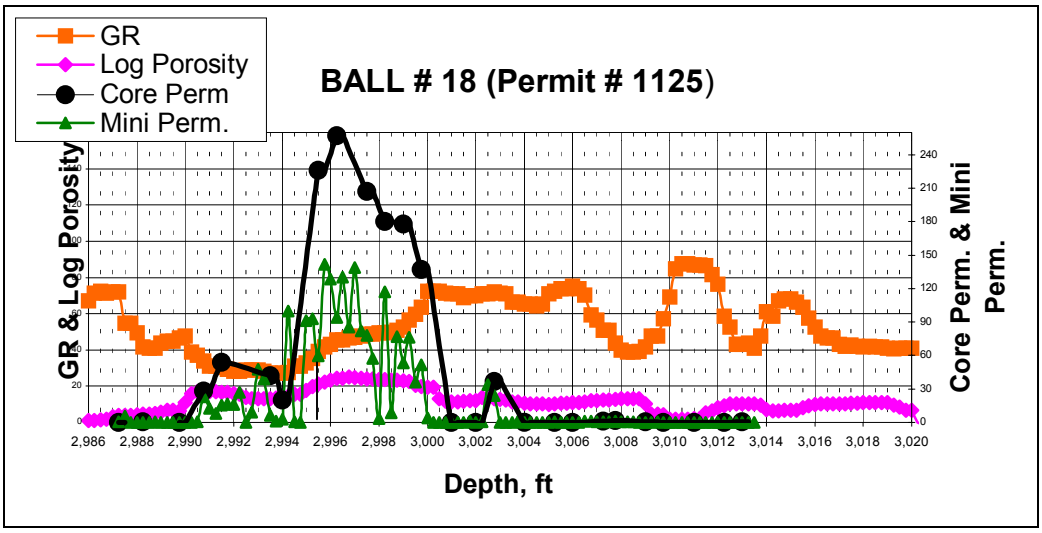

Figure A.13 Ball # 18 Gamma Ray-Log Porosity and Core Measurements

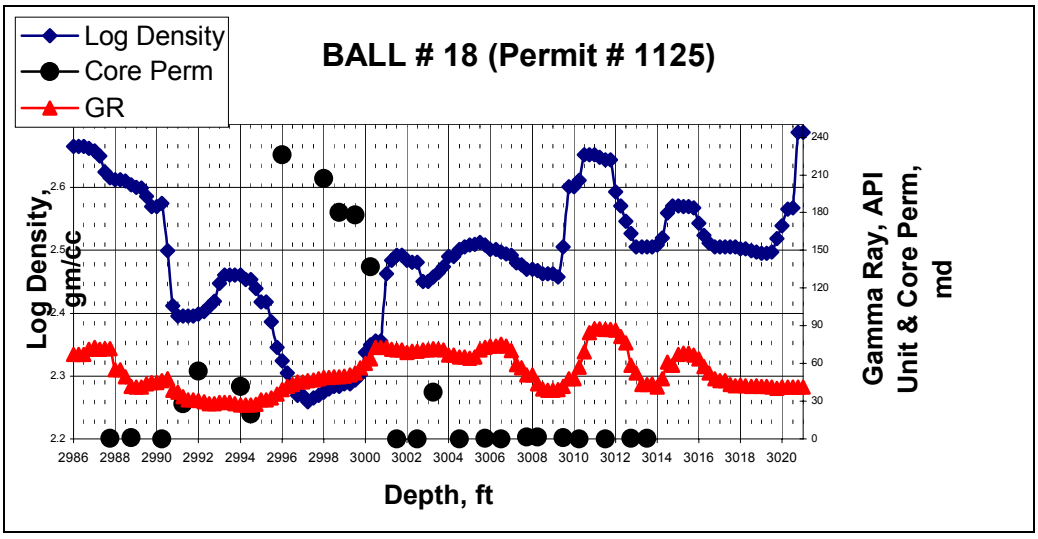

Figure A.14 Ball # 18 Gamma Ray-Log Density and Core Permeability

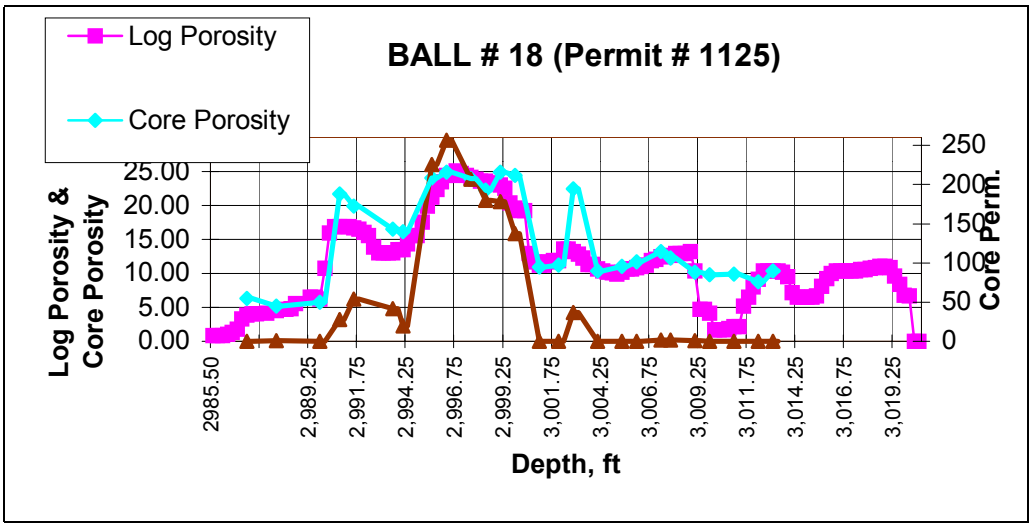

Figure A.15 Ball # 18 Log Porosity versus Core Porosity with Core Permeability

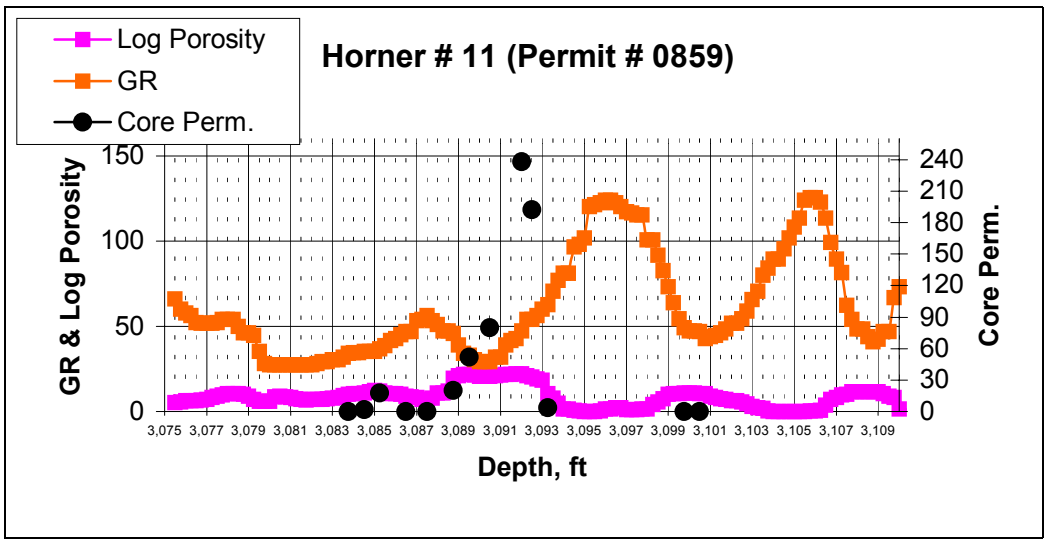

Figure A.16 Horner # 11 Gamma Ray-Log Porosity and Core Measurements

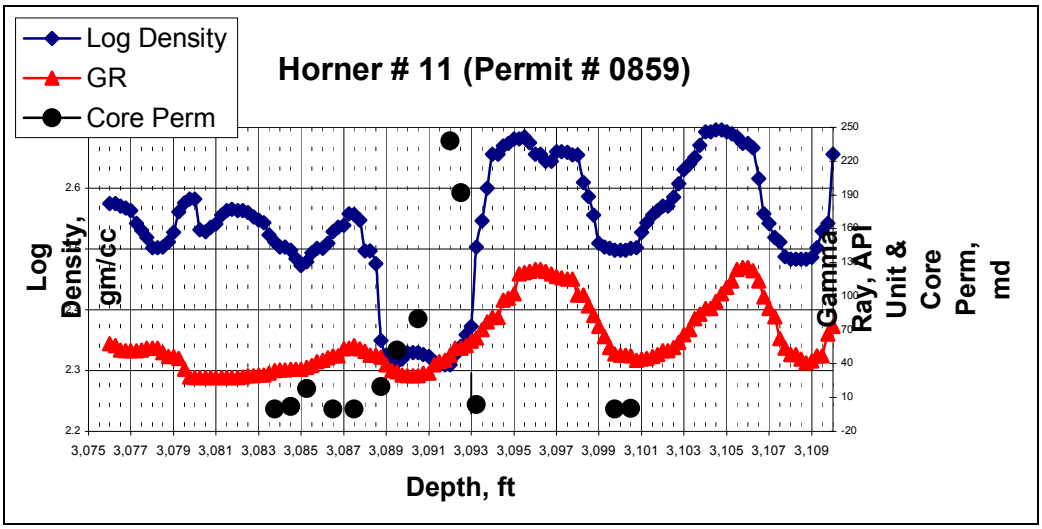

Figure A.17 Horner # 11 Gamma Ray-Log Density and Core Permeability

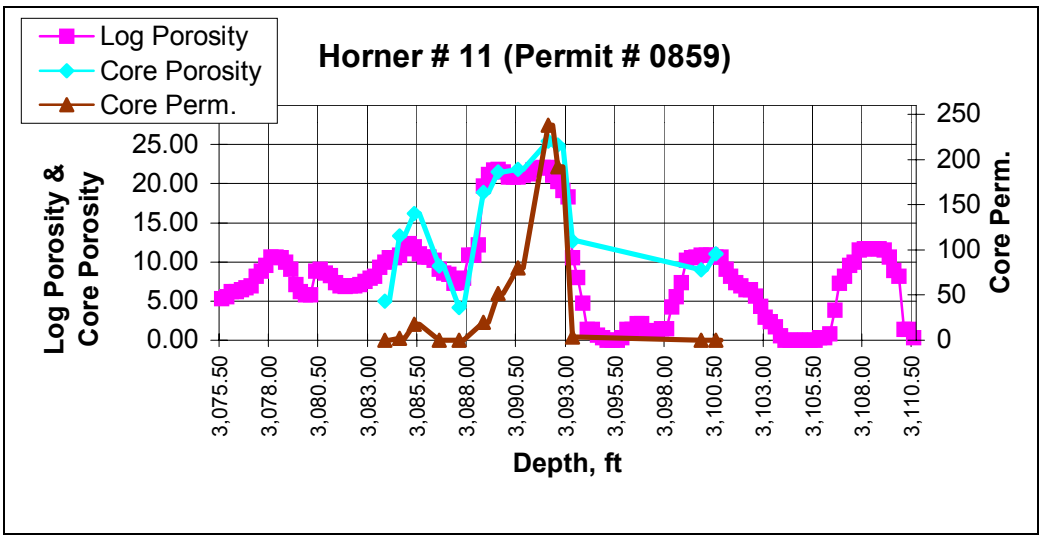

Figure A.18 Horner # 11 Log Porosity versus Core Porosity with Core Permeability

Table A.1
T. Heirs # 8

Depth	GR	Log Density	Log Porosity	Core Porosity	Core Perm	Miniperm
2783.000	105.292	2.628	3.10%			0.01
2783.250	94.150	2.619	3.60%			0.84
2783.500	64.067	2.582	5.80%			0.01
2783.750	60.724	2.563	7.00%			0.01
2784.000	58.496	2.512	10.00%			0.01
2784.250	47.911	2.507	10.30%			0.01
2784.500	47.911	2.507	10.30%			0.01
2784.750	43.454	2.495	11.00%			0.01
2785.000	40.669	2.52	9.50%			0.01
2785.250	38.440	2.519	9.60%	4.00%	0.11	0.28
2785.500	34.540	2.516	9.80%			0.01
2785.750	32.869	2.533	8.80%			0.01
2786.000	32.869	2.533	8.80%			0.01
2786.250	33.983	2.537	8.50%	6.40%	0.12	0.01
2786.500	36.769	2.54	8.30%			0.23
2786.750	38.440	2.544	8.10%			0.05
2787.000	37.883	2.552	7.60%			0.67
2787.250	39.554	2.551	7.70%			3.2
2787.500	42.897	2.548	7.90%			0.53
2787.750	42.897	2.548	7.90%			0.46
2788.000	45.125	2.533	8.80%			0.01
2788.250	47.354	2.504	10.50%			0.01
2788.500	49.582	2.503	10.50%			0.38
2788.750	51.811	2.495	11.00%	13.10%	0.92	0.01
2789.000	51.253	2.488	11.40%			0.01
2789.250	51.253	2.488	11.40%	10.90%	0.31	0.01
2789.500	47.911	2.469	12.60%			0.01
2789.750	43.454	2.473	12.30%			0.01
2790.000	37.326	2.469	12.60%			0.2
2790.250	37.326	2.467	12.70%			1.07
2790.500	37.326	2.467	12.70%			3.99
2790.750	37.326	2.467	12.70%			5.57
2791.000	37.326	2.471	12.40%			4.27
2791.250	38.440	2.471	12.40%			7.08
2791.500	39.554	2.473	12.30%	14.10%	6.5	5.59
2791.750	40.111	2.473	12.30%			3.93
2792.000	46.797	2.471	12.40%			1.38
2792.250	46.797	2.471	12.40%			3.13
2792.500	47.911	2.467	12.70%	14.60%	3.8	4.72
2792.750	49.025	2.464	12.90%			17.95

Table A.1

T. Heirs # 8

Depth	GR	Log Density	Log Porosity	Core Porosity	Core Perm	Miniperm
2793.00	52.925	2.452	13.60%			5.83
2793.25	52.925	2.433	14.70%			6.87
2793.50	52.368	2.402	16.50%			5.7
2793.75	51.811	2.392	17.10%	16.20%	8.1	6.97
2794.00	51.811	2.392	17.10%			7.39
2794.25	50.139	2.387	17.40%			8.26
2794.50	49.582	2.384	17.60%			7.88
2794.75	49.025	2.384	17.60%	17.70%	18	7.26
2795.00	48.468	2.367	18.60%			8.69
2795.25	49.025	2.365	18.80%	18.70%	22	7.64
2795.50	49.025	2.365	18.80%			10.47
2795.75	51.811	2.363	18.90%			9.08
2796.000	52.925	2.359	19.10%	19.40%	23	10.35
2796.250	54.596	2.354	19.40%			12.52
2796.500	55.710	2.352	19.50%	19.40%	21	6.59
2796.750	58.496	2.351	19.60%			7.62

Table A.2
Horner # 9

Depth	GR	Log Density	Log Porosity	Core Porosity	Core Perm	Miniperm
2891.50	44.63	2.57	6.30%			0.01
2891.75	41.32	2.56	7.30%	6.10%	3.3	1.14
2892.00	38.02	2.53	8.70%			13.4
2892.25	35.81	2.51	10.10%			1.54
2892.50	34.71	2.49	11.30%			4.29
2892.75	34.71	2.48	12.10%			1.14
2893.00	34.71	2.48	12.10%	10.00%	40	0.41
2893.25	34.16	2.47	12.70%			0.66
2893.50	33.06	2.46	13.20%	12.60%	55	10.81
2893.75	32.51	2.45	13.80%			6.63
2894.00	34.16	2.44	14.20%			0.01
2894.25	36.36	2.43	14.60%			0.43
2894.50	36.36	2.43	14.60%			6.83
2894.75	38.02	2.43	15.10%			9.88
2895.00	39.67	2.42	15.60%	18.90%	92	27.55
2895.25	40.77	2.41	16.00%			33.02
2895.50	42.98	2.39	17.10%			34.49
2895.75	42.42	2.38	17.80%	17.60%	80	32.09
2896.00	42.42	2.37	18.50%			41.57
2896.25	42.42	2.37	18.50%			46.26
2896.50	41.87	2.35	19.80%	19.40%	84	25.27
2896.75	41.32	2.34	20.00%			10.64
2897.00	41.32	2.34	20.20%			34.83
2897.25	40.77	2.34	20.20%			51.34
2897.50	40.77	2.34	20.20%			24.91
2897.75	41.32	2.34	20.20%			31.3
2898.00	41.32	2.34	20.20%			24.5
2898.25	41.32	2.34	20.20%	21.70%	123	18.61
2898.50	41.32	2.34	20.40%			47.08
2898.75	41.87	2.33	20.60%	21.60%	136	25.16
2899.00	42.42	2.33	20.70%			12.87
2899.25	44.08	2.32	21.30%			44.54
2899.50	44.63	2.3	22.90%			71.82
2899.75	44.63	2.3	22.90%			21.59
2900.00	45.73	2.29	23.30%	23.20%	160	80.8
2900.25	47.38	2.29	23.30%			30.55
2900.50	49.04	2.29	23.50%			85.07
2900.75	49.59	2.28	23.60%			24.44
2901.00	50.69	2.28	23.80%	22.10%	135	30.41
2901.25	51.24	2.28	24.00%			27.07
2901.50	51.24	2.28	24.00%			26.39
2901.75	51.79	2.27	24.20%			58.8

Table A.2
Horner # 9

Depth	GR	Log Density	Log Porosity	Core Porosity	Core Perm	Miniperm
2902.00	52.34	2.27	24.20%	23.10%	144	49.53
2902.25	52.89	2.28	24.10%			73.82
2902.50	53.99	2.28	23.90%			70.55
2902.75	55.1	2.28	23.90%			107.35
2903.00	55.65	2.28	23.60%	23.20%	124	25.05
2903.25	55.65	2.28	23.60%			46.88
2903.50	55.65	2.29	23.30%	24.10%	148	86.69
2903.75	55.65	2.29	23.10%			32.88
2904.00	56.2	2.3	22.80%			10.48
2904.25	57.85	2.32	21.70%			50.21
2904.50	61.16	2.32	21.50%	24.00%	203	44.08
2904.75	61.71	2.33	21.00%			74.49
2905.00	61.71	2.33	21.00%			62.9
2905.25	63.36	2.35	19.60%			135.24
2905.50	66.12	2.36	19.30%	24.40%	214	103.16
2905.75	69.42	2.37	18.60%			120.78
2906.00	73.28	2.38	18.20%			95.16
2906.25	76.58	2.43	14.90%			82.17
2906.50	80.44	2.45	13.90%			80.69
2906.75	80.44	2.45	13.90%			0.01
2907.00	83.75	2.46	13.30%			0.01

Table A.3
Ball # 19

Depth	GR	Log Density	Log Porosity	Core Porosity	Core Perm	Miniperm
3092.00	28.255	2.501	10.65			0.47
3092.25	29.917	2.492	11.19	12.5	4.24	9.63
3092.50	31.025	2.486	11.55			1.65
3092.75	32.687	2.476	12.14	9.7	11	0.74
3093.00	34.349	2.465	12.8			3.12
3093.25	35.457	2.457	13.27			3.5
3093.50	36.565	2.448	13.81			3.25
3093.75	36.565	2.448	13.81			0.58
3094.00	37.119	2.437	14.46			0.01
3094.25	37.119	2.429	14.94	16.7	38	10.1
3094.50	38.781	2.429	14.94			9.07

Table A.3
Ball # 19

Depth	GR	Log Density	Log Porosity	Core Porosity	Core Perm	Miniperm
3094.75	39.889	2.424	15.24	17	31	27.49
3095.00	41.551	2.424	15.24			8.65
3095.25	42.659	2.425	15.18			1.61
3095.50	42.105	2.425	15.18			4.97
3095.75	42.105	2.426	15.12			6.21
3096.00	40.997	2.469	12.56			0.01
3096.25	38.781	2.49	11.31			0.01
3096.50	36.565	2.499	10.77			0.01
3096.75	36.011	2.505	10.42			0.01
3097.00	35.457	2.509	10.18			0.01
3097.25	37.119	2.509	10.18	9.7	0.27	0.23
3097.50	37.119	2.512	10			0.01
3097.75	38.781	2.516	9.76			0.01
3098.00	40.997	2.519	9.58	8.1	0.16	0.01
3098.25	42.659	2.498	10.83			0.01
3098.50	44.321	2.486	11.55			0.01
3098.75	46.537	2.477	12.08			0.01
3099.00	45.429	2.477	12.08			0.01
3099.25	42.659	2.473	12.32	13.3	17	0.01
3099.50	42.659	2.469	12.56			0.99
3099.75	39.889	2.433	14.7			14.3
3100.00	37.119	2.396	16.9	20.3	41	13.5
3100.25	35.457	2.377	18.04			16.28
3100.50	33.795	2.373	18.27			18.08
3100.75	34.903	2.373	18.27			33.15
3101.00	36.565	2.373	18.27			20.29
3101.25	36.565	2.369	18.51	21.4	65	20.39
3101.50	38.227	2.367	18.63			21.9
3101.75	39.889	2.373	18.27			17.17
3102.00	41.551	2.399	16.73	17.4	17	17.98
3102.25	43.767	2.421	15.42			11.28
3102.50	44.321	2.429	14.94			1.59
3102.75	43.767	2.429	14.94			0.01
3103.00	43.767	2.432	14.76	11	6.79	0.01
3103.25	43.767	2.433	14.7			0.01
3103.50	43.213	2.432	14.76			1.05

Table A.3

Ball # 19

Depth	GR	Log Density	Log Porosity	Core Porosity	Core Perm	Miniperm
3103.75	43.213	2.387	17.44			8.02
3104.00	44.321	2.377	18.04	19.7	73	15.93
3104.25	44.321	2.367	18.63			17.68
3104.50	44.875	2.367	18.63			17.44
3104.75	43.213	2.367	18.63			28.9
3105.00	43.213	2.365	18.75	20.8	60	28.01
3105.25	45.429	2.365	18.75			43.44
3105.50	44.875	2.365	18.75			16.64
3105.75	44.321	2.365	18.75			29.54
3106.00	43.767	2.367	18.63	13.4	1.16	4.69
3106.25	42.105	2.367	18.63			18.8
3106.50	40.443	2.37	18.45			0.18
3106.75	40.443	2.365	18.75			0.01
3107.00	39.889	2.362	18.93			12.94
3107.25	39.335	2.358	19.17	21.7	110	26.24
3107.50	40.443	2.322	21.31			16.46
3107.75	40.997	2.307	22.2			21.59
3108.00	40.443	2.307	22.2	22	106	27.96
3108.25	43.767	2.303	22.44			36.78
3108.50	43.767	2.298	22.74			19.89
3108.75	43.767	2.293	23.04	22.9	207	37.84
3109.00	43.213	2.293	23.04			34.58
3109.25	43.213	2.293	23.04			28.89
3109.50	42.659	2.286	23.45	23.2	179	48.23
3109.75	42.105	2.286	23.45			59.52
3110.00	40.997	2.29	23.21			37.05
3110.25	40.997	2.293	23.04			49.62
3110.50	40.997	2.296	22.86			77.1
3110.75	40.443	2.3	22.62	24	124	0.01
3111.00	36.565	2.305	22.32			23.13
3111.25	36.565	2.309	22.08			26.66
3111.50	38.227	2.309	22.08			41.7
3111.75	39.335	2.325	21.13			33.32
3112.00	44.321	2.355	19.35	18.4	26	31.11
3112.25	44.321	2.355	19.35			12.41
3112.50	50.97	2.36	19.05	18.9	34	6.6
3112.75	54.848	2.403	16.49			23.62
3113.00	60.388	2.413	15.89			14.79
3113.25	73.13	2.413	15.89			17.36
3113.50	74.238	2.477	12.08			4.86
3113.75	83.657	2.503	10.54	10.7	1.33	1.82
3114.00	82.548	2.571	6.49			0.14

Table A.4
LeMasters # 13

Depth	GR	Log Density	Log Porosity	Core Porosity	Core Perm	Miniperm
3032.00	30.11	2.549	7.80%	4.30%	0.15	0.56
3032.25						1.25
3032.50	28.98	2.555	7.40%	5.30%	0.72	0.97
3032.75						0.72
3033.00	26.14	2.55	7.70%			0.25
3033.25						0.32
3033.50	23.86	2.548	7.90%			0.2
3033.75						0.22
3034.00	25	2.549	7.80%	4.90%	0.28	0.49
3034.25						0.34
3034.50	27.27	2.559	7.20%	7.10%	0.27	0.05
3034.75						0.18
3035.00	29.55	2.569	6.60%			0.32
3034.25						0.14
3035.50	30.68	2.573	6.40%			0.1
3035.75						0.01
3036.00	30.11	2.583	5.80%	3.40%	0.12	0.01
3036.25						0.01
3036.50	28.41	2.579	6.00%	3.50%	0.22	0.01
3036.75						0.01
3037.00	28.98	2.569	6.60%			0.01
3037.25						0.01
3037.50	31.25	2.563	7.00%			0.01
3037.75						0.01
3038.00	32.96	2.553	7.60%			0.01
3038.25						0.01
3038.50	36.36	2.542	8.20%	6.60%	0.18	0.01
3038.75						0.01
3039.00	38.07	2.538	8.50%			0.01
3039.25						0.01
3039.50	39.21	2.533	8.80%			0.01
3039.75						0.01
3040.00	42.61	2.53	8.90%			0.01
3040.25						0.01
3040.50	43.75	2.533	8.80%			0.01
3040.75						0.01
3041.00	45.46	2.532	8.80%			0.01
3041.25						0.01
3041.50	46.59	2.538	8.50%			0.01
3041.75						0.01
3042.00	46.59	2.542	8.20%			0.01
3042.25						0.01
3042.50	44.89	2.532	8.80%	5.70%	0.19	0.01
3042.75						0.01
3043.00	43.75	2.525	9.20%	9.50%	0.29	0.01

Table A.4

LeMasters # 13

Depth	GR	Log Density	Log Porosity	Core Porosity	Core Perm	Miniperm
3043.50	39.77	2.508	10.20%			0.57
3043.75						1.14
3044.00	39.77	2.499	10.80%			0.78
3044.25						0.69
3044.50	41.48	2.494	11.10%			1.24
3044.75						0.74
3045.00	43.75	2.495	11.00%	10.20%	0.67	1.21
3045.25						0.76
3045.50	52.27	2.53	8.90%			1.01
3045.25						1.22
3046.00	67.05	2.587	5.50%	8.90%	0.21	0.01
3046.25						0.01
3046.50	76.14	2.604	4.50%			0.01
3046.75						0.01
3047.00	86.93	2.586	5.60%			0.39
3047.25						0.61
3047.50	76.71	2.505	10.40%			0.51
3047.75						0.42
3048.00	57.39	2.484	11.70%			4.37
3048.25						10.59
3048.50	49.43	2.416	15.70%			12.25
3048.75						14.94
3049.00	43.18	2.38	17.90%	19.40%	37	22.88
3049.25						15.88
3049.50	42.61	2.404	16.40%			4.38
3049.75						0.01
3050.00	44.32	2.477	12.10%	11.00%	1.51	0.39
3050.25						0.01
3050.50	44.89	2.485	11.60%			0.98
3050.75						1.13
3051.00	46.59	2.505	10.40%	6.90%	0.11	0.81
3051.25						7.01
3051.50	43.75	2.46	13.10%			3.19
3051.75						15.63
3052.00	43.18	2.451	13.60%	14.50%	19	8.03
3052.25						6.54
3052.50	42.61	2.434	14.60%			6.7
3052.75						4.44
3053.00	43.18	2.46	13.10%	16.30%	11	0.71
3053.25						0.31
3053.50	42.61	2.474	12.30%			0.56
3053.75						1.07

Table A.4
LeMasters # 13

Depth	GR	Log Density	Log Porosity	Core Porosity	Core Perm	Miniperm
3054.00	42.05	2.484	11.70%			0.6
3054.25						0.5
3054.50	40.91	2.504	10.50%			0.56
3055.75						0.41
3055.00	39.77	2.505	10.40%			0.45
3055.25						0.57
3055.50	42.05	2.518	9.60%			0.12
3055.75						0.84
3056.00	43.18	2.525	9.20%			1.13

Table A.5
Ball # 18

Depth	GR	Log Density	Log Porosity	Core Porosity	Core Perm	Miniperm
2987.25	72.022	2.615	3.87	6.3	0.26	0.74
2987.50	54.848	2.612	4.05			5.53
2987.75	54.848	2.612	4.05			0.01
2988.00	49.307	2.61	4.17			0.01
2988.25	41.551	2.604	4.52	5.2	0.77	0.01
2988.50	40.997	2.6	4.76			0.01
2988.75	40.997	2.599	4.82			0.69
2989.00	43.767	2.586	5.6			0.01
2989.25	44.875	2.57	6.55			0.01
2989.50	44.875	2.57	6.55			0.01
2989.75	46.537	2.575	6.25	5.8	0.14	0.01
2990.00	47.645	2.499	10.77			0.01
2990.25	38.781	2.412	15.95			0.01
2990.50	37.119	2.396	16.9			0.48
2990.75	33.795	2.396	16.9	21.7	28	23.19
2991.00	31.025	2.396	16.9			12.86
2991.25	31.025	2.396	16.9			7.82
2991.50	30.471	2.399	16.73	19.9	54	15.22
2991.75	29.363	2.403	16.49			16.54
2992.00	28.255	2.411	16.01			16.05
2992.25	28.255	2.419	15.54			26.73
2992.50	28.809	2.447	13.87			0.01
2992.75	28.809	2.461	13.04			9.22
2993.00	28.809	2.461	13.04			47.61

Table A.5
Ball # 18

Depth	GR	Log Density	Log Porosity	Core Porosity	Core Perm	Miniperm
2993.25	28.255	2.461	13.04			38.84
2993.50	27.147	2.461	13.04	16.5	42	6.18
2993.75	27.147	2.454	13.45			1.29
2994.00	27.147	2.454	13.45	16.1	20	2.76
2994.25	27.701	2.439	14.35			99.82
2994.50	31.025	2.418	15.6			0.39
2994.75	31.025	2.418	15.6			0.06
2995.00	32.687	2.386	17.5			91.38
2995.25	35.457	2.346	19.88			92.78
2995.50	39.335	2.324	21.19	24.1	226	59.59
2995.75	41.551	2.305	22.32			141.62
2996.00	43.213	2.286	23.45			128.31
2996.25	45.429	2.269	24.46	24.9	257	94.26
2996.50	45.429	2.269	24.46			130.29
2996.75	46.537	2.259	25.06			85.42
2997.00	47.091	2.265	24.7			138.7
2997.25	47.645	2.269	24.46			82.26
2997.50	48.753	2.274	24.17	24	207	78.01
2997.75	48.753	2.279	23.87			57.26
2998.00	49.307	2.284	23.57			3.5
2998.25	49.307	2.284	23.57	22.3	180	117.37
2998.50	49.861	2.288	23.33			8.5
2998.75	50.97	2.288	23.33			76.85
2999.00	52.632	2.294	22.98	24.9	178	53.64
2999.25	56.51	2.302	22.5			76.14
2999.50	59.834	2.337	20.42			35.98
2999.75	63.712	2.35	19.64	24.4	137	51.54
3000.00	72.576	2.356	19.29			3.76
3000.25	72.576	2.356	19.29			0.01
3000.50	72.576	2.463	12.92			0.01
3000.75	71.468	2.484	11.67			0.04
3001.00	70.914	2.492	11.19			0.01
3001.25	70.914	2.492	11.19			0.01
3001.50	68.698	2.484	11.67			0.01
3001.75	69.806	2.481	11.85			1.03
3002.00	69.806	2.481	11.85			0.01
3002.25	70.914	2.451	13.63			0.84
3002.50	70.914	2.451	13.63			34.04
3002.75	72.022	2.458	13.21	22.5	37	23.86
3003.00	71.468	2.465	12.8			0.01
3003.25	70.914	2.474	12.26			0.01

Table A.5
Ball # 18

Depth	GR	Log Density	Log Porosity	Core Porosity	Core Perm	Miniperm
3003.50	66.482	2.49	11.31			0.01
3003.75	66.482	2.49	11.31			1.33
3004.00	65.374	2.501	10.65			0.01
3004.25	65.374	2.506	10.36			0.01
3004.50	64.266	2.509	10.18			0.01
3004.75	65.374	2.51	10.12			0.26
3005.00	70.914	2.513	9.94			0.1
3005.25	72.576	2.509	10.18	11	0.26	0.4
3005.50	73.684	2.501	10.65			0.01
3005.75	73.684	2.501	10.65			0.01
3006.00	75.346	2.497	10.89			0.01
3006.25	73.684	2.494	11.07			0.01
3006.50	70.36	2.492	11.19			1.08
3006.75	59.28	2.48	11.9			0.89
3007.00	56.51	2.477	12.08			0.78
3007.25	50.97	2.47	12.5	13.2	1.4	0.79
3007.50	50.97	2.47	12.5			0.69
3007.75	43.767	2.468	12.62	12.3	1.5	0.97
3008.00	39.889	2.463	12.92			0.7
3008.25	38.781	2.463	12.92			0.74
3008.50	38.781	2.463	12.92			0.81
3008.75	39.335	2.458	13.21			0.21
3009.00	41.551	2.506	10.36	10.2	0.79	0.22
3009.25	47.645	2.601	4.7			0.09
3009.50	47.645	2.601	4.7			0.78
3009.75	57.064	2.611	4.11	9.8	0.25	0.16
3010.00	69.252	2.652	1.67			0.01
3010.25	84.765	2.652	1.67			0.01
3010.50	87.535	2.652	1.67			0.01
3010.75	87.535	2.648	1.9			0.01
3011.00	86.981	2.644	2.14	9.9	0.11	0.01
3011.25	86.981	2.644	2.14			0.01
3011.50	86.427	2.593	5.18			0.23
3011.75	81.44	2.571	6.49			0.11
3012.00	76.454	2.546	7.98			0.13
3012.25	58.726	2.527	9.11	8.8	0.26	0.05
3012.50	52.632	2.506	10.36			0.12
3012.75	43.213	2.505	10.42			0.23
3013.00	43.213	2.505	10.42	10.4	0.38	0.22
3013.25	43.767	2.505	10.42			0.23

Table A.6

Horner # 11

Depth	GR	Log Density	Log Porosity	Core Porosity	Core Perm
3084.25	34.711	2.503	10.50%		
3084.50	35.262	2.498	10.80%	13.30%	2.1
3084.75	35.262	2.484	11.70%		
3085.00	35.262	2.473	12.30%		
3085.25	36.915	2.479	12.00%	16.20%	18
3085.50	38.567	2.494	11.10%		
3085.75	41.873	2.501	10.70%		
3086.00	42.975	2.501	10.70%		
3086.25	45.179	2.509	10.20%		
3086.50	46.832	2.528	9.00%		
3086.75	46.832	2.536	8.60%		
3087.00	53.444	2.539	8.40%		
3087.25	53.994	2.558	7.30%		
3087.50	56.198	2.557	7.30%		
3087.75	53.444	2.547	7.90%		
3088.00	51.24	2.497	10.90%		
3088.25	47.383	2.497	10.90%		
3088.50	47.383	2.476	12.10%		
3088.75	45.73	2.349	19.70%	18.90%	20
3089.00	39.118	2.325	21.10%		
3089.25	34.16	2.315	21.70%		
3089.50	33.058	2.314	21.80%	21.50%	52
3089.75	30.303	2.319	21.50%		
3090.00	29.201	2.33	20.80%		
3090.25	29.201	2.33	20.80%		
3090.50	29.201	2.33	20.80%	21.80%	80
3090.75	31.956	2.326	21.10%		
3091.00	31.956	2.323	21.30%		
3091.25	39.118	2.315	21.70%		
3091.50	41.873	2.311	22.00%		
3091.75	42.975	2.309	22.10%		
3092.00	47.383	2.309	22.10%	25.40%	238
3092.25	53.994	2.326	21.10%		
3092.50	53.994	2.34	20.20%	24.90%	192
3092.75	56.198	2.359	19.10%		
3093.00	60.055	2.373	18.30%		
3093.25	62.81	2.503	10.50%	12.70%	3.6
3093.50	70.523	2.546	8.00%		

APPENDIX B.

Appendix B. presents cumulative flow capacity versus cumulative storage capacity graphs for each core well. The graphs and supporting tables use core measurements for porosity and permeability. Flow unit indicators are shown on each graph.

Figure B.1 Cumulative Flow Capacity versus Cumulative Storage Capacity (Core Results) T. Heirs # 8

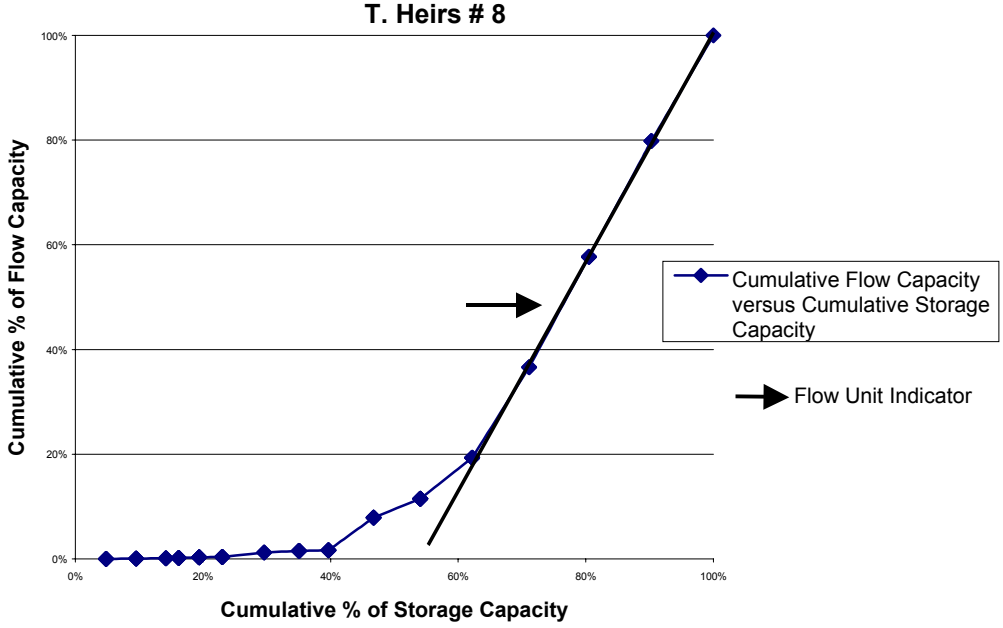

Figure B.2 Cumulative Flow Capacity versus Cumulative Storage Capacity (Core Results) Horner # 9

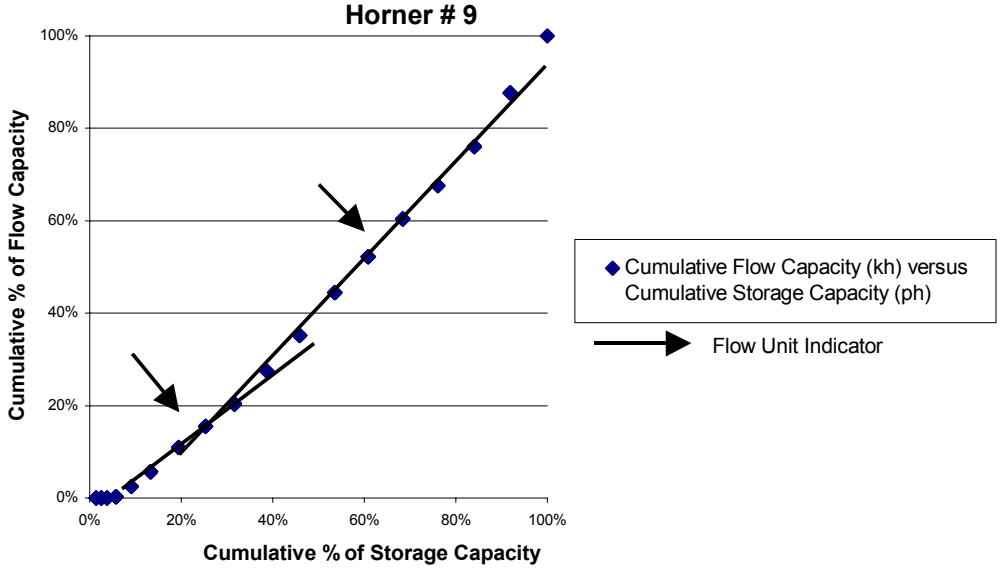

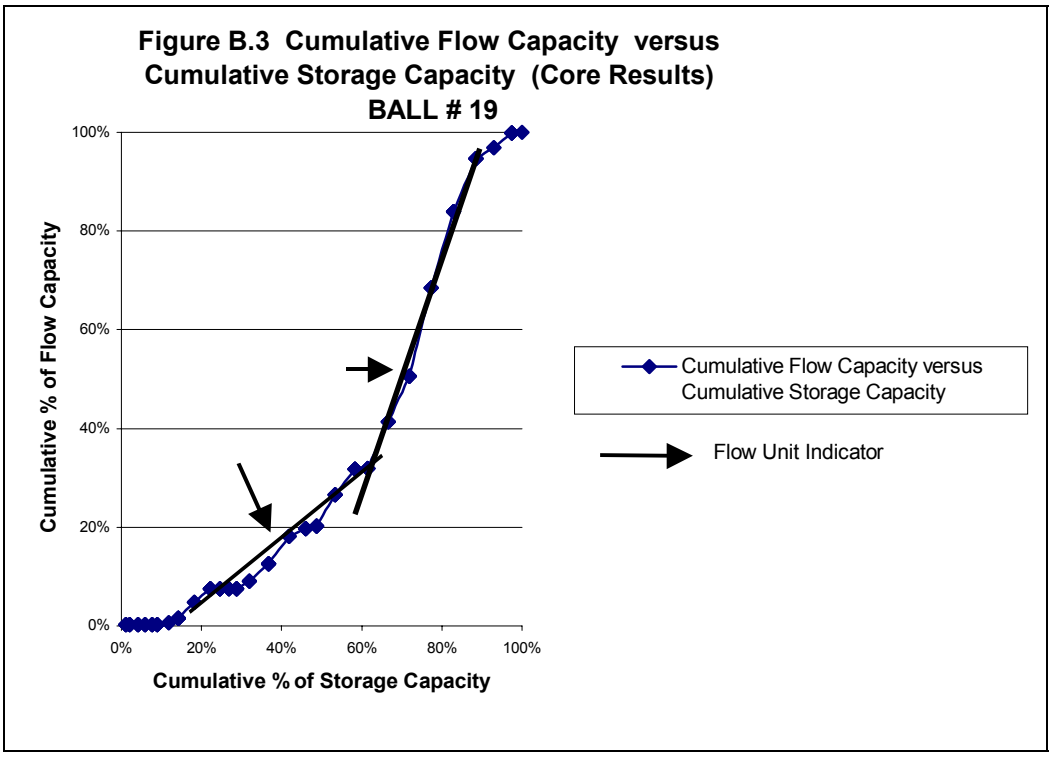
Figure B.3 Cumulative Flow Capacity versus Cumulative Storage Capacity (Core Results) BALL # 19
100%
80%
60%
40%
20%
0%
Cumulative % of Flow Capacity
0%
20%
40%
60%
80%
100%
Cumulative % of Storage Capacity
Cumulative Flow Capacity versus Cumulative Storage Capacity
Flow Unit Indicator

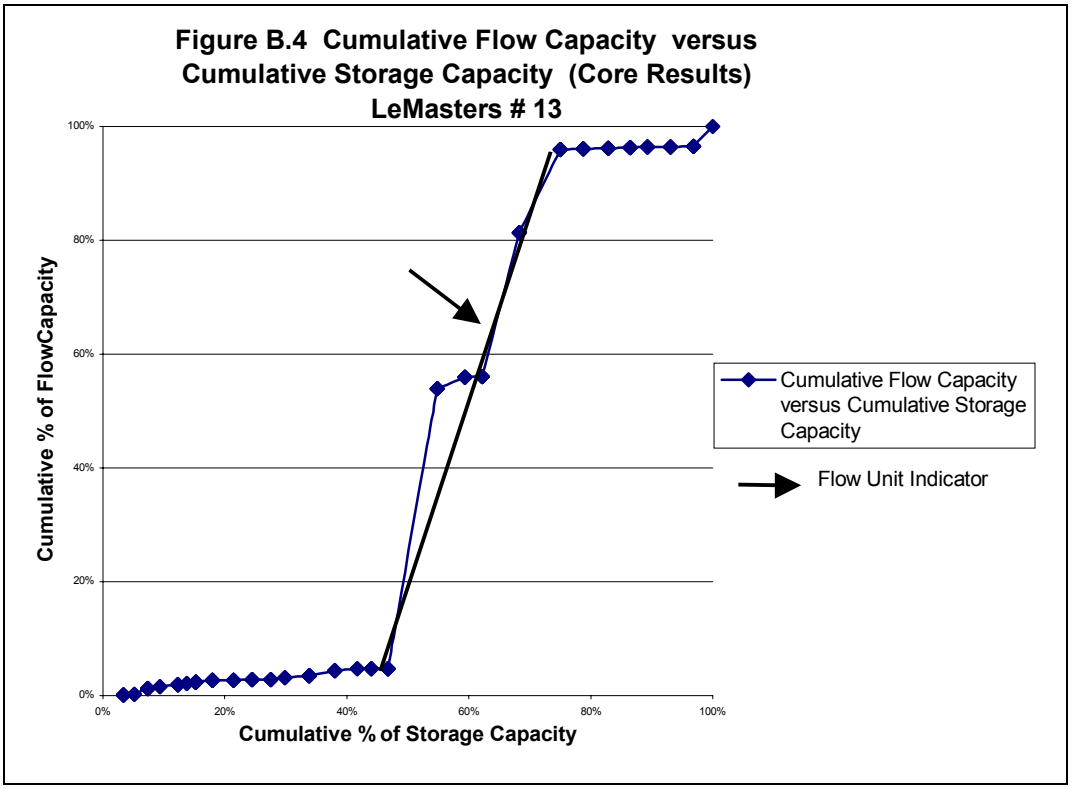
Figure B.4 Cumulative Flow Capacity versus Cumulative Storage Capacity (Core Results) LeMasters # 13
100%
80%
60%
40%
20%
0%
Cumulative % of FlowCapacity
0%
20%
40%
60%
80%
100%
Cumulative % of Storage Capacity
Cumulative Flow Capacity versus Cumulative Storage Capacity
Flow Unit Indicator

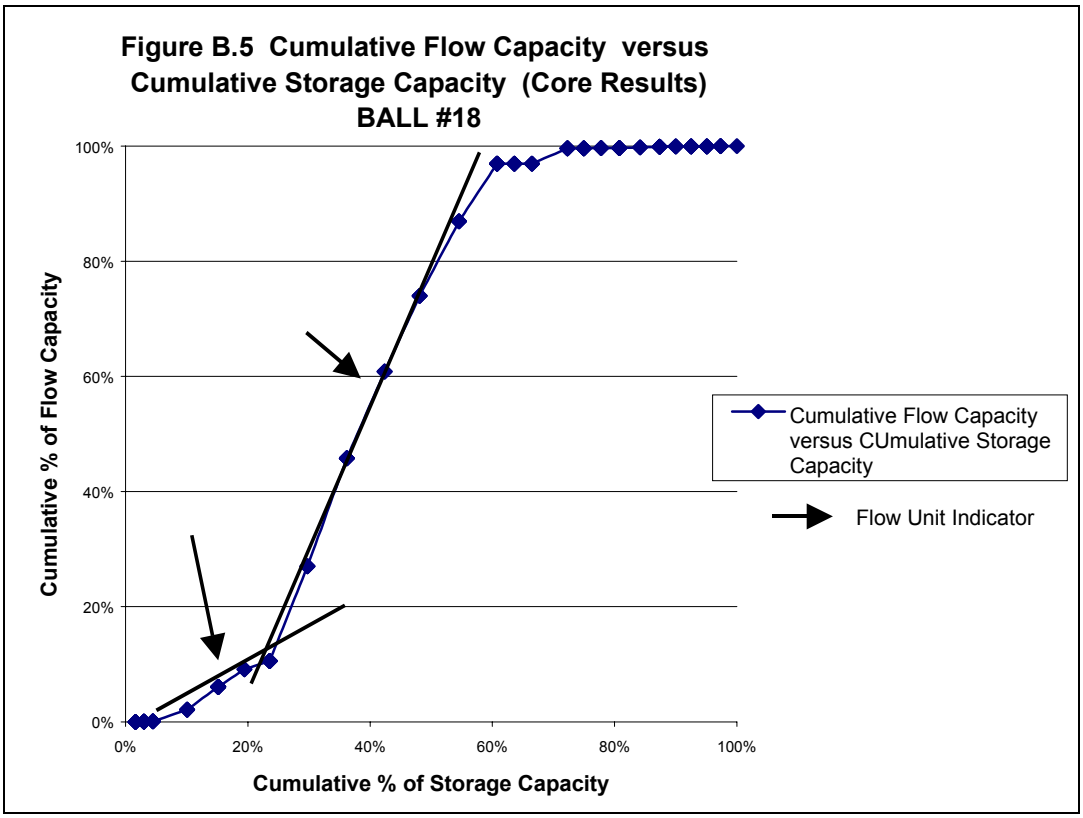
Figure B.5 Cumulative Flow Capacity versus Cumulative Storage Capacity (Core Results) BALL #18
100%
80%
60%
40%
20%
0%
Cumulative % of Flow Capacity
0%
20%
40%
60%
80%
100%
Cumulative % of Storage Capacity
Cumulative Flow Capacity versus CUmulative Storage Capacity
Flow Unit Indicator

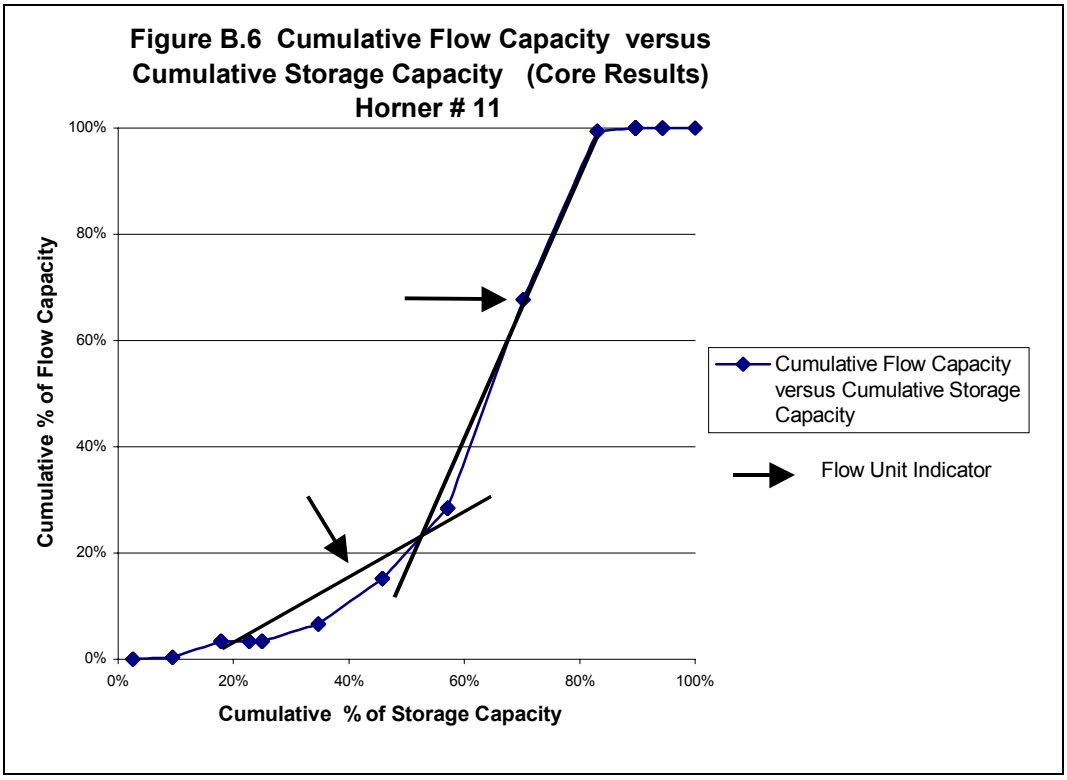
Figure B.6 Cumulative Flow Capacity versus Cumulative Storage Capacity (Core Results) Horner # 11
100%
80%
60%
40%
20%
0%
Cumulative % of Flow Capacity
0%
20%
40%
60%
80%
100%
Cumulative % of Storage Capacity
Cumulative Flow Capacity versus Cumulative Storage Capacity
Flow Unit Indicator

Table B.1 Cumulative k-h versus Cumulative p-h

Well Name: T. Heirs # 8 - Core Results
(Core Porosity and Permeability Used)

Depth (Feet)	Core Porosity	Core Perm	k-h	por-h	cumkh %	cum ph %
2782.50	9.6	0.02	0.02	9.6	0.02%	4.82%
2782.80					0.02%	4.82%
2783.00					0.02%	4.82%
2783.30					0.02%	4.82%
2783.50	9.4	0.03	0.03	9.4	0.05%	9.55%
2783.80					0.05%	9.55%
2784.00					0.05%	9.55%
2784.30					0.05%	9.55%
2784.50	9.2	0.06	0.06	9.2	0.11%	14.17%
2784.80					0.11%	14.17%
2785.00					0.11%	14.17%
2785.30	4	0.11	0.11	4	0.21%	16.18%
2785.50					0.21%	16.18%
2785.80					0.21%	16.18%
2786.00					0.21%	16.18%
2786.30	6.4	0.12	0.12	6.4	0.33%	19.40%
2786.50					0.33%	19.40%
2786.80					0.33%	19.40%
2787.00					0.33%	19.40%
2787.30					0.33%	19.40%
2787.50	7.2	0.02	0.02	7.2	0.35%	23.02%
2787.80					0.35%	23.02%
2788.00					0.35%	23.02%
2788.30					0.35%	23.02%
2788.50					0.35%	23.02%
2788.80	13.1	0.92	0.92	13.1	1.23%	29.60%
2789.00					1.23%	29.60%
2789.30	10.9	0.31	0.31	10.9	1.53%	35.08%
2789.50					1.53%	35.08%
2789.80					1.53%	35.08%
2790.00					1.53%	35.08%
2790.30					1.53%	35.08%
2790.50	9.1	0.1	0.1	9.1	1.62%	39.65%
2790.80					1.62%	39.65%
2791.00					1.62%	39.65%
2791.30					1.62%	39.65%
2791.50	14.1	6.5	6.5	14.1	7.87%	46.73%
2791.80					7.87%	46.73%
2792.00					7.87%	46.73%
2792.30					7.87%	46.73%

Table B.1 Cumulative k-h versus Cumulative p-h

Well Name: T. Heirs # 8 - Core Results
(Core Porosity and Permeability Used)

Depth (Feet)	Core Porosity	Core Perm	k-h	por-h	cumkh %	cum ph %
2792.50	14.6	3.8	3.8	14.6	11.52%	54.07%
2792.80					11.52%	54.07%
2793.00					11.52%	54.07%
2793.30					11.52%	54.07%
2793.50					11.52%	54.07%
2793.80	16.2	8.1	8.1	16.2	19.30%	62.21%
2794.00					19.30%	62.21%
2794.30					19.30%	62.21%
2794.50					19.30%	62.21%
2794.80	17.7	18	18	17.7	36.59%	71.11%
2795.00					36.59%	71.11%
2795.30	18.7	22	22	18.7	57.73%	80.50%
2795.50					57.73%	80.50%
2795.80					57.73%	80.50%
2796.00	19.4	23	23	19.4	79.83%	90.25%
2796.30					79.83%	90.25%
2796.50	19.4	21	21	19.4	100.00%	100.00%
			104.09	199		

Table B.2 Cumulative k-h versus Cumulative p-h

Well Name: Horner # 9 - Core Results
(Core Porosity and Permeability Used)

Depth (Feet)	Core Porosity	Core Perm	k-h	por-h	cumkh %	cum ph %
2888.75	4.1	0.1	0.1	4.1	1.35%	0.01%
2889.00					1.35%	0.01%
2889.25					1.35%	0.01%
2889.50					1.35%	0.01%
2889.75	3.6	0.2	0.2	3.6	2.54%	0.02%
2890.00					2.54%	0.02%
2890.25					2.54%	0.02%
2890.50					2.54%	0.02%
2890.75	3.7	0.1	0.1	3.7	3.76%	0.02%
2891.00					3.76%	0.02%
2891.25					3.76%	0.02%
2891.50					3.76%	0.02%
2891.75	6.1	3.3	3.3	6.1	5.77%	0.21%
2892.00					5.77%	0.21%
2892.25					5.77%	0.21%
2892.50					5.77%	0.21%
2892.75					5.77%	0.21%
2893.00	10	40	40	10	9.06%	2.51%
2893.25					9.06%	2.51%
2893.50	12.6	55	55	12.6	13.22%	5.67%
2893.75					13.22%	5.67%
2894.00					13.22%	5.67%
2894.25					13.22%	5.67%
2894.50					13.22%	5.67%
2894.75					13.22%	5.67%
2895.00	18.9	92	92	18.9	19.45%	10.95%
2895.25					19.45%	10.95%
2895.50					19.45%	10.95%
2895.75	17.6	80	80	17.6	25.25%	15.54%
2896.00					25.25%	15.54%
2896.25					25.25%	15.54%
2896.50	19.4	84	84	19.4	31.64%	20.37%
2896.75					31.64%	20.37%
2897.00					31.64%	20.37%
2897.25					31.64%	20.37%
2897.50					31.64%	20.37%
2897.75					31.64%	20.37%
2898.00					31.64%	20.37%
2898.25	21.7	123	123	21.7	38.79%	27.43%
2898.50					38.79%	27.43%
2898.75	21.6	136	136	21.6	45.91%	35.24%
2899.00					45.91%	35.24%

Table B.2 Cumulative k-h versus Cumulative p-h

Well Name: Horner # 9 - Core Results
(Core Porosity and Permeability Used)

Depth (Feet)	Core Porosity	Core Perm	k-h	por-h	cumkh %	cum ph %
2899.25					45.91%	35.24%
2899.50					45.91%	35.24%
2899.75					45.91%	35.24%
2900.00	23.2	160	160	23.2	53.56%	44.42%
2900.25					53.56%	44.42%
2900.50					53.56%	44.42%
2900.75					53.56%	44.42%
2901.00	22.1	135	135	22.1	60.84%	52.17%
2901.25					60.84%	52.17%
2901.50					60.84%	52.17%
2901.75					60.84%	52.17%
2902.00	23.1	144	144	23.1	68.46%	60.44%
2902.25					68.46%	60.44%
2902.50					68.46%	60.44%
2902.75					68.46%	60.44%
2903.00	23.2	124	124	23.2	76.10%	67.56%
2903.25					76.10%	67.56%
2903.50	24.1	148	148	24.1	84.05%	76.06%
2903.75					84.05%	76.06%
2904.00					84.05%	76.06%
2904.25					84.05%	76.06%
2904.50	24	203	203	24	91.96%	87.71%
2904.75					91.96%	87.71%
2905.00					91.96%	87.71%
2905.25					91.96%	87.71%
2905.50	24.4	214	214	24.4	100.00%	100.00%
			1741.7	303		

Table B.3 Cumulative k-h versus Cumulative p-h

Well Name: Ball # 19 - Core Results
(Core Porosity and Permeability Used)

Depth (Feet)	Core Porosity	Core Perm	k-h	por-h	cumkh %	cum ph %
3086.25	4.6	2.44	2.44	4.6	0.21%	1.09%
3086.50					0.21%	1.09%
3086.75					0.21%	1.09%
3087.00					0.21%	1.09%
3087.25	4.3			4.3	0.21%	2.12%
3087.50					0.21%	2.12%
3087.75					0.21%	2.12%
3088.00					0.21%	2.12%
3088.25	8.5	0.03	0.03	8.5	0.21%	4.14%
3088.50					0.21%	4.14%
3088.75					0.21%	4.14%
3089.00					0.21%	4.14%
3089.25	7.3	0.08	0.08	7.3	0.22%	5.88%
3089.50					0.22%	5.88%
3089.75					0.22%	5.88%
3090.00					0.22%	5.88%
3090.25	7.2	0.08	0.08	7.2	0.23%	7.59%
3090.50					0.23%	7.59%
3090.75					0.23%	7.59%
3091.00					0.23%	7.59%
3091.25	5.5	0.09	0.09	5.5	0.24%	8.90%
3091.50					0.24%	8.90%
3091.75					0.24%	8.90%
3092.00					0.24%	8.90%
3092.25	12.5	4.24	4.24	12.5	0.60%	11.88%
3092.50					0.60%	11.88%
3092.75	9.7	11	11	9.7	1.55%	14.18%
3093.00					1.55%	14.18%
3093.25					1.55%	14.18%
3093.50					1.55%	14.18%
3093.75					1.55%	14.18%
3094.00					1.55%	14.18%
3094.25	16.7	38	38	16.7	4.84%	18.16%
3094.50					4.84%	18.16%
3094.75	17	31	31	17	7.52%	22.20%
3095.00					7.52%	22.20%
3095.25					7.52%	22.20%
3095.50					7.52%	22.20%
3095.75					7.52%	22.20%
3096.00	10	0.08	0.08	10	7.53%	24.58%
3096.25					7.53%	24.58%
3096.50					7.53%	24.58%
3096.75					7.53%	24.58%

Table B.3 Cumulative k-h versus Cumulative p-h

Well Name: Ball # 19 - Core Results
(Core Porosity and Permeability Used)

Depth (Feet)	Core Porosity	Core Perm	k-h	por-h	cumkh %	cum ph %
3097.00					7.53%	24.58%
3097.25	9.7	0.27	0.27	9.7	7.55%	26.89%
3097.50					7.55%	26.89%
3097.75					7.55%	26.89%
3098.00	8.1	0.16	0.16	8.1	7.57%	28.82%
3098.25					7.57%	28.82%
3098.50					7.57%	28.82%
3098.75					7.57%	28.82%
3099.00					7.57%	28.82%
3099.25	13.3	17	17	13.3	9.04%	31.98%
3099.50					9.04%	31.98%
3099.75					9.04%	31.98%
3100.00	20.3	41	41	20.3	12.59%	36.82%
3100.25					12.59%	36.82%
3100.50					12.59%	36.82%
3100.75					12.59%	36.82%
3101.00					12.59%	36.82%
3101.25	21.4	65	65	21.4	18.21%	41.91%
3101.50					18.21%	41.91%
3101.75					18.21%	41.91%
3102.00	17.4	17	17	17.4	19.68%	46.05%
3102.25					19.68%	46.05%
3102.50					19.68%	46.05%
3102.75					19.68%	46.05%
3103.00	11	6.79	6.79	11	20.27%	48.67%
3103.25					20.27%	48.67%
3103.50					20.27%	48.67%
3103.75					20.27%	48.67%
3104.00	19.7	73	73	19.7	26.59%	53.36%
3104.25					26.59%	53.36%
3104.50					26.59%	53.36%
3104.75					26.59%	53.36%
3105.00	20.8	60	60	20.8	31.78%	58.31%
3105.25					31.78%	58.31%
3105.50					31.78%	58.31%
3105.75					31.78%	58.31%
3106.00	13.4	1.16	1.16	13.4	31.88%	61.49%
3106.25					31.88%	61.49%
3106.50					31.88%	61.49%
3106.75					31.88%	61.49%
3107.00					31.88%	61.49%
3107.25	21.7	110	110	21.7	41.39%	66.66%
3107.50					41.39%	66.66%

Table B.3 Cumulative k-h versus Cumulative p-h

Well Name: Ball # 19 - Core Results
(Core Porosity and Permeability Used)

Depth (Feet)	Core Porosity	Core Perm	k-h	por-h	cumkh %	cum ph %
3107.75					41.39%	66.66%
3108.00	22	106	106	22	50.57%	71.89%
3108.25					50.57%	71.89%
3108.50					50.57%	71.89%
3108.75	22.9	207	207	22.9	68.48%	77.34%
3109.00					68.48%	77.34%
3109.25					68.48%	77.34%
3109.50	23.2	179	179	23.2	83.96%	82.87%
3109.75					83.96%	82.87%
3110.00					83.96%	82.87%
3110.25					83.96%	82.87%
3110.50					83.96%	82.87%
3110.75	24	124	124	24	94.69%	88.58%
3111.00					94.69%	88.58%
3111.25					94.69%	88.58%
3111.50					94.69%	88.58%
3111.75					94.69%	88.58%
3112.00	18.4	26	26	18.4	96.94%	92.96%
3112.25					96.94%	92.96%
3112.50	18.9	34	34	18.9	99.88%	97.45%
3112.75					99.88%	97.45%
3113.00					99.88%	97.45%
3113.25					99.88%	97.45%
3113.50					99.88%	97.45%
3113.75	10.7	1.33	1.33	10.7	100.00%	100.00%
3114.00					100.00%	100.00%
3114.25					100.00%	100.00%
3114.50					100.00%	100.00%
3114.75					100.00%	100.00%
3115.00					100.00%	100.00%
3115.25					100.00%	100.00%
3115.50					100.00%	100.00%
3115.75					100.00%	100.00%
3116.00					100.00%	100.00%
3116.25					100.00%	100.00%
3116.50					100.00%	100.00%
3116.75					100.00%	100.00%
3117.00					100.00%	100.00%
3117.25					100.00%	100.00%
3117.50					100.00%	100.00%
3117.75					100.00%	100.00%
3118.00					100.00%	100.00%
3118.25					100.00%	100.00%

Table B.3 Cumulative k-h versus Cumulative p-h

Well Name: Ball # 19 - Core Results
(Core Porosity and Permeability Used)

Depth (Feet)	Core Porosity	Core Perm	k-h	por-h	cumkh %	cum ph %
3118.50					100.00%	100.00%
3118.75					100.00%	100.00%
3119.00					100.00%	100.00%
3119.25					100.00%	100.00%
3119.50					100.00%	100.00%
3119.75					100.00%	100.00%
3120.00					100.00%	100.00%
3120.25					100.00%	100.00%
3120.50					100.00%	100.00%
3120.75					100.00%	100.00%
3121.00					100.00%	
			1156	420		

Table B.4 Cumulative k-h versus Cumulative p-h

Well Name: LeMasters # 13 - Core Results
(Core Porosity and Permeability Used)

Depth (Feet)	Core Porosity	Core Perm	k-h	por-h	cumkh %	cum ph %
3030.80	8.2	0.05	0.1	8.2	0.07%	3.39%
3031.00					0.07%	3.39%
3031.30					0.07%	3.39%
3031.50					0.07%	3.39%
3031.80					0.07%	3.39%
3032.00	4.3	0.15	0.2	4.3	0.27%	5.17%
3032.30					0.27%	5.17%
3032.50	5.3	0.72	0.7	5.3	1.22%	7.36%
3032.80					1.22%	7.36%
3033.00					1.22%	7.36%
3033.30					1.22%	7.36%
3033.50					1.22%	7.36%
3033.80					1.22%	7.36%
3034.00	4.9	0.28	0.3	4.9	1.60%	9.39%
3034.30					1.60%	9.39%
3034.50	7.1	0.27	0.3	7.1	1.96%	12.33%
3034.80					1.96%	12.33%
3035.00					1.96%	12.33%
3035.30					1.96%	12.33%
3035.50					1.96%	12.33%
3035.80					1.96%	12.33%
3036.00	3.4	0.12	0.1	3.4	2.11%	13.74%
3036.30					2.11%	13.74%
3036.50	3.5	0.22	0.2	3.5	2.41%	15.18%
3036.80					2.41%	15.18%
3037.00					2.41%	15.18%
3037.30					2.41%	15.18%
3037.50					2.41%	15.18%
3037.80					2.41%	15.18%
3038.00					2.41%	15.18%
3038.30					2.41%	15.18%
3038.50	6.6	0.18	0.2	6.6	2.65%	17.91%
3038.80					2.65%	17.91%
3039.00					2.65%	17.91%
3039.30					2.65%	17.91%
3039.50					2.65%	17.91%
3039.80	8.4	0.06	0.1	8.4	2.73%	21.39%
3040.00					2.73%	21.39%
3040.30					2.73%	21.39%
3040.50					2.73%	21.39%
3040.80	7.4	0.06	0.1	7.4	2.81%	24.45%
3041.00					2.81%	24.45%
3041.30					2.81%	24.45%

Table B.4 Cumulative k-h versus Cumulative p-h

Well Name: LeMasters # 13 - Core Results
(Core Porosity and Permeability Used)

Depth (Feet)	Core Porosity	Core Perm	k-h	por-h	cumkh %	cum ph %
3041.50					2.81%	24.45%
3041.80	7.4	0.04	0	7.4	2.86%	27.51%
3042.00					2.86%	27.51%
3042.30					2.86%	27.51%
3042.50	5.7	0.19	0.2	5.7	3.11%	29.87%
3042.80					3.11%	29.87%
3043.00	9.5	0.29	0.3	9.5	3.50%	33.80%
3043.30					3.50%	33.80%
3043.50					3.50%	33.80%
3043.80					3.50%	33.80%
3044.00					3.50%	33.80%
3044.30					3.50%	33.80%
3044.50					3.50%	33.80%
3044.80					3.50%	33.80%
3045.00	10.2	0.67	0.7	10	4.39%	38.02%
3045.30					4.39%	38.02%
3045.50					4.39%	38.02%
3045.80					4.39%	38.02%
3046.00	8.9	0.21	0.2	8.9	4.67%	41.70%
3046.30					4.67%	41.70%
3046.50	5.7			5.7	4.67%	44.06%
3046.80					4.67%	44.06%
3047.00					4.67%	44.06%
3047.30					4.67%	44.06%
3047.50	6.6	0.04	0	6.6	4.72%	46.79%
3047.80					4.72%	46.79%
3048.00					4.72%	46.79%
3048.30					4.72%	46.79%
3048.50					4.72%	46.79%
3048.80					4.72%	46.79%
3049.00	19.4	37	37	19	53.93%	54.82%
3049.30					53.93%	54.82%
3049.50					53.93%	54.82%
3049.80					53.93%	54.82%
3050.00	11	1.51	1.5	11	55.94%	59.37%
3050.30					55.94%	59.37%
3050.50					55.94%	59.37%
3050.80					55.94%	59.37%
3051.00	6.9	0.11	0.1	6.9	56.08%	62.23%
3051.30					56.08%	62.23%
3051.50					56.08%	62.23%
3051.80					56.08%	62.23%
3052.00	14.5	19	19	15	81.35%	68.23%

Table B.4 Cumulative k-h versus Cumulative p-h

Well Name: LeMasters # 13 - Core Results
(Core Porosity and Permeability Used)

Depth (Feet)	Core Porosity	Core Perm	k-h	por-h	cumkh %	cum ph %
3052.30					81.35%	68.23%
3052.50					81.35%	68.23%
3052.80					81.35%	68.23%
3053.00	16.3	11	11	16	95.98%	74.97%
3053.30					95.98%	74.97%
3053.50					95.98%	74.97%
3053.80					95.98%	74.97%
3054.00	9.2	0.07	0.1	9.2	96.08%	78.78%
3054.30					96.08%	78.78%
3054.50					96.08%	78.78%
3054.80					96.08%	78.78%
3055.00	9.8	0.1	0.1	9.8	96.21%	82.83%
3055.30					96.21%	82.83%
3055.50					96.21%	82.83%
3055.80					96.21%	82.83%
3056.00	8.7	0.09	0.1	8.7	96.33%	86.43%
3056.30					96.33%	86.43%
3056.50					96.33%	86.43%
3056.80					96.33%	86.43%
3057.00	6.8	0.02	0	6.8	96.36%	89.24%
3057.30					96.36%	89.24%
3057.50					96.36%	89.24%
3057.80					96.36%	89.24%
3058.00	9.3	0.04	0	9.3	96.41%	93.09%
3058.30					96.41%	93.09%
3058.50					96.41%	93.09%
3058.80					96.41%	93.09%
3059.00	9.1	0.04	0	9.1	96.46%	96.86%
3059.30					96.46%	96.86%
3059.50					96.46%	96.86%
3059.80					96.46%	96.86%
3060.00	7.6	2.66	2.7	7.6	100.00%	100.00%
		242		75		

Table B.5 Cumulative k-h versus Cumulative p-h

Well Name: Ball # 18 - Core Results
(Core Porosity and Permeability Used)

Depth (Feet)	Core Porosity	Core Perm	k-h	por-h	cumkh %	cum ph %
2987.25	6.3	0.26	0.26	6.3	0.02%	1.62%
2987.50					0.02%	1.62%
2987.75					0.02%	1.62%
2988.00					0.02%	1.62%
2988.25	5.2	0.77	0.77	5.2	0.08%	2.96%
2988.50					0.08%	2.96%
2988.75					0.08%	2.96%
2989.00					0.08%	2.96%
2989.25					0.08%	2.96%
2989.50					0.08%	2.96%
2989.75	5.8	0.14	0.14	5.8	0.09%	4.45%
2990.00					0.09%	4.45%
2990.25					0.09%	4.45%
2990.50					0.09%	4.45%
2990.75	21.7	28	28	21.7	2.13%	10.04%
2991.00					2.13%	10.04%
2991.25					2.13%	10.04%
2991.50	19.9	54	54	19.9	6.06%	15.16%
2991.75					6.06%	15.16%
2992.00					6.06%	15.16%
2992.25					6.06%	15.16%
2992.50					6.06%	15.16%
2992.75					6.06%	15.16%
2993.00					6.06%	15.16%
2993.25					6.06%	15.16%
2993.50	16.5	42	42	16.5	9.12%	19.41%
2993.75					9.12%	19.41%
2994.00	16.1	20	20	16.1	10.58%	23.56%
2994.25					10.58%	23.56%
2994.50					10.58%	23.56%
2994.75					10.58%	23.56%
2995.00					10.58%	23.56%
2995.25					10.58%	23.56%
2995.50	24.1	226	226	24.1	27.05%	29.76%
2995.75					27.05%	29.76%
2996.00					27.05%	29.76%
2996.25	24.9	257	257	24.9	45.77%	36.17%
2996.50					45.77%	36.17%
2996.75					45.77%	36.17%
2997.00					45.77%	36.17%
2997.25					45.77%	36.17%
2997.50	24	207	207	24	60.85%	42.35%
2997.75					60.85%	42.35%

Table B.5 Cumulative k-h versus Cumulative p-h

Well Name: Ball # 18 - Core Results
(Core Porosity and Permeability Used)

Depth (Feet)	Core Porosity	Core Perm	k-h	por-h	cumkh %	cum ph %
2998.00					60.85%	42.35%
2998.25	22.3	180	180	22.3	73.97%	48.09%
2998.50					73.97%	48.09%
2998.75					73.97%	48.09%
2999.00	24.9	178	178	24.9	86.94%	54.51%
2999.25					86.94%	54.51%
2999.50					86.94%	54.51%
2999.75	24.4	137	137	24.4	96.92%	60.79%
3000.00					96.92%	60.79%
3000.25					96.92%	60.79%
3000.50					96.92%	60.79%
3000.75					96.92%	60.79%
3001.00	10.9	0.06	0.06	10.9	96.93%	63.59%
3001.25					96.93%	63.59%
3001.50					96.93%	63.59%
3001.75					96.93%	63.59%
3002.00	11.2	0.05	0.05	11.2	96.93%	66.48%
3002.25					96.93%	66.48%
3002.50					96.93%	66.48%
3002.75	22.5	37	37	22.5	99.63%	72.27%
3003.00					99.63%	72.27%
3003.25					99.63%	72.27%
3003.50					99.63%	72.27%
3003.75					99.63%	72.27%
3004.00	10.4	0.1	0.1	10.4	99.63%	74.95%
3004.25					99.63%	74.95%
3004.50					99.63%	74.95%
3004.75					99.63%	74.95%
3005.00					99.63%	74.95%
3005.25	11	0.26	0.26	11	99.65%	77.78%
3005.50					99.65%	77.78%
3005.75					99.65%	77.78%
3006.00	11.7	0.07	0.07	11.7	99.66%	80.79%
3006.25					99.66%	80.79%
3006.50					99.66%	80.79%
3006.75					99.66%	80.79%
3007.00					99.66%	80.79%
3007.25	13.2	1.4	1.4	13.2	99.76%	84.19%
3007.50					99.76%	84.19%
3007.75	12.3	1.5	1.5	12.3	99.87%	87.36%
3008.00					99.87%	87.36%
3008.25					99.87%	87.36%
3008.50					99.87%	87.36%

Table B.5 Cumulative k-h versus Cumulative p-h

Well Name: Ball # 18 - Core Results
(Core Porosity and Permeability Used)

Depth (Feet)	Core Porosity	Core Perm	k-h	por-h	cumkh %	cum ph %
3008.75					99.87%	87.36%
3009.00	10.2	0.79	0.79	10.2	99.93%	89.98%
3009.25					99.93%	89.98%
3009.50					99.93%	89.98%
3009.75	9.8	0.25	0.25	9.8	99.95%	92.51%
3010.00					99.95%	92.51%
3010.25					99.95%	92.51%
3010.50					99.95%	92.51%
3010.75					99.95%	92.51%
3011.00	9.9	0.11	0.11	9.9	99.95%	95.06%
3011.25					99.95%	95.06%
3011.50					99.95%	95.06%
3011.75					99.95%	95.06%
3012.00					99.95%	95.06%
3012.25	8.8	0.26	0.26	8.8	99.97%	97.32%
3012.50					99.97%	97.32%
3012.75					99.97%	97.32%
3013.00	10.4	0.38	0.38	10.4	100.00%	100.00%
			1372	388		

Table B.6 Cumulative k-h versus Cumulative p-h

Well Name: Horner # 11 - Core Results
(Core Porosity and Permeability Used)

Depth (Feet)	Core Porosity	Core Perm	k-h	por-h	cumkh %	cum ph %
3083.75	5	0.1	0.1	5	0.02%	2.59%
3084.00					0.02%	2.59%
3084.25					0.02%	2.59%
3084.50	13.3	2.1	2.1	13.3	0.36%	9.46%
3084.75					0.36%	9.46%
3085.00					0.36%	9.46%
3085.25	16.2	18	18	16.2	3.33%	17.84%
3085.50					3.33%	17.84%
3085.75					3.33%	17.84%
3086.00					3.33%	17.84%
3086.25					3.33%	17.84%
3086.50	9.5	0.1	0.1	9.5	3.35%	22.75%
3086.75					3.35%	22.75%
3087.00					3.35%	22.75%
3087.25					3.35%	22.75%
3087.50	4.2	0.1	0.1	4.2	3.36%	24.92%
3087.75					3.36%	24.92%
3088.00					3.36%	24.92%
3088.25					3.36%	24.92%
3088.50					3.36%	24.92%
3088.75	18.9	20	20	18.9	6.66%	34.69%
3089.00					6.66%	34.69%
3089.25					6.66%	34.69%
3089.50	21.5	52	52	21.5	15.24%	45.81%
3089.75					15.24%	45.81%
3090.00					15.24%	45.81%
3090.25					15.24%	45.81%
3090.50	21.8	80	80	21.8	28.43%	57.08%
3090.75					28.43%	57.08%
3091.00					28.43%	57.08%
3091.25					28.43%	57.08%
3091.50					28.43%	57.08%
3091.75					28.43%	57.08%
3092.00	25.4	238	238	25.4	67.69%	70.22%
3092.25					67.69%	70.22%
3092.50	24.9	192	192	24.9	99.36%	83.09%
3092.75					99.36%	83.09%
3093.00					99.36%	83.09%
3093.25	12.7	3.6	3.6	12.7	99.95%	89.66%
3093.50					99.95%	89.66%
3093.75					99.95%	89.66%
3094.00					99.95%	89.66%
3094.25					99.95%	89.66%

Table B.6 Cumulative k-h versus Cumulative p-h

Well Name: Horner # 11 - Core Results
(Core Porosity and Permeability Used)

Depth (Feet)	Core Porosity	Core Perm	k-h	por-h	cumkh %	cum ph %
3094.50					99.95%	89.66%
3094.75					99.95%	89.66%
3095.00					99.95%	89.66%
3095.25					99.95%	89.66%
3095.50					99.95%	89.66%
3095.75					99.95%	89.66%
3096.00					99.95%	89.66%
3096.25					99.95%	89.66%
3096.50					99.95%	89.66%
3096.75					99.95%	89.66%
3097.00					99.95%	89.66%
3097.25					99.95%	89.66%
3097.50					99.95%	89.66%
3097.75					99.95%	89.66%
3098.00					99.95%	89.66%
3098.25					99.95%	89.66%
3098.50					99.95%	89.66%
3098.75					99.95%	89.66%
3099.00					99.95%	89.66%
3099.25					99.95%	89.66%
3099.50					99.95%	89.66%
3099.75	9	0.1	0.1	9	99.97%	94.31%
3100.00					99.97%	94.31%
3100.25					99.97%	94.31%
3100.50					99.97%	94.31%
3100.75	11	0.2	0.2	11	100.00%	100.00%
			606.3	193.4		

Table B.7 Potential Flow Unit Boundary Point Analysis
Core Permeability and Core Measurement

Well Name	Flow Unit Interval (Feet)	Flow Unit Interval (Feet)	Observation
T. Heirs # 8	2791.50 - 2794.00	2794.00 - 2796.00	k in all sections low. Distance between core points vary.
Horner # 9	2892.75 - 2898.00	2898.00 - 2905.50	k much better overall. Much higher in second zone.
Ball # 19	3086.25 - 3106.00	3107.25 - 3110.75	Much higher k in second zone.
LeMasters # 13	3047.00 - 3053.00		Appears to be single zone. Very low k.
Ball # 18	2987.50 - 2994.00	2994.00 - 2999.75	High k second zone. Below sand no k, but sand @ 3002.75 - 3013.00
Horner # 11	3084.50 - 3090.50	3092.00 - 3093.00	Some good k lower zone. High k zone. Possible few points of sand below.

APPENDIX C.

Appendix C. presents cumulative flow capacity versus cumulative storage capacity graphs for each core well. The graphs use log measurements for porosity and minipermeameter measurements for permeability.

Figure C.1 Cumulative Flow Capacity versus Cumulative Storage Capacity (Miniperm) T. Heirs # 8

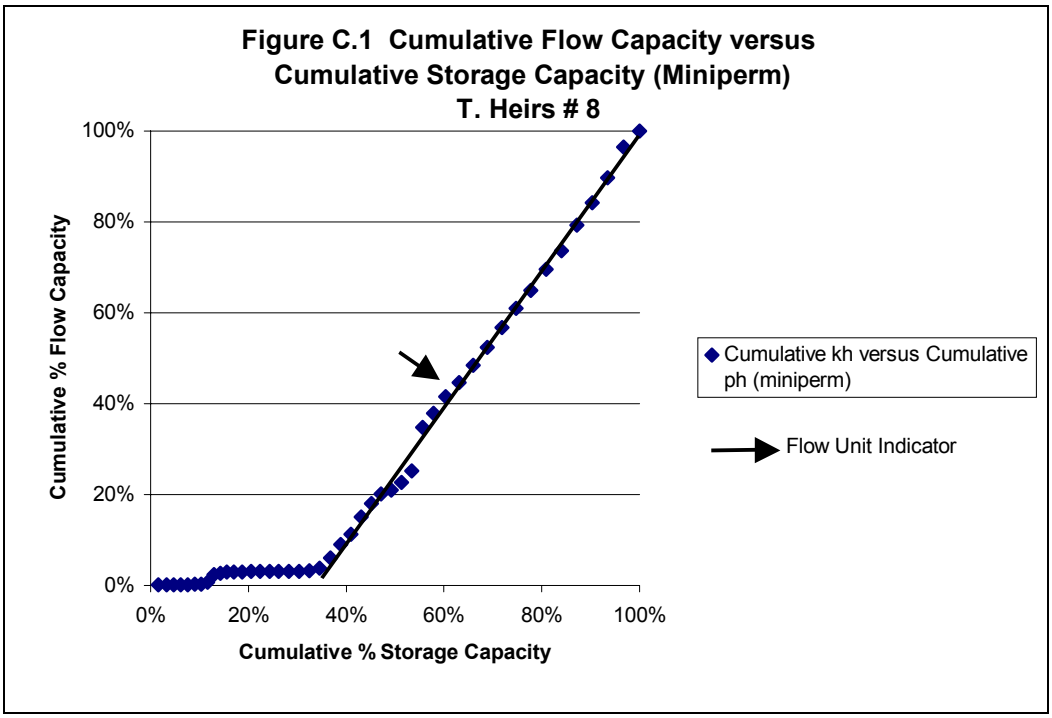

Figure C.2 Cumulative Flow Capacity versus Cumulative Storage Capacity (Miniperm) Horner # 9

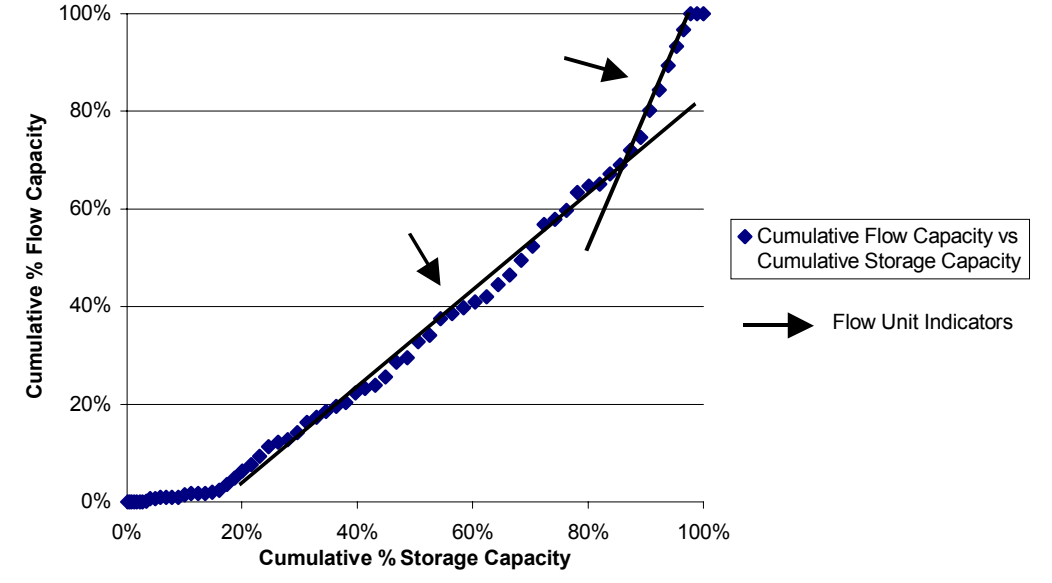

Figure C.3 Cumulative Flow Capacity versus Cumulative Storage Capacity (Miniperm) Ball # 19

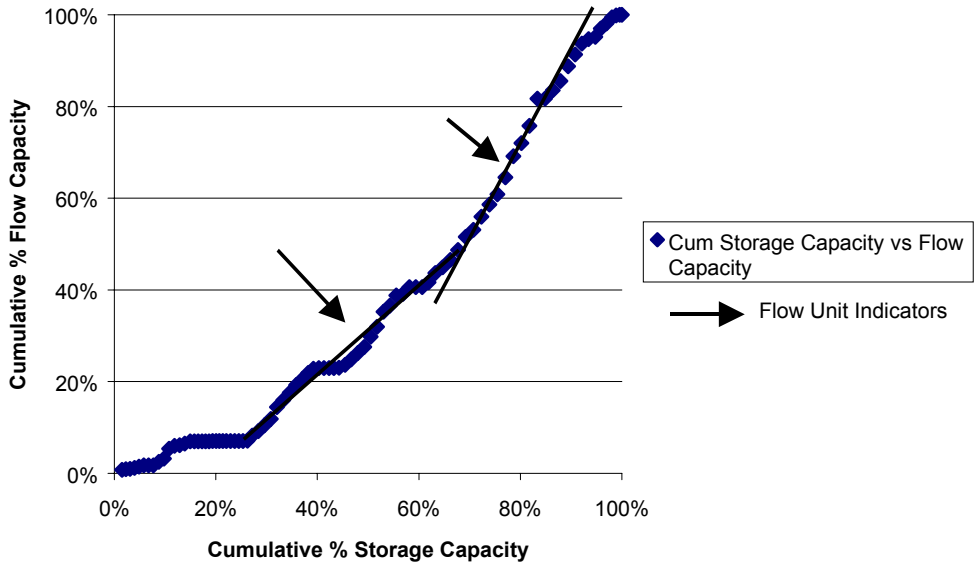

Figure C.4 Cumulative Flow Capacity versus Cumulative Storage Capacity LeMasters # 13 (Miniperm)

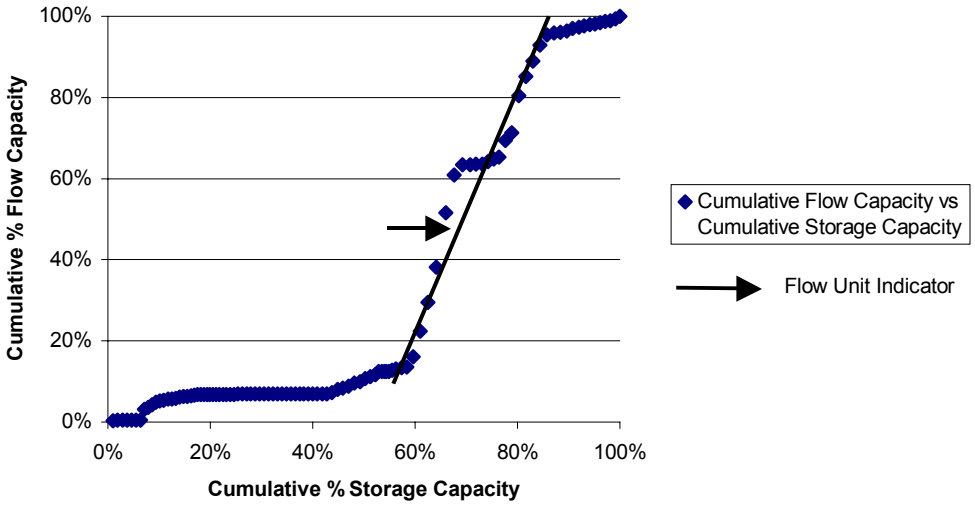

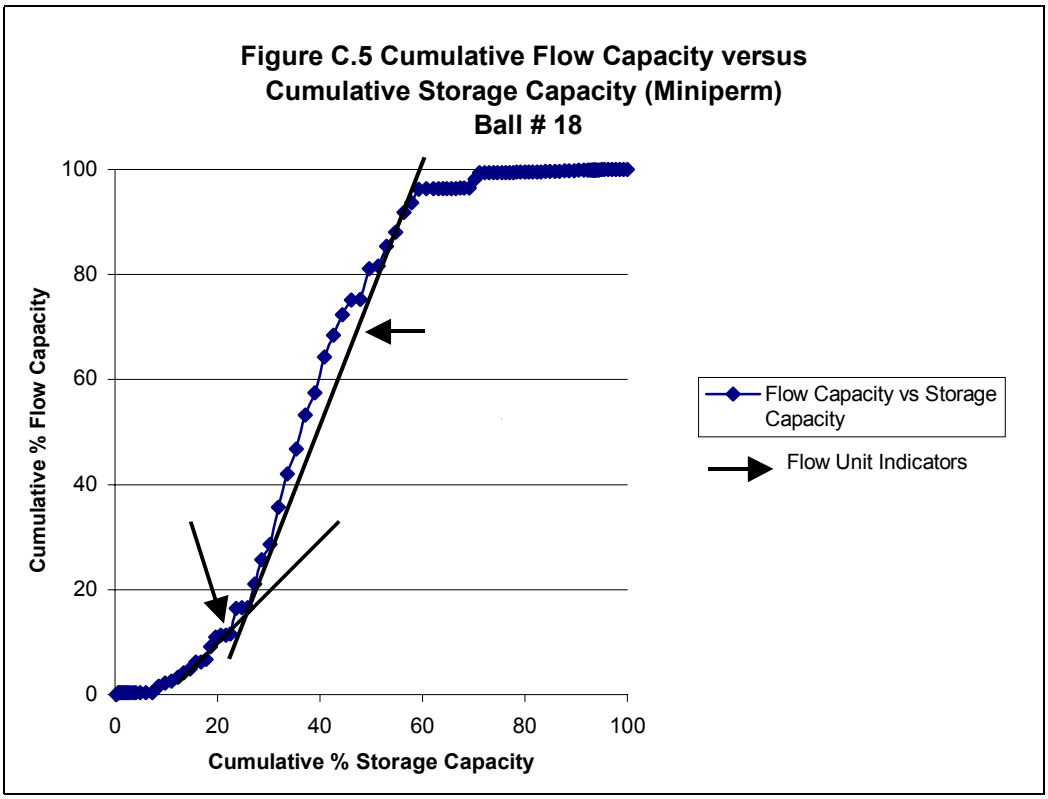
Figure C.5 Cumulative Flow Capacity versus
Cumulative Storage Capacity (Miniperm)
Ball # 18
Cumulative % Flow Capacity
100
80
60
40
20
0
0
20
40
60
80
100
Cumulative % Storage Capacity
Flow Capacity vs Storage Capacity
Flow Unit Indicators

Table C.1 Cumulative kh versus Cumulative Por-h (Minipermeameter Readings)

Well Name: T. Heirs # 8

Depth	Log Porosity	Log Density	Miniperm Perm.	kh	Cum kh %	Por-h	Cum Por-h %
2785.25	0.095833	2.519	0.280998	0.07025	0.001508	0.023958	0.016061
2785.50	0.097619	2.5160	0.0100	0.00	0.0016	0.024405	0.0324
2785.75	0.0875	2.5330	0.0100	0.00	0.0016	0.021875	0.0471
2786.00	0.0875	2.5330	0.0100	0.00	0.0017	0.021875	0.0618
2786.25	0.085119	2.5370	0.0100	0.00	0.0017	0.02128	0.0760
2786.50	0.083333	2.5400	0.2279	0.06	0.0029	0.020833	0.0900
2786.75	0.080952	2.5440	0.0491	0.01	0.0032	0.020238	0.1036
2787.00	0.07619	2.5520	0.6748	0.17	0.0068	0.019048	0.1163
2787.25	0.076786	2.5510	3.1960	0.80	0.0240	0.019196	0.1292
2787.50	0.078571	2.5480	0.5264	0.13	0.0268	0.019643	0.1424
2787.75	0.078571	2.5480	0.4585	0.11	0.0293	0.019643	0.1555
2788.00	0.0875	2.5330	0.0100	0.00	0.0293	0.021875	0.1702
2788.25	0.104762	2.5040	0.0100	0.00	0.0294	0.02619	0.1877
2788.50	0.105357	2.5030	0.3779	0.09	0.0314	0.026339	0.2054
2788.75	0.110119	2.4950	0.0100	0.00	0.0315	0.02753	0.2239
2789.00	0.114286	2.4880	0.0100	0.00	0.0315	0.028571	0.2430
2789.25	0.114286	2.4880	0.0100	0.00	0.0316	0.028571	0.2622
2789.50	0.125595	2.4690	0.0100	0.00	0.0316	0.031399	0.2832
2789.75	0.123214	2.4730	0.0100	0.00	0.0317	0.030804	0.3039
2790.00	0.125595	2.4690	0.2035	0.05	0.0328	0.031399	0.3249
2790.25	0.126786	2.4670	1.0651	0.27	0.0385	0.031696	0.3462
2790.50	0.126786	2.4670	3.9927	1.00	0.0599	0.031696	0.3674
2790.75	0.126786	2.4670	5.5744	1.39	0.0898	0.031696	0.3887
2791.00	0.124405	2.4710	4.2682	1.07	0.1128	0.031101	0.4095
2791.25	0.124405	2.4710	7.0817	1.77	0.1508	0.031101	0.4304
2791.50	0.123214	2.4730	5.5858	1.40	0.1808	0.030804	0.4510
2791.75	0.123214	2.4730	3.9277	0.98	0.2018	0.030804	0.4717
2792.00	0.124405	2.4710	1.3847	0.35	0.2093	0.031101	0.4925
2792.25	0.124405	2.4710	3.1343	0.78	0.2261	0.031101	0.5134
2792.50	0.126786	2.4670	4.7175	1.18	0.2514	0.031696	0.5346
2792.75	0.128571	2.4640	17.9513	4.49	0.3478	0.032143	0.5562
2793.00	0.135714	2.4520	5.8257	1.46	0.3791	0.033929	0.5789
2793.25	0.147024	2.4330	6.8743	1.72	0.4160	0.036756	0.6036
2793.50	0.165476	2.4020	5.6983	1.42	0.4466	0.041369	0.6313
2793.75	0.171429	2.3920	6.9719	1.74	0.4840	0.042857	0.6600
2794.00	0.171429	2.3920	7.3910	1.85	0.5237	0.042857	0.6887
2794.25	0.174405	2.3870	8.2618	2.07	0.5680	0.043601	0.7180
2794.50	0.17619	2.3840	7.8833	1.97	0.6103	0.044048	0.7475
2794.75	0.17619	2.3840	7.2555	1.81	0.6493	0.044048	0.7770
2795.00	0.18631	2.3670	8.6903	2.17	0.6959	0.046577	0.8083
2795.25	0.1875	2.3650	7.6390	1.91	0.7369	0.046875	0.8397
2795.50	0.1875	2.3650	10.4653	2.62	0.7931	0.046875	0.8711
2795.75	0.18869	2.3630	9.0789	2.27	0.8419	0.047173	0.9027
2796.00	0.191071	2.3590	10.3483	2.59	0.8974	0.047768	0.9348

Table C.1 Cumulative kh versus Cumulative Por-h (Minipermeameter Readings)

Well Name: T. Heirs # 8

Depth	Log Porosity	Log Density	Miniperm Perm.	kh	Cum kh %	Por-h	Cum Por-h %
2796.25	0.194048	2.3540	12.5202	3.13	0.9646	0.048512	0.9673
2796.50	0.195238	2.3520	6.5908	1.65	1.0000	0.04881	1.0000
				46.57		1.491667	

Table C.2 Cumulative kh versus Cumulative Por-h (Minipermeameter Readings)

Well Name: Horner # 9

Depth	Log Porosity	Log Density	Miniperm Perm.	kh	Cum kh %	Por-h	Cum Por-h %
2890.00	0.0381	2.627	0.0100	0.0025	0.0000	0.0095	0.0058
2890.25	0.0435	2.616	0.0100	0.0025	0.0000	0.0109	0.0094
2890.50	0.0500	2.607	0.0100	0.0025	0.0000	0.0125	0.0135
2890.75	0.0565	2.596	0.8830	0.2208	0.0004	0.0141	0.0182
2891.00	0.0565	2.585	0.0100	0.0025	0.0004	0.0141	0.0229
2891.25	0.0631	2.585	0.0100	0.0025	0.0004	0.0158	0.0281
2891.50	0.0726	2.574	1.1439	0.2860	0.0009	0.0182	0.0342
2891.75	0.0869	2.558	13.4000	3.3500	0.0064	0.0217	0.0414
2892.00	0.1012	2.534	1.5399	0.3850	0.0070	0.0253	0.0498
2892.25	0.1131	2.51	4.2946	1.0737	0.0088	0.0283	0.0591
2892.50	0.1208	2.49	1.1409	0.2852	0.0092	0.0302	0.0692
2892.75	0.1208	2.477	0.4074	0.1018	0.0094	0.0302	0.0792
2893.00	0.1274	2.477	0.6606	0.1652	0.0097	0.0318	0.0897
2893.25	0.1321	2.466	10.8100	2.7025	0.0141	0.0330	0.1007
2893.50	0.1375	2.458	6.6348	1.6587	0.0168	0.0344	0.1121
2893.75	0.1417	2.449	0.0100	0.0025	0.0168	0.0354	0.1239
2894.00	0.1464	2.442	0.4317	0.1079	0.0170	0.0366	0.1360
2894.25	0.1464	2.434	6.8302	1.7075	0.0198	0.0366	0.1481
2894.50	0.1512	2.434	9.8841	2.4710	0.0239	0.0378	0.1607
2894.75	0.1560	2.426	27.5515	6.8879	0.0352	0.0390	0.1736
2895.00	0.1595	2.418	33.0244	8.2561	0.0488	0.0399	0.1868
2895.25	0.1714	2.412	34.4939	8.6235	0.0630	0.0429	0.2011
2895.50	0.1780	2.392	32.0937	8.0234	0.0762	0.0445	0.2158
2895.75	0.1845	2.381	41.5721	10.3930	0.0932	0.0461	0.2311
2896.00	0.1845	2.37	46.2598	11.5650	0.1122	0.0461	0.2464
2896.25	0.1982	2.37	25.2676	6.3169	0.1226	0.0496	0.2629
2896.50	0.2000	2.347	10.6375	2.6594	0.1270	0.0500	0.2794
2896.75	0.2018	2.344	34.8349	8.7087	0.1413	0.0504	0.2962
2897.00	0.2018	2.341	51.3400	12.8350	0.1624	0.0504	0.3129
2897.25	0.2018	2.341	24.9110	6.2277	0.1727	0.0504	0.3296
2897.50	0.2018	2.341	31.2962	7.8240	0.1855	0.0504	0.3464
2897.75	0.2018	2.341	24.5029	6.1257	0.1956	0.0504	0.3631
2898.00	0.2018	2.341	18.6077	4.6519	0.2032	0.0504	0.3798
2898.25	0.2036	2.341	47.0826	11.7707	0.2226	0.0509	0.3967
2898.50	0.2060	2.338	25.1597	6.2899	0.2329	0.0515	0.4138
2898.75	0.2071	2.334	12.8708	3.2177	0.2382	0.0518	0.4310
2899.00	0.2131	2.332	44.5364	11.1341	0.2565	0.0533	0.4487
2899.25	0.2292	2.322	71.8191	17.9548	0.2860	0.0573	0.4677
2899.50	0.2292	2.295	21.5921	5.3980	0.2949	0.0573	0.4867
2899.75	0.2327	2.295	80.8000	20.2000	0.3281	0.0582	0.5060
2900.00	0.2333	2.289	30.5458	7.6364	0.3407	0.0583	0.5253
2900.25	0.2351	2.288	85.0700	21.2675	0.3756	0.0588	0.5448
2900.50	0.2357	2.285	24.4367	6.1092	0.3857	0.0589	0.5644
2900.75	0.2375	2.284	30.4148	7.6037	0.3982	0.0594	0.5841

Table C.2 Cumulative kh versus Cumulative Por-h (Minipermeameter Readings)

Well Name: Horner # 9

Depth	Log Porosity	Log Density	Miniperm Perm.	kh	Cum kh %	Por-h	Cum Por-h %
2901.00	0.2399	2.281	27.0736	6.7684	0.4093	0.0600	0.6040
2901.25	0.2399	2.277	26.3850	6.5963	0.4201	0.0600	0.6239
2901.50	0.2417	2.277	58.8000	14.7000	0.4443	0.0604	0.6439
2901.75	0.2417	2.274	49.5306	12.3826	0.4647	0.0604	0.6639
2902.00	0.2411	2.274	73.8187	18.4547	0.4950	0.0603	0.6839
2902.25	0.2393	2.275	70.5482	17.6371	0.5240	0.0598	0.7038
2902.50	0.2387	2.278	107.3500	26.8375	0.5681	0.0597	0.7236
2902.75	0.2357	2.279	25.0521	6.2630	0.5784	0.0589	0.7431
2903.00	0.2357	2.284	46.8822	11.7206	0.5977	0.0589	0.7627
2903.25	0.2333	2.284	86.6900	21.6725	0.6333	0.0583	0.7820
2903.50	0.2310	2.288	32.8846	8.2211	0.6468	0.0577	0.8012
2903.75	0.2280	2.292	10.4806	2.6201	0.6511	0.0570	0.8201
2904.00	0.2173	2.297	50.2100	12.5525	0.6718	0.0543	0.8381
2904.25	0.2155	2.315	44.0806	11.0202	0.6899	0.0539	0.8560
2904.50	0.2101	2.318	74.4946	18.6237	0.7205	0.0525	0.8734
2904.75	0.2101	2.327	62.8958	15.7239	0.7463	0.0525	0.8908
2905.00	0.1958	2.327	135.2400	33.8100	0.8019	0.0490	0.9070
2905.25	0.1929	2.351	103.1568	25.7892	0.8443	0.0482	0.9230
2905.50	0.1863	2.356	120.7821	30.1955	0.8940	0.0466	0.9385
2905.75	0.1815	2.367	95.1579	23.7895	0.9331	0.0454	0.9535
2906.00	0.1494	2.375	82.1700	20.5425	0.9668	0.0374	0.9659
2906.25	0.1387	2.429	80.6947	20.1737	1.0000	0.0347	0.9774
2906.50	0.1387	2.447	0.0100	0.0025	1.0000	0.0347	0.9889
2906.75	0.1333	2.447	0.0100	0.0025	1.0000	0.0333	1.0000
2907.00		2.456		608.3126		3.0146	

Table C.3 Cumulative kh versus Cumulative Por-h (Minipermeameter Readings)

Well Name: Ball # 19

Depth	Log Porosity	Log Density	Miniperm Perm.	kh	Cum kh %	Por-h	Cum Por-h %
3092.00	0.1065	2.501	0.4690	0.1173	0.0004	0.0266	0.0072
3092.25	0.1119	2.492	9.6252	2.4063	0.0078	0.0280	0.0148
3092.5	0.1155	2.486	1.6543	0.4136	0.0090	0.0289	0.0227
3092.75	0.1214	2.476	0.7410	0.1853	0.0096	0.0304	0.0309
3093.00	0.1280	2.465	3.1201	0.7800	0.0120	0.0320	0.0396
3093.25	0.1327	2.457	3.4990	0.8748	0.0147	0.0332	0.0486
3093.50	0.1381	2.448	3.2476	0.8119	0.0172	0.0345	0.0580
3093.75	0.1381	2.448	0.5783	0.1446	0.0176	0.0345	0.0674
3094.00	0.1446	2.437	0.0100	0.0025	0.0176	0.0362	0.0772
3094.25	0.1494	2.429	10.1040	2.5260	0.0254	0.0374	0.0874
3094.50	0.1494	2.429	9.0680	2.2670	0.0324	0.0374	0.0975
3094.75	0.1524	2.424	27.4903	6.8726	0.0535	0.0381	0.1079
3095.00	0.1524	2.424	8.6515	2.1629	0.0602	0.0381	0.1182
3095.25	0.1518	2.425	1.6059	0.4015	0.0614	0.0379	0.1285
3095.50	0.1518	2.425	4.9664	1.2416	0.0652	0.0379	0.1388
3095.75	0.1512	2.426	6.2090	1.5523	0.0700	0.0378	0.1491
3096.00	0.1256	2.469	0.0100	0.0025	0.0700	0.0314	0.1577
3096.25	0.1131	2.490	0.0100	0.0025	0.0700	0.0283	0.1653
3096.50	0.1077	2.499	0.0100	0.0025	0.0700	0.0269	0.1727
3096.75	0.1042	2.505	0.0100	0.0025	0.0700	0.0260	0.1797
3097.00	0.1018	2.509	0.0100	0.0025	0.0700	0.0254	0.1866
3097.25	0.1018	2.509	0.2263	0.0566	0.0702	0.0254	0.1936
3097.50	0.1000	2.512	0.0100	0.0025	0.0702	0.0250	0.2003
3097.75	0.0976	2.516	0.0100	0.0025	0.0702	0.0244	0.2070
3098.00	0.0958	2.519	0.0100	0.0025	0.0702	0.0240	0.2135
3098.25	0.1083	2.498	0.0100	0.0025	0.0702	0.0271	0.2208
3098.50	0.1155	2.486	0.0100	0.0025	0.0702	0.0289	0.2287
3098.75	0.1208	2.477	0.0100	0.0025	0.0702	0.0302	0.2369
3099.00	0.1208	2.477	0.0100	0.0025	0.0702	0.0302	0.2451
3099.25	0.1232	2.473	0.0100	0.0025	0.0703	0.0308	0.2535
3099.50	0.1256	2.469	0.9861	0.2465	0.0710	0.0314	0.2620
3099.75	0.1470	2.433	14.2959	3.5740	0.0820	0.0368	0.2720
3100.00	0.1690	2.396	13.5000	3.3750	0.0924	0.0423	0.2835
3100.25	0.1804	2.377	16.2820	4.0705	0.1049	0.0451	0.2957
3100.50	0.1827	2.373	18.0824	4.5206	0.1188	0.0457	0.3081
3100.75	0.1827	2.373	33.1488	8.2872	0.1443	0.0457	0.3206
3101.00	0.1827	2.373	20.2898	5.0724	0.1599	0.0457	0.3330
3101.25	0.1851	2.369	20.3892	5.0973	0.1756	0.0463	0.3455
3101.50	0.1863	2.367	21.9033	5.4758	0.1924	0.0466	0.3582
3101.75	0.1827	2.373	17.1661	4.2915	0.2056	0.0457	0.3706
3102.25	0.1542	2.421	11.2808	2.8202	0.2281	0.0385	0.3924
3102.50	0.1494	2.429	1.5862	0.3965	0.2293	0.0374	0.4026
3102.75	0.1494	2.429	0.0100	0.0025	0.2293	0.0374	0.4127
3103.00	0.1476	2.432	0.0100	0.0025	0.2293	0.0369	0.4228

Table C.3 Cumulative kh versus Cumulative Por-h (Minipermeameter Readings)

Well Name: Ball # 19

Depth	Log Porosity	Log Density	Miniperm Perm.	kh	Cum kh %	Por-h	Cum Por-h %
3101.75	0.1827	2.373	17.1661	4.2915	0.2056	0.0457	0.3706
3102.25	0.1542	2.421	11.2808	2.8202	0.2281	0.0385	0.3924
3102.50	0.1494	2.429	1.5862	0.3965	0.2293	0.0374	0.4026
3102.75	0.1494	2.429	0.0100	0.0025	0.2293	0.0374	0.4127
3103.00	0.1476	2.432	0.0100	0.0025	0.2293	0.0369	0.4228
3103.00	0.1476	2.432	0.0100	0.0025	0.2293	0.0369	0.4228
3104.25	0.1863	2.367	17.6836	4.4209	0.2621	0.0466	0.4795
3104.50	0.1863	2.367	17.4356	4.3589	0.2755	0.0466	0.4922
3104.75	0.1863	2.367	28.9000	7.2250	0.2978	0.0466	0.5049
3105.00	0.1875	2.365	28.0094	7.0023	0.3193	0.0469	0.5176
3105.25	0.1875	2.365	43.4398	10.8599	0.3527	0.0469	0.5303
3105.50	0.1875	2.365	16.6449	4.1612	0.3655	0.0469	0.5431
3105.75	0.1875	2.365	29.5354	7.3838	0.3882	0.0469	0.5558
3106.00	0.1863	2.367	4.6923	1.1731	0.3918	0.0466	0.5685
3106.25	0.1863	2.367	18.8024	4.7006	0.4062	0.0466	0.5811
3106.50	0.1845	2.370	0.1780	0.0445	0.4064	0.0461	0.5936
3106.75	0.1875	2.365	0.0100	0.0025	0.4064	0.0469	0.6064
3107.00	0.1893	2.362	12.9367	3.2342	0.4163	0.0473	0.6192
3107.25	0.1917	2.358	26.2400	6.5600	0.4365	0.0479	0.6323
3107.50	0.2131	2.322	16.4645	4.1161	0.4492	0.0533	0.6467
3107.75	0.2220	2.307	21.5918	5.3980	0.4658	0.0555	0.6618
3108.00	0.2220	2.307	27.9564	6.9891	0.4872	0.0555	0.6769
3108.25	0.2244	2.303	36.7811	9.1953	0.5155	0.0561	0.6921
3108.50	0.2274	2.298	19.8911	4.9728	0.5308	0.0568	0.7076
3108.75	0.2304	2.293	37.8392	9.4598	0.5599	0.0576	0.7232
3109.00	0.2304	2.293	34.5830	8.6458	0.5865	0.0576	0.7389
3109.25	0.2304	2.293	28.8869	7.2217	0.6087	0.0576	0.7545
3109.50	0.2345	2.286	48.2341	12.0585	0.6458	0.0586	0.7705
3109.75	0.2345	2.286	59.5243	14.8811	0.6915	0.0586	0.7864
3110.00	0.2321	2.290	37.0504	9.2626	0.7200	0.0580	0.8022
3110.25	0.2304	2.293	49.6232	12.4058	0.7581	0.0576	0.8178
3110.50	0.2286	2.296	77.0974	19.2744	0.8174	0.0571	0.8333
3110.75	0.2262	2.300	0.0100	0.0025	0.8174	0.0565	0.8487
3111.00	0.2232	2.305	23.1314	5.7828	0.8352	0.0558	0.8639
3111.25	0.2208	2.309	26.6593	6.6648	0.8557	0.0552	0.8789
3111.50	0.2208	2.309	41.6980	10.4245	0.8877	0.0552	0.8939
3111.75	0.2113	2.325	33.3160	8.3290	0.9134	0.0528	0.9082
3112.25	0.1935	2.355	12.4062	3.1015	0.9468	0.0484	0.9345
3112.5	0.1905	2.360	6.5959	1.6490	0.9519	0.0476	0.9474
3112.75	0.1649	2.403	23.6243	5.9061	0.9700	0.0412	0.9586
3113.00	0.1589	2.413	14.7889	3.6972	0.9814	0.0397	0.9694
3113.25	0.1589	2.413	17.3599	4.3400	0.9948	0.0397	0.9802
3113.50	0.1208	2.477	4.8599	1.2150	0.9985	0.0302	0.9884
3113.75	0.1054	2.503	1.8235	0.4559	0.9999	0.0263	0.9956

Table C.3 Cumulative kh versus Cumulative Por-h (Minipermeameter Readings)

Well Name: Ball # 19

Depth	Log Porosity	Log Density	Miniperm Perm.	kh	Cum kh %	Por-h	Cum Por-h %
3114.00	0.0649	2.571	0.1378	0.0345	1.0000	0.0162	1.0000
				325.2191		3.6804	

Table C.4 Cumulative kh versus Cumulative Por-h (Minipermeameter Readings)

Well Name: LeMasters # 13

Depth	Log Porosity	Log Density	Miniperm Perm.	kh	Cum kh %	Por-h	Cum Por-h %
3030.00	0.0946	2.521	0.6421	0.1605	0.0037	0.0237	0.0094
3030.25	0.0946	2.521	0.0412	0.0103	0.0040	0.0237	0.0189
3030.50	0.0946	2.521	0.0100	0.0025	0.0040	0.0237	0.0283
3030.75	0.0914	2.5265	0.0100	0.0025	0.0041	0.0228	0.0374
3031.00	0.0881	2.532	0.0100	0.0025	0.0042	0.0220	0.0462
3031.25	0.0863	2.535	0.1014	0.0253	0.0048	0.0216	0.0548
3031.50	0.0845	2.538	0.1230	0.0308	0.0055	0.0211	0.0632
3031.75	0.0813	2.5435	4.5938	1.1485	0.0323	0.0203	0.0713
3032.00	0.0780	2.549	0.5637	0.1409	0.0356	0.0195	0.0790
3032.25	0.0762	2.552	1.2516	0.3129	0.0429	0.0190	0.0866
3032.50	0.0744	2.555	0.9737	0.2434	0.0486	0.0186	0.0941
3032.75	0.0759	2.5525	0.7179	0.1795	0.0528	0.0190	0.1016
3033.00	0.0774	2.55	0.2536	0.0634	0.0542	0.0193	0.1093
3033.25	0.0780	2.549	0.3176	0.0794	0.0561	0.0195	0.1171
3033.50	0.0786	2.548	0.2019	0.0505	0.0573	0.0196	0.1249
3033.75	0.0783	2.5485	0.2180	0.0545	0.0585	0.0196	0.1327
3034.00	0.0780	2.549	0.4881	0.1220	0.0614	0.0195	0.1405
3034.25	0.0750	2.554	0.3417	0.0854	0.0634	0.0188	0.1480
3034.50	0.0720	2.559	0.0528	0.0132	0.0637	0.0180	0.1551
3034.75	0.0690	2.564	0.1782	0.0446	0.0647	0.0173	0.1620
3035.00	0.0661	2.569	0.3239	0.0810	0.0666	0.0165	0.1686
3035.25	0.0649	2.571	0.1413	0.0353	0.0674	0.0162	0.1751
3035.50	0.0637	2.573	0.0951	0.0238	0.0680	0.0159	0.1814
3035.75	0.0607	2.578	0.0100	0.0025	0.0681	0.0152	0.1875
3036.00	0.0577	2.583	0.0100	0.0025	0.0681	0.0144	0.1932
3036.25	0.0589	2.581	0.0100	0.0025	0.0682	0.0147	0.1991
3036.50	0.0601	2.579	0.0100	0.0025	0.0682	0.0150	0.2051
3036.75	0.0631	2.574	0.0100	0.0025	0.0683	0.0158	0.2114
3037.00	0.0661	2.569	0.0100	0.0025	0.0684	0.0165	0.2179
3037.25	0.0679	2.566	0.0100	0.0025	0.0684	0.0170	0.2247
3037.50	0.0696	2.563	0.0100	0.0025	0.0685	0.0174	0.2316
3037.75	0.0726	2.558	0.0100	0.0025	0.0685	0.0182	0.2389
3038.00	0.0756	2.553	0.0100	0.0025	0.0686	0.0189	0.2464
3038.25	0.0789	2.5475	0.0100	0.0025	0.0686	0.0197	0.2543
3038.50	0.0821	2.542	0.0100	0.0025	0.0687	0.0205	0.2624
3038.75	0.0833	2.54	0.0100	0.0025	0.0688	0.0208	0.2707
3039.00	0.0845	2.538	0.0100	0.0025	0.0688	0.0211	0.2792
3039.25	0.0860	2.5355	0.0100	0.0025	0.0689	0.0215	0.2877
3039.50	0.0875	2.533	0.0100	0.0025	0.0689	0.0219	0.2964
3039.75	0.0884	2.5315	0.0100	0.0025	0.0690	0.0221	0.3053
3040.25	0.0884	2.5315	0.0100	0.0025	0.0691	0.0221	0.3230
3040.50	0.0875	2.533	0.0100	0.0025	0.0692	0.0219	0.3317
3040.75	0.0878	2.5325	0.0100	0.0025	0.0692	0.0219	0.3404
3041.00	0.0881	2.532	0.0100	0.0025	0.0693	0.0220	0.3492

Table C.4 Cumulative kh versus Cumulative Por-h (Minipermeameter Readings)

Well Name: LeMasters # 13

Depth	Log Porosity	Log Density	Miniperm Perm.	kh	Cum kh %	Por-h	Cum Por-h %
3041.25	0.0863	2.535	0.0100	0.0025	0.0693	0.0216	0.3578
3041.50	0.0845	2.538	0.0100	0.0025	0.0694	0.0211	0.3662
3041.75	0.0833	2.54	0.0100	0.0025	0.0695	0.0208	0.3745
3042.00	0.0821	2.542	0.0100	0.0025	0.0695	0.0205	0.3827
3042.25	0.0851	2.537	0.0100	0.0025	0.0696	0.0213	0.3912
3042.50	0.0881	2.532	0.0100	0.0025	0.0696	0.0220	0.4000
3042.75	0.0902	2.5285	0.0100	0.0025	0.0697	0.0225	0.4089
3043.00	0.0923	2.525	0.0100	0.0025	0.0698	0.0231	0.4181
3043.25	0.0973	2.5165	0.0100	0.0025	0.0698	0.0243	0.4278
3043.50	0.1024	2.508	0.5673	0.1418	0.0731	0.0256	0.4380
3043.75	0.1051	2.5035	1.1433	0.2858	0.0798	0.0263	0.4485
3044.00	0.1077	2.499	0.7807	0.1952	0.0844	0.0269	0.4592
3044.25	0.1092	2.4965	0.6904	0.1726	0.0884	0.0273	0.4701
3044.50	0.1107	2.494	1.2410	0.3102	0.0956	0.0277	0.4811
3044.75	0.1104	2.4945	0.7391	0.1848	0.0999	0.0276	0.4921
3045.00	0.1101	2.495	1.2144	0.3036	0.1070	0.0275	0.5031
3045.25	0.0997	2.5125	0.7577	0.1894	0.1115	0.0249	0.5130
3045.50	0.0893	2.53	1.0071	0.2518	0.1173	0.0223	0.5219
3045.75	0.0723	2.5585	1.2182	0.3046	0.1244	0.0181	0.5291
3046.00	0.0554	2.587	0.0100	0.0025	0.1245	0.0138	0.5347
3046.25	0.0503	2.5955	0.0100	0.0025	0.1246	0.0126	0.5397
3046.50	0.0452	2.604	0.0100	0.0025	0.1246	0.0113	0.5442
3046.75	0.0506	2.595	0.0100	0.0025	0.1247	0.0126	0.5492
3047.00	0.0560	2.586	0.3936	0.0984	0.1270	0.0140	0.5548
3047.25	0.0801	2.5455	0.6110	0.1528	0.1305	0.0200	0.5628
3047.50	0.1042	2.505	0.5092	0.1273	0.1335	0.0260	0.5731
3047.75	0.1104	2.4945	0.4229	0.1057	0.1360	0.0276	0.5841
3048.00	0.1167	2.484	4.3701	1.0925	0.1615	0.0292	0.5958
3048.25	0.1369	2.45	10.5897	2.6474	0.2233	0.0342	0.6094
3048.50	0.1571	2.416	12.2493	3.0623	0.2948	0.0393	0.6251
3048.75	0.1679	2.398	14.9449	3.7362	0.3820	0.0420	0.6418
3049.00	0.1786	2.38	22.8823	5.7206	0.5156	0.0446	0.6596
3049.25	0.1714	2.392	15.8823	3.9706	0.6083	0.0429	0.6767
3049.50	0.1643	2.404	4.3813	1.0953	0.6339	0.0411	0.6930
3049.75	0.1426	2.4405	0.0100	0.0025	0.6339	0.0356	0.7072
3050.00	0.1208	2.477	0.3942	0.0986	0.6362	0.0302	0.7193
3050.50	0.1161	2.485	0.9759	0.2440	0.6420	0.0290	0.7426
3050.75	0.1101	2.495	1.1329	0.2832	0.6486	0.0275	0.7536
3051.00	0.1042	2.505	0.8146	0.2036	0.6533	0.0260	0.7640
3051.25	0.1176	2.4825	7.0110	1.7528	0.6943	0.0294	0.7757
3051.50	0.1310	2.46	3.1885	0.7971	0.7129	0.0327	0.7887
3051.75	0.1336	2.4555	15.6280	3.9070	0.8041	0.0334	0.8021
3052.00	0.1363	2.451	8.0326	2.0081	0.8510	0.0341	0.8156
3052.25	0.1414	2.4425	6.5426	1.6356	0.8892	0.0353	0.8297

Table C.4 Cumulative kh versus Cumulative Por-h (Minipermeameter Readings)

Well Name: LeMasters # 13

Depth	Log Porosity	Log Density	Miniperm Perm.	kh	Cum kh %	Por-h	Cum Por-h %
3052.50	0.1464	2.434	6.7041	1.6760	0.9283	0.0366	0.8443
3052.75	0.1387	2.447	4.4446	1.1111	0.9542	0.0347	0.8581
3053.00	0.1310	2.46	0.7080	0.1770	0.9584	0.0327	0.8712
3053.25	0.1268	2.467	0.3136	0.0784	0.9602	0.0317	0.8838
3053.50	0.1226	2.474	0.5627	0.1407	0.9635	0.0307	0.8960
3053.75	0.1196	2.479	1.0716	0.2679	0.9698	0.0299	0.9079
3054.00	0.1167	2.484	0.6017	0.1504	0.9733	0.0292	0.9196
3054.25	0.1107	2.494	0.4980	0.1245	0.9762	0.0277	0.9306
3054.50	0.1048	2.504	0.5603	0.1401	0.9794	0.0262	0.9410
3054.75	0.1045	2.5045	0.4124	0.1031	0.9818	0.0261	0.9514
3055.00	0.1042	2.505	0.4471	0.1118	0.9845	0.0260	0.9618
3055.25	0.1003	2.5115	0.5733	0.1433	0.9878	0.0251	0.9718
3055.50	0.0964	2.518	0.1180	0.0295	0.9885	0.0241	0.9814
3055.75	0.0943	2.5215	0.8389	0.2097	0.9934	0.0236	0.9908
3056.00	0.0923	2.525	1.1327	0.2832	1.0000	0.0231	1.0000
				42.8309		2.5094	

Table C.5 Cumulative kh versus Cumulative Por-h (Minipermeameter Readings)

Well Name: Ball # 18

Depth	Log Porosity	Log Density	Miniperm Perm.	kh	Cum kh %	Por-h	Cum Por-h %
2987.25	0.0387	2.615	0.7412	0.1853	0.0368	0.0097	0.2841
2987.50	0.0405	2.612	5.5260	1.3815	0.3115	0.0101	0.5814
2987.75	0.0405	2.612	0.0100	0.0025	0.3120	0.0101	0.8786
2988.00	0.0417	2.61	0.0100	0.0025	0.3125	0.0104	1.1846
2988.25	0.0452	2.604	0.0100	0.0025	0.3130	0.0113	1.5168
2988.50	0.0476	2.6	0.0100	0.0025	0.3135	0.0119	1.8665
2988.75	0.0482	2.599	0.6941	0.1735	0.3480	0.0121	2.2206
2989.00	0.0560	2.586	0.0100	0.0025	0.3485	0.0140	2.6315
2989.25	0.0655	2.57	0.0100	0.0025	0.3490	0.0164	3.1123
2989.50	0.0655	2.57	0.0100	0.0025	0.3495	0.0164	3.5931
2989.75	0.0625	2.575	0.0100	0.0025	0.3500	0.0156	4.0521
2990.00	0.1077	2.499	0.0100	0.0025	0.3505	0.0269	4.8433
2990.25	0.1595	2.412	0.0100	0.0025	0.3510	0.0399	6.0148
2990.50	0.1690	2.396	0.4835	0.1209	0.3750	0.0423	7.2562
2990.75	0.1690	2.396	23.1855	5.7964	1.5275	0.0423	8.4976
2991.00	0.1690	2.396	12.8595	3.2149	2.1666	0.0423	9.7390
2991.25	0.1690	2.396	7.8246	1.9561	2.5556	0.0423	10.9805
2991.50	0.1673	2.399	15.2162	3.8040	3.3119	0.0418	12.2088
2991.75	0.1649	2.403	16.5372	4.1343	4.1339	0.0412	13.4196
2992.00	0.1601	2.411	16.0521	4.0130	4.9317	0.0400	14.5954
2992.25	0.1554	2.419	26.7324	6.6831	6.2605	0.0388	15.7363
2992.50	0.1387	2.447	0.0100	0.0025	6.2610	0.0347	16.7548
2992.75	0.1304	2.461	9.2193	2.3048	6.7192	0.0326	17.7121
2993.00	0.1304	2.461	47.6147	11.9037	9.0859	0.0326	18.6694
2993.25	0.1304	2.461	38.8404	9.7101	11.0165	0.0326	19.6267
2993.50	0.1304	2.461	6.1751	1.5438	11.3234	0.0326	20.5840
2993.75	0.1345	2.454	1.2925	0.3231	11.3877	0.0336	21.5719
2994.00	0.1345	2.454	2.7648	0.6912	11.5251	0.0336	22.5598
2994.25	0.1435	2.439	99.8200	24.9550	16.4867	0.0359	23.6132
2994.50	0.1560	2.418	0.3904	0.0976	16.5061	0.0390	24.7585
2994.75	0.1560	2.418	0.0602	0.0150	16.5091	0.0390	25.9037
2995.00	0.1750	2.386	91.3754	22.8439	21.0509	0.0438	27.1889
2995.25	0.1988	2.346	92.7815	23.1954	25.6626	0.0497	28.6489
2995.50	0.2119	2.324	59.5880	14.8970	28.6244	0.0530	30.2050
2995.75	0.2232	2.305	141.6210	35.4052	35.6637	0.0558	31.8442
2996.00	0.2345	2.286	128.3129	32.0782	42.0415	0.0586	33.5665
2996.25	0.2446	2.269	94.2611	23.5653	46.7268	0.0612	35.3630
2996.50	0.2446	2.269	130.2949	32.5737	53.2031	0.0612	37.1596
2996.75	0.2506	2.259	85.4206	21.3552	57.4489	0.0626	38.9999
2997.00	0.2470	2.265	138.6999	34.6750	64.3430	0.0618	40.8139
2997.25	0.2446	2.269	82.2567	20.5642	68.4316	0.0612	42.6105
2997.50	0.2417	2.274	78.0076	19.5019	72.3090	0.0604	44.3852
2997.75	0.2387	2.279	57.2574	14.3144	75.1550	0.0597	46.1380
2998.25	0.2357	2.284	117.3729	29.3432	81.1632	0.0589	49.6000

Table C.5 Cumulative kh versus Cumulative Por-h (Minipermeameter Readings)

Well Name: Ball # 18

Depth	Log Porosity	Log Density	Miniperm Perm.	kh	Cum kh %	Por-h	Cum Por-h %
2998.50	0.2333	2.288	8.5026	2.1256	81.5858	0.0583	51.3135
2998.75	0.2333	2.288	76.8486	19.2122	85.4056	0.0583	53.0271
2999.00	0.2298	2.294	53.6382	13.4096	88.0717	0.0574	54.7143
2999.25	0.2250	2.302	76.1389	19.0347	91.8562	0.0563	56.3667
2999.50	0.2042	2.337	35.9760	8.9940	93.6443	0.0510	57.8660
2999.75	0.1964	2.35	51.5400	12.8850	96.2061	0.0491	59.3085
3000.00	0.1929	2.356	3.7603	0.9401	96.3931	0.0482	60.7247
3000.25	0.1929	2.356	0.0100	0.0025	96.3935	0.0482	62.1410
3000.50	0.1292	2.463	0.0100	0.0025	96.3940	0.0323	63.0896
3000.75	0.1167	2.484	0.0438	0.0109	96.3962	0.0292	63.9463
3001.00	0.1119	2.492	0.0100	0.0025	96.3967	0.0280	64.7681
3001.25	0.1119	2.492	0.0100	0.0025	96.3972	0.0280	65.5899
3001.50	0.1167	2.484	0.0100	0.0025	96.3977	0.0292	66.4466
3001.75	0.1185	2.481	1.0346	0.2586	96.4491	0.0296	67.3165
3002.00	0.1185	2.481	0.0100	0.0025	96.4496	0.0296	68.1864
3002.25	0.1363	2.451	0.8449	0.2112	96.4916	0.0341	69.1874
3002.50	0.1363	2.451	34.0370	8.5092	98.1834	0.0341	70.1884
3002.75	0.1321	2.458	23.8569	5.9642	99.3692	0.0330	71.1588
3003.00	0.1280	2.465	0.0100	0.0025	99.3697	0.0320	72.0986
3003.25	0.1226	2.474	0.0100	0.0025	99.3702	0.0307	72.9991
3003.50	0.1131	2.49	0.0100	0.0025	99.3707	0.0283	73.8296
3003.75	0.1131	2.49	1.3266	0.3317	99.4367	0.0283	74.6601
3004.00	0.1065	2.501	0.0100	0.0025	99.4372	0.0266	75.4426
3004.25	0.1036	2.506	0.0100	0.0025	99.4377	0.0259	76.2032
3004.50	0.1018	2.509	0.0100	0.0025	99.4382	0.0254	76.9506
3004.75	0.1012	2.51	0.2567	0.0642	99.4509	0.0253	77.6938
3005.00	0.0994	2.513	0.1021	0.0255	99.4560	0.0249	78.4237
3005.25	0.1018	2.509	0.4004	0.1001	99.4759	0.0254	79.1712
3005.50	0.1065	2.501	0.0100	0.0025	99.4764	0.0266	79.9537
3005.75	0.1065	2.501	0.0100	0.0025	99.4769	0.0266	80.7361
3006.00	0.1089	2.497	0.0100	0.0025	99.4774	0.0272	81.5360
3006.25	0.1107	2.494	0.0100	0.0025	99.4779	0.0277	82.3491
3006.50	0.1119	2.492	1.0839	0.2710	99.5318	0.0280	83.1709
3006.75	0.1190	2.48	0.8926	0.2231	99.5761	0.0298	84.0451
3007.00	0.1208	2.477	0.7823	0.1956	99.6150	0.0302	84.9325
3007.25	0.1250	2.47	0.7872	0.1968	99.6541	0.0313	85.8504
3007.50	0.1250	2.47	0.6916	0.1729	99.6885	0.0313	86.7684
3007.75	0.1262	2.468	0.9719	0.2430	99.7368	0.0315	87.6951
3008.00	0.1292	2.463	0.7010	0.1752	99.7717	0.0323	88.6436
3008.25	0.1292	2.463	0.7406	0.1851	99.8085	0.0323	89.5922
3008.50	0.1292	2.463	0.8141	0.2035	99.8489	0.0323	90.5407
3008.75	0.1321	2.458	0.2126	0.0531	99.8595	0.0330	91.5111
3009.00	0.1036	2.506	0.2178	0.0545	99.8703	0.0259	92.2717
3009.25	0.0470	2.601	0.0906	0.0227	99.8748	0.0118	92.6170

Table C.5 Cumulative kh versus Cumulative Por-h (Minipermeameter Readings)

Well Name: Ball # 18

Depth	Log Porosity	Log Density	Miniperm Perm.	kh	Cum kh %	Por-h	Cum Por-h %
3009.50	0.0470	2.601	0.7780	0.1945	99.9135	0.0118	92.9624
3009.75	0.0411	2.611	0.1595	0.0399	99.9214	0.0103	93.2640
3010.00	0.0167	2.652	0.0100	0.0025	99.9219	0.0042	93.3864
3010.25	0.0167	2.652	0.0100	0.0025	99.9224	0.0042	93.5088
3010.50	0.0167	2.652	0.0100	0.0025	99.9229	0.0042	93.6312
3010.75	0.0190	2.648	0.0100	0.0025	99.9234	0.0048	93.7710
3011.00	0.0214	2.644	0.0100	0.0025	99.9239	0.0054	93.9284
3011.25	0.0214	2.644	0.0100	0.0025	99.9244	0.0054	94.0858
3011.50	0.0518	2.593	0.2342	0.0585	99.9361	0.0129	94.4661
3011.75	0.0649	2.571	0.1149	0.0287	99.9418	0.0162	94.9425
3012.00	0.0798	2.546	0.1280	0.0320	99.9481	0.0199	95.5283
3012.25	0.0911	2.527	0.0492	0.0123	99.9506	0.0228	96.1971
3012.50	0.1036	2.506	0.1214	0.0304	99.9566	0.0259	96.9576
3012.75	0.1042	2.505	0.2261	0.0565	99.9678	0.0260	97.7226
3013.00	0.1042	2.505	0.2231	0.0558	99.9789	0.0260	98.4876
3013.25	0.1042	2.505	0.2253	0.0563	99.9901	0.0260	99.2525
3013.50	0.1018	2.509	0.1985	0.0496	100.0000	0.0254	100.0000
				502.9664		3.4043	

Table C.6 Potential Flow Unit Boundary Point Analysis
Miniperm Values and Core Porosity
(see Appendix C. for detail data)

Well Name	Flow Unit Interval (Feet)	Flow Unit Interval (Feet)	Observation
T. Heirs # 8	2785.00 - 2791.00 (No k)	2791.00 - 2795.00 (Looks like single FU)	Similar shape to core plot. Lower section very low k, don't include.
Horner # 9	2895.00 - 2905.00	2905.00 - 2906.00	FU1 has k = 20 - 70 md FU2 has k = 90 - 135 md
Ball # 19	3100.00 - 3107.00	3107.00 - 3114.00	Steady k in upper zone. Second FU has higher k.
LeMasters # 13	3048.50 - 3049.00	3051.50- 3052.75	Appears to be one unit. Low k streak in center @ 3049.00 - 3051.50 feet.
Ball # 18	2987.50 - 2994.50	2994.50 - 3000.00	Upper section up to 50 md Lower section high k.
Horner # 11	3084.00 - 3088.00	3088.00 - 3093.00	High k in lower section.

APPENDIX D.

Appendix D. presents permeability versus porosity scatter plots (semi-log) and associated tables for each core well. The core porosity and permeability were used for values in Appendixes D. and E. The log porosity is included as a part of these tables but was not used for computations.

Figure D.1 Permeability-Porosity Scatter Plot
T.Heirs # 8

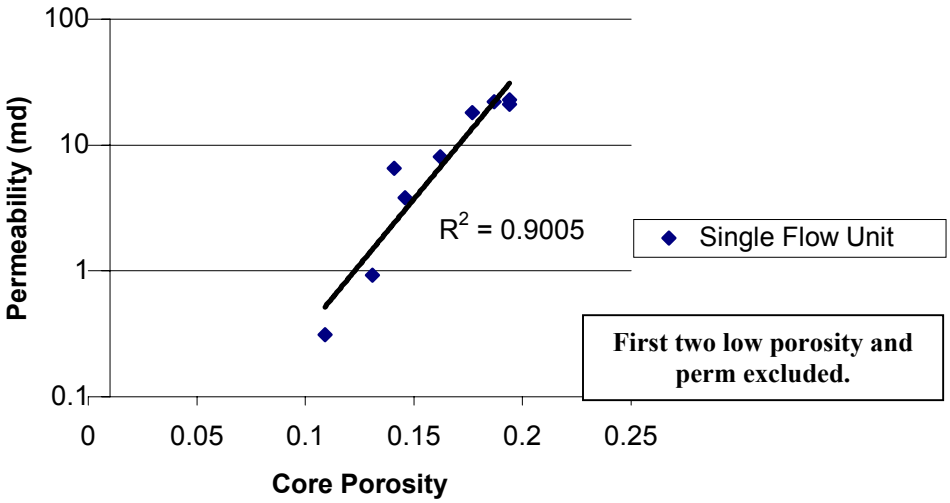

Figure D.2 Permeability-Porosity Scatter Plot
Horner # 9

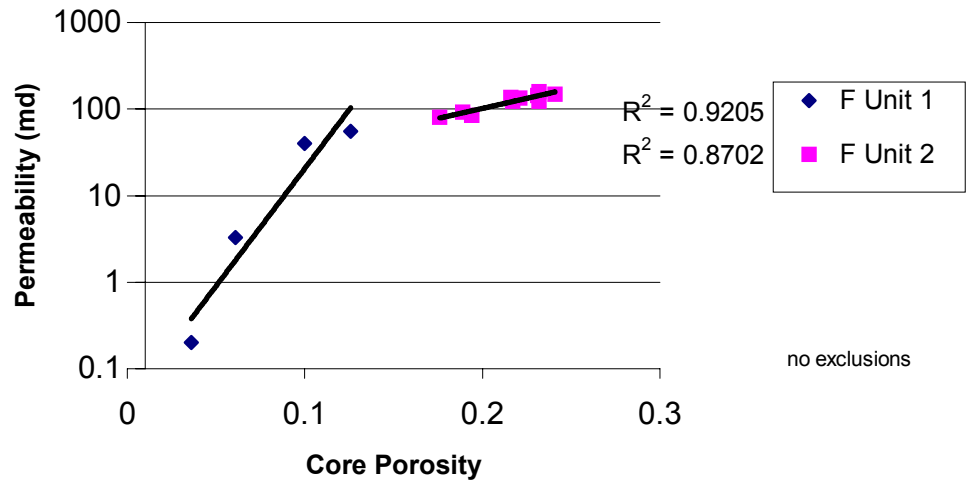

Figure D.3 Permeability-Porosity Scatter Plot
Ball # 19

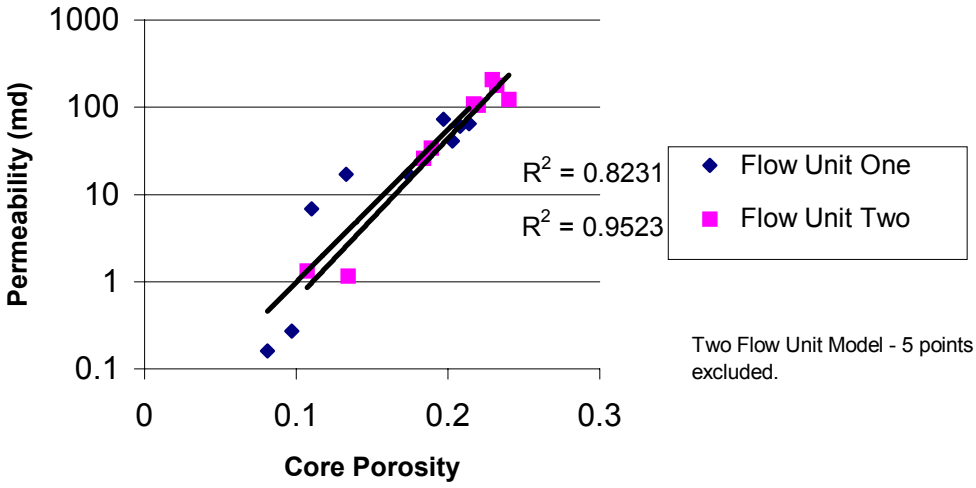

Figure D.4 Permeability-Porosity Scatter Plot
LeMasters # 13

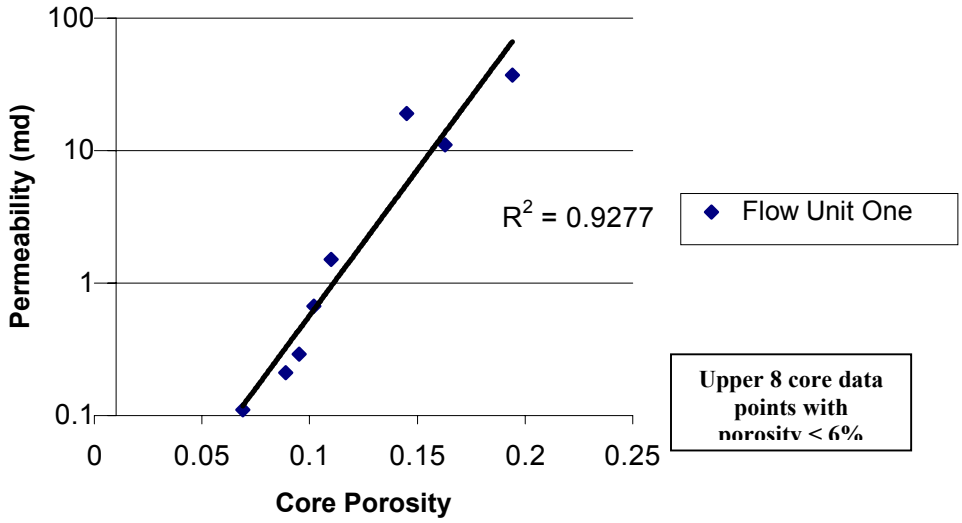

Figure D.5 Permeability-Porosity Scatter Plot
Ball # 18

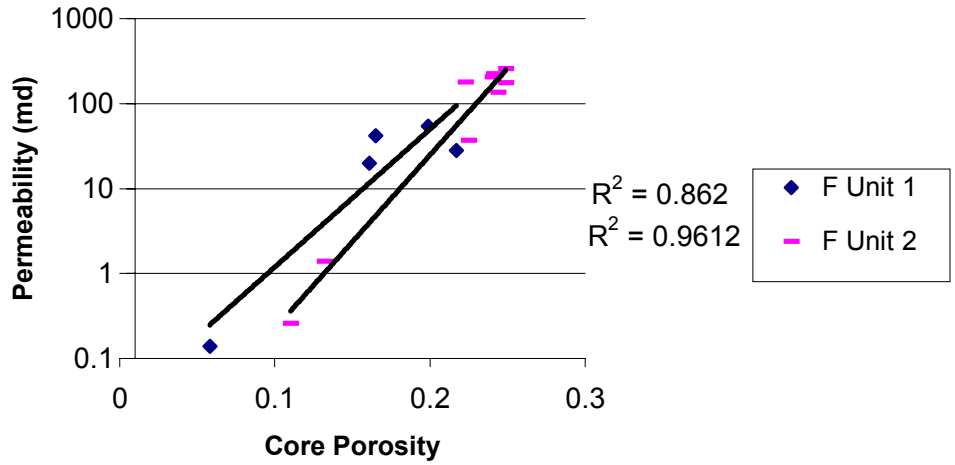

Figure D.6 Permeability-Porosity Scatter Plot
Horner # 11

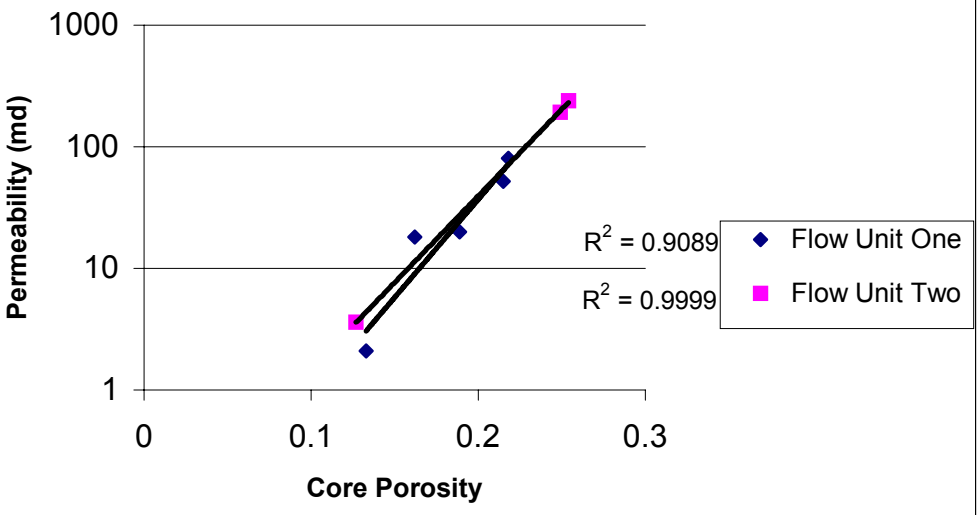

Figure D.7 Permeability-Porosity Scatter Plot
Composite Six Core Wells

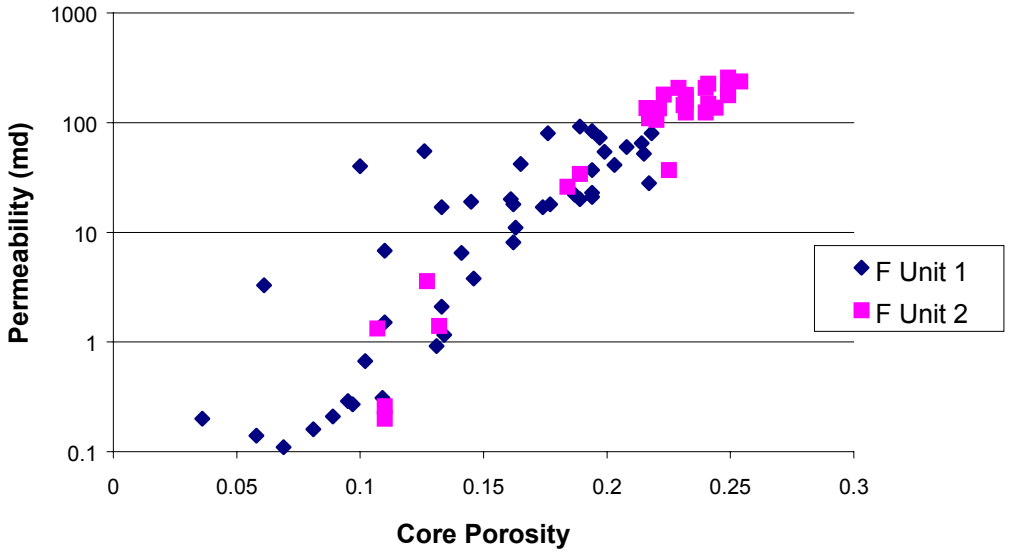

Figure D.8 Permeability-Porosity Scatter Plot
Composite Six Core Wells

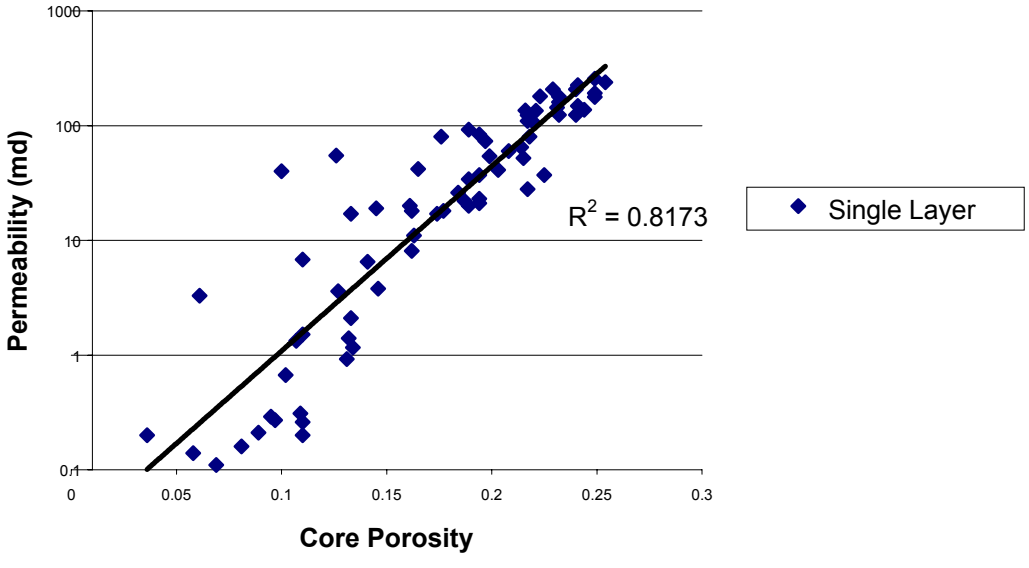

Table D.1 Data for Figures D.1 and E.1
Well Name: T. Heirs # 8
Single Flow Unit Model
Highest Correlation with Two Points Excluded
Best Fit Results

DEPTH	F Unit	gr	cpor/1- c por	density	log por	core por	k/c por	.0314 * sqrt k/c por	k (md)	exc
2785.25		38.44	0.041667	2.519	0.09583	0.04	2.75	0.052071	0.11	out
2786.75		38.44	0.068376	2.544	0.08095	0.064	1.875	0.042996	0.12	out
2788.75	1	51.811	0.150748	2.495	0.11012	0.131	7.0229	0.083212	0.92	
2789.25	1	51.253	0.122335	2.488	0.11429	0.109	2.84404	0.052954	0.31	
2791.5	1	39.554	0.164144	2.473	0.12321	0.141	46.0993	0.213195	6.5	
2792.5	1	47.911	0.17096	2.467	0.12679	0.146	26.0274	0.160194	3.8	
2793.75	1	51.811	0.193317	2.392	0.17143	0.162	50	0.222032	8.1	
2794.75	1	49.025	0.215067	2.384	0.17619	0.177	101.695	0.31665	18	
2795.25	1	49.025	0.230012	2.365	0.1875	0.187	117.647	0.340581	22	
2796	1	52.925	0.240695	2.359	0.19107	0.194	118.557	0.341895	23	
2797.5	1	74.652	0.240695	2.354	0.19405	0.194	108.247	0.326692	21	

Table D.2 Data for Figures D.2 and E.2
Well Name: Horner # 9
Two Flow Unit Model
Correlation with Zero Points Excluded
Best Fit Results

Depth	F Unit	gr	c por/1-c por	Log Dens	Log Por	Core Por	k/ c por	.0314 * Sqrt k/c por	k (md)	exc
2890	1	98.072	0.037344	2.627	0.03155	0.036	5.55556	0.074011	0.2	
2891.75	1	41.322	0.064963	2.558	0.07262	0.061	54.0984	0.230952	3.3	
2893	1	34.711	0.111111	2.477	0.12083	0.1	400	0.628	40	
2893.5	1	33.058	0.144165	2.458	0.13214	0.126	436.508	0.656033	55	
2895	1	39.669	0.233046	2.418	0.15595	0.189	486.772	0.692776	92	
2895.75	1	42.424	0.213592	2.381	0.17798	0.176	454.545	0.66945	80	
2896.5	1	41.873	0.240695	2.347	0.19821	0.194	432.99	0.653384	84	
2898.25	2	41.322	0.277139	2.341	0.20179	0.217	566.82	0.747571	123	
2898.75	2	41.873	0.27551	2.334	0.20595	0.216	629.63	0.787902	136	
2900	2	45.73	0.302083	2.289	0.23274	0.232	689.655	0.824604	160	
2901	2	50.689	0.283697	2.281	0.2375	0.221	610.86	0.776069	135	
2902	2	52.342	0.30039	2.274	0.24167	0.231	623.377	0.78398	144	
2903	2	55.647	0.302083	2.284	0.23571	0.232	534.483	0.725933	124	
2903.5	2	55.647	0.317523	2.288	0.23333	0.241	614.108	0.77813	148	

Table D.3 Data for Figures D.3 and E.3
Well Name: Ball # 19
Two Flow Unit Model
Five Points Excluded
Best Fit Results

		Uses Core Porosity			Log	Core		.0314 *		
DEPTH	F Unit	gr	por/1-por	density	porosity	Porosity	k/por	sqrt(k/por)	k (md)	exc
3086.25		84.211	0.048218	2.652	0.01667	0.046	53.0435	0.228689	2.44	exc
3092.25		29.917	0.142857	2.492	0.1119	0.125	33.92	0.182876	4.24	exc
3092.75		32.687	0.10742	2.476	0.12143	0.097	113.402	0.33438	11	exc
3094.25	1	37.119	0.20048	2.429	0.1494	0.167	227.545	0.473656	38	exc
3094.75	1	39.889	0.204819	2.424	0.15238	0.17	182.353	0.42402	31	exc
3097.25	1	37.119	0.10742	2.509	0.10179	0.097	2.78351	0.052387	0.27	
3098	1	40.997	0.088139	2.519	0.09583	0.081	1.97531	0.044131	0.16	
3099.25	1	42.659	0.153403	2.473	0.12321	0.133	127.82	0.355	17	
3100	1	37.119	0.254705	2.396	0.16905	0.203	201.97	0.446245	41	
3101.25	1	36.565	0.272265	2.369	0.18512	0.214	303.738	0.547242	65	
3102	1	41.551	0.210654	2.399	0.16726	0.174	97.7011	0.31037	17	
3103	1	43.767	0.123596	2.432	0.14762	0.11	61.7273	0.246699	6.79	
3104	1	44.321	0.24533	2.377	0.18036	0.197	370.558	0.604447	73	
3105	1	43.213	0.262626	2.365	0.1875	0.208	288.462	0.533302	60	
3106	1	43.767	0.154734	2.367	0.18631	0.134	8.65672	0.092386	1.16	
3107.25	2	39.335	0.277139	2.358	0.19167	0.217	506.912	0.706962	110	
3108	2	40.443	0.282051	2.307	0.22202	0.22	481.818	0.689241	106	
3108.75	2	43.767	0.297017	2.293	0.23036	0.229	903.93	0.944055	207	
3109.5	2	42.659	0.302083	2.286	0.23452	0.232	771.552	0.872192	179	
3110.75	2	40.443	0.31579	2.3	0.22619	0.24	516.667	0.713732	124	
3112	2	44.321	0.22549	2.355	0.19345	0.184	141.304	0.373257	26	
3112.5	2	50.97	0.233046	2.36	0.19048	0.189	179.894	0.421151	34	
3113.75		83.657	0.119821	2.503	0.10536	0.107	12.4299	0.110704	1.33	

Table D.4 Data for Figures D.4 and E.4
Well Name: LeMasters # 13
Two Flow Unit Model
Highest Correlation with Eight Points Excluded
Best Fit Results

				Log	Log	Core		0.0314		
DEPTH	F Unit	gr	cpor/1-cpor	Dens	Por	Por	k/cpor	sqrt k/por	k (md)	exc
3031.75		30.114	0.044932	2.544	0.08125	0.043	3.48837	0.058646	0.15	exc
3032.25		29.546	0.055966	2.552	0.07619	0.053	13.5849	0.115733	0.72	exc
3034.25		26.137	0.051525	2.554	0.075	0.049	5.71429	0.07506	0.28	exc
3034.75		28.409	0.076426	2.564	0.06905	0.071	3.80282	0.061233	0.27	exc
3036		30.114	0.035197	2.583	0.05774	0.034	3.52941	0.05899	0.12	exc
3036.5		28.409	0.036269	2.579	0.06012	0.035	6.28571	0.078724	0.22	exc
3038.5		36.364	0.070664	2.542	0.08214	0.066	2.72727	0.051855	0.18	exc
3042.5		44.886	0.060445	2.532	0.0881	0.057	3.33333	0.057328	0.19	exc
3043.25	1	41.762	0.104972	2.517	0.09732	0.095	3.05263	0.054861	0.29	
3045.25	1	48.012	0.113586	2.513	0.0997	0.102	6.56863	0.080476	0.67	
3045.75	1	59.659	0.097695	2.559	0.07232	0.089	2.35955	0.048233	0.21	
3048.75	1	46.307	0.240695	2.398	0.16786	0.194	190.722	0.43364	37	
3050	1	44.318	0.123596	2.477	0.12083	0.11	13.7273	0.116338	1.51	
3051	1	46.591	0.074114	2.505	0.10417	0.069	1.5942	0.039646	0.11	
3052.25	1	42.898	0.169591	2.443	0.14137	0.145	131.034	0.359437	19	
3052.75	1	42.898	0.194743	2.447	0.13869	0.163	67.4847	0.257948	11	

Table D.5 Data for Figures D.5 and E.5
Well Name: Ball # 18
Two Flow Unit Model
Highest Correlation with Eight Points Excluded
Best Fit Results

				Log	Log	Core		0.0314		
DEPTH	F Unit	gr	por/1-por	Dens	Por	Por	k/por	sqrt k/por	k (md)	exc
2987.25		72.022	0.067236	2.615	0.03869	0.063	4.12698	0.063789	0.26	exc
2988.25		41.551	0.054852	2.604	0.04524	0.052	14.8077	0.12083	0.77	exc
2989.75	1	46.537	0.061571	2.575	0.0625	0.058	2.41379	0.048784	0.14	
2990.75	1	33.795	0.277139	2.396	0.16905	0.217	129.032	0.35668	28	
2991.5	1	30.471	0.24844	2.399	0.16726	0.199	271.357	0.517249	54	
2993.5	1	27.147	0.197605	2.461	0.13036	0.165	254.545	0.500971	42	
2994	1	27.147	0.191895	2.454	0.13452	0.161	124.224	0.349971	20	
2995.5	2	39.335	0.317523	2.324	0.2119	0.241	937.759	0.961558	226	
2996.25	2	45.429	0.331558	2.269	0.24464	0.249	1032.13	1.00878	257	
2997.5	2	48.753	0.31579	2.274	0.24167	0.24	862.5	0.922166	207	
2998.25	2	49.307	0.287001	2.284	0.23571	0.223	807.175	0.8921	180	
2999	2	52.632	0.331558	2.294	0.22976	0.249	714.859	0.839537	178	
2999.75	2	63.712	0.322751	2.35	0.19643	0.244	561.475	0.744038	137	
3002.75	2	72.022	0.290323	2.458	0.13214	0.225	164.444	0.402661	37	
3005.25	2	72.576	0.123596	2.509	0.10179	0.11	2.36364	0.048275	0.26	
3007.25	2	50.97	0.152074	2.47	0.125	0.132	10.6061	0.10226	1.4	
3007.75		43.767	0.140251	2.468	0.12619	0.123	12.1951	0.109654	1.5	exc
3009		41.551	0.113586	2.506	0.10357	0.102	7.7451	0.087386	0.79	exc
3009.75		57.064	0.108648	2.611	0.04107	0.098	2.55102	0.050152	0.25	exc
3011		86.981	0.109878	2.644	0.02143	0.099	1.11111	0.033099	0.11	exc
3012.25		58.726	0.096491	2.527	0.09107	0.088	2.95455	0.053973	0.26	exc
3013		43.213	0.116071	2.505	0.10417	0.104	3.65385	0.060021	0.38	exc

Table D.6 Perm-Porosity Scatter Plot Data
Well Name: Horner # 11
Two Flow Unit Model
Highest Correlation with One Points Excluded
Best Fit Results
Data for Figures D.6 and E.6

								0.0314		
DEPTH	F Unit	gr	: por/1-c poi	density	log por	core por	k/c por	Sqrt k/c por	k (md)	exc
3084.5	1	35.262	0.153403	2.498	0.10833	0.133	15.7895	0.124771	2.1	
3085.25	1	36.915	0.193317	2.479	0.11964	0.162	111.111	0.330985	18	
3088.75	1	45.73	0.233046	2.349	0.19702	0.189	105.82	0.323008	20	
3089.5	1	33.058	0.273885	2.314	0.21786	0.215	241.86	0.488329	52	
3090.5	1	29.201	0.278772	2.33	0.20833	0.218	366.972	0.601515	80	
3092	2	47.383	0.340483	2.309	0.22083	0.254	937.008	0.961172	238	
3092.5	2	53.994	0.331558	2.34	0.20238	0.249	771.084	0.871928	192	
3093.25	2	62.81	0.145475	2.503	0.10536	0.127	28.3465	0.167178	3.6	
3100.5	2	46.832	0.123596	2.501	0.10655	0.11	1.81818	0.04234	0.2	exc

APPENDIX E.

Appendix E. presents flow zone indicator scatter plots and associated tables for each core well. Supporting data for Appendix E. is included as a part of Appendix D.

Figure E.1 Flow Zone Indicator versus Normalized Porosity T. Heirs # 8

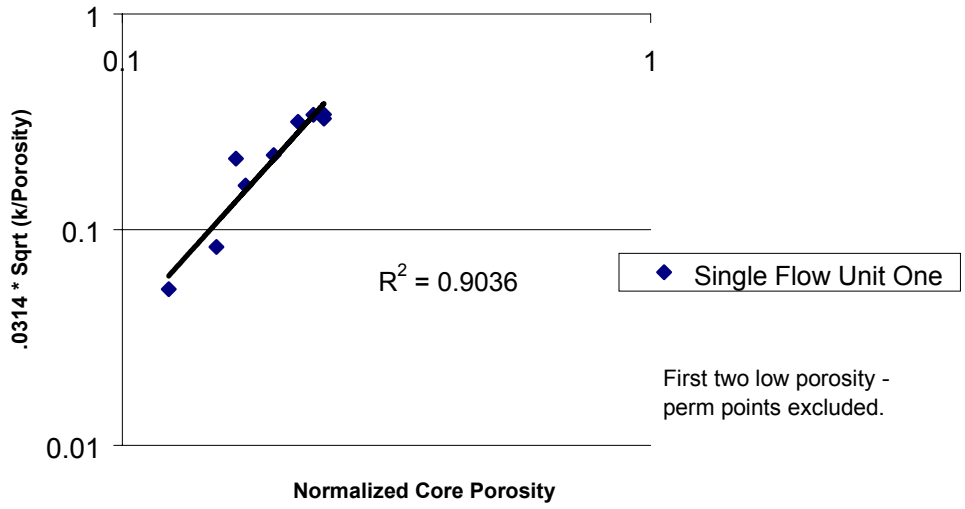

Figure E.2 Flow Zone Indicator versus Normalized Porosity Horner # 9

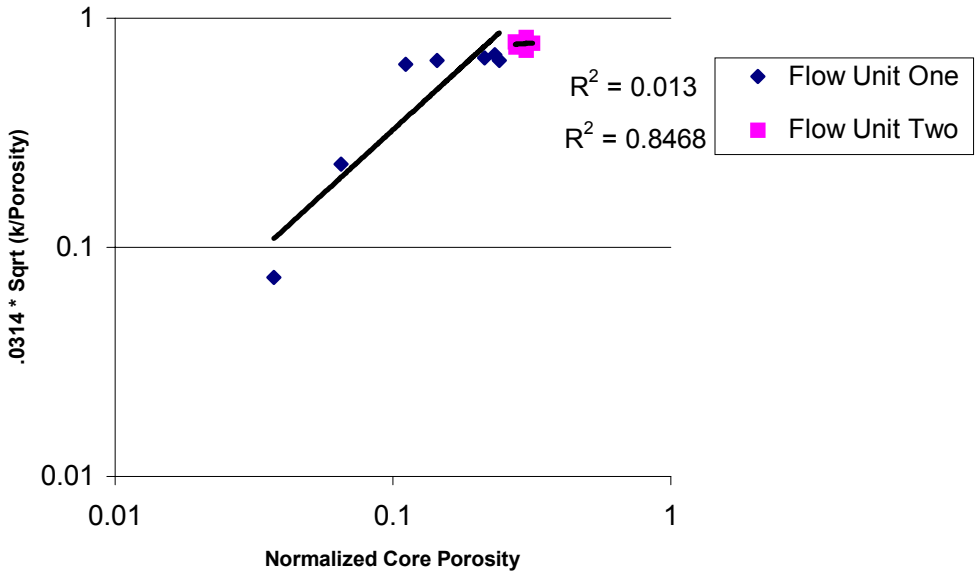

Figure E.3 Flow Zone Indicator versus Normalized Porosity Ball # 19

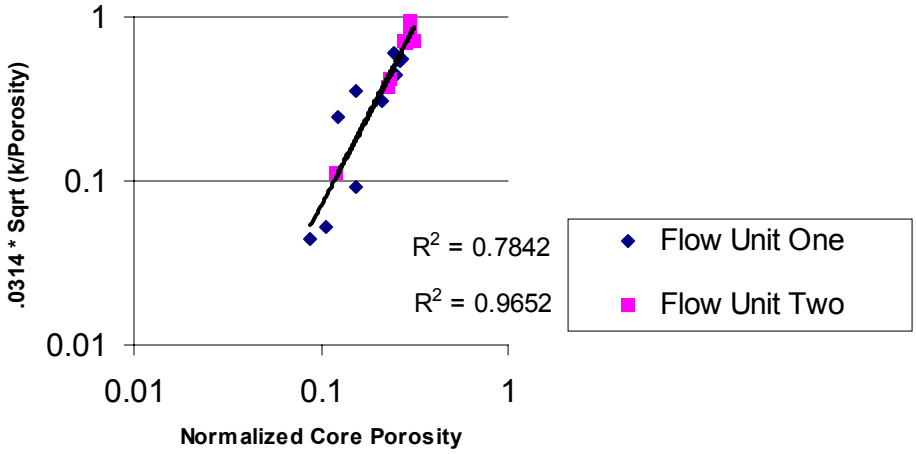

Figure E.4 Flow Zone Indicator versus Normalized Porosity LeMasters # 13

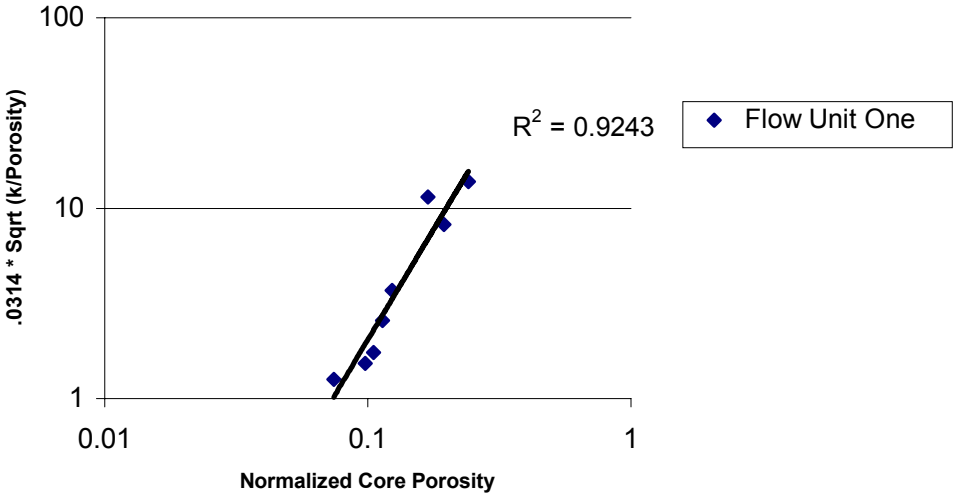

Figure E.5 Flow Zone Indicator versus Normalized Porosity Ball # 18

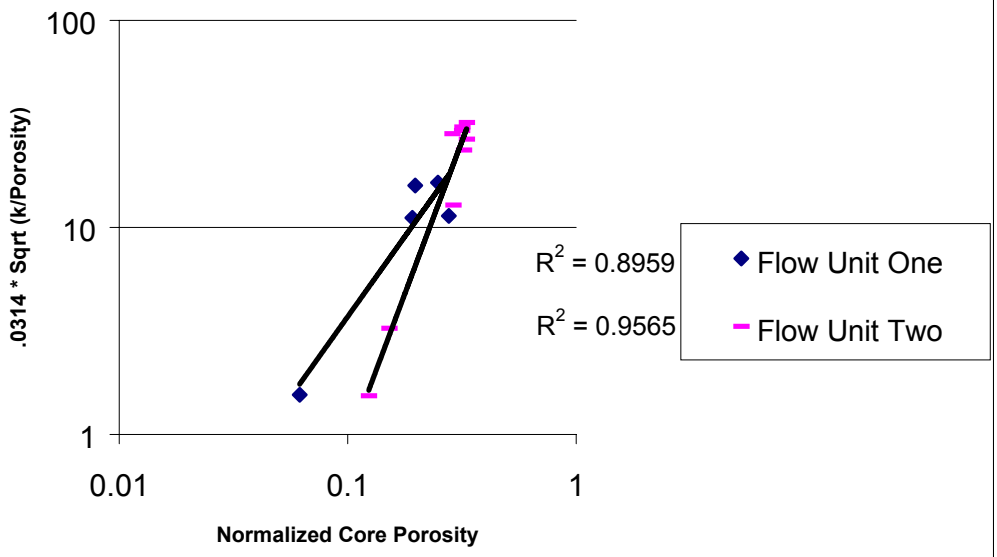

Figure E.6 Flow Zone Indicator versus Normalized Porosity Horner # 11

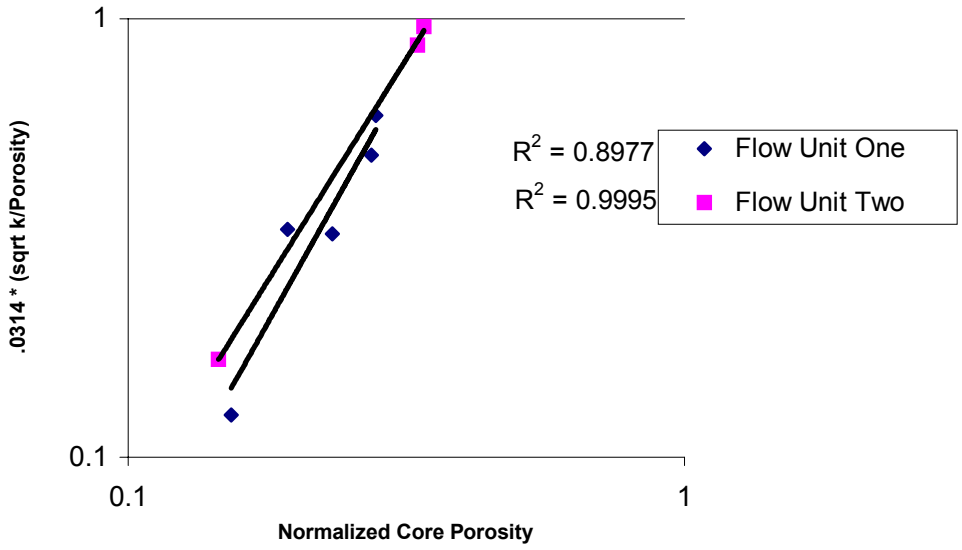

Figure E.7 Flow Zone Indicator versus Normalized Porosity - Composite Six Core Wells

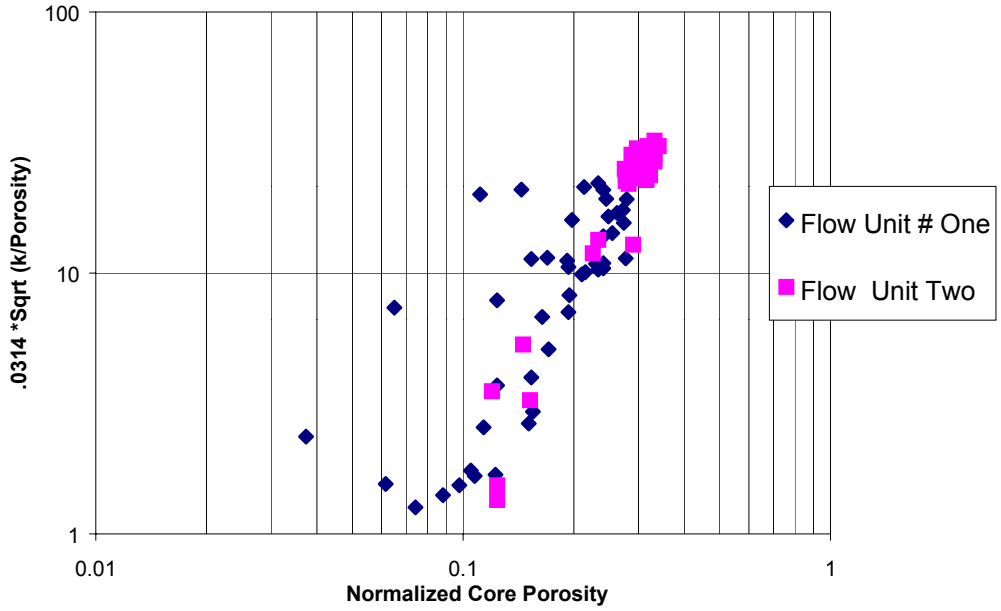

Figure E.8 Flow Zone Indicator versus Normalized Porosity - Composite Six Core Wells

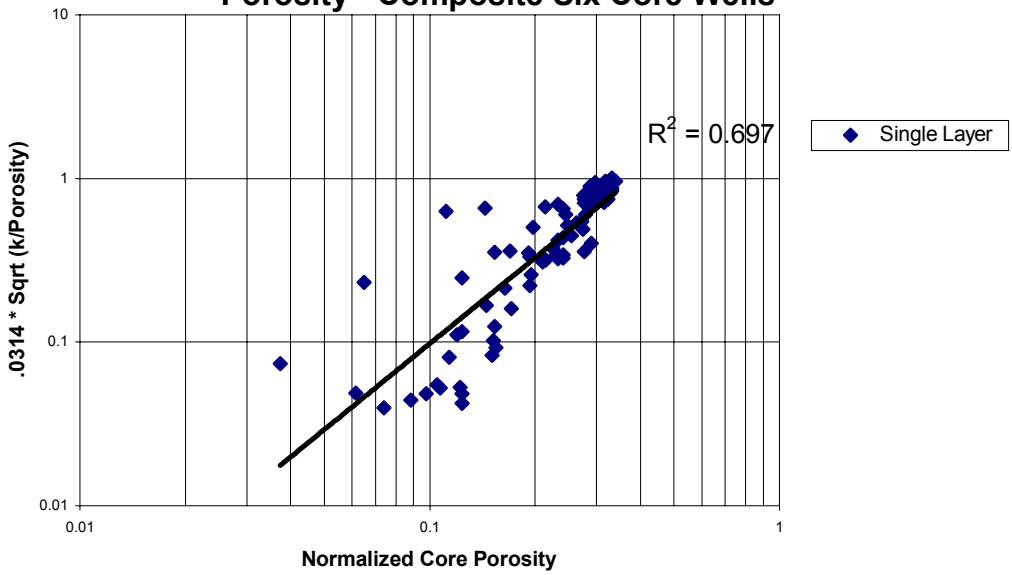

APPENDIX F.

Appendix F. presents the results of Kohonen Artificial Neural Network analysis for two and three output categories.

Table F.1 Kohonen Network (Two Output Categories)

ANN Analysis of Core Data Set
Winning Neuron is Set at 1.0
Analysis for Two Sets

ANN Inputs =====>		input	input	input	input	input	input	input		
Well Name	**Depth**	**gr**	**rhob**	**gr'**	**rhob'**	**gr bl**	**rhob bl**	**k (md)**	**Nwk 1**	**Nwk 2**
Ball # 18	2987.25	72.02	2.615	-34.35	-0.026	107	2.72	0.26	1	0
Ball # 18	2988	49.31	2.61	-26.59	-0.016	107	2.72	0.77	1	0
Ball # 18	2989	43.77	2.586	7.756	-0.058	107	2.72	0.06	1	0
Ball # 18	2990	47.65	2.499	-15.51	-0.326	107	2.72	0.14	1	0
Ball # 18	2991	31.03	2.396	-5.54	0	107	2.72	28	1	0
		Beginning of transition zone								
Ball # 18	2992	28.26	2.411	-2.216	0.032	107	2.72	54	0	1
Ball # 18	2993	28.81	2.461	-1.108	0	107	2.72	42	1	0
Ball # 18	2994	27.15	2.454	1.108	-0.03	107	2.72	20	1	0
		End of FU 1 and beginning of FU 2								
Ball # 18	2995	32.69	2.386	8.864	-0.144	107	2.72	226	0	1
Ball # 18	2996	43.21	2.286	7.756	-0.072	107	2.72	257	0	1
Ball # 18	2997	47.09	2.265	2.216	0.02	107	2.72	207	0	1
Ball # 18	2998	49.31	2.284	1.108	0.01	107	2.72	180	0	1
Ball # 18	2999	52.63	2.294	11.08	0.028	107	2.72	178	0	1
Ball # 18	3000	72.58	2.356	17.728	0.012	107	2.72	137	0	1
		End of FU 2 and low k below								
Ball # 18	3001	70.91	2.492	-1.108	0.016	107	2.72	0.06	1	0
Ball # 18	3002	69.81	2.481	2.216	-0.06	107	2.72	0.05	1	0
Ball # 18	3003	71.47	2.465	-2.216	0.032	107	2.72	37	1	0
Ball # 18	3004	65.37	2.501	-2.216	0.032	107	2.72	0.1	1	0
Ball # 18	3005	70.91	2.513	14.404	-0.002	107	2.72	0.26	1	0
Ball # 18	3006	75.35	2.497	0	-0.014	107	2.72	0.07	1	0
Ball # 18	3007	56.51	2.477	-16.62	-0.02	107	2.72	1.4	1	0
Ball # 18	3008	39.89	2.463	-9.972	-0.01	107	2.72	1.5	1	0
Ball # 18	3009	41.55	2.506	16.62	0.286	107	2.72	0.79	1	0
Ball # 18	3010	69.25	2.652	55.402	0.082	107	2.72	0.25	1	0
Ball # 18	3011	86.98	2.644	-1.108	-0.008	107	2.72	0.11	1	0
Ball # 18	3012	76.45	2.546	-45.43	-0.088	107	2.72	0.26	1	0
Ball # 18	3013	43.21	2.505	1.108	0	107	2.72	0.38	1	0

Table F.1 Kohonen Network (Two Output Categories)

ANN Analysis of Core Data Set
Winning Neuron is Set at 1.0
Analysis for Two Sets

ANN Inputs =====>		input	input	input	input	input	input	input		
Well Name	**Depth**	**gr**	**rhob**	**gr'**	**rhob'**	**gr bl**	**rhob bl**	**k (md)**	**Nwk 1**	**Nwk 2**
Ball # 19	3086	90.86	2.663	-23.27	-0.052	123	2.71	2.44	1	0
Ball # 19	3087	63.71	2.618	-54.29	-0.034	123	2.71	0.01	1	0
Ball # 19	3088	48.75	2.572	-1.108	-0.026	123	2.71	0.03	1	0
Ball # 19	3089	41.55	2.569	-11.08	-0.006	123	2.71	0.08	1	0
Ball # 19	3090	28.81	2.556	-6.648	-0.014	123	2.71	0.08	1	0
Ball # 19	3091	27.15	2.528	2.216	-0.036	123	2.71	0.09	1	0
Ball # 19	3092	28.26	2.501	3.324	-0.018	123	2.71	4.24	1	0
Ball # 19	3093	34.35	2.465	5.54	-0.038	123	2.71	11	1	0
Ball # 19	3094	37.12	2.437	1.108	-0.038	123	2.71	38	1	0
Ball # 19	3095	41.55	2.424	5.54	0.002	123	2.71	31	1	0
Ball # 19	3096	41	2.469	-6.648	0.128	123	2.71	0.08	1	0
Ball # 19	3097	35.46	2.509	2.216	0.008	123	2.71	0.27	1	0
Ball # 19	3098	41	2.519	7.756	-0.036	123	2.71	0.16	1	0
Ball # 19	3099	45.43	2.477	-7.756	-0.008	123	2.71	17	1	0
Ball # 19	3100	37.12	2.396	-8.864	-0.112	123	2.71	41	1	0
		Beginning of transition zone								
Ball # 19	3101	36.57	2.373	3.324	-0.008	123	2.71	65	0	1
Ball # 19	3102	41.55	2.399	7.756	0.096	123	2.71	17	1	0
Ball # 19	3103	43.77	2.432	0	0.008	123	2.71	6.79	1	0
Ball # 19	3104	44.32	2.377	2.216	-0.04	123	2.71	73	0	1
Ball # 19	3105	43.21	2.365	4.432	-0.004	123	2.71	60	1	0
Ball # 19	3106	43.77	2.367	-4.432	0.004	123	2.71	1.16	1	0
		Beginning of FU 2 and end of transition								
Ball # 19	3107	39.89	2.362	-2.216	-0.014	123	2.71	110	0	1
Ball # 19	3108	40.44	2.307	5.54	-0.008	123	2.71	106	0	1
Ball # 19	3109	43.21	2.293	-1.108	0	123	2.71	207	0	1
Ball # 19	3110	41	2.29	-2.216	0.014	123	2.71	179	0	1
Ball # 19	3111	36.57	2.305	-7.756	0.018	123	2.71	124	0	1
		End of FU 2								
Ball # 19	3112	44.32	2.355	9.972	0.06	123	2.71	26	1	0
Ball # 19	3113	60.39	2.413	36.564	0.02	123	2.71	34	1	0
Ball # 19	3114	82.55	2.571	-2.218	0.152	123	2.71	1.33	1	0

Table F.1 Kohonen Network (Two Output Categories)

ANN Analysis of Core Data Set
Winning Neuron is Set at 1.0
Analysis for Two Sets

ANN Inputs =====>		input	input	input	input	input	input	input		
Well Name	**Depth**	**gr**	**rhob**	**gr'**	**rhob'**	**gr bl**	**rhob bl**	**k (md)**	**Nwk 1**	**Nwk 2**
Horner # 11	3083.75	34.16	2.512	5.51	-0.04	122	2.7	0.1	1	0
Horner # 11	3084.5	35.26	2.498	1.102	-0.038	122	2.7	2.1	1	0
Horner # 11	3085.5	38.57	2.494	9.916	0.044	122	2.7	18	1	0
Horner # 11	3086.5	46.83	2.528	3.306	0.054	122	2.7	0.1	1	0
Horner # 11	3087.5	56.2	2.557	-1.1	-0.022	122	2.7	0.1	1	0
Horner # 11	3088.5	47.38	2.476	-3.306	-0.296	122	2.7	20	1	0
Horner # 11	3089.5	33.06	2.314	-7.714	0.008	122	2.7	52	1	0
		Beginning of FU 2 and end of FU 1								
Horner # 11	3090.5	29.2	2.33	5.51	-0.008	122	2.7	80	0	1
Horner # 11	3091.5	41.87	2.311	7.714	-0.012	122	2.7	238	0	1
Horner # 11	3092.5	53.99	2.34	4.408	0.066	122	2.7	192	0	1
		End of FU 2 and back to FU 1								
Horner # 11	3093.25	62.81	2.503	20.936	0.346	122	2.7	3.6	1	0
Horner # 11	3099.75	49.04	2.498	-14.32	-0.006	122	2.7	0.1	1	0
Horner # 11	3100.5	46.83	2.501	-8.816	0.008	122	2.7	0.2	1	0
Horner # 9	2889	120.7	2.652	2.204	-0.014	130	2.71	0.1	1	0
Horner # 9	2890	98.07	2.627	-55.1	-0.044	130	2.71	0.2	1	0
Horner # 9	2891	47.93	2.585	-16.53	-0.022	130	2.71	0.1	1	0
Horner # 9	2892	38.02	2.534	-11.02	-0.096	130	2.71	3.3	1	0
Horner # 9	2893	34.71	2.477	-1.102	-0.022	130	2.71	40	1	0
Horner # 9	2894	34.16	2.442	7.714	-0.03	130	2.71	55	1	0
		End of FU 1 and beginning of FU 2								
Horner # 9	2895	39.67	2.418	5.508	-0.028	130	2.71	92	0	1
Horner # 9	2896	42.42	2.37	0	-0.022	130	2.71	80	0	1
Horner # 9	2897	41.32	2.341	-1.102	-0.006	130	2.71	84	0	1
Horner # 9	2898	41.32	2.341	0	0	130	2.71	123	0	1
Horner # 9	2899	42.42	2.332	4.408	-0.024	130	2.71	136	0	1
Horner # 9	2900	45.73	2.289	5.51	-0.014	130	2.71	160	0	1
Horner # 9	2901	50.69	2.281	3.306	-0.014	130	2.71	135	0	1
Horner # 9	2902	52.34	2.274	2.204	0.002	130	2.71	144	0	1
Horner # 9	2903	55.65	2.284	1.102	0.01	130	2.71	124	0	1
Horner # 9	2904	56.2	2.297	4.408	0.046	130	2.71	148	0	1
Horner # 9	2905	61.71	2.327	3.306	0.048	130	2.71	203	0	1
Horner # 9	2906	73.28	2.375	14.326	0.124	130	2.71	214	0	1

Table F.1 Kohonen Network (Two Output Categories)

ANN Analysis of Core Data Set
Winning Neuron is Set at 1.0
Analysis for Two Sets

ANN Inputs =====>		input	input	input	input	input	input	input		
Well Name	**Depth**	**gr**	**rhob**	**gr'**	**rhob'**	**gr bl**	**rhob bl**	**k (md)**	**Nwk 1**	**Nwk 2**
LeMas # 13	3030.75	28.13	2.527	1.136	0.022	115	2.72	0.05	1	0
LeMas # 13	3031.75	30.11	2.544	0	0.022	115	2.72	0.15	1	0
LeMas # 13	3032.75	27.56	2.553	-5.682	-0.01	115	2.72	0.72	1	0
LeMas # 13	3033.75	24.43	2.549	2.272	0.002	115	2.72	0.28	1	0
LeMas # 13	3034.75	28.41	2.564	4.544	0.02	115	2.72	0.27	1	0
LeMas # 13	3035.75	30.4	2.578	-1.136	0.02	115	2.72	0.12	1	0
LeMas # 13	3036.75	28.69	2.574	1.136	-0.02	115	2.72	0.22	1	0
LeMas # 13	3037.75	32.1	2.558	3.41	-0.02	115	2.72	0.1	1	0
LeMas # 13	3038.75	37.22	2.54	3.408	-0.008	115	2.72	0.18	1	0
LeMas # 13	3039.75	40.91	2.532	6.818	-0.006	115	2.72	0.06	1	0
LeMas # 13	3040.75	44.6	2.533	3.41	-0.002	115	2.72	0.06	1	0
LeMas # 13	3041.75	46.59	2.54	0	0.008	115	2.72	0.04	1	0
LeMas # 13	3042.75	44.32	2.529	-2.272	-0.014	115	2.72	0.19	1	0
LeMas # 13	3043.75	39.77	2.504	0	-0.018	115	2.72	0.29	1	0
LeMas # 13	3044.75	42.61	2.495	4.546	0.002	115	2.72	0.67	1	0
LeMas # 13	3045.75	59.66	2.559	29.544	0.114	115	2.72	0.21	1	0
LeMas # 13	3046.25	71.59	2.596	18.182	0.034	115	2.72	0.01	1	0
LeMas # 13	3048	57.39	2.484	-27.27	-0.089	115	2.72	0.04	1	0
LeMas # 13	3048.75	46.31	2.398	-12.5	-0.072	115	2.72	37	1	0
LeMas # 13	3049.75	43.47	2.441	3.408	0.146	115	2.72	1.51	1	0
LeMas # 13	3050.75	45.74	2.495	3.41	0.04	115	2.72	0.11	1	0
LeMas # 13	3052	43.18	2.451	-1.136	-0.026	115	2.72	19	1	0
LeMas # 13	3052.75	42.9	2.447	1.136	0.052	115	2.72	11	1	0
LeMas # 13	3053.75	42.33	2.479	-1.138	0.02	115	2.72	0.07	1	0
LeMas # 13	3054.75	40.34	2.505	-2.272	0.002	115	2.72	0.1	1	0
LeMas # 13	3055.75	42.61	2.522	2.274	0.014	115	2.72	0.09	1	0
LeMas # 13	3056.75	44.6	2.528	-3.41	-0.008	115	2.72	0.02	1	0
LeMas # 13	3057.75	41.76	2.495	-3.41	-0.016	115	2.72	0.04	1	0
LeMas # 13	3058.75	47.73	2.51	22.728	0.088	115	2.72	0.04	1	0
LeMas # 13	3059.75	76.7	2.599	47.726	0.146	115	2.72	0.05	1	0

Table F.1 Kohonen Network (Two Output Categories)

ANN Analysis of Core Data Set
Winning Neuron is Set at 1.0
Analysis for Two Sets

ANN Inputs =====>		input	input	input	input	input	input	input		
Well Name	**Depth**	**gr**	**rhob**	**gr'**	**rhob'**	**gr bl**	**rhob bl**	**k (md)**	**Nwk 1**	**Nwk 2**
T Heirs # 8	2781.5	105.9	2.617	27.854	0.034	145	2.71	0.02	1	0
T Heirs # 8	2782.5	116.4	2.634	-40.11	-0.018	145	2.71	0.03	1	0
T Heirs # 8	2783.5	64.07	2.582	-66.85	-0.112	145	2.71	0.06	1	0
T Heirs # 8	2784.5	47.91	2.507	-8.914	-0.024	145	2.71	0.11	1	0
T Heirs # 8	2785.5	34.54	2.516	-11.14	0.028	145	2.71	0.12	1	0
T Heirs # 8	2786.5	36.77	2.54	8.914	0.014	145	2.71	0.02	1	0
T Heirs # 8	2787.5	42.9	2.548	6.686	-0.006	145	2.71	0.92	1	0
T Heirs # 8	2788.5	49.58	2.503	8.914	-0.018	145	2.71	0.31	1	0
T Heirs # 8	2789.5	47.91	2.469	-15.6	-0.03	145	2.71	0.1	1	0
T Heirs # 8	2790.5	37.33	2.467	0	0	145	2.71	6.5	1	0
T Heirs # 8	2791.5	39.55	2.473	3.342	0.004	145	2.71	3.8	1	0
T Heirs # 8	2792.5	47.91	2.467	4.456	-0.014	145	2.71	8.1	1	0
T Heirs # 8	2793.5	52.37	2.402	-2.228	-0.082	145	2.71	18	1	0
T Heirs # 8	2794.5	49.58	2.384	-2.228	-0.006	145	2.71	22	1	0
T Heirs # 8	2795.5	49.03	2.365	5.572	-0.004	145	2.71	23	1	0
T Heirs # 8	2796.5	55.71	2.352	7.8	-0.006	145	2.71	21	1	0

Table F.2 Kohonen Network (Three Output Categories)

ANN Analysis of Core Data Set
Winning Neuron is Set at 1.0
Analysis for Three Sets

ANN Inputs =====>		input	input	input	input	input	input	input			
									Network		
Well Name	Depth	gr	rhob	gr'	rhob'	gr bl	rhob bl	k (md)	1	2	3
Ball # 18	2987.25	72.02	2.615	-34.35	-0.026	107	2.72	0.26	1	0	0
Ball # 18	2988	49.31	2.61	-26.59	-0.016	107	2.72	0.77	1	0	0
Ball # 18	2989	43.77	2.586	7.756	-0.058	107	2.72	0.06	1	0	0
Ball # 18	2990	47.65	2.499	-15.51	-0.326	107	2.72	0.14	1	0	0
Ball # 18	2991	31.03	2.396	-5.54	0	107	2.72	28	1	0	0
		Beginning of transition zone									
Ball # 18	2992	28.26	2.411	-2.216	0.032	107	2.72	54	0	1	0
Ball # 18	2993	28.81	2.461	-1.108	0	107	2.72	42	0	1	0
Ball # 18	2994	27.15	2.454	1.108	-0.03	107	2.72	20	1	0	0
		End of FU 1 and beginning of FU 2									
Ball # 18	2995	32.69	2.386	8.864	-0.144	107	2.72	226	0	0	1
Ball # 18	2996	43.21	2.286	7.756	-0.072	107	2.72	257	0	0	1
Ball # 18	2997	47.09	2.265	2.216	0.02	107	2.72	207	0	0	1
Ball # 18	2998	49.31	2.284	1.108	0.01	107	2.72	180	0	0	1
Ball # 18	2999	52.63	2.294	11.08	0.028	107	2.72	178	0	0	1
Ball # 18	3000	72.58	2.356	17.728	0.012	107	2.72	137	0	0	1
		End of FU 2 and low k below									
Ball # 18	3001	70.91	2.492	-1.108	0.016	107	2.72	0.06	1	0	0
Ball # 18	3002	69.81	2.481	2.216	-0.06	107	2.72	0.05	1	0	0
Ball # 18	3003	71.47	2.465	-2.216	0.032	107	2.72	37	1	0	0
Ball # 18	3004	65.37	2.501	-2.216	0.032	107	2.72	0.1	1	0	0
Ball # 18	3005	70.91	2.513	14.404	-0.002	107	2.72	0.26	1	0	0
Ball # 18	3006	75.35	2.497	0	-0.014	107	2.72	0.07	1	0	0
Ball # 18	3007	56.51	2.477	-16.62	-0.02	107	2.72	1.4	1	0	0
Ball # 18	3008	39.89	2.463	-9.972	-0.01	107	2.72	1.5	1	0	0
Ball # 18	3009	41.55	2.506	16.62	0.286	107	2.72	0.79	1	0	0
Ball # 18	3010	69.25	2.652	55.402	0.082	107	2.72	0.25	1	0	0
Ball # 18	3011	86.98	2.644	-1.108	-0.008	107	2.72	0.11	1	0	0
Ball # 18	3012	76.45	2.546	-45.43	-0.088	107	2.72	0.26	1	0	0
Ball # 18	3013	43.21	2.505	1.108	0	107	2.72	0.38	1	0	0

Table F.2 Kohonen Network (Three Output Categories)

ANN Analysis of Core Data Set
Winning Neuron is Set at 1.0
Analysis for Three Sets

ANN Inputs =====>		input	input	input	input	input	input	input			
									Network		
Well Name	Depth	gr	rhob	gr'	rhob'	gr bl	rhob bl	k (md)	1	2	3
Ball # 19	3086	90.86	2.663	-23.27	-0.052	123	2.71	2.44	1	0	0
Ball # 19	3087	63.71	2.618	-54.29	-0.034	123	2.71	0.01	1	0	0
Ball # 19	3088	48.75	2.572	-1.108	-0.026	123	2.71	0.03	1	0	0
Ball # 19	3089	41.55	2.569	-11.08	-0.006	123	2.71	0.08	1	0	0
Ball # 19	3090	28.81	2.556	-6.648	-0.014	123	2.71	0.08	1	0	0
Ball # 19	3091	27.15	2.528	2.216	-0.036	123	2.71	0.09	1	0	0
Ball # 19	3092	28.26	2.501	3.324	-0.018	123	2.71	4.24	1	0	0
Ball # 19	3093	34.35	2.465	5.54	-0.038	123	2.71	11	1	0	0
Ball # 19	3094	37.12	2.437	1.108	-0.038	123	2.71	38	1	0	0
Ball # 19	3095	41.55	2.424	5.54	0.002	123	2.71	31	1	0	0
Ball # 19	3096	41	2.469	-6.648	0.128	123	2.71	0.08	1	0	0
Ball # 19	3097	35.46	2.509	2.216	0.008	123	2.71	0.27	1	0	0
Ball # 19	3098	41	2.519	7.756	-0.036	123	2.71	0.16	1	0	0
Ball # 19	3099	45.43	2.477	-7.756	-0.008	123	2.71	17	1	0	0
		Beginning of transition zone									
Ball # 19	3100	37.12	2.396	-8.864	-0.112	123	2.71	41	0	1	0
Ball # 19	3101	36.57	2.373	3.324	-0.008	123	2.71	65	0	1	0
Ball # 19	3102	41.55	2.399	7.756	0.096	123	2.71	17	1	0	0
Ball # 19	3103	43.77	2.432	0	0.008	123	2.71	6.79	1	0	0
Ball # 19	3104	44.32	2.377	2.216	-0.04	123	2.71	73	0	0	1
Ball # 19	3105	43.21	2.365	4.432	-0.004	123	2.71	60	0	1	0
Ball # 19	3106	43.77	2.367	-4.432	0.004	123	2.71	1.16	1	0	0
		Beginning of FU 2 and end of transition									
Ball # 19	3107	39.89	2.362	-2.216	-0.014	123	2.71	110	0	0	1
Ball # 19	3108	40.44	2.307	5.54	-0.008	123	2.71	106	0	0	1
Ball # 19	3109	43.21	2.293	-1.108	0	123	2.71	207	0	0	1
Ball # 19	3110	41	2.29	-2.216	0.014	123	2.71	179	0	0	1
Ball # 19	3111	36.57	2.305	-7.756	0.018	123	2.71	124	0	0	1
		End of FU 2									
Ball # 19	3112	44.32	2.355	9.972	0.06	123	2.71	26	1	0	0
Ball # 19	3113	60.39	2.413	36.564	0.02	123	2.71	34	1	0	0
Ball # 19	3114	82.55	2.571	-2.218	0.152	123	2.71	1.33	1	0	0

Table F.2 Kohonen Network (Three Output Categories)
ANN Analysis of Core Data Set
Winning Neuron is Set at 1.0
Analysis for Three Sets

ANN Inputs =====>		input	input	input	input	input	input	input			
										Network	
Well Name	Depth	gr	rhob	gr'	rhob'	gr bl	rhob bl	k (md)	1	2	3
Horner # 11	3083.75	34.16	2.512	5.51	-0.04	122	2.7	0.1	1	0	0
Horner # 11	3084.5	35.26	2.498	1.102	-0.038	122	2.7	2.1	1	0	0
Horner # 11	3085.5	38.57	2.494	9.916	0.044	122	2.7	18	1	0	0
Horner # 11	3086.5	46.83	2.528	3.306	0.054	122	2.7	0.1	1	0	0
Horner # 11	3087.5	56.2	2.557	-1.1	-0.022	122	2.7	0.1	1	0	0
Horner # 11	3088.5	47.38	2.476	-3.306	-0.296	122	2.7	20	1	0	0
		Beginning of transition									
Horner # 11	3089.5	33.06	2.314	-7.714	0.008	122	2.7	52	0	1	0
		Beginning of FU 2 and end of FU 1									
Horner # 11	3090.5	29.2	2.33	5.51	-0.008	122	2.7	80	0	0	1
Horner # 11	3091.5	41.87	2.311	7.714	-0.012	122	2.7	238	0	0	1
Horner # 11	3092.5	53.99	2.34	4.408	0.066	122	2.7	192	0	0	1
		End of FU 2 and back to FU 1									
Horner # 11	3093.25	62.81	2.503	20.936	0.346	122	2.7	3.6	1	0	0
Horner # 11	3099.75	49.04	2.498	-14.32	-0.006	122	2.7	0.1	1	0	0
Horner # 11	3100.5	46.83	2.501	-8.816	0.008	122	2.7	0.2	1	0	0
Horner # 9	2889	120.7	2.652	2.204	-0.014	130	2.71	0.1	1	0	0
Horner # 9	2890	98.07	2.627	-55.1	-0.044	130	2.71	0.2	1	0	0
Horner # 9	2891	47.93	2.585	-16.53	-0.022	130	2.71	0.1	1	0	0
Horner # 9	2892	38.02	2.534	-11.02	-0.096	130	2.71	3.3	1	0	0
		Beginning of transition									
Horner # 9	2893	34.71	2.477	-1.102	-0.022	130	2.71	40	0	1	0
Horner # 9	2894	34.16	2.442	7.714	-0.03	130	2.71	55	0	1	0
		End of FU 1 and beginning of FU 2									
Horner # 9	2895	39.67	2.418	5.508	-0.028	130	2.71	92	0	0	1
Horner # 9	2896	42.42	2.37	0	-0.022	130	2.71	80	0	0	1
Horner # 9	2897	41.32	2.341	-1.102	-0.006	130	2.71	84	0	0	1
Horner # 9	2898	41.32	2.341	0	0	130	2.71	123	0	0	1
Horner # 9	2899	42.42	2.332	4.408	-0.024	130	2.71	136	0	0	1
Horner # 9	2900	45.73	2.289	5.51	-0.014	130	2.71	160	0	0	1
Horner # 9	2901	50.69	2.281	3.306	-0.014	130	2.71	135	0	0	1
Horner # 9	2902	52.34	2.274	2.204	0.002	130	2.71	144	0	0	1
Horner # 9	2903	55.65	2.284	1.102	0.01	130	2.71	124	0	0	1
Horner # 9	2904	56.2	2.297	4.408	0.046	130	2.71	148	0	0	1
Horner # 9	2905	61.71	2.327	3.306	0.048	130	2.71	203	0	0	1
Horner # 9	2906	73.28	2.375	14.326	0.124	130	2.71	214	0	0	1

Table F.2 Kohonen Network (Three Output Categories)

ANN Analysis of Core Data Set
Winning Neuron is Set at 1.0
Analysis for Three Sets

ANN Inputs =====>		input	input	input	input	input	input	input			
									Network		
Well Name	Depth	gr	rhob	gr'	rhob'	gr bl	rhob bl	k (md)	1	2	3
LeMas # 13	3030.75	28.13	2.527	1.136	0.022	115	2.72	0.05	1	0	0
LeMas # 13	3031.75	30.11	2.544	0	0.022	115	2.72	0.15	1	0	0
LeMas # 13	3032.75	27.56	2.553	-5.682	-0.01	115	2.72	0.72	1	0	0
LeMas # 13	3033.75	24.43	2.549	2.272	0.002	115	2.72	0.28	1	0	0
LeMas # 13	3034.75	28.41	2.564	4.544	0.02	115	2.72	0.27	1	0	0
LeMas # 13	3035.75	30.4	2.578	-1.136	0.02	115	2.72	0.12	1	0	0
LeMas # 13	3036.75	28.69	2.574	1.136	-0.02	115	2.72	0.22	1	0	0
LeMas # 13	3037.75	32.1	2.558	3.41	-0.02	115	2.72	0.1	1	0	0
LeMas # 13	3038.75	37.22	2.54	3.408	-0.008	115	2.72	0.18	1	0	0
LeMas # 13	3039.75	40.91	2.532	6.818	-0.006	115	2.72	0.06	1	0	0
LeMas # 13	3040.75	44.6	2.533	3.41	-0.002	115	2.72	0.06	1	0	0
LeMas # 13	3041.75	46.59	2.54	0	0.008	115	2.72	0.04	1	0	0
LeMas # 13	3042.75	44.32	2.529	-2.272	-0.014	115	2.72	0.19	1	0	0
LeMas # 13	3043.75	39.77	2.504	0	-0.018	115	2.72	0.29	1	0	0
LeMas # 13	3044.75	42.61	2.495	4.546	0.002	115	2.72	0.67	1	0	0
LeMas # 13	3045.75	59.66	2.559	29.544	0.114	115	2.72	0.21	1	0	0
LeMas # 13	3046.25	71.59	2.596	18.182	0.034	115	2.72	0.01	1	0	0
LeMas # 13	3048	57.39	2.484	-27.27	-0.089	115	2.72	0.04	1	0	0
LeMas # 13	3048.75	46.31	2.398	-12.5	-0.072	115	2.72	37	1	0	0
LeMas # 13	3049.75	43.47	2.441	3.408	0.146	115	2.72	1.51	1	0	0
LeMas # 13	3050.75	45.74	2.495	3.41	0.04	115	2.72	0.11	1	0	0
LeMas # 13	3052	43.18	2.451	-1.136	-0.026	115	2.72	19	1	0	0
LeMas # 13	3052.75	42.9	2.447	1.136	0.052	115	2.72	11	1	0	0
LeMas # 13	3053.75	42.33	2.479	-1.138	0.02	115	2.72	0.07	1	0	0
LeMas # 13	3054.75	40.34	2.505	-2.272	0.002	115	2.72	0.1	1	0	0
LeMas # 13	3055.75	42.61	2.522	2.274	0.014	115	2.72	0.09	1	0	0
LeMas # 13	3056.75	44.6	2.528	-3.41	-0.008	115	2.72	0.02	1	0	0
LeMas # 13	3057.75	41.76	2.495	-3.41	-0.016	115	2.72	0.04	1	0	0
LeMas # 13	3058.75	47.73	2.51	22.728	0.088	115	2.72	0.04	1	0	0
LeMas # 13	3059.75	76.7	2.599	47.726	0.146	115	2.72	0.05	1	0	0

Table F.2 Kohonen Network (Three Output Categories)

ANN Analysis of Core Data Set
Winning Neuron is Set at 1.0
Analysis for Three Sets

ANN Inputs =====>		input	input	input	input	input	input	input			
									Network		
Well Name	Depth	gr	rhob	gr'	rhob'	gr bl	rhob bl	k (md)	1	2	3
T Heirs # 8	2781.5	105.9	2.617	27.854	0.034	145	2.71	0.02	1	0	0
T Heirs # 8	2782.5	116.4	2.634	-40.11	-0.018	145	2.71	0.03	1	0	0
T Heirs # 8	2783.5	64.07	2.582	-66.85	-0.112	145	2.71	0.06	1	0	0
T Heirs # 8	2784.5	47.91	2.507	-8.914	-0.024	145	2.71	0.11	1	0	0
T Heirs # 8	2785.5	34.54	2.516	-11.14	0.028	145	2.71	0.12	1	0	0
T Heirs # 8	2786.5	36.77	2.54	8.914	0.014	145	2.71	0.02	1	0	0
T Heirs # 8	2787.5	42.9	2.548	6.686	-0.006	145	2.71	0.92	1	0	0
T Heirs # 8	2788.5	49.58	2.503	8.914	-0.018	145	2.71	0.31	1	0	0
T Heirs # 8	2789.5	47.91	2.469	-15.6	-0.03	145	2.71	0.1	1	0	0
T Heirs # 8	2790.5	37.33	2.467	0	0	145	2.71	6.5	1	0	0
T Heirs # 8	2791.5	39.55	2.473	3.342	0.004	145	2.71	3.8	1	0	0
T Heirs # 8	2792.5	47.91	2.467	4.456	-0.014	145	2.71	8.1	1	0	0
T Heirs # 8	2793.5	52.37	2.402	-2.228	-0.082	145	2.71	18	1	0	0
T Heirs # 8	2794.5	49.58	2.384	-2.228	-0.006	145	2.71	22	1	0	0
T Heirs # 8	2795.5	49.03	2.365	5.572	-0.004	145	2.71	23	1	0	0
T Heirs # 8	2796.5	55.71	2.352	7.8	-0.006	145	2.71	21	1	0	0

Table F.3 Kohonen Network (Two Output Categories)

ANN Analysis of Most Recent Data Set
Winning Neuron is Set at 1.0
Analysis for Two Sets

ANN Inputs ======>			input log	input log	input gr	input rhob	input	input rhob	input k	C	Category Results	
Well Name	**Depth**	**FU**	**gr**	**density**	**slope**	**slope**	**gr bl**	**bl**	**md**	**G**	**1**	**2**
Horner # 11	3084.5	1	35.26	2.498	1.1	-0.04	122	2.7	2.1	t	1	0
Horner # 11	3085.25	1	36.92	2.479	6.61	0.042	122	2.7	18	t	1	0
Horner # 11	3088.75	1	45.73	2.349	-16.5	-0.3	122	2.7	20	p	1	0
Horner # 11	3088.75	1	45.73	2.349	-16.5	-0.3	122	2.7	20		1	0
Horner # 11	3089.5	1	33.06	2.314	-7.71	0.008	122	2.7	52	t	1	0
Horner # 11	3090.5	1	29.2	2.33	5.51	-0.01	122	2.7	80	t	0	1
Horner # 11	3092	2	47.38	2.309	22	0.034	122	2.7	238	t	0	1
Horner # 11	3092.5	2	53.99	2.34	4.41	0.066	122	2.7	192	t	0	1
T Heirs # 8	2785.25	1	38.44	2.519	-12.3	-0.01	145	2.71	0.1	T	1	0
T Heirs # 8	2786.75	1	38.44	2.544	2.23	0.024	145	2.71	0.1	T	1	0
T Heirs # 8	2788.75	1	51.81	2.495	3.34	-0.03	145	2.71	0.9	T	1	0
T Heirs # 8	2789.25	1	51.25	2.488	-6.68	-0.04	145	2.71	0.3	p	1	0
T Heirs # 8	2789.25	1	51.25	2.488	-6.68	-0.04	145	2.71	0.3		1	0
T Heirs # 8	2791.5	1	39.55	2.473	3.34	0.004	145	2.71	6.5	T	1	0
T Heirs # 8	2792.5	1	47.91	2.467	4.46	-0.01	145	2.71	3.8	T	1	0
T Heirs # 8	2793.75	1	51.81	2.392	-1.11	-0.02	145	2.71	8.1	T	1	0
T Heirs # 8	2794.75	1	49.03	2.384	-2.23	-0.03	145	2.71	18	T	1	0
T Heirs # 8	2795.25	1	49.03	2.365	1.11	-0	145	2.71	22	p	1	0
T Heirs # 8	2795.25	1	49.03	2.365	1.11	-0	145	2.71	22		1	0
T Heirs # 8	2796	1	52.93	2.359	5.57	-0.02	145	2.71	23	T	1	0
T Heirs # 8	2797.5	1	74.65	2.354	21.2	0.038	145	2.71	21	T	1	0
Horner # 9	2890	1	98.07	2.627	-55.1	-0.04	130	2.71	0.2	T	1	0
Horner # 9	2891.75	1	41.32	2.558	-13.2	-0.08	130	2.71	3.3	T	1	0
Horner # 9	2893	1	34.71	2.477	-1.1	-0.02	130	2.71	40	p	1	0
Horner # 9	2893	1	34.71	2.477	-1.1	-0.02	130	2.71	40		1	0
Horner # 9	2893.5	1	33.06	2.458	-3.31	-0.03	130	2.71	55	T	1	0
Horner # 9	2895	1	39.67	2.418	5.51	-0.03	130	2.71	92	T	0	1
Horner # 9	2895.75	1	42.42	2.381	-1.1	-0.04	130	2.71	80	T	0	1
Horner # 9	2896.5	1	41.87	2.347	-2.2	-0.05	130	2.71	84	T	0	1
Horner # 9	2898.25	2	41.32	2.341	0	-0.01	130	2.71	123	p	0	1
Horner # 9	2898.25	2	41.32	2.341	0	-0.01	130	2.71	123		0	1
Horner # 9	2898.75	2	41.87	2.334	2.2	-0.01	130	2.71	136	T	0	1
Horner # 9	2900	2	45.73	2.289	5.51	-0.01	130	2.71	160	T	0	1
Horner # 9	2901	2	50.69	2.281	3.31	-0.01	130	2.71	135	T	0	1
Horner # 9	2902	2	52.34	2.274	2.2	0.002	130	2.71	144	T	0	1
Horner # 9	2903	2	55.65	2.284	1.1	0.01	130	2.71	124	p	0	1
Horner # 9	2903	2	55.65	2.284	1.1	0.01	130	2.71	124		0	1
Horner # 9	2903.5	2	55.65	2.288	0	0.016	130	2.71	148	T	0	1

Table F.3 Kohonen Network (Two Output Categories)

ANN Analysis of Most Recent Data Set
Winning Neuron is Set at 1.0
Analysis for Two Sets

ANN Inputs ======>			input	input	input	input	input	input	input		Category Results	
			log	log	gr	rhob		rhob	k	C		
Well Name	**Depth**	**FU**	**gr**	**density**	**slope**	**slope**	**gr bl**	**bl**	**md**	**G**	**1**	**2**
Ball # 19	3086.25	1	84.21	2.652	-13.3	-0.02	123	2.71	2.4	P	1	0
Ball # 19	3086.25	1	84.21	2.652	-13.3	-0.02	123	2.71	2.4		1	0
Ball # 19	3092.25	1	29.92	2.492	5.54	-0.03	123	2.71	4.2	T	1	0
Ball # 19	3092.75	1	32.69	2.476	6.65	-0.04	123	2.71	11	T	1	0
Ball # 19	3094.25	1	37.12	2.429	3.32	-0.02	123	2.71	38	T	1	0
Ball # 19	3094.75	1	39.89	2.424	5.54	-0.01	123	2.71	31	T	1	0
Ball # 19	3097.25	1	37.12	2.509	3.32	0.006	123	2.71	0.3	P	1	0
Ball # 19	3097.25	1	37.12	2.509	3.32	0.006	123	2.71	0.3		1	0
Ball # 19	3098	1	41	2.519	7.76	-0.04	123	2.71	0.2	T	1	0
Ball # 19	3099.25	1	42.66	2.473	-5.54	-0.02	123	2.71	17	T	1	0
Ball # 19	3100	1	37.12	2.396	-8.86	-0.11	123	2.71	41	T	1	0
Ball # 19	3101.25	1	36.57	2.369	3.32	-0.01	123	2.71	65	T	0	1
Ball # 19	3102	1	41.55	2.399	7.76	0.096	123	2.71	17	T	1	0
Ball # 19	3103	1	43.77	2.432	0	0.008	123	2.71	6.8	T	1	0
Ball # 19	3104	1	44.32	2.377	2.22	-0.04	123	2.71	73	T	0	1
Ball # 19	3105	1	43.21	2.365	4.43	-0	123	2.71	60	T	0	1
Ball # 19	3106	1	43.77	2.367	-4.43	0.004	123	2.71	1.2	T	1	0
Ball # 19	3107.25	2	39.34	2.358	1.11	-0.08	123	2.71	110	P	0	1
Ball # 19	3107.25	2	39.34	2.358	1.11	-0.08	123	2.71	110		0	1
Ball # 19	3108	2	40.44	2.307	5.54	-0.01	123	2.71	106	T	0	1
Ball # 19	3108.75	2	43.77	2.293	-1.11	-0.01	123	2.71	207	T	0	1
Ball # 19	3109.5	2	42.66	2.286	-2.22	-0.01	123	2.71	179	T	0	1
Ball # 19	3110.75	2	40.44	2.3	-8.86	0.018	123	2.71	124	T	0	1
LeMas #13	3031.75	1	30.11	2.544	0	0.022	115	2.72	0.2	p	1	0
LeMas #13	3031.75	1	30.11	2.544	0	0.022	115	2.72	0.2		1	0
LeMas #13	3032.25	1	29.55	2.552	-2.27	0.012	115	2.72	0.7	T	1	0
LeMas #13	3034.25	1	26.14	2.554	4.55	0.02	115	2.72	0.3	T	1	0
LeMas #13	3034.75	1	28.41	2.564	4.54	0.02	115	2.72	0.3	T	1	0
LeMas #13	3036	1	30.11	2.583	-2.27	0.006	115	2.72	0.1	T	1	0
LeMas #13	3036.5	1	28.41	2.579	-1.14	-0.01	115	2.72	0.2	p	1	0
LeMas #13	3036.5	1	28.41	2.579	-1.14	-0.01	115	2.72	0.2		1	0
LeMas #13	3038.5	1	36.36	2.542	5.11	-0.02	115	2.72	0.2	T	1	0
LeMas #13	3042.5	1	44.89	2.532	-2.84	-0.02	115	2.72	0.2	T	1	0
LeMas #13	3043.25	1	41.76	2.517	-7.95	-0.03	115	2.72	0.3	P	1	0
LeMas #13	3043.25	1	41.76	2.517	-7.95	-0.03	115	2.72	0.3		1	0
LeMas #13	3045.25	1	48.01	2.513	17	0.07	115	2.72	0.7	T	1	0
LeMas #13	3045.75	1	59.66	2.559	29.5	0.114	115	2.72	0.2	T	1	0
LeMas #13	3048.75	1	46.31	2.398	-12.5	-0.07	115	2.72	37	P	1	0
LeMas #13	3048.75	1	46.31	2.398	-12.5	-0.07	115	2.72	37		1	0
LeMas #13	3050	1	44.32	2.477	2.27	0.081	115	2.72	1.5	T	1	0

Table F.3 Kohonen Network (Two Output Categories)

ANN Analysis of Most Recent Data Set
Winning Neuron is Set at 1.0
Analysis for Two Sets

ANN Inputs ======>			input	input	input	input	input	input	input		Category Results
			log	log	gr	rhob		rhob	k C		
Well Name	**Depth**	**FU**	**gr**	**density**	**slope**	**slope**	**gr bl**	**bl**	**md G**	**1**	**2**
LeMas #13	3051	1	46.59	2.505	-1.14	-0.03	115	2.72	0.1T	1	0
LeMas #13	3052.25	1	42.9	2.443	-1.14	-0.03	115	2.72	19T	1	0
LeMas #13	3052.75	1	42.9	2.447	1.14	0.052	115	2.72	11T	1	0
Ball # 18	2987.25	1	72.02	2.615	-34.3	-0.03	107	2.72	0.3v	1	0
Ball # 18	2988.25	1	41.55	2.604	-16.6	-0.02	107	2.72	0.8v	1	0
Ball # 18	2989.75	1	46.54	2.575	5.54	-0.14	107	2.72	0.1P	1	0
Ball # 18	2990.75	1	33.8	2.396	-12.2	0	107	2.72	28v	1	0
Ball # 18	2991.5	1	30.47	2.399	-3.32	0.014	107	2.72	54v	0	1
Ball # 18	2993.5	1	27.15	2.461	-2.22	-0.01	107	2.72	42v	1	0
Ball # 18	2994	1	27.15	2.454	1.11	-0.03	107	2.72	20v	1	0
Ball # 18	2995.5	2	39.34	2.324	12.2	-0.08	107	2.72	226P	0	1
Ball # 18	2996.25	2	45.43	2.269	4.43	-0.03	107	2.72	257v	0	1
Ball # 18	2997.5	2	48.75	2.274	2.22	0.02	107	2.72	207v	0	1
Ball # 18	2998.25	2	49.31	2.284	1.11	0.008	107	2.72	180v	0	1
Ball # 18	2999	2	52.63	2.294	11.1	0.028	107	2.72	178v	0	1
Ball # 18	2999.75	2	63.71	2.35	25.5	0.038	107	2.72	137P	0	1

Table F.4 Kohonen Network (Three Output Categories)

ANN Analysis of Most Recent Data Set
Winning Neuron is Set at 1.0
Analysis for Two Sets

ANN Inputs	======>		input	input	input	input	input	input	input		Category Results		
			log	log	gr	rhob		rhob	k	C			
Well Name	**Depth**	**FU**	**gr**	**density**	**slope**	**slope**	**gr bl**	**bl**	**md**	**G**	**1**	**2**	**3**
Horner # 11	3084.5	1	35.26	2.498	1.1	-0.04	122	2.7	2.1	t	1	0	0
Horner # 11	3085.3	1	36.92	2.479	6.61	0.04	122	2.7	18	t	1	0	0
Horner # 11	3088.8	1	45.73	2.349	-16.5	-0.3	122	2.7	20	p	1	0	0
Horner # 11	3088.8	1	45.73	2.349	-16.5	-0.3	122	2.7	20		1	0	0
Horner # 11	3089.5	1	33.06	2.314	-7.71	0.01	122	2.7	52	t	1	0	0
Horner # 11	3090.5	1	29.2	2.33	5.51	-0.01	122	2.7	80	t	0	0	1
Horner # 11	3092	2	47.38	2.309	22	0.03	122	2.7	238	t	0	0	1
Horner # 11	3092.5	2	53.99	2.34	4.41	0.07	122	2.7	192	t	0	0	1
T Heirs # 8	2785.3	1	38.44	2.519	-12.3	-0.01	145	2.71	0.1	T	1	0	0
T Heirs # 8	2786.8	1	38.44	2.544	2.23	0.02	145	2.71	0.1	T	1	0	0
T Heirs # 8	2788.8	1	51.81	2.495	3.34	-0.03	145	2.71	0.9	T	1	0	0
T Heirs # 8	2789.3	1	51.25	2.488	-6.68	-0.04	145	2.71	0.3	p	1	0	0
T Heirs # 8	2789.3	1	51.25	2.488	-6.68	-0.04	145	2.71	0.3		1	0	0
T Heirs # 8	2791.5	1	39.55	2.473	3.34	0	145	2.71	6.5	T	1	0	0
T Heirs # 8	2792.5	1	47.91	2.467	4.46	-0.01	145	2.71	3.8	T	1	0	0
T Heirs # 8	2793.8	1	51.81	2.392	-1.11	-0.02	145	2.71	8.1	T	1	0	0
T Heirs # 8	2794.8	1	49.03	2.384	-2.23	-0.03	145	2.71	18	T	1	0	0
T Heirs # 8	2795.3	1	49.03	2.365	1.11	-0	145	2.71	22	p	1	0	0
T Heirs # 8	2795.3	1	49.03	2.365	1.11	-0	145	2.71	22		1	0	0
T Heirs # 8	2796	1	52.93	2.359	5.57	-0.02	145	2.71	23	T	1	0	0
T Heirs # 8	2797.5	1	74.65	2.354	21.2	0.04	145	2.71	21	T	1	0	0
Horner # 9	2890	1	98.07	2.627	-55.1	-0.04	130	2.71	0.2	T	1	0	0
Horner # 9	2891.8	1	41.32	2.558	-13.2	-0.08	130	2.71	3.3	T	1	0	0
Horner # 9	2893	1	34.71	2.477	-1.1	-0.02	130	2.71	40	p	1	0	0
Horner # 9	2893	1	34.71	2.477	-1.1	-0.02	130	2.71	40		1	0	0
Horner # 9	2893.5	1	33.06	2.458	-3.31	-0.03	130	2.71	55	T	1	0	0
Horner # 9	2895	1	39.67	2.418	5.51	-0.03	130	2.71	92	T	0	0	1
Horner # 9	2895.8	1	42.42	2.381	-1.1	-0.04	130	2.71	80	T	0	0	1
Horner # 9	2896.5	1	41.87	2.347	-2.2	-0.05	130	2.71	84	T	0	0	1
Horner # 9	2898.3	2	41.32	2.341	0	-0.01	130	2.71	123	p	0	0	1
Horner # 9	2898.3	2	41.32	2.341	0	-0.01	130	2.71	123		0	0	1
Horner # 9	2898.8	2	41.87	2.334	2.2	-0.01	130	2.71	136	T	0	0	1
Horner # 9	2900	2	45.73	2.289	5.51	-0.01	130	2.71	160	T	0	0	1
Horner # 9	2901	2	50.69	2.281	3.31	-0.01	130	2.71	135	T	0	0	1
Horner # 9	2902	2	52.34	2.274	2.2	0	130	2.71	144	T	0	0	1
Horner # 9	2903	2	55.65	2.284	1.1	0.01	130	2.71	124	p	0	0	1
Horner # 9	2903	2	55.65	2.284	1.1	0.01	130	2.71	124		0	0	1
Horner # 9	2903.5	2	55.65	2.288	0	0.02	130	2.71	148	T	0	0	1

Table F.4 Kohonen Network (Three Output Categories)

ANN Analysis of Most Recent Data Set
Winning Neuron is Set at 1.0
Analysis for Two Sets

ANN Inputs	======>		input log	input log	input gr	input rhob	input	input rhob	input k	C	Category Results		
Well Name	**Depth**	**FU**	**gr**	**density**	**slope**	**slope**	**gr bl**	**bl**	**md**	**G**	**1**	**2**	**3**
Ball # 19	3086.3	1	84.21	2.652	-13.3	-0.02	123	2.71	2.4	P	1	0	0
Ball # 19	3086.3	1	84.21	2.652	-13.3	-0.02	123	2.71	2.4		1	0	0
Ball # 19	3092.3	1	29.92	2.492	5.54	-0.03	123	2.71	4.2	T	1	0	0
Ball # 19	3092.8	1	32.69	2.476	6.65	-0.04	123	2.71	11	T	1	0	0
Ball # 19	3094.3	1	37.12	2.429	3.32	-0.02	123	2.71	38	T	1	0	0
Ball # 19	3094.8	1	39.89	2.424	5.54	-0.01	123	2.71	31	T	1	0	0
Ball # 19	3097.3	1	37.12	2.509	3.32	0.01	123	2.71	0.3	P	1	0	0
Ball # 19	3097.3	1	37.12	2.509	3.32	0.01	123	2.71	0.3		1	0	0
Ball # 19	3098	1	41	2.519	7.76	-0.04	123	2.71	0.2	T	1	0	0
Ball # 19	3099.3	1	42.66	2.473	-5.54	-0.02	123	2.71	17	T	1	0	0
Ball # 19	3100	1	37.12	2.396	-8.86	-0.11	123	2.71	41	T	1	0	0
Ball # 19	3101.3	1	36.57	2.369	3.32	-0.01	123	2.71	65	T	0	0	1
Ball # 19	3102	1	41.55	2.399	7.76	0.1	123	2.71	17	T	1	0	0
Ball # 19	3103	1	43.77	2.432	0	0.01	123	2.71	6.8	T	1	0	0
Ball # 19	3104	1	44.32	2.377	2.22	-0.04	123	2.71	73	T	0	0	1
Ball # 19	3105	1	43.21	2.365	4.43	-0	123	2.71	60	T	1	0	0
Ball # 19	3106	1	43.77	2.367	-4.43	0	123	2.71	1.2	T	1	0	0
Ball # 19	3107.3	2	39.34	2.358	1.11	-0.08	123	2.71	110	P	0	0	1
Ball # 19	3107.3	2	39.34	2.358	1.11	-0.08	123	2.71	110		0	0	1
Ball # 19	3108	2	40.44	2.307	5.54	-0.01	123	2.71	106	T	0	0	1
Ball # 19	3108.8	2	43.77	2.293	-1.11	-0.01	123	2.71	207	T	0	0	1
Ball # 19	3109.5	2	42.66	2.286	-2.22	-0.01	123	2.71	179	T	0	0	1
Ball # 19	3110.8	2	40.44	2.3	-8.86	0.02	123	2.71	124	T	0	0	1
LeMas #13	3031.8	1	30.11	2.5435	0	0.02	115	2.72	0.2	p	1	0	0
LeMas #13	3031.8	1	30.11	2.5435	0	0.02	115	2.72	0.2		1	0	0
LeMas #13	3032.3	1	29.55	2.552	-2.27	0.01	115	2.72	0.7	T	1	0	0
LeMas #13	3034.3	1	26.14	2.554	4.55	0.02	115	2.72	0.3	T	1	0	0
LeMas #13	3034.8	1	28.41	2.564	4.54	0.02	115	2.72	0.3	T	1	0	0
LeMas #13	3036	1	30.11	2.583	-2.27	0.01	115	2.72	0.1	T	1	0	0
LeMas #13	3036.5	1	28.41	2.579	-1.14	-0.01	115	2.72	0.2	p	1	0	0
LeMas #13	3036.5	1	28.41	2.579	-1.14	-0.01	115	2.72	0.2		1	0	0
LeMas #13	3038.5	1	36.36	2.542	5.11	-0.02	115	2.72	0.2	T	1	0	0
LeMas #13	3042.5	1	44.89	2.532	-2.84	-0.02	115	2.72	0.2	T	1	0	0
LeMas #13	3043.3	1	41.76	2.5165	-7.95	-0.03	115	2.72	0.3	P	1	0	0
LeMas #13	3043.3	1	41.76	2.5165	-7.95	-0.03	115	2.72	0.3		1	0	0
LeMas #13	3045.3	1	48.01	2.5125	17	0.07	115	2.72	0.7	T	1	0	0
LeMas #13	3045.8	1	59.66	2.5585	29.5	0.11	115	2.72	0.2	T	1	0	0
LeMas #13	3048.8	1	46.31	2.398	-12.5	-0.07	115	2.72	37	P	1	0	0
LeMas #13	3048.8	1	46.31	2.398	-12.5	-0.07	115	2.72	37		1	0	0
LeMas #13	3050	1	44.32	2.477	2.27	0.08	115	2.72	1.5	T	1	0	0

Table F.4 Kohonen Network (Three Output Categories)

ANN Analysis of Most Recent Data Set
Winning Neuron is Set at 1.0
Analysis for Two Sets

ANN Inputs ======>			input	input	input	input	input	input	input		Category Results		
			log	log	gr	rhob		rhob	k	C			
Well Name	**Depth**	**FU**	**gr**	**density**	**slope**	**slope**	**gr bl**	**bl**	**md**	**G**	**1**	**2**	**3**
LeMas #13	3051	1	46.59	2.505	-1.14	-0.03	115	2.72	0.1	T	1	0	0
LeMas #13	3052.3	1	42.9	2.4425	-1.14	-0.03	115	2.72	19	T	1	0	0
LeMas #13	3052.8	1	42.9	2.447	1.14	0.05	115	2.72	11	T	1	0	0
Ball # 18	2987.3	1	72.02	2.615	-34.3	-0.03	107	2.72	0.3	v	1	0	0
Ball # 18	2988.3	1	41.55	2.604	-16.6	-0.02	107	2.72	0.8	v	1	0	0
Ball # 18	2989.8	1	46.54	2.575	5.54	-0.14	107	2.72	0.1	P	1	0	0
Ball # 18	2990.8	1	33.8	2.396	-12.2	0	107	2.72	28	v	1	0	0
Ball # 18	2991.5	1	30.47	2.399	-3.32	0.01	107	2.72	54	v	0	0	1
Ball # 18	2993.5	1	27.15	2.461	-2.22	-0.01	107	2.72	42	v	1	0	0
Ball # 18	2994	1	27.15	2.454	1.11	-0.03	107	2.72	20	v	1	0	0
Ball # 18	2995.5	2	39.34	2.324	12.2	-0.08	107	2.72	226	P	0	0	1
Ball # 18	2996.3	2	45.43	2.269	4.43	-0.03	107	2.72	257	v	0	0	1
Ball # 18	2997.5	2	48.75	2.274	2.22	0.02	107	2.72	207	v	0	0	1
Ball # 18	2998.3	2	49.31	2.284	1.11	0.01	107	2.72	180	v	0	0	1
Ball # 18	2999	2	52.63	2.294	11.1	0.03	107	2.72	178	v	0	0	1
Ball # 18	2999.8	2	63.71	2.35	25.5	0.04	107	2.72	137	P	0	0	1

APPENDIX G.

Appendix G. details graphs comparing core data to minpermeameter data for cumulative flow capacity versus cumulative storage capacity for each core well having miniperm data. Appendixes B. and C. can be referenced for each type of graph and the supporting tables of data.

Figure G.1 T. Heirs # 8 Cumulative Flow Capacity versus Cumulative Storage Capacity (Core and Miniperm)

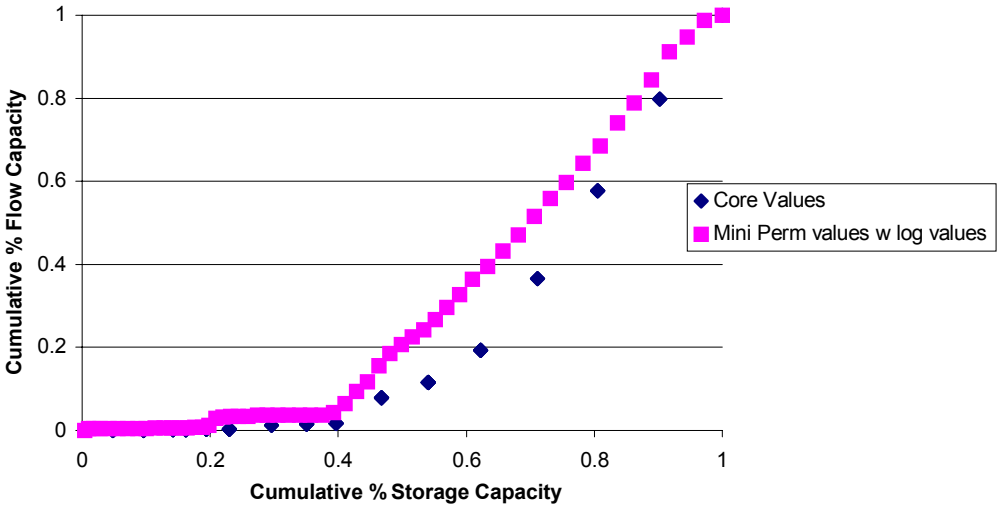

Figure G.2 Horner # 9 Cumulative Flow Capacity versus Cumulative Storage Capacity (Core and Miniperm)

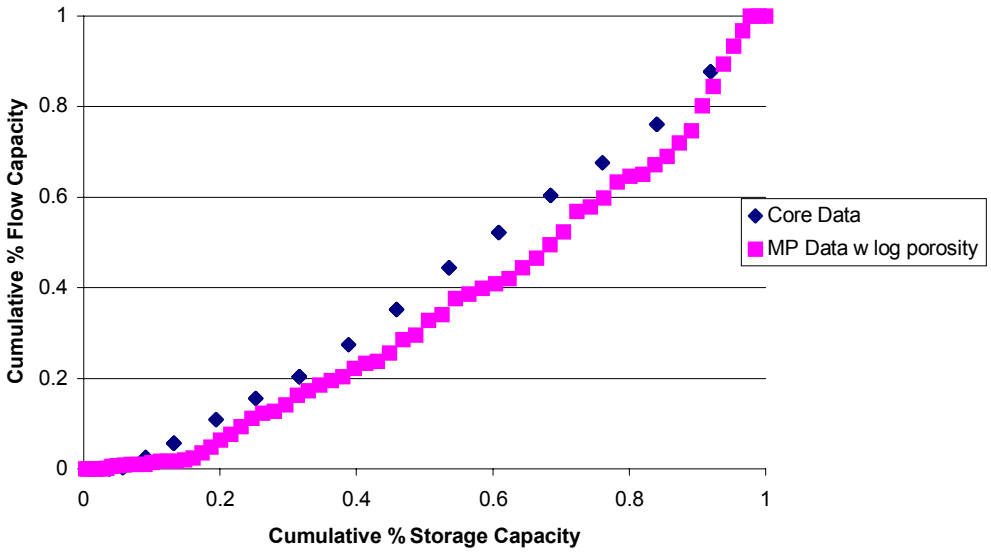

Figure G.3 Ball # 19 Cumulative Flow Capacity versus Cumulative Storage Capacity (Core and Miniperm)

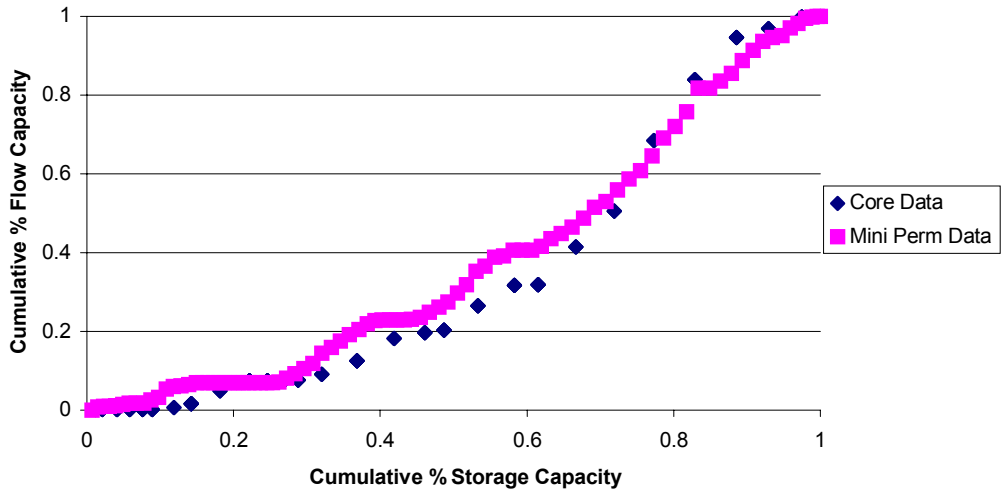

Figure G.4 LeMasters # 13 Cumulative Flow Capacity versus Cumulative Storage Capacity (Core and Miniperm)

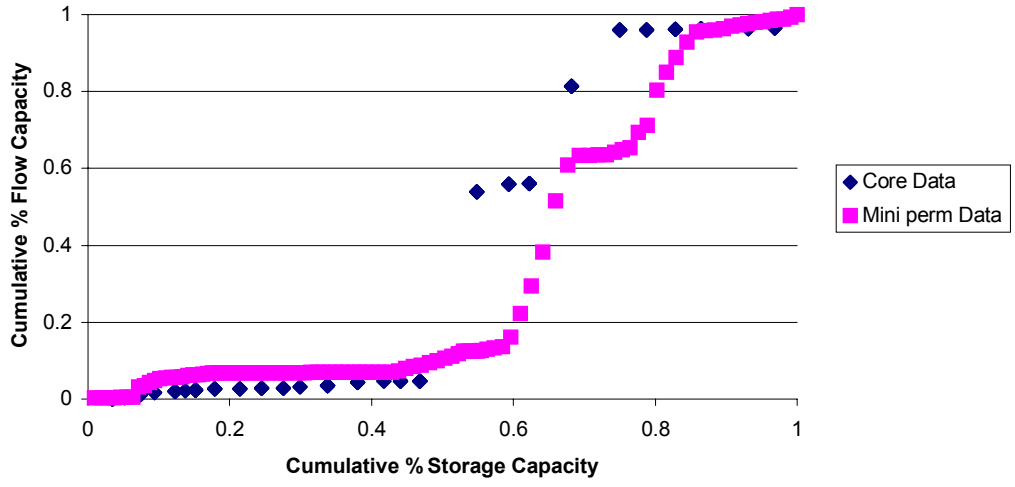

Figure G.5 Ball # 18 Cumulative Flow Capacity versus Cumulative Storage Capacity (Core and Miniperm)

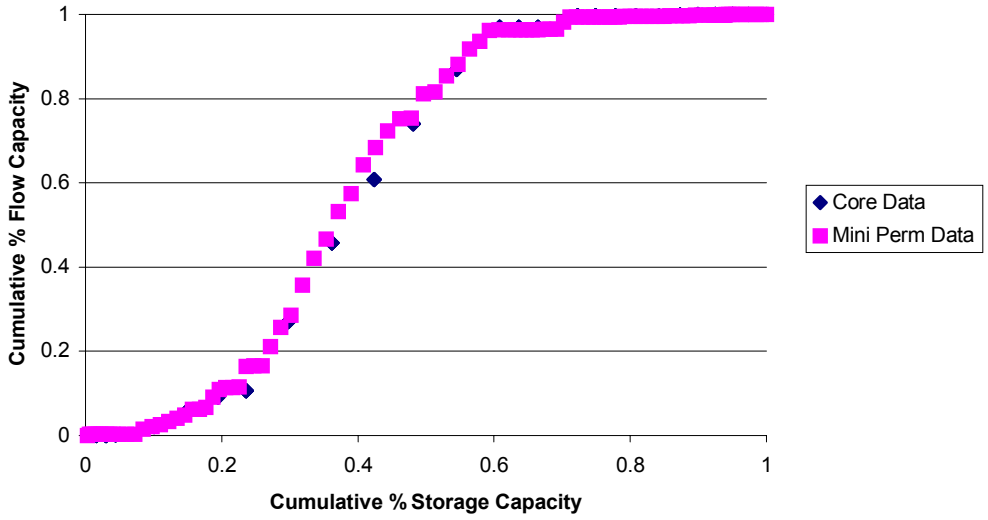

APPENDIX H.

Table H.1 and H.2 are the final backpropagation models for permeability prediction. Table H.3 is the final backpropagation model (4-FU) for flow unit prediction. Figures H.1 – H.6 are graphs of actual versus predicted permeability for each core well.

Table H.1 Neural Network Model for Permeability Prediction
Model 1-K
(Seven Inputs with Constant Test Set)

		INPUT							OUTPUT	
Well Name	Depth	flow unit	gr	density	gr slope	rhob slope	gr bl	rhob bl	k (md)	Cgy A
Horner # 11	3084.50	1	35.262	2.498	1.102	-0.038	122	2.7	2.1	p
Horner # 11	3085.25	1	36.915	2.479	6.61	0.042	122	2.7	18	T
Horner # 11	3088.75	1	45.73	2.349	-16.5	-0.302	122	2.7	20	T
Horner # 11	3089.50	1	33.058	2.314	-7.71	0.008	122	2.7	52	p
Horner # 11	3090.50	1	29.201	2.33	5.51	-0.008	122	2.7	80	p
Horner # 11	3092.00	2	47.383	2.309	22.04	0.034	122	2.7	238	p
Horner # 11	3092.50	2	53.994	2.34	4.408	0.066	122	2.7	192	T
T. Heirs # 8	2785.25	1	38.44	2.519	-12.3	-0.008	145	2.71	0.11	T
T. Heirs # 8	2786.75	1	38.44	2.544	2.228	0.024	145	2.71	0.12	T
T. Heirs # 8	2788.75	1	51.811	2.495	3.342	-0.03	145	2.71	0.92	T
T. Heirs # 8	2789.25	1	51.253	2.488	-6.68	-0.038	145	2.71	0.31	T
T. Heirs # 8	2791.50	1	39.554	2.473	3.342	0.004	145	2.71	6.5	T
T. Heirs # 8	2792.50	1	47.911	2.467	4.456	-0.014	145	2.71	3.8	p
T. Heirs # 8	2793.75	1	51.811	2.392	-1.11	-0.02	145	2.71	8.1	T
T. Heirs # 8	2794.75	1	49.025	2.384	-2.23	-0.034	145	2.71	18	T
T. Heirs # 8	2795.25	1	49.025	2.365	1.114	-0.004	145	2.71	22	T
T. Heirs # 8	2796.00	1	52.925	2.359	5.57	-0.018	145	2.71	23	T
T. Heirs # 8	2797.50	1	74.652	2.354	21.17	0.038	145	2.71	21	T
Horner # 9	2890.00	1	98.072	2.627	-55.1	-0.044	130	2.71	0.2	T
Horner # 9	2891.75	1	41.322	2.558	-13.2	-0.08	130	2.71	3.3	T
Horner # 9	2893.00	1	34.711	2.477	-1.1	-0.022	130	2.71	40	T
Horner # 9	2893.50	1	33.058	2.458	-3.31	-0.034	130	2.71	55	p
Horner # 9	2895.00	1	39.669	2.418	5.508	-0.028	130	2.71	92	p
Horner # 9	2895.75	1	42.424	2.381	-1.1	-0.044	130	2.71	80	T
Horner # 9	2896.50	1	41.873	2.347	-2.2	-0.052	130	2.71	84	p
Horner # 9	2898.25	2	41.322	2.341	0	-0.006	130	2.71	123	T
Horner # 9	2898.75	2	41.873	2.334	2.204	-0.012	130	2.71	136	T
Horner # 9	2900.00	2	45.73	2.289	5.51	-0.014	130	2.71	160	T
Horner # 9	2901.00	2	50.689	2.281	3.306	-0.014	130	2.71	135	T
Horner # 9	2902.00	2	52.342	2.274	2.204	0.002	130	2.71	144	p
Horner # 9	2903.00	2	55.647	2.284	1.102	0.01	130	2.71	124	p
Horner # 9	2903.50	2	55.647	2.288	0	0.016	130	2.71	148	T

Table H.1 Neural Network Model for Permeability Prediction
Model 1-K
(Seven Inputs with Constant Test Set)

		INPUT							OUTPUT	
Well Name	Depth	flow unit	gr	density	gr slope	rhob slope	gr bl	rhob bl	k (md)	Cgy A
Ball # 19	3086.25	1	84.211	2.652	-13.3	-0.022	123	2.71	2.44	T
Ball # 19	3092.25	1	29.917	2.492	5.54	-0.03	123	2.71	4.24	T
Ball # 19	3092.75	1	32.687	2.476	6.648	-0.042	123	2.71	11	T
Ball # 19	3094.25	1	37.119	2.429	3.324	-0.016	123	2.71	38	T
Ball # 19	3094.75	1	39.889	2.424	5.54	-0.01	123	2.71	31	p
Ball # 19	3097.25	1	37.119	2.509	3.324	0.006	123	2.71	0.27	T
Ball # 19	3098.00	1	40.997	2.519	7.756	-0.036	123	2.71	0.16	T
Ball # 19	3099.25	1	42.659	2.473	-5.54	-0.016	123	2.71	17	T
Ball # 19	3100.00	1	37.119	2.396	-8.86	-0.112	123	2.71	41	T
Ball # 19	3101.25	1	36.565	2.369	3.324	-0.012	123	2.71	65	T
Ball # 19	3102.00	1	41.551	2.399	7.756	0.096	123	2.71	17	p
Ball # 19	3103.00	1	43.767	2.432	0	0.008	123	2.71	6.79	p
Ball # 19	3104.00	1	44.321	2.377	2.216	-0.04	123	2.71	73	T
Ball # 19	3105.00	1	43.213	2.365	4.432	-0.004	123	2.71	60	T
Ball # 19	3106.00	1	43.767	2.367	-4.43	0.004	123	2.71	1.16	p
Ball # 19	3107.25	2	39.335	2.358	1.108	-0.08	123	2.71	110	T
Ball # 19	3108.00	2	40.443	2.307	5.54	-0.008	123	2.71	106	T
Ball # 19	3108.75	2	43.767	2.293	-1.11	-0.01	123	2.71	207	p
Ball # 19	3109.50	2	42.659	2.286	-2.22	-0.014	123	2.71	179	T
Ball # 19	3110.75	2	40.443	2.3	-8.86	0.018	123	2.71	124	T
LeMasters # 13	3031.75	1	30.114	2.544	0	0.022	115	2.72	0.15	T
LeMasters # 13	3032.25	1	29.546	2.552	-2.27	0.012	115	2.72	0.72	T
LeMasters # 13	3034.25	1	26.137	2.554	4.546	0.02	115	2.72	0.28	T
LeMasters # 13	3034.75	1	28.409	2.564	4.544	0.02	115	2.72	0.27	T
LeMasters # 13	3036.00	1	30.114	2.583	-2.27	0.006	115	2.72	0.12	T
LeMasters # 13	3036.50	1	28.409	2.579	-1.14	-0.014	115	2.72	0.22	T
LeMasters # 13	3038.50	1	36.364	2.542	5.113	-0.015	115	2.72	0.18	T
LeMasters # 13	3042.50	1	44.886	2.532	-2.84	-0.017	115	2.72	0.19	T
LeMasters # 13	3043.25	1	41.762	2.517	-7.95	-0.034	115	2.72	0.29	T
LeMasters # 13	3045.25	1	48.012	2.513	17.05	0.07	115	2.72	0.67	T
LeMasters # 13	3045.75	1	59.659	2.559	29.54	0.114	115	2.72	0.21	T
LeMasters # 13	3048.75	1	46.307	2.398	-12.5	-0.072	115	2.72	37	T
LeMasters # 13	3050.00	1	44.318	2.477	2.272	0.081	115	2.72	1.51	p
LeMasters # 13	3051.00	1	46.591	2.505	-1.14	-0.025	115	2.72	0.11	T
LeMasters # 13	3052.25	1	42.898	2.443	-1.14	-0.034	115	2.72	19	T
LeMasters # 13	3052.75	1	42.898	2.447	1.136	0.052	115	2.72	11	p

Table H.1 Neural Network Model for Permeability Prediction

Model 1-K

(Seven Inputs with Constant Test Set)

		INPUT							OUTPUT	
Well Name	Depth	flow unit	gr	density	gr slope	rhob slope	gr bl	rhob bl	k (md)	Cgy A
Ball # 18	2987.25	1	72.022	2.615	-34.3	-0.026	107	2.72	0.26	T
Ball # 18	2988.25	1	41.551	2.604	-16.6	-0.02	107	2.72	0.77	T
Ball # 18	2989.75	1	46.537	2.575	5.54	-0.142	107	2.72	0.14	T
Ball # 18	2990.75	1	33.795	2.396	-12.2	0	107	2.72	28	p
Ball # 18	2991.50	1	30.471	2.399	-3.32	0.014	107	2.72	54	T
Ball # 18	2993.50	1	27.147	2.461	-2.22	-0.014	107	2.72	42	T
Ball # 18	2994.00	1	27.147	2.454	1.108	-0.03	107	2.72	20	T
Ball # 18	2995.50	2	39.335	2.324	12.19	-0.082	107	2.72	226	T
Ball # 18	2996.25	2	45.429	2.269	4.432	-0.034	107	2.72	257	T
Ball # 18	2997.50	2	48.753	2.274	2.216	0.02	107	2.72	207	T
Ball # 18	2998.25	2	49.307	2.284	1.108	0.008	107	2.72	180	T
Ball # 18	2999.00	2	52.632	2.294	11.08	0.028	107	2.72	178	p
Ball # 18	2999.75	2	63.712	2.35	25.48	0.038	107	2.72	137	P

Table H.2 Neural Network Model for Permeability Prediction
Model 2-K
(Seven Inputs with Constant Test Set)

		INPUT							OUTPUT	
Well Name	Depth	flow unit	gr	density	gr slope	rhob slope	gr bl	rhob bl	k (md)	Cgy A
Horner # 11	3084.50	1	35.262	2.498	1.102	-0.038	122	2.7	2.1	p
Horner # 11	3085.30	1	36.915	2.479	6.61	0.042	122	2.7	18	t
Horner # 11	3088.80	1	45.73	2.349	-16.53	-0.302	122	2.7	20	t
Horner # 11	3089.50	1	33.058	2.314	-7.714	0.008	122	2.7	52	p
Horner # 11	3090.50	1	29.201	2.33	5.51	-0.008	122	2.7	80	t
Horner # 11	3092.00	2	47.383	2.309	22.04	0.034	122	2.7	238	p
Horner # 11	3092.50	2	53.994	2.34	4.408	0.066	122	2.7	192	t
Horner # 11	3093.30	1	62.81	2.503	20.94	0.346	122	2.7	3.6	t
Horner # 11	3100.50	1	46.832	2.501	-8.816	0.008	122	2.7	0.2	t
T. Heirs # 8	2785.30	1	38.44	2.519	-12.26	-0.008	145	2.71	0.11	T
T. Heirs # 8	2786.80	1	38.44	2.544	2.228	0.024	145	2.71	0.12	T
T. Heirs # 8	2788.80	1	51.811	2.495	3.342	-0.03	145	2.71	0.92	T
T. Heirs # 8	2789.30	1	51.253	2.488	-6.684	-0.038	145	2.71	0.31	T
T. Heirs # 8	2791.50	1	39.554	2.473	3.342	0.004	145	2.71	6.5	T
T. Heirs # 8	2792.50	1	47.911	2.467	4.456	-0.014	145	2.71	3.8	T
T. Heirs # 8	2793.80	1	51.811	2.392	-1.114	-0.02	145	2.71	8.1	T
T. Heirs # 8	2794.80	1	49.025	2.384	-2.228	-0.034	145	2.71	18	T
T. Heirs # 8	2795.30	1	49.025	2.365	1.114	-0.004	145	2.71	22	T
T. Heirs # 8	2796.00	1	52.925	2.359	5.57	-0.018	145	2.71	23	T
T. Heirs # 8	2797.50	1	74.652	2.354	21.17	0.038	145	2.71	21	T
Horner # 9	2890.00	1	98.072	2.627	-55.1	-0.044	130	2.71	0.2	T
Horner # 9	2891.80	1	41.322	2.558	-13.22	-0.08	130	2.71	3.3	T
Horner # 9	2893.00	1	34.711	2.477	-1.102	-0.022	130	2.71	40	t
Horner # 9	2893.50	1	33.058	2.458	-3.306	-0.034	130	2.71	55	p
Horner # 9	2895.00	1	39.669	2.418	5.508	-0.028	130	2.71	92	p
Horner # 9	2895.80	1	42.424	2.381	-1.102	-0.044	130	2.71	80	T
Horner # 9	2896.50	1	41.873	2.347	-2.204	-0.052	130	2.71	84	p
Horner # 9	2898.30	2	41.322	2.341	0	-0.006	130	2.71	123	t
Horner # 9	2898.80	2	41.873	2.334	2.204	-0.012	130	2.71	136	T
Horner # 9	2900.00	2	45.73	2.289	5.51	-0.014	130	2.71	160	p
Horner # 9	2901.00	2	50.689	2.281	3.306	-0.014	130	2.71	135	T
Horner # 9	2902.00	2	52.342	2.274	2.204	0.002	130	2.71	144	T
Horner # 9	2903.00	2	55.647	2.284	1.102	0.01	130	2.71	124	p
Horner # 9	2903.50	2	55.647	2.288	0	0.016	130	2.71	148	T

Table H.2 Neural Network Model for Permeability Prediction
Model 2-K
(Seven Inputs with Constant Test Set)

		INPUT							OUTPUT	
Well Name	Depth	flow unit	gr	density	gr slope	rhob slope	gr bl	rhob bl	k (md)	Cgy A
Ball # 19	3086.30	1	84.211	2.652	-13.3	-0.022	123	2.71	2.44	t
Ball # 19	3092.30	1	29.917	2.492	5.54	-0.03	123	2.71	4.24	T
Ball # 19	3092.80	1	32.687	2.476	6.648	-0.042	123	2.71	11	T
Ball # 19	3094.30	1	37.119	2.429	3.324	-0.016	123	2.71	38	T
Ball # 19	3094.80	1	39.889	2.424	5.54	-0.01	123	2.71	31	p
Ball # 19	3097.30	1	37.119	2.509	3.324	0.006	123	2.71	0.27	t
Ball # 19	3098.00	1	40.997	2.519	7.756	-0.036	123	2.71	0.16	T
Ball # 19	3099.30	1	42.659	2.473	-5.54	-0.016	123	2.71	17	T
Ball # 19	3100.00	1	37.119	2.396	-8.864	-0.112	123	2.71	41	T
Ball # 19	3101.30	1	36.565	2.369	3.324	-0.012	123	2.71	65	T
Ball # 19	3102.00	1	41.551	2.399	7.756	0.096	123	2.71	17	T
Ball # 19	3103.00	1	43.767	2.432	0	0.008	123	2.71	6.79	p
Ball # 19	3104.00	1	44.321	2.377	2.216	-0.04	123	2.71	73	T
Ball # 19	3105.00	1	43.213	2.365	4.432	-0.004	123	2.71	60	T
Ball # 19	3106.00	1	43.767	2.367	-4.432	0.004	123	2.71	1.16	p
Ball # 19	3107.30	2	39.335	2.358	1.108	-0.08	123	2.71	110	t
Ball # 19	3108.00	2	40.443	2.307	5.54	-0.008	123	2.71	106	p
Ball # 19	3108.80	2	43.767	2.293	-1.108	-0.01	123	2.71	207	p
Ball # 19	3109.50	2	42.659	2.286	-2.216	-0.014	123	2.71	179	T
Ball # 19	3110.80	2	40.443	2.3	-8.864	0.018	123	2.71	124	T
Ball # 19	3112.00	1	44.321	2.355	9.972	0.06	123	2.71	26	T
Ball # 19	3112.50	1	50.97	2.36	21.05	0.096	123	2.71	34	p
Ball # 19	3113.80	1	83.657	2.503	16.62	0.188	123	2.71	1.33	t
LeMasters # 13	3031.80	1	30.114	2.544	0	0.022	115	2.72	0.15	T
LeMasters # 13	3032.30	1	29.5455	2.552	-2.274	0.012	115	2.72	0.72	T
LeMasters # 13	3034.30	1	26.1365	2.554	4.546	0.02	115	2.72	0.28	T
LeMasters # 13	3034.80	1	28.409	2.564	4.544	0.02	115	2.72	0.27	T
LeMasters # 13	3036.00	1	30.114	2.583	-2.273	0.006	115	2.72	0.12	T
LeMasters # 13	3036.50	1	28.409	2.579	-1.137	-0.014	115	2.72	0.22	T
LeMasters # 13	3038.50	1	36.364	2.542	5.113	-0.015	115	2.72	0.18	T
LeMasters # 13	3042.50	1	44.886	2.532	-2.841	-0.017	115	2.72	0.19	T
LeMasters # 13	3043.30	1	41.7615	2.517	-7.954	-0.034	115	2.72	0.29	T
LeMasters # 13	3045.30	1	48.0115	2.513	17.05	0.07	115	2.72	0.67	T
LeMasters # 13	3045.80	1	59.659	2.559	29.54	0.114	115	2.72	0.21	T
LeMasters # 13	3048.80	1	46.307	2.398	-12.5	-0.072	115	2.72	37	T
LeMasters # 13	3050.00	1	44.318	2.477	2.272	0.081	115	2.72	1.51	p
LeMasters # 13	3051.00	1	46.591	2.505	-1.136	-0.025	115	2.72	0.11	T
LeMasters # 13	3052.30	1	42.898	2.443	-1.136	-0.034	115	2.72	19	T
LeMasters # 13	3052.80	1	42.898	2.447	1.136	0.052	115	2.72	11	p

Table H.2 Neural Network Model for Permeability Prediction
Model 2-K
(Seven Inputs with Constant Test Set)

		INPUT							OUTPUT	
Well Name	Depth	flow unit	gr	density	gr slope	rhob slope	gr bl	rhob bl	k (md)	Cgy A
Ball # 18	2987.30	1	72.022	2.615	-34.35	-0.026	107	2.72	0.26	t
Ball # 18	2988.30	1	41.551	2.604	-16.62	-0.02	107	2.72	0.77	t
Ball # 18	2989.80	1	46.537	2.575	5.54	-0.142	107	2.72	0.14	t
Ball # 18	2990.80	1	33.795	2.396	-12.19	0	107	2.72	28	p
Ball # 18	2991.50	1	30.471	2.399	-3.324	0.014	107	2.72	54	t
Ball # 18	2993.50	1	27.147	2.461	-2.216	-0.014	107	2.72	42	t
Ball # 18	2994.00	1	27.147	2.454	1.108	-0.03	107	2.72	20	t
Ball # 18	2995.50	2	39.335	2.324	12.19	-0.082	107	2.72	226	t
Ball # 18	2996.30	2	45.429	2.269	4.432	-0.034	107	2.72	257	p
Ball # 18	2997.50	2	48.753	2.274	2.216	0.02	107	2.72	207	t
Ball # 18	2998.30	2	49.307	2.284	1.108	0.008	107	2.72	180	t
Ball # 18	2999.00	2	52.632	2.294	11.08	0.028	107	2.72	178	t
Ball # 18	2999.80	2	63.712	2.35	25.48	0.038	107	2.72	137	P
Ball # 18	3002.80	1	72.022	2.458	1.108	0.028	107	2.72	37	t
Ball # 18	3005.30	1	72.576	2.509	5.54	-0.024	107	2.72	0.26	t
Ball # 18	3007.30	1	50.97	2.47	-11.08	-0.014	107	2.72	1.4	p
Ball # 18	3007.80	1	43.767	2.468	-22.16	-0.014	107	2.72	1.5	t
Ball # 18	3009.00	1	41.551	2.506	16.62	0.286	107	2.72	0.79	t
Ball # 18	3009.80	1	57.064	2.611	43.21	0.102	107	2.72	0.25	t
Ball # 18	3011.00	1	86.981	2.644	-1.108	-0.008	107	2.72	0.11	t
Ball # 18	3012.30	1	58.726	2.527	-47.64	-0.08	107	2.72	0.26	t
Ball # 18	3013.00	1	43.213	2.505	1.108	0	107	2.72	0.38	t

Table H.3 Table of ANN Model for Flow Unit Prediction

Model 4-FU

(Constant Test Set)

		OUTPUT	INPUT ----------						INPUT
		flow			**gr**	**rhob**	**gr**	**rhob**	Cat
Well Name	Depth	**unit**	**gr**	**density**	**slope**	**slope**	**bl**	**bl**	A
T Heirs # 8	2789.50	1	47.91	2.469	-15.60	-0.030	145	2.71	T
T Heirs # 8	2789.75	1	43.45	2.473	-21.17	0.000	145	2.71	T
T Heirs # 8	2790.00	1	37.33	2.469	-12.26	-0.012	145	2.71	T
T Heirs # 8	2790.25	1	37.33	2.467	0.00	-0.004	145	2.71	T
T Heirs # 8	2790.50	1	37.33	2.467	0.00	0.000	145	2.71	T
T Heirs # 8	2790.75	1	37.33	2.467	0.00	0.008	145	2.71	T
T Heirs # 8	2791.00	1	37.33	2.471	2.23	0.008	145	2.71	T
T Heirs # 8	2791.25	1	38.44	2.471	4.46	0.004	145	2.71	T
T Heirs # 8	2791.50	1	39.55	2.473	3.34	0.004	145	2.71	T
T Heirs # 8	2791.75	1	40.11	2.473	14.49	-0.004	145	2.71	T
T Heirs # 8	2792.00	1	46.8	2.471	13.37	-0.004	145	2.71	T
T Heirs # 8	2792.25	1	46.8	2.471	2.23	-0.008	145	2.71	T
T Heirs # 8	2792.50	1	47.91	2.467	4.46	-0.014	145	2.71	T
T Heirs # 8	2792.75	1	49.03	2.464	10.03	-0.030	145	2.71	T
T Heirs # 8	2793.00	1	52.93	2.452	7.80	-0.062	145	2.71	T
T Heirs # 8	2793.25	1	52.93	2.433	-1.11	-0.100	145	2.71	T
T Heirs # 8	2793.50	1	52.37	2.402	-2.23	-0.082	145	2.71	T
T Heirs # 8	2793.75	1	51.81	2.392	-1.11	-0.020	145	2.71	T
T Heirs # 8	2794.00	1	51.81	2.392	-3.34	-0.010	145	2.71	T
T Heirs # 8	2794.25	1	50.14	2.387	-4.46	-0.016	145	2.71	T
T Heirs # 8	2794.50	1	49.58	2.384	-2.23	-0.006	145	2.71	T
T Heirs # 8	2794.75	1	49.03	2.384	-2.23	-0.034	145	2.71	T
T Heirs # 8	2795.00	1	48.47	2.367	0.00	-0.038	145	2.71	T
T Heirs # 8	2795.25	1	49.03	2.365	1.11	-0.004	145	2.71	T
T Heirs # 8	2795.50	1	49.03	2.365	5.57	-0.004	145	2.71	T
T Heirs # 8	2795.75	1	51.81	2.363	7.80	-0.012	145	2.71	T
T Heirs # 8	2796.00	1	52.93	2.359	5.57	-0.018	145	2.71	T
T Heirs # 8	2796.25	1	54.6	2.354	5.57	-0.014	145	2.71	T
T Heirs # 8	2796.50	1	55.71	2.352	7.80	-0.006	145	2.71	T
T Heirs # 8	2796.75	1	58.5	2.351	5.57	-0.002	145	2.71	T
T Heirs # 8	2797.00	1	58.5	2.351	11.14	-0.008	145	2.71	T

Table H.3 Table of ANN Model for Flow Unit Prediction

Model 4-FU

(Constant Test Set)

		OUTPUT	INPUT---------- INPUT						
		flow			gr	rhob	gr	rhob	Cat
Well Name	Depth	unit	gr	density	slope	slope	bl	bl	A
LeMasters # 13	3048.00	1	57.39	2.484	-27.27	-0.089	115	2.72	T
LeMasters # 13	3048.25	1	53.41	2.450	-15.91	-0.136	115	2.72	T
LeMasters # 13	3048.50	1	49.43	2.416	-14.20	-0.104	115	2.72	T
LeMasters # 13	3048.75	1	46.31	2.398	-12.50	-0.072	115	2.72	T
LeMasters # 13	3049.00	1	43.18	2.380	-6.82	-0.012	115	2.72	T
LeMasters # 13	3049.25	1	42.90	2.392	-1.14	0.048	115	2.72	T
LeMasters # 13	3049.50	1	42.61	2.404	1.14	0.097	115	2.72	T
LeMasters # 13	3049.75	1	43.47	2.441	3.41	0.146	115	2.72	T
LeMasters # 13	3050.00	1	44.32	2.477	2.27	0.081	115	2.72	p
LeMasters # 13	3050.25	1	44.60	2.481	1.14	0.016	115	2.72	T
LeMasters # 13	3050.50	1	44.89	2.485	2.27	0.028	115	2.72	T
LeMasters # 13	3050.75	1	45.74	2.495	3.41	0.040	115	2.72	T
LeMasters # 13	3051.00	1	46.59	2.505	-1.14	-0.025	115	2.72	T
LeMasters # 13	3051.25	1	45.17	2.483	-5.68	-0.090	115	2.72	T
LeMasters # 13	3051.50	1	43.75	2.460	-3.41	-0.054	115	2.72	T
LeMasters # 13	3051.75	1	43.47	2.456	-1.14	-0.018	115	2.72	T
LeMasters # 13	3052.00	1	43.18	2.451	-1.14	-0.026	115	2.72	T
LeMasters # 13	3052.25	1	42.90	2.443	-1.14	-0.034	115	2.72	T
LeMasters # 13	3052.50	1	42.61	2.434	0.00	0.009	115	2.72	T
LeMasters # 13	3052.75	1	42.90	2.447	1.14	0.052	115	2.72	p
LeMasters # 13	3053.00	1	43.18	2.460	0.00	0.040	115	2.72	T
LeMasters # 13	3053.25	1	42.90	2.467	-1.14	0.028	115	2.72	T
LeMasters # 13	3053.50	1	42.61	2.474	-1.14	0.024	115	2.72	T
LeMasters # 13	3053.75	1	42.33	2.479	-1.14	0.020	115	2.72	T
LeMasters # 13	3054.00	1	42.05	2.484	-1.70	0.030	115	2.72	T

Table H.3 Table of ANN Model for Flow Unit Prediction

Model 4-FU

(Constant Test Set)

		OUTPUT	INPUT						INPUT
Well Name	Depth	flow unit	gr	density	gr slope	rhob slope	gr bl	rhob bl	Cat A
Horner # 9	2892.75	1	34.71	2.48	0.00	-0.026	130	2.71	T
Horner # 9	2893.00	1	34.71	2.48	-1.10	-0.022	130	2.71	T
Horner # 9	2893.25	1	34.16	2.47	-3.31	-0.038	130	2.71	T
Horner # 9	2893.50	1	33.06	2.46	-3.31	-0.034	130	2.71	p
Horner # 9	2893.75	1	32.51	2.45	2.20	-0.032	130	2.71	T
Horner # 9	2894.00	1	34.16	2.44	7.71	-0.030	130	2.71	T
Horner # 9	2894.25	1	36.36	2.43	4.41	-0.016	130	2.71	T
Horner # 9	2894.50	1	36.36	2.43	3.31	-0.016	130	2.71	T
Horner # 9	2894.75	1	38.02	2.43	6.61	-0.032	130	2.71	T
Horner # 9	2895.00	1	39.67	2.42	5.51	-0.028	130	2.71	p
Horner # 9	2895.25	1	40.77	2.41	6.61	-0.052	130	2.71	T
Horner # 9	2895.50	1	42.98	2.39	3.31	-0.062	130	2.71	T
Horner # 9	2895.75	1	42.42	2.38	-1.10	-0.044	130	2.71	T
Horner # 9	2896.00	1	42.42	2.37	0.00	-0.022	130	2.71	T
Horner # 9	2896.25	1	42.42	2.37	-1.10	-0.046	130	2.71	T
Horner # 9	2896.50	2	41.87	2.35	-2.20	-0.052	130	2.71	p
Horner # 9	2896.75	2	41.32	2.34	-1.10	-0.012	130	2.71	T
Horner # 9	2897.00	2	41.32	2.34	-1.10	-0.006	130	2.71	T
Horner # 9	2897.25	2	40.77	2.34	-1.10	0.000	130	2.71	T
Horner # 9	2897.50	2	40.77	2.34	1.10	0.000	130	2.71	T
Horner # 9	2897.75	2	41.32	2.34	1.10	0.000	130	2.71	T
Horner # 9	2898.00	2	41.32	2.34	0.00	0.000	130	2.71	T
Horner # 9	2898.25	2	41.32	2.34	0.00	-0.006	130	2.71	T
Horner # 9	2898.50	2	41.32	2.34	1.10	-0.014	130	2.71	T
Horner # 9	2898.75	2	41.87	2.33	2.20	-0.012	130	2.71	T
Horner # 9	2899.00	2	42.42	2.33	4.41	-0.024	130	2.71	T
Horner # 9	2899.25	2	44.08	2.32	4.41	-0.074	130	2.71	T
Horner # 9	2899.50	3	44.63	2.30	1.10	-0.054	130	2.71	T
Horner # 9	2899.75	3	44.63	2.30	2.20	-0.012	130	2.71	T
Horner # 9	2900.00	3	45.73	2.29	5.51	-0.014	130	2.71	p
Horner # 9	2900.25	3	47.38	2.29	6.61	-0.008	130	2.71	T
Horner # 9	2900.50	3	49.04	2.29	4.41	-0.008	130	2.71	T
Horner # 9	2900.75	3	49.59	2.28	3.31	-0.008	130	2.71	T
Horner # 9	2901.00	3	50.69	2.28	3.31	-0.014	130	2.71	T
Horner # 9	2901.25	3	51.24	2.28	1.10	-0.008	130	2.71	T
Horner # 9	2901.50	3	51.24	2.28	1.10	-0.006	130	2.71	T
Horner # 9	2901.75	3	51.79	2.27	2.20	-0.006	130	2.71	T
Horner # 9	2902.00	3	52.34	2.27	2.20	0.002	130	2.71	T

Table H.3 Table of ANN Model for Flow Unit Prediction

Model 4-FU

(Constant Test Set)

		OUTPUT	INPUT----------						INPUT
		flow			gr	rhob	gr	rhob	Cat
Well Name	Depth	unit	gr	density	slope	slope	bl	bl	A
Horner # 9	2902.75	3	55.10	2.28	3.31	0.012	130	2.71	T
Horner # 9	2903.00	3	55.65	2.28	1.10	0.010	130	2.71	p
Horner # 9	2903.25	3	55.65	2.28	0.00	0.008	130	2.71	T
Horner # 9	2903.50	3	55.65	2.29	0.00	0.016	130	2.71	T
Horner # 9	2903.75	3	55.65	2.29	1.10	0.018	130	2.71	T
Horner # 9	2904.00	3	56.20	2.30	4.41	0.046	130	2.71	T
Horner # 9	2904.25	3	57.85	2.32	9.92	0.042	130	2.71	T
Horner # 9	2904.50	3	61.16	2.32	7.71	0.024	130	2.71	T
Horner # 9	2904.75	2	61.71	2.33	1.10	0.018	130	2.71	T
Horner # 9	2905.00	2	61.71	2.33	3.31	0.048	130	2.71	T
Horner # 9	2905.25	1	63.36	2.35	8.82	0.058	130	2.71	T
Horner # 9	2905.50	1	66.12	2.36	12.12	0.032	130	2.71	T
Horner # 9	2905.75	1	69.42	2.37	14.32	0.038	130	2.71	T
Horner # 9	2906.00	1	73.28	2.38	14.33	0.124	130	2.71	T
Horner # 9	2906.25	1	76.58	2.43	14.33	0.144	130	2.71	T
Horner # 9	2906.50	1	80.44	2.45	7.71	0.036	130	2.71	T

Table H.3 Table of ANN Model for Flow Unit Prediction
Model 4-FU
(Constant Test Set)

		OUTPUT	INPUT						
		flow			gr	rhob	gr	rhob	Cat
Well Name	Depth	unit	gr	density	slope	slope	bl	bl	A
Ball # 19	3092.50	1	31.03	2.486	5.54	-0.032	123	2.71	T
Ball # 19	3092.75	1	32.69	2.476	6.65	-0.042	123	2.71	T
Ball # 19	3093.00	1	34.35	2.465	5.54	-0.038	123	2.71	T
Ball # 19	3093.25	1	35.46	2.457	4.43	-0.034	123	2.71	T
Ball # 19	3093.50	1	36.57	2.448	2.22	-0.018	123	2.71	T
Ball # 19	3093.75	1	36.57	2.448	1.11	-0.022	123	2.71	T
Ball # 19	3094.00	1	37.12	2.437	1.11	-0.038	123	2.71	T
Ball # 19	3094.25	1	37.12	2.429	3.32	-0.016	123	2.71	T
Ball # 19	3094.50	1	38.78	2.429	5.54	-0.010	123	2.71	T
Ball # 19	3094.75	1	39.89	2.424	5.54	-0.010	123	2.71	p
Ball # 19	3095.00	1	41.55	2.424	5.54	0.002	123	2.71	T
Ball # 19	3095.25	1	42.66	2.425	1.11	0.002	123	2.71	T
Ball # 19	3095.50	1	42.11	2.425	-1.11	0.002	123	2.71	T
Ball # 19	3095.75	1	42.11	2.426	-2.22	0.088	123	2.71	T
Ball # 19	3096.00	1	41	2.469	-6.65	0.128	123	2.71	T
Ball # 19	3096.25	1	38.78	2.49	-8.86	0.060	123	2.71	T
Ball # 19	3096.50	1	36.57	2.499	-5.54	0.030	123	2.71	T
Ball # 19	3096.75	1	36.01	2.505	-2.22	0.020	123	2.71	T
Ball # 19	3097.00	1	35.46	2.509	2.22	0.008	123	2.71	T
Ball # 19	3097.25	1	37.12	2.509	3.32	0.006	123	2.71	T
Ball # 19	3097.50	1	37.12	2.512	3.32	0.014	123	2.71	T
Ball # 19	3097.75	1	38.78	2.516	7.76	0.014	123	2.71	T
Ball # 19	3098.00	1	41	2.519	7.76	-0.036	123	2.71	T
Ball # 19	3098.25	1	42.66	2.498	6.65	-0.066	123	2.71	T
Ball # 19	3098.50	1	44.32	2.486	7.76	-0.042	123	2.71	T
Ball # 19	3098.75	1	46.54	2.477	2.22	-0.018	123	2.71	T
Ball # 19	3099.00	1	45.43	2.477	-7.76	-0.008	123	2.71	T
Ball # 19	3099.25	1	42.66	2.473	-5.54	-0.016	123	2.71	T
Ball # 19	3099.50	1	42.66	2.469	-5.54	-0.080	123	2.71	T
Ball # 19	3099.75	1	39.89	2.433	-11.08	-0.146	123	2.71	T
Ball # 19	3100.00	1	37.12	2.396	-8.86	-0.112	123	2.71	T
Ball # 19	3100.25	1	35.46	2.377	-6.65	-0.046	123	2.71	T
Ball # 19	3100.50	1	33.8	2.373	-1.11	-0.008	123	2.71	T
Ball # 19	3100.75	1	34.9	2.373	5.54	0.000	123	2.71	T
Ball # 19	3101.00	1	36.57	2.373	3.32	-0.008	123	2.71	T
Ball # 19	3101.25	1	36.57	2.369	3.32	-0.012	123	2.71	T
Ball # 19	3101.50	1	38.23	2.367	6.65	0.008	123	2.71	T
Ball # 19	3101.75	1	39.89	2.373	6.65	0.064	123	2.71	T
Ball # 19	3102.00	1	41.55	2.399	7.76	0.096	123	2.71	T

Table H.3 Table of ANN Model for Flow Unit Prediction

Model 4-FU

(Constant Test Set)

		OUPUT	INPUT----------						INPUT
		flow			gr	rhob	gr	rhob	Cat
Well Name	Depth	unit	gr	density	slope	slope	bl	bl	A
Ball # 19	3102.25	1	43.77	2.421	5.54	0.060	123	2.71	T
Ball # 19	3102.50	1	44.32	2.429	0.00	0.016	123	2.71	T
Ball # 19	3102.75	1	43.77	2.429	-1.11	0.006	123	2.71	T
Ball # 19	3103.00	1	43.77	2.432	0.00	0.008	123	2.71	p
Ball # 19	3103.25	1	43.77	2.433	-1.11	0.000	123	2.71	T
Ball # 19	3103.50	1	43.21	2.432	-1.11	-0.092	123	2.71	T
Ball # 19	3103.75	1	43.21	2.387	2.22	-0.110	123	2.71	T
Ball # 19	3104.00	1	44.32	2.377	2.22	-0.040	123	2.71	T
Ball # 19	3104.25	1	44.32	2.367	1.11	-0.020	123	2.71	T
Ball # 19	3104.50	1	44.88	2.367	-2.22	0.000	123	2.71	T
Ball # 19	3104.75	1	43.21	2.367	-3.32	-0.004	123	2.71	T
Ball # 19	3105.00	1	43.21	2.365	4.43	-0.004	123	2.71	T
Ball # 19	3105.25	1	45.43	2.365	3.32	0.000	123	2.71	T
Ball # 19	3105.50	1	44.88	2.365	-2.22	0.000	123	2.71	T
Ball # 19	3105.75	1	44.32	2.365	-2.22	0.004	123	2.71	T
Ball # 19	3106.00	1	43.77	2.367	-4.43	0.004	123	2.71	p
Ball # 19	3106.25	1	42.11	2.367	-6.65	0.006	123	2.71	T
Ball # 19	3106.50	1	40.44	2.37	-3.32	-0.004	123	2.71	T
Ball # 19	3106.75	1	40.44	2.365	-1.11	-0.016	123	2.71	T
Ball # 19	3107.00	2	39.89	2.362	-2.22	-0.014	123	2.71	T
Ball # 19	3107.25	2	39.34	2.358	1.11	-0.080	123	2.71	T
Ball # 19	3107.50	3	40.44	2.322	3.32	-0.102	123	2.71	T
Ball # 19	3107.75	3	41	2.307	0.00	-0.030	123	2.71	T
Ball # 19	3108.00	3	40.44	2.307	5.54	-0.008	123	2.71	p
Ball # 19	3108.25	3	43.77	2.303	6.65	-0.018	123	2.71	T
Ball # 19	3108.50	3	43.77	2.298	0.00	-0.020	123	2.71	T
Ball # 19	3108.75	3	43.77	2.293	-1.11	-0.010	123	2.71	p
Ball # 19	3109.00	3	43.21	2.293	-1.11	0.000	123	2.71	T
Ball # 19	3109.25	3	43.21	2.293	-1.11	-0.014	123	2.71	T
Ball # 19	3109.50	3	42.66	2.286	-2.22	-0.014	123	2.71	T
Ball # 19	3109.75	3	42.11	2.286	-3.32	0.008	123	2.71	T
Ball # 19	3110.00	3	41	2.29	-2.22	0.014	123	2.71	T
Ball # 19	3110.25	3	41	2.293	0.00	0.012	123	2.71	T
Ball # 19	3110.50	3	41	2.296	-1.11	0.014	123	2.71	T
Ball # 19	3110.75	3	40.44	2.3	-8.86	0.018	123	2.71	T

Table H.3 Table of ANN Model for Flow Unit Prediction
Model 4-FU
(Constant Test Set)

		OUTPUT	INPUT----------						INPUT
		flow			gr	rhob	gr	rhob	Cat
Well Name	Depth	unit	gr	density	slope	slope	bl	bl	A
Ball # 19	3111.00	3	36.57	2.305	-7.76	0.018	123	2.71	T
Ball # 19	3111.25	3	36.57	2.309	3.32	0.008	123	2.71	T
Ball # 19	3111.50	3	38.23	2.309	5.54	0.032	123	2.71	T
Ball # 19	3111.75	3	39.34	2.325	12.19	0.092	123	2.71	T
Ball # 19	3112.00	2	44.32	2.355	9.97	0.060	123	2.71	T
Ball # 19	3112.25	1	44.32	2.355	13.30	0.010	123	2.71	T
Ball # 19	3112.50	1	50.97	2.36	21.05	0.096	123	2.71	p
Ball # 19	3112.75	1	54.85	2.403	18.84	0.106	123	2.71	T
Ball # 19	3113.00	1	60.39	2.413	36.56	0.020	123	2.71	T
Ball # 19	3113.25	1	73.13	2.413	27.70	0.128	123	2.71	T
Ball # 19	3113.50	1	74.24	2.477	21.05	0.180	123	2.71	T

Table H.3 Table of ANN Model for Flow Unit Prediction
Model 4-FU
(Constant Test Set)

		OUTPUT	INPUT----------						INPUT
		flow			gr	rhob	gr	rhob	Cat
Well Name	Depth	unit	gr	density	slope	slope	bl	bl	A
Ball # 18	2990.25	1	38.78	2.412	-21.05	-0.206	107	2.72	T
Ball # 18	2990.50	1	37.12	2.396	-9.97	-0.032	107	2.72	T
Ball # 18	2990.75	1	33.8	2.396	-12.19	0.000	107	2.72	p
Ball # 18	2991.00	1	31.03	2.396	-5.54	0.000	107	2.72	T
Ball # 18	2991.25	1	31.03	2.396	-1.11	0.006	107	2.72	T
Ball # 18	2991.50	1	30.47	2.399	-3.32	0.014	107	2.72	T
Ball # 18	2991.75	1	29.36	2.403	-4.43	0.024	107	2.72	T
Ball # 18	2992.00	1	28.26	2.411	-2.22	0.032	107	2.72	T
Ball # 18	2992.25	1	28.26	2.419	1.11	0.072	107	2.72	T
Ball # 18	2992.50	1	28.81	2.447	1.11	0.084	107	2.72	T
Ball # 18	2992.75	1	28.81	2.461	0.00	0.028	107	2.72	T
Ball # 18	2993.00	1	28.81	2.461	-1.11	0.000	107	2.72	T
Ball # 18	2993.25	1	28.26	2.461	-3.32	0.000	107	2.72	T
Ball # 18	2993.50	1	27.15	2.461	-2.22	-0.014	107	2.72	T
Ball # 18	2993.75	1	27.15	2.454	0.00	-0.014	107	2.72	T
Ball # 18	2994.00	1	27.15	2.454	1.11	-0.030	107	2.72	T
Ball # 18	2994.25	1	27.7	2.439	7.76	-0.072	107	2.72	T

Table H.3 Table of ANN Model for Flow Unit Prediction

Model 4-FU

(Constant Test Set)

		OUTPUT	INPUT----------						INPUT
		flow			gr	rhob	gr	rhob	Cat
Well Name	Depth	unit	gr	density	slope	slope	bl	bl	A
Ball # 18	2994.50	1	31.03	2.418	6.65	-0.042	107	2.72	T
Ball # 18	2994.75	1	31.03	2.418	3.32	-0.064	107	2.72	T
Ball # 18	2995.00	1	32.69	2.386	8.86	-0.144	107	2.72	T
Ball # 18	2995.25	1	35.46	2.346	13.30	-0.124	107	2.72	T
Ball # 18	2995.50	2	39.34	2.324	12.19	-0.082	107	2.72	T
Ball # 18	2995.75	2	41.55	2.305	7.76	-0.076	107	2.72	T
Ball # 18	2996.00	3	43.21	2.286	7.76	-0.072	107	2.72	T
Ball # 18	2996.25	3	45.43	2.269	4.43	-0.034	107	2.72	p
Ball # 18	2996.50	3	45.43	2.269	2.22	-0.020	107	2.72	T
Ball # 18	2996.75	3	46.54	2.259	3.32	-0.008	107	2.72	T
Ball # 18	2997.00	3	47.09	2.265	2.22	0.020	107	2.72	T
Ball # 18	2997.25	3	47.65	2.269	3.32	0.018	107	2.72	T
Ball # 18	2997.50	3	48.75	2.274	2.22	0.020	107	2.72	T
Ball # 18	2997.75	3	48.75	2.279	1.11	0.020	107	2.72	T
Ball # 18	2998.00	3	49.31	2.284	1.11	0.010	107	2.72	T
Ball # 18	2998.25	3	49.31	2.284	1.11	0.008	107	2.72	T
Ball # 18	2998.50	3	49.86	2.288	3.33	0.008	107	2.72	T
Ball # 18	2998.75	3	50.97	2.288	5.54	0.012	107	2.72	T
Ball # 18	2999.00	3	52.63	2.294	11.08	0.028	107	2.72	T
Ball # 18	2999.25	3	56.51	2.302	14.40	0.086	107	2.72	T
Ball # 18	2999.50	3	59.83	2.337	14.40	0.096	107	2.72	T
Ball # 18	2999.75	3	63.71	2.35	25.48	0.038	107	2.72	p
Ball # 18	3000.00	2	72.58	2.356	17.73	0.012	107	2.72	T
Ball # 18	3000.25	2	72.58	2.356	0.00	0.214	107	2.72	T
Ball # 18	3000.50	1	72.58	2.463	-2.22	0.256	107	2.72	T
Ball # 18	3000.75	1	71.47	2.484	-3.32	0.058	107	2.72	T
Ball # 18	3001.00	1	70.91	2.492	-1.11	0.016	107	2.72	T
Ball # 18	3001.25	1	70.91	2.492	-4.43	-0.016	107	2.72	T
Ball # 18	3001.50	1	68.7	2.484	-2.22	-0.022	107	2.72	T
Ball # 18	3001.75	1	69.81	2.481	2.22	-0.006	107	2.72	T
Ball # 18	3002.00	1	69.81	2.481	2.22	-0.060	107	2.72	T
Ball # 18	3002.25	1	70.91	2.451	2.22	-0.060	107	2.72	T
Ball # 18	3002.50	1	70.91	2.451	2.22	0.014	107	2.72	T
Ball # 18	3002.75	1	72.02	2.458	1.11	0.028	107	2.72	T
Ball # 18	3003.00	1	71.47	2.465	-2.22	0.032	107	2.72	T
Ball # 18	3003.25	1	70.91	2.474	-9.97	0.050	107	2.72	T

Table H.3 Table of ANN Model for Flow Unit Prediction
Model 4-FU
(Constant Test Set)

		OUTPUT	INPUT----------						INPUT
		flow			**gr**	**rhob**	**gr**	**rhob**	Cat
Well Name	Depth	**unit**	**gr**	**density**	**slope**	**slope**	**bl**	**bl**	A
Ball # 18	3003.50	1	66.48	2.49	-8.86	0.032	107	2.72	T
Ball # 18	3003.75	1	66.48	2.49	-2.22	0.022	107	2.72	T
Ball # 18	3004.00	1	65.37	2.501	-2.22	0.032	107	2.72	T
Ball # 18	3004.25	1	65.37	2.506	-2.22	0.016	107	2.72	T
Ball # 18	3004.50	1	64.27	2.509	0.00	0.008	107	2.72	T
Ball # 18	3004.75	1	65.37	2.51	13.30	0.008	107	2.72	T
Ball # 18	3005.00	1	70.91	2.513	14.40	-0.002	107	2.72	T
Ball # 18	3005.25	1	72.58	2.509	5.54	-0.024	107	2.72	T
Ball # 18	3005.50	1	73.68	2.501	2.22	-0.016	107	2.72	T
Ball # 18	3005.75	1	73.68	2.501	3.32	-0.008	107	2.72	T
Ball # 18	3006.00	1	75.35	2.497	0.00	-0.014	107	2.72	T
Ball # 18	3006.25	1	73.68	2.494	-9.97	-0.010	107	2.72	T
Ball # 18	3006.50	1	70.36	2.492	-28.81	-0.028	107	2.72	T
Ball # 18	3006.75	1	59.28	2.48	-27.70	-0.030	107	2.72	T
Ball # 18	3007.00	1	56.51	2.477	-16.62	-0.020	107	2.72	T
Ball # 18	3007.25	1	50.97	2.47	-11.08	-0.014	107	2.72	p
Ball # 18	3007.50	1	50.97	2.47	-14.41	-0.004	107	2.72	T
Ball # 18	3007.75	1	43.77	2.468	-22.16	-0.014	107	2.72	T
Ball # 18	3008.00	1	39.89	2.463	-9.97	-0.010	107	2.72	T
Ball # 18	3008.25	1	38.78	2.463	-2.22	0.000	107	2.72	T

Table H.3 Table of ANN Model for Flow Unit Prediction
Model 4-FU
(Constant Test Set**)**

		OUTPUT	INPUT----------						INPUT
		flow			**gr**	**rhob**	**gr**	**rhob**	Cat
Well Name	Depth	**unit**	**gr**	**density**	**slope**	**slope**	**bl**	**bl**	A
Horner # 11	3,084.50	1	35.26	2.498	1.10	-0.038	122	2.71	p
Horner # 11	3084.75	1	35.26	2.484	0	-0.05	122	2.71	T
Horner # 11	3085.00	1	35.26	2.473	3.306	-0.01	122	2.71	T
Horner # 11	3085.25	1	36.92	2.479	6.61	0.042	122	2.71	T
Horner # 11	3085.50	1	38.57	2.494	9.916	0.044	122	2.71	T
Horner # 11	3085.75	1	41.87	2.501	8.816	0.014	122	2.71	T

Table H.3 Table of ANN Model for Flow Unit Prediction

Model 4-FU

(Constant Test Set)

		OUTPUT	INPUT						INPUT
Well Name	Depth	flow unit	gr	density	gr slope	rhob slope	gr bl	rhob bl	Cat A
Horner # 11	3086.00	1	42.98	2.501	6.612	0.016	122	2.71	T
Horner # 11	3086.25	1	45.18	2.509	7.714	0.054	122	2.71	T
Horner # 11	3086.50	1	46.83	2.528	3.306	0.054	122	2.71	T
Horner # 11	3086.75	1	46.83	2.536	13.22	0.022	122	2.71	T
Horner # 11	3087.00	1	53.44	2.539	14.32	0.044	122	2.71	T
Horner # 11	3087.25	1	53.99	2.558	5.508	0.036	122	2.71	T
Horner # 11	3087.50	1	56.2	2.557	-1.1	-0.022	122	2.71	T
Horner # 11	3087.75	1	53.44	2.547	-9.916	-0.12	122	2.71	T
Horner # 11	3088.00	1	51.24	2.497	-12.12	-0.1	122	2.71	T
Horner # 11	3088.25	1	47.38	2.497	-7.714	-0.042	122	2.71	T
Horner # 11	3088.50	1	47.38	2.476	-3.306	-0.296	122	2.71	T
Horner # 11	3088.75	2	45.73	2.349	-16.53	-0.302	122	2.71	T
Horner # 11	3089.00	2	39.12	2.325	-23.14	-0.068	122	2.71	T
Horner # 11	3089.25	2	34.16	2.315	-12.12	-0.022	122	2.71	T
Horner # 11	3089.50	2	33.06	2.314	-7.714	0.008	122	2.71	p
Horner # 11	3089.75	2	30.3	2.319	-7.714	0.032	122	2.71	T
Horner # 11	3090.00	2	29.2	2.33	-2.204	0.022	122	2.71	T
Horner # 11	3090.25	2	29.2	2.33	0	0	122	2.71	T
Horner # 11	3090.50	2	29.2	2.33	5.51	-0.008	122	2.71	T
Horner # 11	3090.75	2	31.96	2.326	5.51	-0.014	122	2.71	T
Horner # 11	3091.00	2	31.96	2.323	14.32	-0.022	122	2.71	T
Horner # 11	3091.25	3	39.12	2.315	19.83	-0.024	122	2.71	T
Horner # 11	3091.50	3	41.87	2.311	7.714	-0.012	122	2.71	T
Horner # 11	3091.75	3	42.98	2.309	11.02	-0.004	122	2.71	T
Horner # 11	3092.00	3	47.38	2.309	22.04	0.034	122	2.71	p
Horner # 11	3092.25	3	53.99	2.326	13.22	0.062	122	2.71	T
Horner # 11	3092.50	3	53.99	2.34	4.408	0.066	122	2.71	T
Horner # 11	3092.75	1	56.2	2.359	12.12	0.066	122	2.71	T
Horner # 11	3093.00	1	60.06	2.373	13.22	0.288	122	2.71	T

Table H.4
Summary of Final Flow Units

Well Name	Flow Unit One (Feet)	Flow Unit Two (Feet)
T Heirs # 8	2789.50 - 2797.00	None
LeMasters # 13	3048.00 - 3054.00	None
Horner # 9	2892.75 - 2899.25	2899.25 - 2904.50
Ball # 19	3092.50 - 3107.25	3107.25 - 3111.75
Ball # 18	2990.25 - 2995.75	2995.75 - 2999.75
Horner # 11	3084.50 - 3091.00	3091.00 - 3092.50

Figure H.1 Horner # 11
(Predicted versus Actual Permeability)

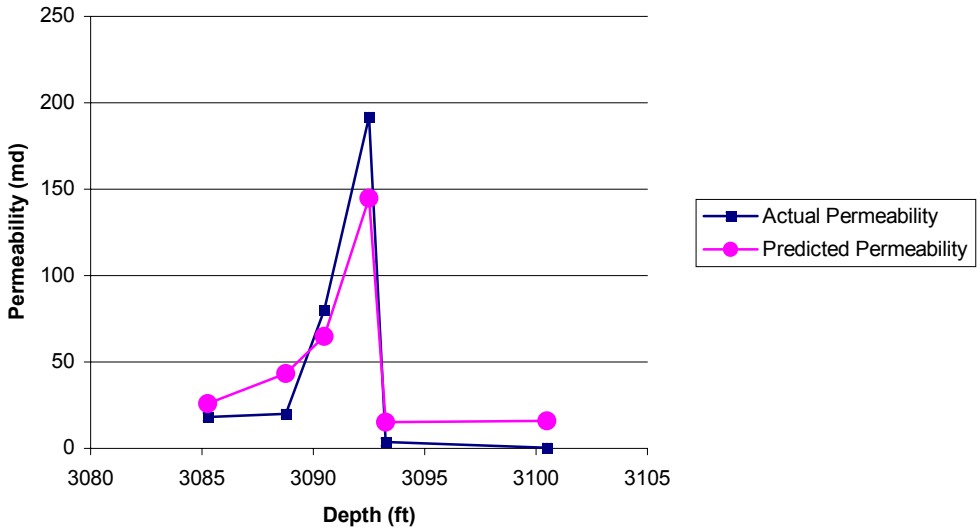

Figure H.2 T. Heirs # 8
(Predicted versus Actual Permeability)

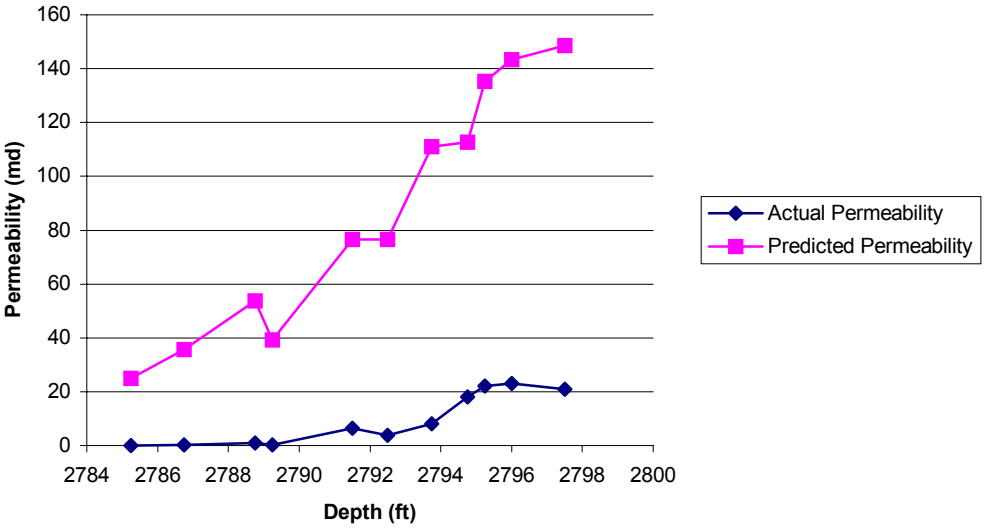

Figure H.3 Horner # 9
(Predicted versus Actual Permeability)

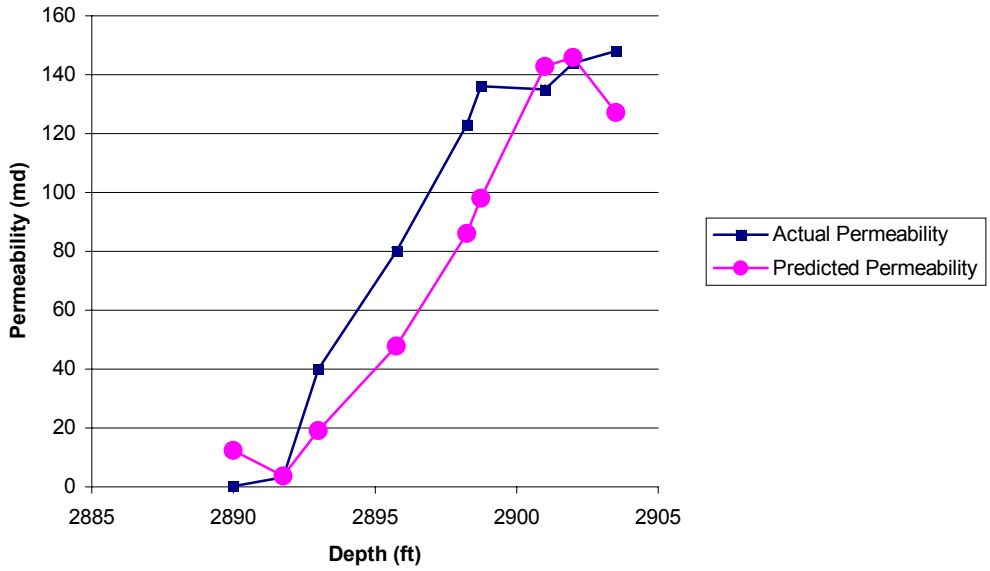

Figure H.4 Ball # 19
(Predicted versus Actual Permeability)

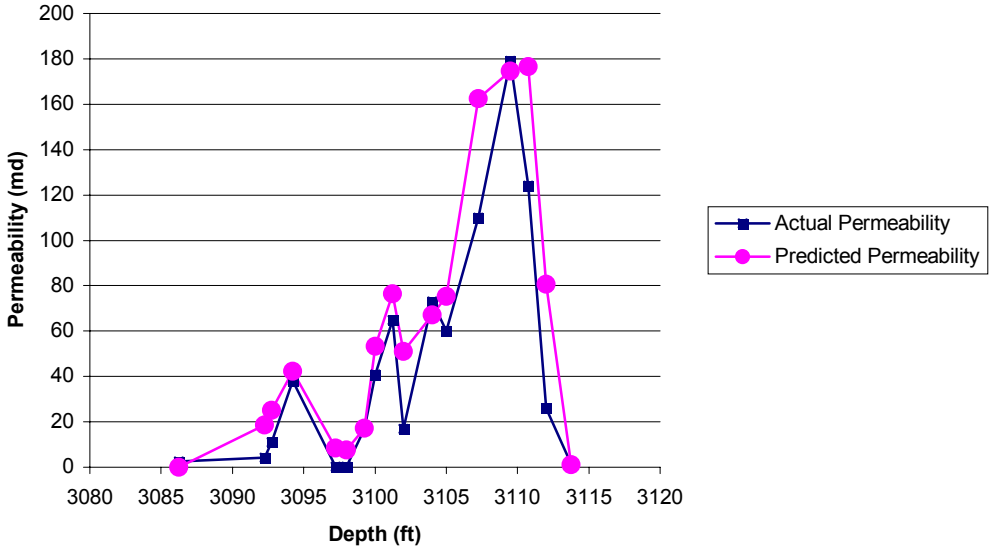

Appendix H. Figure 5.0 LeMasters # 13
(predicted vs actual permeability)

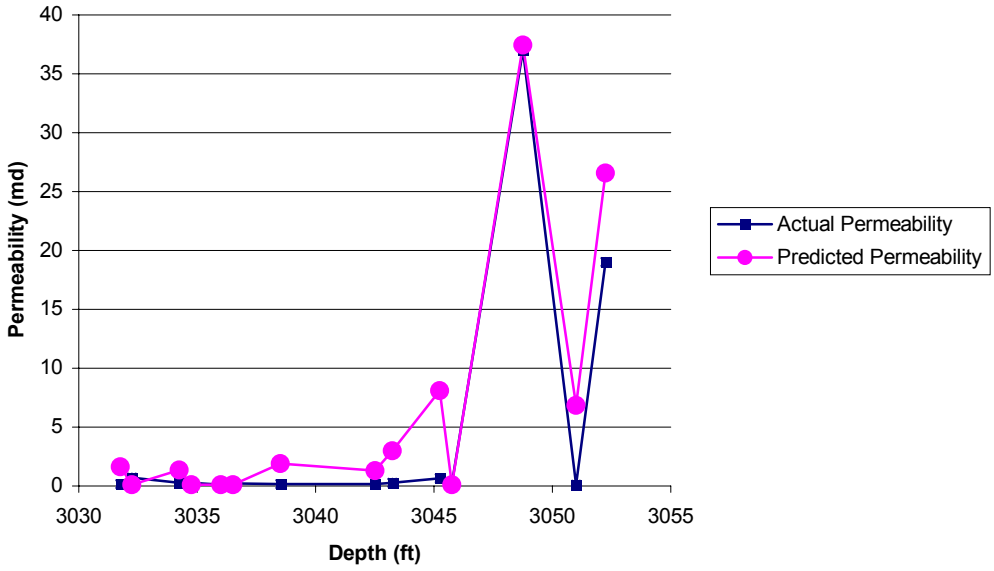

Figure H.6 Ball # 18
(Predicted versus Actual Permeability)

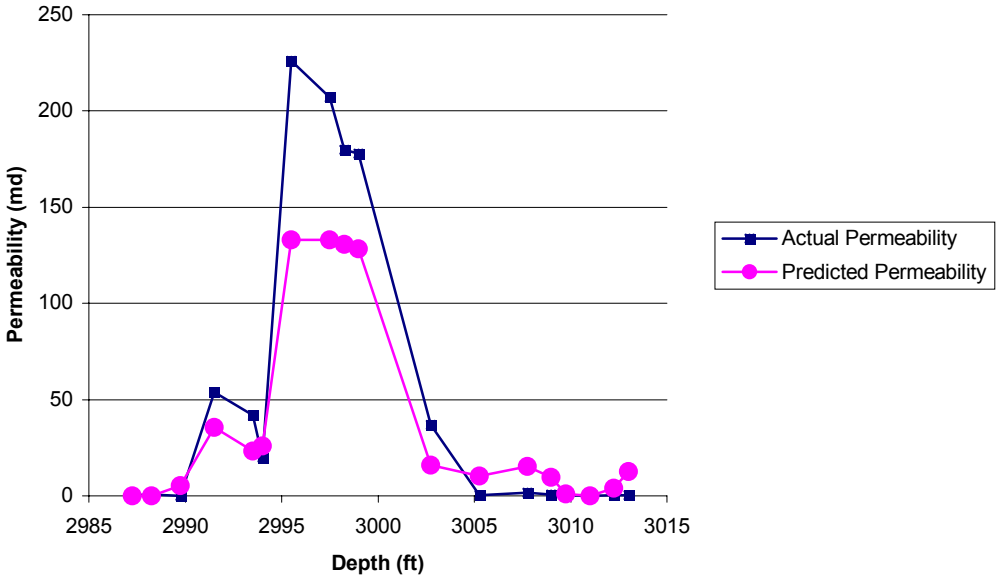

APPENDIX I.

Tables I.1 and I.2 are the individual well summaries of predicted permeability within each flow unit. The tables include flow capacity and storage capacity data for each well. The summaries are for the 125 wells in the field.

Table I.1 Summary of Results from ANN Permeability Prediction for Field Application Flow Unit One - Detail

Well Name	Pred FU	x Coord	y Coord	H Thick	Avg Por	Avg Pred k	Por-h	kh
THOMPSON HEIRS 8	1	1661311	350310	7.5	0.1598	11.11	1.20	83.35
LEMASTERS, E B O-13	1	1670619	356894	5.50	0.1430	15.80	0.79	86.90
REILLY, IRENE 13	1	1662365	363701	1.25	0.1216	0.11	0.15	0.14
HORNER, PETER 9	1	1663331	347187	6.25	0.1725	63.89	1.08	399.31
BALL, F R 19	1	1665845	349376	3.25	0.1420	17.92	0.46	58.24
BALL, F R 18	1	1664052	350419	5.00	0.1540	38.02	0.77	190.10
HORNER, P 11	1	1662865	348286	2	0.2000	73.93	0.40	147.86
WRIGHT, C 5	1	1661036	339889	3	0.1230	20.37	0.37	61.11
ASH, EMELINE 5	1	1663819	347763	3.75	0.1627	14.65	0.61	54.94
LEMASTERS, F M 9	1	1661747	348093	0.25	0.1220	16.46	0.03	4.12
PENNICK, M H 7	1	1662221	348695	1.5	0.1598	50.53	0.24	75.80
HORNER, PETER 12	1	1663196	347699	5.5	0.1717	29.36	0.94	161.48
BALL, F R 21	1	1665028	349532	6	0.1892	69.93	1.14	419.59
THOMPSON HEIRS 10	1	1662173	350142	2.5	0.1621	58.08	0.41	145.20
PENNICK, M H 9	1	1663954	351371	0.25	0.1231	29.02	0.03	7.26
LEMASTERS, F M 10	1	1660552	348663	6.25	0.1802	30.16	1.13	188.50

Table I.1 Summary of Results from ANN Permeability Prediction for Field Application Flow Unit One - Detail

Well Name	Pred FU	x Coord	y Coord	H Thick	Avg Por	Avg Pred k	Por-h	kh
GORRELL, J B 5	1	1663994	349706	1.75	0.1437	8.50	0.25	14.88
LEMASTERS, A D 20	1	1665538	351784	4.5	0.1470	14.46	0.66	65.07
LEMASTERS, A D I10	1	1664692	353981	2.25	0.1967	63.68	0.44	143.28
BALL, F R J7	1	1665940	350176	8	0.1390	18.76	1.11	150.08
LEMASTERS, L J K13	1	1666841	356429	11.3	0.1778	10.02	2.00	112.73
LEMASTERS, S P J10	1	1665869	353779	0.25	0.1510	44.03	0.04	11.01
LEMASTERS, S P M-10	1	1668301	353642	5.25	0.1415	7.19	0.74	37.73
LEMASTERS, L J M-12	1	1668495	355533	0.25	0.2030	25.27	0.05	6.32
PENNICK, C C M-14	1	1668716	356900	0.75	0.1215	31.99	0.09	23.99
MCCOY, C L-8	1	1667289	351797	11	0.1526	27.16	1.68	298.76
MCCOY, C K-8	1	1666541	351388	1.5	0.1490	9.59	0.22	14.39
LEMASTERS, S P L-10	1	1667813	353029	8.5	0.1389	2.97	1.18	25.25
BALL HEIRS N-11	1	1669445	354720	2.75	0.1307	0.11	0.36	0.30
PENNICK, C C N-13	1	1669552	356430	10.3	0.1737	45.28	1.78	464.12
ALLEN, NANCY M-9	1	1668536	352145	2.25	0.1336	26.10	0.30	58.73
LEMASTERS, J F-8	1	1661699	351908	0.25	0.1350	60.10	0.03	15.03
THOMPSON HRS E-7	1	1661036	350860	5	0.1685	33.62	0.84	168.10
WHARTON, W J D-7	1	1660131	350763	9	0.1746	51.71	1.57	465.39
DAWSON, J H F-14	1	1662361	357053	3	0.1775	51.95	0.53	155.85

Table I.1 Summary of Results from ANN Permeability Prediction for Field Application Flow Unit One - Detail

Well Name	Pred FU	x Coord	y Coord	H Thick	Avg Por	Avg Pred k	Por-h	kh
EDDY, J T N-10-B	1	1669653	353777	9.75	0.1584	14.64	1.54	142.74
DAWSON, J H G-13	1	1662888	356347	1.25	0.1322	8.02	0.17	10.02
LEMASTERS, J H-11	1	1664169	355011	6.25	0.1690	49.90	1.06	311.88
DAWSON, J H F-12	1	1662114	355472	2.5	0.1440	5.36	0.36	13.40
STACKPOLE, R M F-9	1	1662027	352956	4.5	0.1725	25.10	0.78	112.95
HUFFMAN, Q. F-11	1	1662111	354223	12.8	0.1419	19.56	1.81	249.39
BALL, F R J-5	1	1666251	348234	7	0.1624	14.45	1.14	101.15
BALL, F R L-6	1	1667471	349573	4.25	0.1793	63.04	0.76	267.92
MCCOY, C L-8-B	1	1668143	351265	5.75	0.1623	54.67	0.93	314.35
BALL, R L L-7	1	1668182	350314	0.5	0.1224	34.09	0.06	17.05
BALL, F R K-5	1	1666862	348962	2.5	0.1582	12.96	0.40	32.40
MCMILLEN, S J-4	1	1666007	347549	16	0.1750	13.81	2.80	220.96
EDDY, M A O-7	1	1670289	350786	1.25	0.1208	8.86	0.15	11.08
LONGSTRETH, E E-12	1	1660336	355324	1.5	0.1687	87.10	0.25	130.65
GLOVER, ALPHEUS C-9	1	1659053	352938	5.75	0.1558	38.20	0.90	219.65
BALL, F R L-5	1	1667251	348021	0.75	0.1230	39.46	0.09	29.60
BALL, F R M-6	1	1668263	349009	4.5	0.1554	55.08	0.70	247.85
STACKPOLE, U E-11	1	1660623	354421	1	0.1408	30.61	0.14	30.61

Table I.1 Summary of Results from ANN Permeability Prediction for Field Application Flow Unit One - Detail

Well Name	Pred FU	x Coord	y Coord	H Thick	Avg Por	Avg Pred k	Por-h	kh
WRIGHT, P G D-3	1	1659323	346574	6.5	0.1806	63.18	1.17	410.64
ELDER, MARTHA 12	1	1661964	341880	10.5	0.1942	76.12	2.04	799.22
MCINTYRE, E 11	1	1662537	339719	4	0.1639	42.00	0.66	168.00
BAKER, I 5	1	1660658	341599	15.5	0.1433	35.45	2.22	549.55
HAUGHT, JOSHUA 6	1	1659528	343063	0.25	0.1226	38.29	0.03	9.57
PITTS, OLIVER 8	1	1661002	344748	5.75	0.1377	25.42	0.79	146.15
PITTS, OLIVER 9	1	1661994	345384	5.5	0.1530	43.26	0.84	237.93
SWIGER, B A 7	1	1659297	344622	0.25	0.1300	4.43	0.03	1.11
MCINTYRE, J L 12	1	1663109	345121	5.75	0.1723	16.06	0.99	92.35
ELDER, MARTHA 13	1	1662085	343583	4.5	0.1426	13.85	0.64	62.32
ALLEN, NANCY N-8	1	1669370	351399	4	0.1479	39.79	0.59	159.15
BALL, R L N-6	1	1669223	349648	2	0.1335	62.77	0.27	125.53
WYATT, SILAS E-3	1	1660280	346911	10	0.2092	55.18	2.09	551.82
LEMASTERS, L J 3-A	1	1667342	355232	9.5	0.1644	33.17	1.56	315.10
LEMASTERS, A D 13-A	1	1667342	355232	0.25	0.1370	68.74	0.03	17.19
HALL, C T K14	1	1666859	357777	1.75	0.1552	82.21	0.27	143.87
PENNICK, C C J15	1	1666121	357777	4.25	0.1283	15.98	0.55	67.89
PENNICK, C C L15	1	1667485	357777	13	0.1545	27.67	2.01	359.74
NOLAN, HENRY L-16	1	1668293	357777	12.5	0.1888	36.31	2.36	453.90

Table I.1 Summary of Results from ANN Permeability Prediction for Field Application Flow Unit One - Detail

Well Name	Pred FU	x Coord	y Coord	H Thick	Avg Por	Avg Pred k	Por-h	kh
LEMASTERS, A D H-13	1	1663875	357777	10	0.1618	26.11	1.62	261.09
HOGE, F L H-14	1	1663435	357777	6.75	0.1347	17.57	0.91	118.60
NOLAN, HENRY L-17	1	1667777	357777	7.5	0.1344	4.74	1.01	35.52
PENNICK, C C M-15	1	1668790	357777	9.5	0.1428	15.88	1.36	150.84
NOLAN, HENRY M-17	1	1668809	357777	12.5	0.1642	60.44	2.05	755.55
PENNICK, C C L-15B	1	1668133	357777	5	0.1585	1.84	0.79	9.20
LEMASTERS, E B P-12	1	1671304	357777	7.75	0.1619	44.94	1.25	348.32
LEMASTERS, MARY P-14	1	1671831	357777	4	0.1922	40.26	0.77	161.04
REILLY, T W N-17	1	1670315	357777	10.5	0.1713	17.36	1.80	182.28
REILLY, G V L-19	1	1668041	357777	2.75	0.1821	25.73	0.50	70.76
REILLY, G V N-19	1	1669545	357777	3.75	0.2000	59.21	0.75	222.05
REILLY, MARY J O-19	1	1670467	357777	6.75	0.1789	70.44	1.21	475.48
PENNICK, C C O-15	1	1671346	357777	11	0.1445	27.52	1.59	302.69
JAMISON, H M Q-17	1	1673425	357777	3.75	0.1380	11.90	0.52	44.62
WILEY, ISAAC G-22	1	1661620	357777	1.5	0.1490	2.40	0.22	3.61
WILEY, S H G-23	1	1661635	357777	2.75	0.1688	9.58	0.46	26.34
REILLY, IRENE I-20	1	1663804	357777	11.5	0.1896	82.05	2.18	943.52
PENNICK, C C G-15	1	1662785	357777	4.5	0.1812	54.42	0.82	244.89
WILEY, J E G-25	1	1663056	357777	3.25	0.2022	36.12	0.66	117.40

Table I.1 Summary of Results from ANN Permeability Prediction for Field Application Flow Unit One - Detail

Well Name	Pred FU	x Coord	y Coord	H Thick	Avg Por	Avg Pred k	Por-h	kh
FLUHARTY, WM. E-16	1	1661046	357777	1	0.1292	53.87	0.13	53.87
FLUHARTY, J K E-18	1	1661118	357777	10.8	0.1746	44.31	1.88	476.31
FLUHARTY, H G-17	1	1663204	357777	3.5	0.1641	58.44	0.57	204.53
WILEY, I G-22-B	1	1662521	357777	9.5	0.1451	13.12	1.38	124.61
REILLY, IRENE H-19	1	1664183	357777	3.75	0.1618	40.46	0.61	151.71
WILEY, JACOB H-25	1	1664361	357777	4.25	0.1786	22.28	0.76	94.69
MCCOY HRS. H-27	1	1664336	357777	9.25	0.1582	71.71	1.46	663.35
WILEY, A E-26	1	1661466	357777	5.25	0.1576	55.50	0.83	291.36
WILEY, S H E-24	1	1660426	357777	6.75	0.1788	95.08	1.21	641.79
LEMASTERS, E B P-13	1	1671869	357777	5.5	0.1392	36.84	0.77	202.62

Table I.2 Summary of Results from ANN Permeability Prediction for Field Application Flow Unit Two - Detail

Well Name	Pred FU	x Coord	y Coord	H Thick	Avg Por	Avg Pred k	Por-h	kh
HORNER, PETER 8	2	1663331	347187	4.50	0.2350	143.40	1.06	645.30
BALL, F R 19	2	1665845	349376	3.75	0.2270	152.78	0.85	572.93
BALL, F R 18	2	1664052	350419	3.75	0.2360	201.76	0.89	756.60
HORNER, P 11	2	1662865.4	348286	0.75	0.2150	180.14	0.16	135.11
WRIGHT, C 5	2	1661036.1	339889	12.8	0.3010	98.40	3.84	1254.60
ASH, EMELINE 5	2	1663818.6	347763	5.25	0.2420	241.30	1.27	1266.83
LEMASTERS, F M 9	2	1661747.3	348093	2.5	0.2126	124.79	0.53	311.98
PENNICK, M H 7	2	1662221.3	348695	2.75	0.2272	167.83	0.62	461.53
HORNER, PETER 10	2	1662517.8	347635	5.25	0.2636	175.30	1.38	920.33
BALL, F R 21	2	1665028.2	349532	4.25	0.2394	223.17	1.02	948.47
THOMPSON HEIRS 9	2	1661161.2	349256	1.5	0.2044	137.38	0.31	206.07
PENNICK, M H 9	2	1663954	351371	6.75	0.2472	177.00	1.67	1194.75
LEMASTERS, F M 10	2	1660551.8	348663	1.75	0.2147	199.36	0.38	348.88
BALL, F R 20	2	1665067	350333	16	0.2504	175.62	4.01	2809.92
GORRELL, J B 4	2	1665100.4	348584	5.5	0.2452	167.76	1.35	922.68
GORRELL, J B 5	2	1663994.1	349706	6	0.2650	133.53	1.59	801.18
LEMASTERS, A D 20	2	1665537.9	351784	5.75	0.2680	136.67	1.54	785.85
PENNICK, M H 8	2	1663167.6	350205	5	0.2478	123.85	1.24	619.25
BALL, F R J7	2	1665940.3	350176	0.25	0.1340	30.73	0.03	7.68

Table I.2 Summary of Results from ANN Permeability Prediction for Field Application Flow Unit Two - Detail

Well Name	Pred FU	x Coord	y Coord	H Thick	Avg Por	Avg Pred k	Por-h	kh
LEMASTERS, L J K12	2	1666263	355381	6.25	0.2530	121.93	1.58	762.06
LEMASTERS, S P J10	2	1665869.2	353779	6.75	0.2202	143.34	1.49	967.55
LEMASTERS, L J M-12	2	1668495.4	355533	3	0.2181	224.23	0.65	672.69
MCCOY, C K-8	2	1666540.8	351388	0.75	0.1790	130.23	0.13	97.67
LEMASTERS, S P L-10	2	1667813.2	353029	1.5	0.1765	175.29	0.26	262.94
BALL HEIRS N-11	2	1669444.7	354720	2.5	0.2033	118.54	0.51	296.35
LEMASTERS, J F-8	2	1661699.3	351908	3.5	0.1995	107.96	0.70	377.86
LEMASTERS, JASPER 15	2	1661987.4	351070	1.75	0.1943	151.29	0.34	264.76
GLOVER, J N E-8	2	1660843	352065	0.5	0.1289	138.77	0.06	69.39
BALL, F R K-5	2	1666861.9	348962	2	0.1829	105.64	0.37	211.28
LONGSTRETH, E E-12	2	1660336	355324	6.75	0.2400	176.05	1.62	1188.34
BALL, F R L-5	2	1667250.6	348021	4.75	0.2093	128.38	0.99	609.81
ELDER, MARTHA 11	2	1663385.3	343413	3.5	0.2352	140.38	0.82	491.32
STACKPOLE, U E-11	2	1660623.2	354421	2	0.2038	211.21	0.41	422.42
MCINTYRE, E 11	2	1662536.8	339719	1.25	0.1938	188.97	0.24	236.21
HAUGHT, JOSHUA 6	2	1659527.7	343063	8	0.2187	112.34	1.75	898.72
BAKER HRS., D 11	2	1660731.4	343299	2.75	0.1981	144.54	0.54	397.49
PITTS, OLIVER 8	2	1661002.2	344748	2	0.2094	135.08	0.42	270.16
SWIGER, B A 7	2	1659297.3	344622	7	0.2827	182.72	1.98	1279.02
No Name	2	1660951.8	345958	6.25	0.2191	178.32	1.37	1114.50

Table I.2 Summary of Results from ANN Permeability Prediction for Field Application Flow Unit Two - Detail

Well Name	Pred FU	x Coord	y Coord	H Thick	Avg Por	Avg Pred k	Por-h	kh
MCINTYRE, J L 12	2	1663108.6	345121	3.5	0.1942	72.57	0.68	254.01
ELDER, MARTHA 13	2	1662085.4	343583	1.5	0.1307	91.94	0.20	137.91
LEMASTERS, A D 13-A	2	1667342.4	355232	3.5	0.2048	122.16	0.72	427.55
HALL, C T K14	2	1666859.1	357777	5.5	0.2216	144.83	1.22	796.57
NOLAN, HENRY L-17	2	1667776.7	357777	3	0.2137	83.01	0.64	249.03
NOLAN, HENRY M-17	2	1668809.5	357777	1.5	0.1545	144.43	0.23	216.65
NOLAN, HENRY N-15	2	1669992.9	357777	0.25	0.2368	56.85	0.06	14.21
PENNICK, C C L-15B	2	1668132.6	357777	1.5	0.2075	131.01	0.31	196.52
REILLY, G V L-19	2	1668040.7	357777	0.75	0.1500	89.62	0.11	67.21
WILEY, ISAAC G-22	2	1661620.1	357777	2.75	0.2002	135.39	0.55	372.32
WILEY, S H G-23	2	1661635.2	357777	0.25	0.1470	120.67	0.04	30.17
REILLY, IRENE G-20	2	1661747	357777	4	0.2280	190.14	0.91	760.56
FLUHARTY, WM. E-14	2	1661209.8	357777	4.25	0.2541	78.41	1.08	333.26
PENNICK, C C G-15	2	1662784.9	357777	0.75	0.1558	68.92	0.12	51.69
WILEY, ANDERSON F-25	2	1662059.2	357777	9.5	0.2735	129.66	2.60	1231.77
WILEY, J E G-25	2	1663056	357777	0.25	0.1550	141.75	0.04	35.44
FLUHARTY, WM. E-15	2	1661075.6	357777	6	0.2976	66.74	1.79	400.45
WILEY, ISAAC H-22	2	1663970	357777	4.5	0.2512	126.08	1.13	567.35
CUNNINGHAM, D F-18-B	2	1662124.3	357777	5	0.2623	171.40	1.31	857.00

Table I.2 Summary of Results from ANN Permeability Prediction for Field Application Flow Unit Two - Detail

Well Name	Pred FU	x Coord	y Coord	H Thick	Avg Por	Avg Pred k	Por-h	kh
MCCOY HRS. H-27	2	1664335.9	357777	0.25	0.1200	69.13	0.03	17.28
MCCOY HRS. G-27	2	1663080.6	357777	8.75	0.2247	134.28	1.97	1174.99
WILEY, S H E-24	2	1660426.1	357777	0.25	0.1279	53.78	0.03	13.45
LEASURE, E I-21	2	1663995.4	357777	6.75	0.2500	136.26	1.69	919.77

VITAE

Benjamin Hale Thomas was born July 5, 1954, in Parkersburg, West Virginia. He is the son of Kenneth Berl Thomas and the late Glenna Marie Rymer Thomas.

He received his B.B.A. degree from Kent State University in 1975, his B.S. degree in Petroleum Engineering from Marietta College in 1981, his M.B.A. from Ashland University in 1987, his M.S. in Petroleum and Natural Gas Engineering in 1997 and his Doctor of Philosophy in Petroleum and Natural Gas Engineering in 2002, both from West Virginia University.

He is a member of the Honor Society of Petroleum Engineers (Pi Epsilon Tau), a member of the Society of Petroleum Engineers (SPE) since 1979, has been active in the Ohio Oil & Gas Association (OOGA), and was Governor appointed to serve on the Technical Advisory Council (TAC) for the Ohio Division of Oil and Gas from 1987 - 2002.

He is married to Connie Ruth Buck Thomas and has one son, Jeremy John Thomas. They currently reside in Dover, Ohio.

He was President of MB Operating Co., Inc., and Chief Executive Officer of Marbel Energy Corporation, both located in Canton, Ohio. In 2000, he retired to complete his Doctorate studies. He plans to teach and research topics related to Petroleum and Natural Gas Engineering.